



UCL

NEUROIMAGING OF SUDDEN UNEXPECTED DEATH IN EPILEPSY (SUDEP)

Luke Allen, PhD thesis

Student number: 16000791

Primary supervisor: Dr. Beate Diehl

Secondary supervisor: Professor Louis Lemieux

UCL Institute of Neurology
Department of Clinical & Experimental Epilepsy

Table of contents

Table of contents	1
Declaration	4
List of figures	5
List of tables	7
Contributing authors & acknowledgements	8
Acknowledgements	8
Author institution information	10
Abbreviations	11
Abstract	14
Impact statement	16
Thesis objectives, outline & acknowledgements	17
Objectives	17
Thesis outline and summary of chapters	17
Chapter 1: Background	21
1.1: Epilepsy	21
1.1.1 Definition	21
1.1.2 Incidence	22
1.1.3 Aetiology	22
1.1.4 Diagnosis and outlook	23
1.1.5 Neuroimaging and epilepsy	24
1.2: SUDEP	25
1.2.1 Definitions and epidemiology	25
1.2.2 Proposed mechanisms	27
1.2.3 SUDEP risk factors	27
1.3: Autonomic and respiratory dysfunction in epilepsy and SUDEP	30
1.3.1 Cardiac alterations	30
1.3.2 Heart rate variability (HRV)	32
1.3.4 Changes in blood pressure	34
1.3.5 Respiratory disturbances	35

1.3.6 Summary of autonomic and respiratory dysfunction in epilepsy and SUDEP	38
1.4: Central control of autonomic and respiratory regulation (a brief overview).....	39
1.5: Neuroimaging of SUDEP	43
1.5.1 Overview	43
1.5.2 Evidence from structural MRI	44
1.5.3 Evidence from resting-state fMRI.....	51
1.5.4 Discussion and considerations	53
1.5.5 Conclusions & outlook.....	55
Chapter 2: Common methods	57
2.1: Ascertainment of SUDEP cases	57
2.2: Magnetic Resonance Imaging and analysis procedures.....	58
2.1. MRI (overview)	58
2.2 Functional MRI and resting-state fMRI (overview)	60
2.3 Image processing and analysis techniques	63
Chapter 3. Structural brain changes associated with SUDEP	76
3.1: Cerebellar, midbrain and limbic volume alterations in SUDEP.	76
3.1.1. Background	76
3.1.2 Methods	77
3.1.3 Results.....	82
3.1.4 Discussion	93
3.2: Brain morphometric alterations accompanying GTCS with hypoxemia: a prospective structural imaging study.....	102
3.2.1 Rationale and motivation	102
3.2.2 Background	103
3.2.3 Methods	104
3.2.4 Results.....	110
3.2.5 Discussion	120
3.2.6 Conclusions.....	129
Chapter 4. Functional brain network alterations related to SUDEP.....	130
4.1: Dysfunctional Brain Networking among Autonomic Regulatory Structures in Temporal Lobe Epilepsy Patients at High Risk of Sudden Unexpected Death in Epilepsy.....	131
4.1.1 Background	131
4.1.2 Methods	132

4.1.3 Results.....	139
4.1.4 Discussion	143
4.1.5 Conclusions.....	153
4.2: Altered modularity and local connectivity amongst cortical and sub-cortical regulatory structures in confirmed cases of SUDEP.....	155
4.2.1 Background.....	155
4.2.2 Methods	156
4.2.3 Results.....	171
4.2.4 Discussion	177
4.2.5 Conclusions.....	185
Chapter 5: Conclusions, limitations and future work.....	187
5.1: Key findings.....	187
5.1.1 Structural brain alterations.....	187
5.1.2 Resting-state functional connectivity and brain network alterations	189
5.2 Overarching limitations, considerations and future work.....	190
5.2.1 Overview.....	190
5.2.2 Limitations of findings and interpretation.....	190
5.2.3 Relationship with epilepsy severity	192
5.2.4 The need for longitudinal experiments to assess progressive brain changes	193
5.2.5 Relationship between structural and RS-FC alterations.....	193
5.2.6 Relevance of findings to identification of preventative interventions.....	194
5.2.7 Future for neuroimaging of SUDEP and towards biomarkers	195
5.3 Concluding remarks.....	199
Supplementary material	200
Supplementary Methods	200
Supplementary tables	201
Supplementary figures.....	214
References	218

Declaration

I Luke A. Allen confirm that the work presented in this thesis is my own. Where information has been derived from other sources, I confirm that this has been indicated in the thesis.

List of figures

Figure 1.1. Cohort-dependency of SUDEP incidence (adapted from Tomson et al., 2008).

Figure 1.2. Post ictal autonomic and breathing dysfunction following GTCS in 10 observed cases of SUDEP.

Figure 1.3. Schematic of a potential, multi-factorial pathway to SUDEP.

Figure 1.4. Summary of structural findings from imaging studies in SUDEP and populations at high-risk of SUDEP.

Figure 1.5. Summary of RS-FC findings in patients at risk of SUDEP.

Figure 2.1. Example T1 and T2 MR images for a representative subject.

Figure 2.2. Example images from morphometric and volumetric processing steps.

Figure 2.3. Simple schematic of ROI extraction and network (whole brain and subnetwork) construction.

Figure 2.4. Example network consisting of three modules, nodes and edges.

Figure 3.1.1. VBM-derived grey matter and ROI volume decreases in SUDEP compared with healthy controls.

Figure 3.1.2. VBM grey matter volume alterations in SUDEP and high-risk subjects, compared with low-risk subjects.

Figure 3.1.3. VBM grey matter volume alterations in SUDEP and high-risk subjects, compared with healthy controls.

Figure 3.1.4. VBM grey matter reductions in non-phenytoin group.

Figure 3.1.5. Results from ROI volume analysis displayed in bar graphs.

Figure 3.1.6. VBM grey matter and ROI volume increases in SUDEP.

Figure 3.1.7. Partial correlations between parahippocampal volume and disease duration.

Figure 3.1.8. Partial correlations between regional volumes and time between MRI and SUDEP.

Figure 3.2.1. Grey matter VBM contrasts with healthy controls for GTCS-hypox and GTCS-hypox-no.

Figure 3.2.2. White matter VBM contrasts for GTCS-hypox compared with with healthy controls.

Figure 3.2.3. ROI volume analysis results displayed in bar graphs.

Figure 3.2.4. Partial correlations between thalamic and hippocampal volume and degree of SpO₂ loss.

Figure 3.2.5. Partial correlations between accumbens and posterior vermis volume and duration of hypoxemia.

Figure 3.2.6. Partial correlations between thalamic volume and GTCS frequency.

Figure 4.2.1. Visualisation of the selected subnetwork and ROI coverage displayed in standard space.

Figure 4.2.2. Hub distribution index computed for one subject.

Figure 4.2.3. Area under the curve (AUC) of an example graph measure (degree centrality) in one subject.

Figure 4.2.4. Reduced modularity in SUDEP and high-risk.

Figure 4.2.5. Elevated participation in SUDEP and high-risk subjects.

Figure 4.2.6. Altered degree centrality across groups compared with healthy controls.

Figure 4.2.7. Subnetwork Hub distribution index across groups.

List of tables

Table 3.1.1. Group characteristics of SUDEP cases, high-risk, low-risk and healthy controls.

Table 3.1.2. Analysis contrasts and results per method

Table 3.2.1. Group demographics and clinical characteristics.

Table 3.2.2. Demographics and clinical characteristics of the GTCS hypoxemia subgroups.

Table 4.1.1. Summary of patients at low and high-risk of SUDEP.

Table 4.1.2. List of decreased connections belonging to the subnetwork of reduced connectivity found in high-risk < low-risk.

Table 4.1.3. List of enhanced connections belonging to the subnetwork of increased connectivity found in high-risk > low-risk.

Table 4.2.1. Clinical characteristics of the SUDEP cases.

Contributing authors & acknowledgements

Acknowledgements

Dr. Beate Diehl (UCL ION) and Professor Louis Lemieux (UCL ION) are the primary and secondary supervisors of this thesis respectively and, as such, were heavily involved in many aspects of the work which it encompasses. This included study design, conception and interpretation of results, manuscript writing and editing, and offering of guidance often extending beyond academic matters. I am incredibly lucky and truly thankful to have had the pleasure of working with two such experts and leaders of their respective fields, to whom I bestow immense thanks, and a wealth of respect and appreciation.

Someone who has hugely influenced the work of this thesis and been incredibly instrumental in extracting the neurobiological meaning of the many results which it contains is Professor Ronald M. Harper (UCLA). Ron's knowledge of central autonomic and respiratory control has been pivotal in shaping hypotheses and determining the outcomes of the following studies. Ron and his team, Dr. Jenifer A Ogren (UCLA) and Dr. Rajesh Kumar (UCLA), have contributed extensively to study design, methodological tuning and manuscript writing and editing in all studies. I am eternally grateful for their support and friendship throughout the duration of this PhD and am incredibly lucky to have been able to work so closely with them.

Catherine A. Scott (UCL ION) maintained project databases, assisted greatly with recruitment and uploading of multi-centre data. Catherine was heavily involved in

neurophysiological and respiratory aspects of experimental studies, and contributed editorially to all manuscripts.

Dr. Sjoerd B. Vos (UCL ION) played a crucial role in organising, extracting and assisting analysis of structural neuroimaging, as well as with manuscript writing and editing in all experimental work. His guidance and friendship over the past 4 years, and on into the future, is closely treasured.

Professor Maxime Guye (AMU) lent his extensive methodological expertise and knowledge of network analysis and graph theory for the resting state fMRI investigations ([4.1](#), [4.2](#)).

Dr. Gavin P. Winton (UCL ION) contributed healthy control data for all volumetric studies ([3.1](#), [3.2](#)) and gave expert guidance on aspects of image analysis design and manuscript editing.

A special thanks is owed to the all of the physiologists and nurses of the Sir Jules thorn Telemetry Unit and the National hospital for Neurology and Neurosurgery (NHNN), for their help in recruiting patients, applying additional recording parameters (electrodes, respiratory belts and pulse oximetry in study [3.2](#)) and much more.

Professor Samden D. Lhatoo, Dr. Nuria Lacuey and Dr. Laura Vilella (UTH), played key roles in synergising collaboration between UCL and UTH, particularly regarding the study in chapter [3.2](#). Dr. Lhatoo contributed editorially in all studies. This included the smooth running of data transfers and quality, and editorial contributions.

Other individuals who contributed to various aspects of manuscript writing and editing, whose input is invaluable and so highly appreciated, are: Professor John S. Duncan (UCL ION), Dr. Britta Wandschneider (UCL ION) and Dr. Simona Balestrini (UCL ION).

Author institution information

UCL ION: University College London Institute of Neurology

UCLA: University College Los Angeles

AMU: Aix Marseille University

UTH: University of Texas at Houston

Abbreviations

ACC: Anterior cingulate cortex

AED: Anti-epileptic drug(s)

AUC: Area under the curve

BNA: Brainnetome atlas

BOLD: Blood Oxygen Level Dependent

BP: Blood pressure

CAT12: Computational anatomy toolbox

CCHS: Congenital Central Hypoventilation Syndrome

CSF: Cerebrospinal fluid

CSR: Center for SUDEP Research

DARTEL: Diffeomorphic anatomical registration through exponential lie algebra

DC: Degree centrality

DPARSFA: Data processing assistant for resting state fMRI analysis

ECG: Electrocardiogram

EEG: Electroencephalography

EEG-fMRI: Electroencephalography functional magnetic resonance imaging

EMU: Epilepsy Monitoring Unit

ENIGMA: Enhancing Neuroimaging Genetics through Meta-Analysis

FC: Functional Connectivity

FCD: Focal cortical dysplasia

FD: Framewise displacement

fMRI: functional Magnetic Resonance Imaging

FOV: Field of view

FSPGR: fast spoiled gradient recalled echo

FWER: Family-wise error rate

FWHM: Full width at half maximum

GIF: Geodesic information flows

GLM: General Linear Model

GM: Grey matter

GSR: Global signal regression

GTCS: Generalized tonic-clonic seizure

HC: Health control

HDI: Hub distribution index

HF: Heart Failure

H-F: High-Frequency

HR: Heart rate

HRV: Heart Rate Variability

HS: Hippocampal sclerosis

Hz: Hertz (1/second)

IBM SPSS: International business machine statistical package for the social sciences

ICA: Ictal Central Apnoea

IED: Inter-ictal epileptic discharges

ILAE: International League Against Epilepsy

JME: Juvenile myoclonic epilepsy

LF: Low Frequency

MEG: Magnetoencephalography

MNI: Montreal neurological institute

MODWT: Maximal overlap discrete wavelet transform

MORTEMUS: Mortality in Epilepsy Monitoring Units Study

MRI: Magnetic Resonance Imaging

MST: Minimal spanning tree

NBS: Network based statistic

OFC: Orbitofrontal cortex

OR: Odds ratio

OSA: Obstructive Sleep Apnoea

PAG: Periaqueductal grey

PBN: Parabrachial Nucleus

PCCA: Post-convulsive Central Apnoea

PGES: Post-ictal generalized EEG Suppression

RMSSD: Root Mean Squared Successive Differences

ROI: Region of interest

RS-FC: Resting state functional connectivity

RS-fMRI: Resting-State functional Magnetic Resonance Imaging

RVLM: Rostral Ventrolateral Medulla

SaO₂: Arterial oxygen saturation

SCN1A: Sodium Voltage-Gated Channel Alpha Subunit 1

SE: Standard error

SpO₂: Peripheral capillary oxygen saturation

SPM: Statistical parametric mapping

SUDEP: Sudden Unexpected Death in Epilepsy

TE: Echo time

TIV: Total intracranial volume

TLE: Temporal Lobe Epilepsy

TPM: Tissue probability map

TR: Repetition time

VBM: Voxel based morphometry

VEEG: Video electroencephalography

VLM: Ventrolateral Medulla

VMPFC: Ventro-medial prefrontal cortex

VT: Video telemetry

WM: White matter

Abstract

Background

Sudden unexpected death in epilepsy (SUDEP) is the leading cause of premature death among people with epilepsy. The precise mechanisms underlying SUDEP remain elusive, though work so far demonstrates a potential centrally mediated event in which autonomic, respiratory and/or arousal processes fail to recover following a significant seizure. Neuroimaging enables non-invasive assessment of the structural and functional architecture among sites and networks involved in regulating such processes; damage or alterations may indicate a central predisposition in those at high-risk and who suffer SUDEP, and provide non-invasive biomarkers.

Methods

In this thesis, structural and functional imaging techniques were employed to address this possibility. Both retrospective investigations of those who succumbed to SUDEP, and prospective studies of those at high-risk, were performed. Voxel-based morphometry, volumetry and resting-state functional magnetic resonance imaging (RS-fMRI) network analysis techniques were utilised to identify and characterise brain structural and functional alterations relative to low-risk subjects and controls.

Results

Brain morphometric and volumetric alterations among sites involved in cardiorespiratory regulation and recovery were found in those who later suffered SUDEP and in matched, living individuals at high risk. Prospective work revealed similar, and additional, structural alterations in those at high-risk which were associated

with the extent of seizure-related hypoxemia; notably among the thalamus, periaqueductal grey (PAG), medulla, vermis and hippocampus.

Network analysis of functional imaging data revealed disturbed patterns of connectivity in high-risk temporal lobe epilepsy (TLE) patients, and altered functional organisation in confirmed cases of SUDEP, among regulatory brain sites as well as the whole brain.

Conclusions

Structural and resting state functional connectivity disturbances were found in patients who suffered SUDEP, and those at elevated risk. Injury and connectivity disturbances may indicate damage or dysfunction within sites and networks involved central regulatory processes, which could facilitate SUDEP. However, further work is required to elucidate the precise mechanisms of volume and functional connectivity alterations, and to provide firm links between centrally mediated autonomic and respiratory dysfunction, SUDEP and related imaging findings.

A more immediate use for the imaging outcomes revealed here may rest with the development of non-invasive biomarkers, which may one day assist in identifying those at risk and evaluating individual risk for SUDEP based on injury to brain sites or altered functional networks.

Impact statement

The work of the present thesis identified alterations in brain morphology and functional connectivity associated with SUDEP and elevated risk. The findings may provide insights into pathophysiological mechanisms and future preventive strategies of SUDEP. A more immediate application of these discoveries should be to guide future imaging studies and wider biotechnological projects to develop and refine imaging-based markers of elevated SUDEP risk. Such biomarkers have the potential to one day prevent the leading cause of premature mortality in those who experience ongoing seizures

Thesis objectives, outline & acknowledgements

Objectives

The overarching aims of the present body of work are to: a) use magnetic resonance imaging (MRI) techniques to characterise brain morphological and connectivity alterations among regulatory brain structures associated with SUDEP and its risk factors; and b) consider how such alterations may enrich our understanding of proposed central mechanisms of SUDEP, and represent non-invasive markers which could be used to prospectively identify those at risk and inform prevention strategies in the future.

Thesis outline and summary of chapters

This thesis consists of 5 main chapters which will be outlined and briefly described below for completeness, including details regarding resultant publications (acknowledgements of individual contributions can be found above in [contributing authors & acknowledgements](#)).

Chapter 1: Background

The purpose of chapter 1 is to provide an introduction to epilepsy and SUDEP, covering key concepts and key previous work which lead to the rationales of the present thesis. The sections in this chapter are as follows: 1. Epilepsy; 2. SUDEP; 3. autonomic and respiratory dysfunction in epilepsy and SUDEP; 4. central control of autonomic and respiratory regulation; and 5. Neuroimaging of SUDEP.

Section 5 of this chapter (Neuroimaging of SUDEP) is an adapted version of a review published in *Frontiers of Neurology* (Allen et al., 2019a), which was written collectively by Luke Allen, Ronald M Harper, Samden D Lhatoo, Louis Lemieux and Beate Diehl.

Chapter 2: Common methodology

This chapter provides an overview of the common methods employed in this thesis and exists to describe briefly and conceptually the techniques used, how they work and why they were suitable to address the questions set out. This includes descriptions of how SUDEP cases were acquired and structural and functional MRI methodology, including basic principles, pre-processing methods and analysis procedures. The two sections of this chapter are: 1. Ascertainment of SUDEP cases; and 2. Magnetic Resonance Imaging and Analysis procedures.

Chapter 3: Structural brain changes associated with SUDEP

In Chapter 3, structural imaging work, consisting of two separate studies, will be detailed as follows:

3.1 “Cerebellar, midbrain and limbic volume alterations in SUDEP.” A retrospective study of 25 SUDEP cases, and matched high-risk, low-risk and healthy controls.

This retrospective study into brain volume alterations in subjects who, after being scanned, subsequently suffered SUDEP was published in *Epilepsia* (Allen et al., 2019b).

3.2 *“Grey matter abnormalities accompanying GTCS with hypoxemia.” A prospective study.*

This prospective investigation into brain morphometric changes associated with hypoxemia in patients with GTCS was carried out in collaboration with colleagues at UTH, and utilised data from both of these sites. The manuscript is currently in preparation to be submitted.

Chapter 4: Functional brain network alterations related to SUDEP

Two retrospective studies were performed to investigate potential functional connectivity alterations in people at high risk and in confirmed cases of SUDEP:

4.1 *“Dysfunctional networking among autonomic and respiratory regulatory structures in temporal lobe epilepsy (TLE) patients at high-risk of SUDEP.”*

The first of these studies (4.1) examined TLE patients stratified into high- and low-risk of SUDEP based on known clinical criteria, and was subsequently published in *Frontiers in Neurology* (Allen et al., 2017).

4.2 *Altered modularity and local connectivity among regulatory brain sites in confirmed SUDEP and those at varied risk.*

The last of the resting-state fMRI studies in this collection of work set out to determine functional network alterations in confirmed cases of SUDEP and matched high-risk, low-risk and healthy controls. This manuscript is currently pending revisions in *Neuroimage Clinical*.

Chapter 5: Conclusions, limitations and future work

Following original research chapters 3 and 4, a summary of all findings, overarching limitations, future work and conclusions will be outlined in chapter 5. This chapter includes the following sections: 1. Key findings; 2. Overarching limitations, considerations and future work; 3. Concluding remarks.

Supplementary material

Finally, additional materials considered inappropriate for the main text of the thesis are compiled here. This includes additional large tables and figures from supplementary analyses.

Chapter 1: Background

In this chapter, overviews of epilepsy and SUDEP are first provided in sections 1 and 2 respectively. This is followed by descriptions of autonomic and respiratory disturbances seen in epilepsy and in observed cases of SUDEP (section 3). A brief overview of the brain sites subserving central autonomic and respiratory control is outlined in section 4. Lastly, the existing literature on neuroimaging of SUDEP is reviewed in section 5.

1.1: Epilepsy

1.1.1 Definition

Epilepsy is a neurological disorder in which a person experiences recurring seizures. Specifically, people with epilepsy have had either at least two unprovoked seizures or one unprovoked seizure with a probability (at least 60%; equivalent to the general recurrence risk following two unprovoked seizures over the next 10 years) of further seizures (Fisher et al., 2014). A seizure is defined as: “a transient occurrence of signs and/or symptoms due to abnormal excessive or synchronous neuronal activity in the brain” (Fisher et al., 2005). The origin and nature of this abnormal neural activity greatly influences the type and extent of observed symptoms (seizures). There are therefore many different types of seizures, with many people experiencing more than one type (Blume et al., 2001). Seizure aetiologies and characteristics are used to define epilepsy syndromes (Scheffer et al., 2017), of which there are many sub-types, including ‘focal’ and ‘generalised’. Focal epilepsies are characterised by seizures which may be

confined to epileptogenic networks within one lobe, or sometimes rapidly engage larger networks in multiple lobes, or one hemisphere of the brain. Seizures in generalised epilepsies involve bilaterally distributed brain networks involving both hemispheres from onset of the seizure (Berg et al., 2010). Seizures, as well as epilepsy syndromes, can be focal, generalised or may progress from a focal to a generalised seizure (i.e. a generalised tonic-clonic seizure; GTCS). The definition of seizure types and nomenclature has undergone rigorous development over the years. Recent changes, as outlined in the most recent ILAE (international league against epilepsy) position paper (Fisher et al., 2017), include revision of what used to be known as simple or complex partial seizures, which are now defined as focal seizures with or without loss of awareness.

1.1.2 Incidence

In developed countries, the incidence of epilepsy is approximately 50 per 100,000 people per year, with a prevalence between 4 – 10 per 1000 people (Sander, 2003). There are around 600,000 people living with epilepsy in the UK, of whom 70% can expect to become seizure free with optimal anti-epileptic drug (AED) treatment (Brodie 2000; Sander 2003, 2004). For the remaining 30% of people with epilepsy, seizures cannot be effectively controlled despite trials on multiple AED types (Sander, 1997).

1.1.3 Aetiology

Epilepsy has a wide range of potential causes including structural, genetic, infectious, metabolic, immune or unknown aetiologies (Scheffer et al., 2017). Structural causes of epilepsy are the most common and relate to abnormalities in the brain which can be detected visibly with neuroimaging (e.g. structural MRI – Magnetic Resonance

Imaging) and carry a substantial risk of being linked to the observed seizures. Structural abnormalities are typically brain lesions such as malformations of cortical development (e.g. focal cortical dysplasia), brain tumours (e.g. a cavernous haemangioma formed by an abnormal collection of blood vessels), damage caused by traumatic brain injury or mesial temporal sclerosis – the most commonly associated feature of temporal lobe epilepsy (Cook et al., 1992; Camacho & Castillo, 2007) – defined by gliosis and cell loss in hippocampal structures including the amygdala.

1.1.4 Diagnosis and outlook

Epilepsy is diagnosed upon the incidence of at least two unprovoked seizures occurring more than 24 hours apart from each other, or after one seizure with a high risk of recurrence (Fisher et al., 2014). Seizure characterisation relates to the anatomical substrate and pathophysiology of the seizure (Engel, 2006). The optimal diagnostic and characterisation procedure (though not always necessary) is video-electroencephalography (VEEG), during which a patient with presumed epilepsy visits a video-telemetry (VT), or epilepsy monitoring (EMU), unit in order to capture the clinical semiology of their seizures alongside inter-ictal (between seizure) electroencephalographic (EEG) changes in the brain. Where eye-witness and patient history is unclear, full localisation may require recording of clinical and EEG information during an episode. It is through this process that the origin and evolution of a patient's seizures may be localised. This investigation, if supported by neuroimaging findings, can help to indicate the epileptogenic zone for targeted neurosurgical intervention, such as the resection of a structural abnormality. Of the medically refractory patients who undergo surgical treatment, approximately half will remain seizure free after 10

years (de Tisi et al., 2011). Full surgical workup allows enhanced characterisation of seizure semiology and localisation, and thus greater chance of seizure freedom. A range of complications and/or comorbidities may accompany pharmaco-resistant epilepsy, including cognitive decline (Thompson and Duncan, 2005), increased risk of psychiatric disease - particularly depression (Kanner, 2003; Boylan et al., 2004), and, most critically, an increased risk of untimely death (Laxer et al., 2014; Shorvon & Tomson, 2011).

1.1.5 Neuroimaging and epilepsy

As well as being employed to visually identify structural pathologies at the individual level, neuroimaging techniques are also used experimentally to explore changes in brain structure or function, beyond what can be quantified visually, and allowing determination of commonalities in groups of patients. Both structural and functional magnetic resonance imaging (MRI) techniques have been widely applied to the study of epilepsy. Notable examples include the characterisation of presurgical thalamic functional networks associated with seizure recurrence (He et al., 2017), and brain structural disturbances found in temporal lobe epilepsy (TLE; Keller & Roberts, 2008; Keller et al., 2013). Changes in brain structure and function, for example grey matter volume and functional connectivity, are demonstrated even in the absence of lesional pathology (Beheshti et al., 2018 and Weaver et al., 2013, respectively). Such studies provide evidence for underlying alterations to brain structure and circuitry in epilepsy when contrasted with healthy populations.

1.2: SUDEP

1.2.1 Definitions and epidemiology

Sudden unexpected death in epilepsy (SUDEP) is the leading cause of premature death among people who experience ongoing seizures (Tomson et al., 2008), and is defined as a non-traumatic, non-accidental, non-drowning death of a person with epilepsy, with or without evidence of a terminal seizure, for which no structural or toxicological cause can be found (Nashef et al, 2012). SUDEP can be further defined as definite, probable, possible, near-SUDEP, not SUDEP or unclassified, as per a recent proposal to unify the definitions of SUDEP (Nashef et al., 2012):

“1. Definite SUDEP: A Sudden, unexpected, witnessed or unwitnessed, nontraumatic and non-drowning death, occurring in benign circumstances, in an individual with epilepsy, with or without evidence for a seizure and excluding documented status epilepticus (seizure duration ≥ 30 min or seizures without recovery in between), in which post-mortem examination does not reveal a cause of death.

2. Probable SUDEP: Same as Definite SUDEP but without autopsy. The victim should have died unexpectedly while in a reasonable state of health, during normal activities, and in benign circumstances, without a known structural cause of death.

3. Possible SUDEP: A competing cause of death is present.

4. Near-SUDEP: A patient with epilepsy survives resuscitation for more than 1 h after a cardiorespiratory arrest that has no structural cause identified after investigation.

5. Not SUDEP: A clear cause of death is known.

6. Unclassified: Incomplete information available; not possible to classify.”

The classification of SUDEP into different sub-types brings to the light the nature of its complexity, and raises the possibility of different types and physiological pathways to SUDEP. However, it comes at the disadvantage of dilution and potential that SUDEP, or SUDEP-related events, may be overlooked, or missed, if we discount other cohorts, including the sudden adult death population in general.

After stroke, SUDEP is the leading cause of years of life lost among neurological diseases, and is responsible for between 500 and 600 deaths per year in the UK (Hanna et al., 2002). The risk of sudden death for any one person with epilepsy has been estimated to be between 24 and 28 times higher than that of the general population (Flicker et al., 1998; Holst et al., 2013); a shocking reality requiring attention. However, the incidence of SUDEP varies greatly depending on patient cohort (Figure 1.1). Incidences range between 0.35 to 2.3 per 1000 patient-years among population-based cohorts, prevalence cohorts, and clinic-based cohorts, whereas incidences for chronic pharmaco-resistant cohorts range between 1 and 6 per 1000 patient-years (Tomson et al, 2008; Shorvon & Tomson, 2011; Figure 1.1). The highest incidence rates are among treatment resistant patients undergoing pre-surgical investigations, or surgical failures, which are reported as high as 6 to 9 per 1000 patient-years (Télliez-Zenteno et al., 2005; Tomson et al., 2008; Ryvlin et al., 2013; Figure 1.1).

1.2.2 Proposed mechanisms

Although the underlying mechanisms of SUDEP remain elusive, seizure-related autonomic (cardiac arrhythmia or hypotension) or respiratory (hypoventilation, apnoea or hypoxia) dysfunction, or a fatal combination of these, are most likely responsible (Nashef et al., 2007; Surges et al., 2009; Massey et al., 2014). Other precipitating processes may also contribute, including sleep (Lamberts, 2012), metabolic, hormonal and genetic actions (Dlouhy, et al., 2016). And whether the fatal respiratory or cardiac observations in SUDEP cases are secondary to profound inhibition of central respiratory or autonomic regulatory sites (Shorvon & Tomson, 2011) is unclear. An abundance of animal and human studies have revealed neurocardiac genes directly linked to cardiac dysfunction and SUDEP (Glasscock, 2014). In mouse models, failure of periaqueductal grey-mediated cardiorespiratory recovery precedes seizure induced death (Kommajosyula et al., 2018), and spreading depolarisation in the brainstem has shown to mediate cardiorespiratory arrest leading to sudden death (Aiba & Noebels, 2015). Overall, many proposed explanations for SUDEP now exist, but clear pathophysiological mechanisms linking epilepsy with sudden and unexpected death in humans with epilepsy remain lacking.

1.2.3 SUDEP risk factors

Recent years have seen the identification and refinement of clinical risk factors associated with SUDEP. By far, the most significant of these is presence and frequency of generalised tonic clonic seizures (GTCS; Harden et al., 2017). Specifically, experiencing more than 3 GTCS per year is ranked as the leading risk factor for SUDEP (DeGiorgio et al., 2017) and is associated with a 15-fold increase in risk

(Hesdorffer et al., 2011; Harden et al., 2017). This relative increase in SUDEP risk equates roughly to an absolute risk of up to ~18 per 1000 patient-years among people with frequent ongoing GTCS (Hesdorffer et al., 2011; 2012). With SUDEP being a primarily nocturnal event (Lamberts et al., 2012), experiencing nocturnal seizures is also associated with increased SUDEP risk.

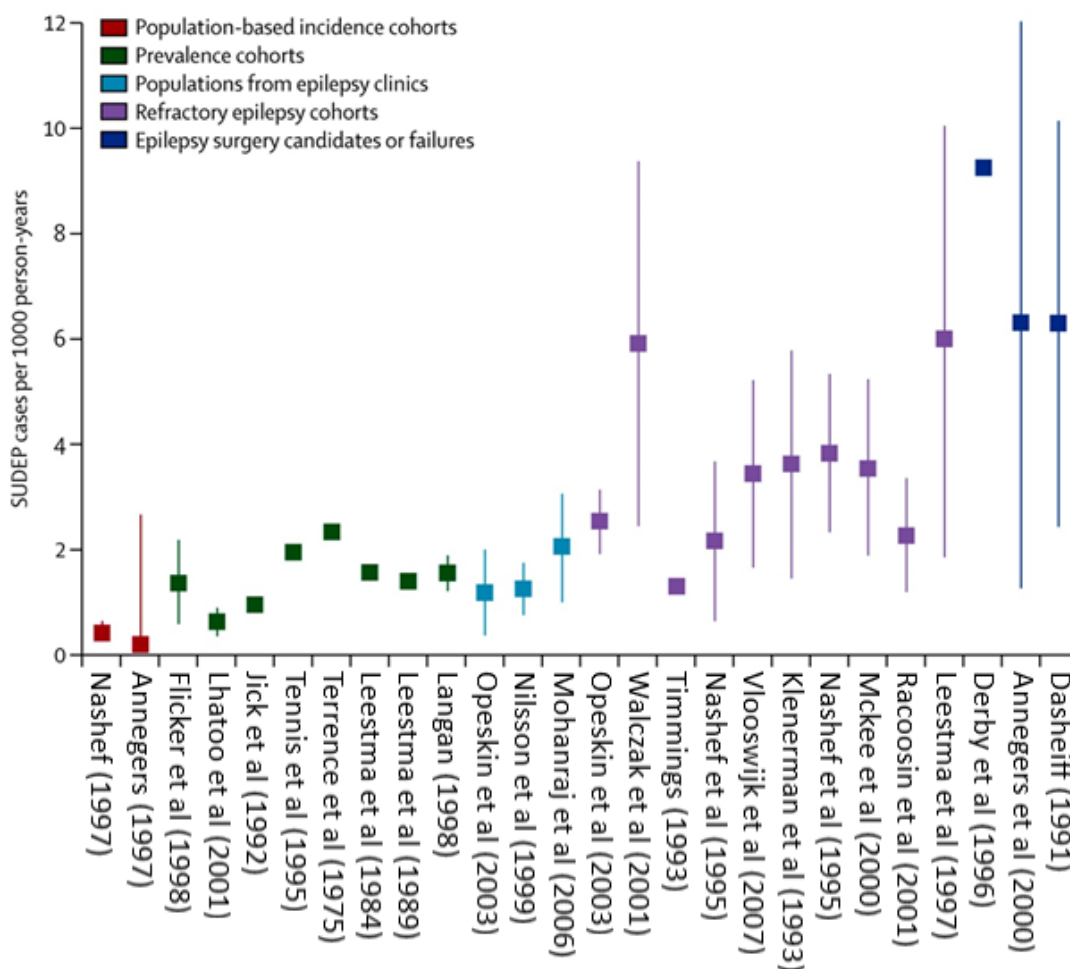


Figure 1.1. Cohort-dependency of SUDEP incidence (adapted from Tomson et al., 2008). Incidence of SUDEP (cases per 1000 person-years) across 24 studies is shown, with higher incidences reported for refractory epilepsy cohorts and surgery candidates or failures, compared with general epilepsy populations (population-based cohorts, prevalence cohorts and populations from epilepsy clinics).

A recent combined risk factor analysis (Hesdorffer et al., 2011) of a wide range of clinical epilepsy characteristics has highlighted the most significant factors associated with SUDEP: 1. age of epilepsy onset less than 16 years; 2. duration of disease greater than 15 years; and 3. more than 3 GTCS experienced per year. The major factors highlighted here can be used to risk-stratify epilepsy cohorts for prospective and retrospective investigations, as has been common among neuroimaging studies of SUDEP (Tang et al., 2014; Wandschneider et al., 2015).

Treatment-related risk factors include lack of AED treatment, which is associated with a substantial increase in SUDEP risk (Langan et al., 2005). Tapering of anti-epileptic medication during EMU admission is also associated with SUDEP risk (Ryvlin et al., 2013). Some studies indicate that monotherapy (use of only one AED) is associated with a lower risk of SUDEP compared with polytherapy (use of more than one AED; Hitiris et al., 2007). In a combined-risk factor analysis of SUDEP (Hesdorffer et al., 2011), polytherapy was associated with increased risk, but not after controlling for frequency of GTCS (Hesdorffer et al., 2012). Overall, these studies show that the use of polytherapy is a marker of epilepsy severity which, in itself, is a risk factor for SUDEP (Shankar et al., 2017).

1.3: Autonomic and respiratory dysfunction in epilepsy and SUDEP

Epileptic seizures are frequently accompanied by changes in autonomic and respiratory function. Given the cardio-respiratory features which appear to be involved in SUDEP, the aim of this section is to briefly summarise the current state of literature involving autonomic and respiratory disturbances observed in epilepsy, during and after seizures and in observed cases of SUDEP.

1.3.1 Cardiac alterations

Abnormal heart rhythms, or cardiac arrhythmias, are known to accompany seizures (van der Lende et al., 2016). Sinus tachycardia (abnormally fast heart rate) is reported during the ictal and post-ictal phase in approximately 90% of seizures (Blumhardt et al., 1986; Di Gennaro et al., 2004), and equally so around the time of seizure onset (Zijlmans et al., 2002). While sinus tachycardia is a type of arrhythmia, it should be noted that such elevations around the time of seizures are more appropriately represented by a physiological response to seizures. Less common are reports of bradycardia (abnormal slowing of the heart rate) and asystole (cessation of the heart-beat), presenting in ~2% (Rugg-Gunn et al., 2004) and less than 1% (Rocamora et al., 2003) respectively. Cardiac rhythm and repolarisation abnormalities are observed most often in patients who are medically refractory, particularly so in males who experience frequent generalised tonic clonic seizures (GTCS) and seizures of longer duration (Rugg-Gunn et al., 2004; Tomson et al., 2008), of whom are at greatest risk of SUDEP.

Peri-ictal heart rate changes have been shown not to significantly differ between seizures with and without loss of awareness (Rugg-Gunn et al., 2004). However, it has been demonstrated that secondarily GTCS are associated with higher ictal heart rates, prolonged post-ictal tachycardia and abnormal shortening of QTc (corrected QT interval) in the early post-ictal phase (Surges et al., 2010). Other severe cardiac and conduction irregularities have also been significantly associated with GTCS, including asystole, atrial fibrillation, sinus arrhythmia, supraventricular tachycardia, atrial premature depolarization, ventricular premature repolarization and bundle branch block (Nei et al., 2000). One study (Opherk et al., 2002) demonstrates that such abnormalities occur in approximately 13% of generalised seizures; although rare in the general epilepsy population, cardiac changes of this kind could be a major contributing factor in the occurrence of SUDEP among people who experience GTCS.

A study exploring the incidence and mechanisms of cardiorespiratory arrests in epilepsy monitoring units (MORTEMUS) found that in 10 monitored cases of SUDEP (Ryvlin et al., 2013), severe cardiac dysfunction occurred in the early post-ictal phase following a GTCS. This was characterised by bradycardia lasting between 20 and 90 seconds in duration and resulted in asystole in 90% of cases (Figure 2). Post-ictal cardiac arrhythmias are common following convulsive seizures and are often associated with SUDEP and near-SUDEP events (van der Lende et al., 2016).

The relationship between localisation and lateralisation of epileptogenic focus and ictal ECG (electrocardiogram) changes is not clear and data area largely inconsistent. One study (Di Gennaro et al., 2004) indicates no effect of epilepsy lateralisation on ECG changes during seizures. However, others show hemispheric and lobular preferences

across the occurrence ECG abnormalities (Leutmezer et al, 2003). This study demonstrated that ictal HR increases are more profound in mesial TLE when compared with extra-temporal or non-lesional epilepsies. Furthermore, ictal onset tachycardia presented more often in seizures involving the right hemisphere, and seizures arising from the temporal lobe occurred, on average, 4 seconds earlier than those seen in extra-temporal lobe seizures. While autonomic disturbances have been reported to present more often in focal seizures involving the temporal lobes than others (Leutmezer et al., 2003; Di Gennaro et al., 2004; Britton et al., 2006), evidence regarding epilepsy localisation and peri-ictal autonomic alterations is conflicting and the picture remains unclear. Lateralisation of autonomic brain function has been demonstrated, but how epilepsy lateralisation impacts the various networks involved is not known.

1.3.2 Heart rate variability (HRV)

Heart rate variability (HRV) is the variation in time between consecutive R-R (heart beat) intervals and can be used to assess autonomic cardiovascular function. A recent meta-analysis (Lotufo et al., 2012) of (inter-ictal) HRV in patients with epilepsy revealed that patients exhibited reduced high-frequency (H-F) HRV – a measure of vagal tone. Time-domain measures of HRV also reveal reductions in patients with epilepsy, including both focal and generalised epilepsy types (Yildiz et al, 2011; Evrengül et al, 2005). HRV studies of only temporal lobe epilepsy (TLE) also demonstrate reductions in HRV in patients (Frysinger et al., 1993; Isojärvi et al., 1998; Massetani et al., 1997; Messenheimer et al., 1990; Tomson et al., 1998). Analyses of long-term inter-ictal

recordings show alterations in the fractal organisation of HR dynamics in patients with TLE (Ansakorpi et al., 2002).

Altered HRV has shown to be more profound in intractable epilepsy patients and among those who experience GTCS (Evrengül et al., 2005; Mukherjee et al., 2009), both of which are associated with increased SUDEP risk. These studies show reductions in H-F (a marker of parasympathetic activity) values and increases in low frequency (LF; a marker of sympathetic activity) values in patients compared with epilepsy and healthy controls. Increases in resting sympathetic tone and lowered parasympathetic tone in these cohorts indicates an imbalance in the systems serving autonomic regulation. Increased SUDEP risk has been associated with reduced measures of RMSSD (root-mean square differences of successive R-R intervals; Stein, 1994) - a further measure of HRV which reflects vagus nerve-mediated autonomic control of the heart - in severely refractory patients (DeGiorgio et al, 2010). Diminished vagal influences, reflected through lowered parasympathetic tone, could result in a reduced ability to recover following enhanced sympathetic strain occurring as a result of seizures. Furthermore, such HRV alterations are shown to be particularly prominent at night (Ronkainen et al., 2005), which is of note given the tendency of SUDEP to occur nocturnally (Lamberts, 2012). A more recent investigation has shown reduced wakeful HRV and extreme ratios of sleep-to-wake HRV in patients who suffered SUDEP, of whom those with SCN1A gene mutations showed more extensive alterations (Myers et al., 2018). Such studies indicate genetic predispositions and HRV measures may provide useful biomarkers for SUDEP. Overall, the HRV changes revealed in epilepsy suggest imbalances in autonomic function, particularly among

refractory epilepsy patients and those who experience GTCS. Such imbalances could alter autonomic recovery processes following extreme events such as seizures.

1.3.4 Changes in blood pressure

Enhanced sympathetic responses occur in the majority of seizures, which involve the commonly reported increases in heart rate and would include elevations in blood pressure (Devinsky, 2004). However, reduced sympathetic activity, or increased parasympathetic drives, are also known to accompany many seizures. As discussed earlier, suppression of cardiac rate (i.e. bradycardia) is known to occur, along with reductions in blood pressure (Van Buren, 1958). Prolonged hypotension has been observed following GTCS (Bozorgi et al., 2013), and correlated with post-ictal generalised EEG suppression (PGES). PGES is a transient diffuse attenuation of the EEG signal, implying central suppression of cortical brain activity after a seizure, and has been discussed as a potential SUDEP biomarker, though its precise role remains ambiguous (Kang et al., 2017). A study examining inter-ictal autonomic nervous system function in epilepsy patients revealed significant elevations in blood pressure and heart rate during orthostasis and cold pressor tests (Devinsky et al., 1994). However, medication levels also correlated with baseline and task-related BP and HR in this study. Enhanced sympathetic and parasympathetic responses are observed around the time of seizures, and alterations are seen in epilepsy during autonomic function tasks. However, work is required to understand altered autonomic responses separate from medication in patients. Autonomic task-related fMRI investigations (Valsalva manoeuvre, hand-grip task and cold pressure test) are of interest and could help to shed light on brain areas related to disturbed autonomic responses.

1.3.5 Respiratory disturbances

Investigations into peri-ictal respiratory changes are less abundant compared to those relating to heart rate changes. However, a range of respiratory disturbances have been documented in conjunction with epileptic seizures. Ictal central apnoea (ICA; cessation of breathing for > 10 seconds) occurs in ~37% of seizures (Lacuey et al., 2018a) and has been observed across multiple seizure types including focal and GTCS (Lacuey et al., 2018; Vilella et al., 2019a; Nashef et al., 1996), and in near-SUDEP incidents (So et al., 2000). Post convulsive central apnoea (PCCA; cessations of breathing occurring post-ictally) is seen in both focal and generalised epilepsies but occurs less frequently than ICA; in ~22% of seizures (Vilella et al., 2019b). MORTEMUS revealed the occurrence of severe respiratory dysfunction (including PCCA) following fatal secondarily GTCS in n=10 monitored cases of SUDEP. This study demonstrated rapid breathing (between 18 – 50 breaths per minute) in the immediate post-ictal phase, followed by a period of normal breathing, leading to transient, and eventually terminal, apnoea which preceded asystole in all cases (Ryvlin et al., 2013; Figure 1.2). PGES also featured in all observed SUDEP cases (Ryvlin et al., 2013), and is known to be associated with post-ictal respiratory depression and immobility, or impaired arousal processes, (Kuo et al., 2016).

Apnoea, if sustained, can lead to severe ictal or post-ictal hypoxemia (Lacuey et al., 2018) – abnormally low concentrations of oxygen in the blood. Hypoxemia has been shown to occur in approximately one third of both focal and generalised seizures, among patients undergoing VT investigations, the degree of which is significantly associated with seizure duration (Bateman et al., 2008). However, apnoea is not the

only pathway to hypoxemia, which may also result from, hypoventilation (Bateman et al., 2008) or pulmonary shunting or edema (Seyal et al., 2010). Either way, hypoxemia around the time of ictal events, particularly GTCS, could establish a scenario for hypoxic or excitotoxic injury to the brain, including sites involved in mediation of autonomic and breathing processes. Acute intermittent episodes of hypoxia are associated with cerebellar deep nuclei injury (Pae et al., 2005), as well as altered functional responses in thalamic, mid-brain, cerebellar and limbic sites (Macey et al., 2005).

GTCS are accompanied by reduced ictal and post-ictal cerebral oxygen saturation (Moseley et al., 2012); the extent of reduced saturation was also greater for those at higher risk of SUDEP. However, hypoxemia is not limited to generalised seizures. A recent case study showed ictal hypoxemia in a patient with focal sub-clinical seizures involving the temporal lobe which persisted after termination of the EEG seizure (Maglajlija et al., 2012). Hypoxemia, as well as establishing the potential for more longer-term damage to critical brain areas, may concurrently impair autonomic, respiratory and arousal processes if involved brain sites are not adequately supplied with oxygen-rich blood they require to function. Such a scenario could form the basis of events leading to SUDEP, though this remains unknown.

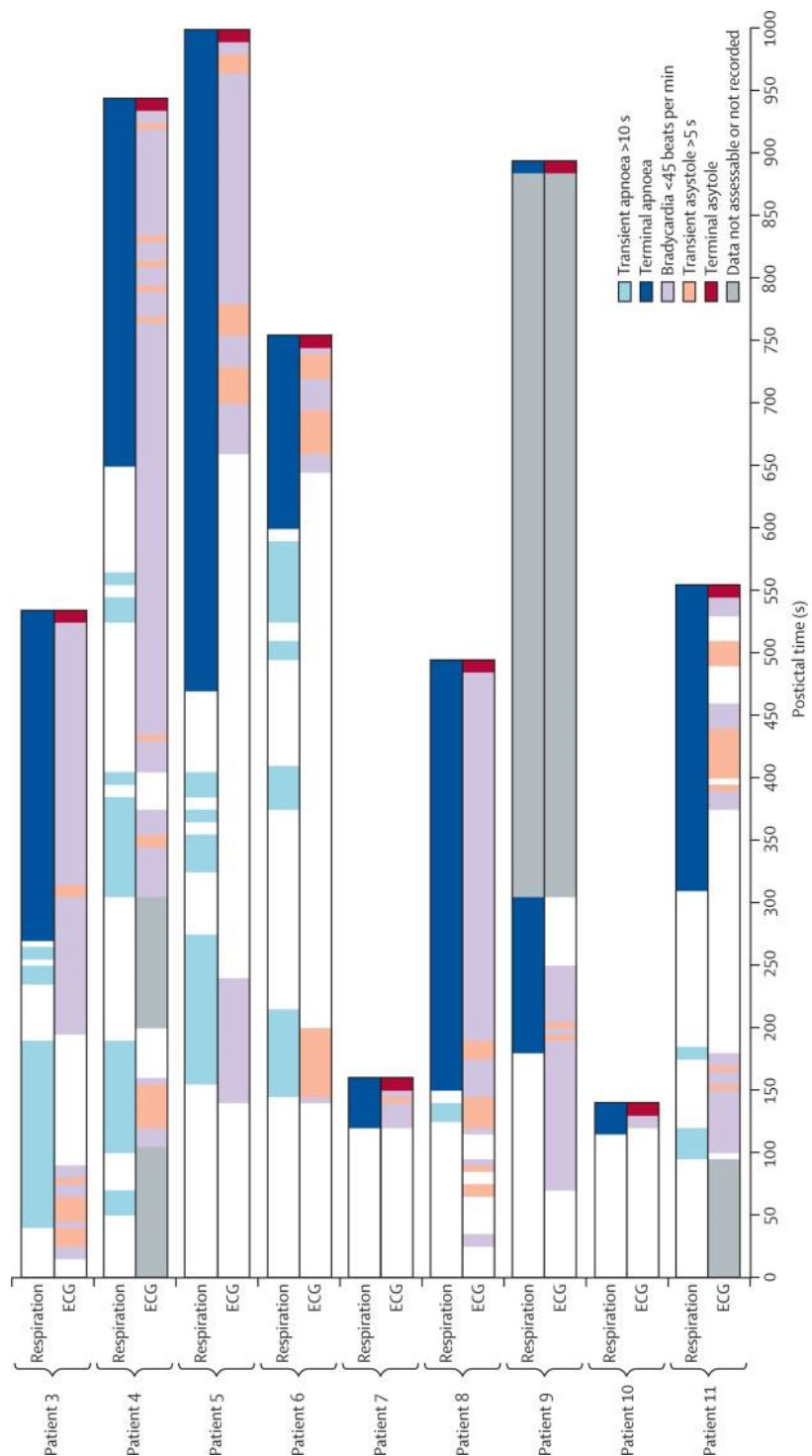


Figure 1.2. Post ictal autonomic and breathing dysfunction following GTCS in 10 observed cases of SUDEP. Adapted from MORTEMUS (Ryvlin et al., 2013). Normal breathing is followed by transient periods of apnoea and bradycardia and resulting in terminal apnoea and asystole.

1.3.6 Summary of autonomic and respiratory dysfunction in epilepsy and SUDEP

Studies from EMUs demonstrate key autonomic and breathing alterations around the time of seizures. Such changes are sometimes observed in conjunction with post-ictal suppression of brain activity, or PGES, though their precise relationship remains unknown. Importantly, crucial evidence from observed cases of SUDEP, e.g. as outlined by MORTEMUS (Ryvlin et al., 2013), indicates a centrally mediated pattern of cardiorespiratory dysfunction following GTCS prior to SUDEP. A natural approach, then, might be to investigate SUDEP in terms of being related to disruption among central neural (brain) structures and processes which mediate cardiorespiratory function, such is the premise of this thesis. In order to consider this, though, the pathways of central autonomic and respiratory control and their organisation throughout the brain must first be considered, as will be discussed in the next section.

1.4: Central control of autonomic and respiratory regulation (a brief overview)

Central regulation of both autonomic and respiratory control is represented throughout an array of structures across several levels of the neuroaxis. Control of regulatory functions extends much beyond the typically designated sites in the medulla and pons of the brainstem which, indeed, mediate final respiratory, sympathetic and parasympathetic outflow. Many cortical and sub-cortical sites, including the cerebellum, contribute to activation, inhibition, and timing of both respiratory and autonomic control.

In the lower brainstem, the ventrolateral medulla (VLM) contains the key premotor neurons responsible for controlling vasomotor tone and cardio-respiratory function (Benarroch, 1993; 2014), and its rostral portion (RVLM) is a key blood-pressure regulatory site (Guyenet, 2006; Wenker et al., 2017). Upper portions of the brainstem, such as the periaqueductal grey (PAG) and parabrachial nucleus (PBN), are involved in relaying and integrating interoceptive information between the brainstem and forebrain (Benarroch, 1993; Saper, 2002).

While not classically associated with autonomic roles, cerebellar influences on blood pressure and cardiovascular functions have long been known (Dow & Maruzzi, 1958). The cerebellum contains autonomic nuclei such as the fastigial nucleus, a small grey matter structure located deep amongst the cerebellar white matter, which projects to the cardiac and blood pressure nuclei in the brainstem (Miura & Reis, 1969; Andrezik et al., 1984) and shares connections with the hypothalamus (Zanchetti et al., 1954)

which integrates autonomic and endocrine responses for homeostatic and adaptive functions (Benarroch, 2014).

Other sub-cortical structures include the thalamus and portions of the basal ganglia. The thalamus is highly interconnected with the cortex and sub-cortex (Behrens et al., 2003) and its posterior portion – the pulvinar – plays a role in oxygen and respiratory regulation (Koos et al., 1998; Koos et al., 2000; Koos et al., 2016). Of the basal ganglia, the caudate and putamen are among the most salient with respect to autonomic and respiratory functions (Pazo & Belforte, 2002; Macey et al., 2016). The caudate plays an especially important role in sleep cycles (Kumar et al., 2009) and the putamen is involved in the integration of sensory information in preparation of movement (Alexander & Crutcher, 1990).

At the cortical level, the insular cortices are known to influence autonomic function, as demonstrated by Oppenheimer (1992, 1996) in early stimulation studies involving human epilepsy patients with implanted intracerebral electrodes. Functional neuroimaging studies support these findings (Henderson et al., 2002; Henderson et al., 2007; Macey et al., 2012) and confirm the earlier noted functional lateralisation of the insulae (Oppenheimer, 1992, 1996), with the right exerting more control parasympathetic functions and the left over sympathetic (Macey et al., 2012). Descending insula visceromotor influences are mediated via the lateral hypothalamus (Loewy, 1982). Furthermore, the insula is a major interoceptive area of the brain, integrating pain, temperature and visceral information (Saper, 2002), via connections with thalamic (Mufson & Mesulam, 1984) and limbic cortices (Saper, 2002; Craig, 2003; Cauda et al., 2011).

Other cortical regions include ventral medial prefrontal and orbitofrontal cortex, which project to the brainstem and hypothalamus (Verberne & Owens, 1998; Öngür and Price, 2000) and repeatedly respond to autonomic and respiratory challenges in functional neuroimaging studies (Shoemaker et al., 2015; Macey et al., 2016). Of the limbic system, the hippocampus, amygdala, cingulate and subcallosal cortex are also involved in autonomic functions (Harper et al., 2015). These regions are highly interconnected and many project directly to nuclei regulating respiratory and autonomic action in the brainstem (Hopkins & Holstege, 1978; Holstege et al., 1985; Verberne & Owens 1998; Owens & Verberne, 2000).

Of concern is that seizures may arise in, or propagate to, central autonomic control sites and disturb the normal function of critical autonomic and other regulatory structures (Rugg-Gunn, 2010). This may be particularly prominent in temporal lobe epilepsy and seizures involving propagation to limbic or brainstem structures (Lacuey et al., 2018b; Maglajlija et al., 2012; Wilson et al., 1990). While the majority of seizures are accompanied by symptoms of autonomic nervous system activation and, in some cases, dysfunction (Devinsky, 2004), investigations into autonomic brain regions in epilepsy are of interest. As discussed previously, the most severe autonomic and respiratory alterations are observed during and after GTCS, and prior to SUDEP (Ryvlin et al., 2013). Such changes (including apnoea, hypotension and hypoxemia) are shown to occur in conjunction with PGES, which may indicate post-ictal cerebral inhibition (Bozorgi et al., 2013). Equally, the autonomic and respiratory alterations observed during and after GTCS could in turn damage or inhibit central regulatory processes. If central neuronal sites and brain circuitry involved in recovery from cardiorespiratory dysfunction, or arousal, are damaged or inhibited, a failure to recover

from a significant cardiorespiratory event post-seizure could be a likely pathway to SUDEP (Figure 1.3). The goal of the current work is thus to investigate potential changes in brain structure and functional connectivity related to SUDEP, elevated risk and known risk factors, such as those observed in EMUs (e.g. hypoxemia).

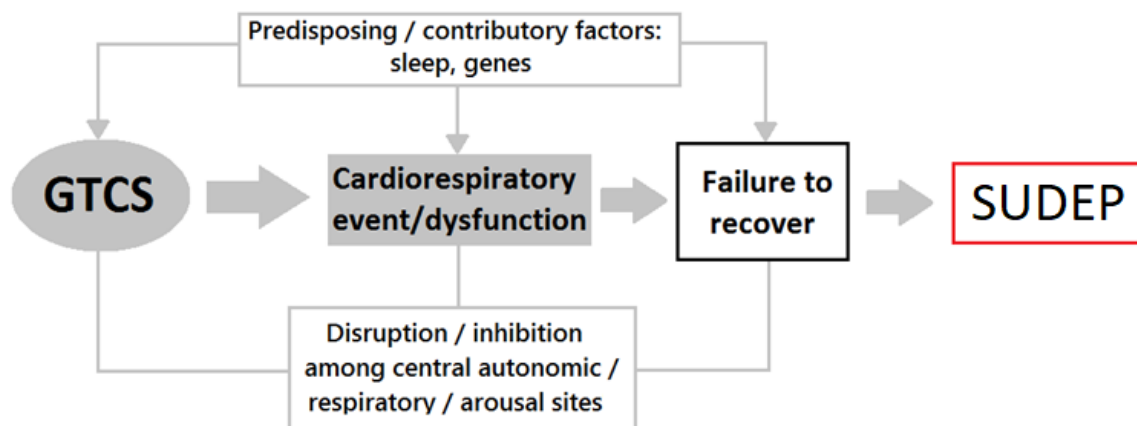


Figure 1.3. Schematic of a potential, multi-factorial pathway to SUDEP. In this model, SUDEP is characterised by a failure to recover from significant cardiorespiratory dysfunction post-GTCS, likely compounded by predisposing genetic and circadian factors and involving disruption or inhibition among central regulatory brain sites.

1.5: Neuroimaging of SUDEP¹

A literature review of existing neuroimaging studies of SUDEP, drawing insights from structural and resting-state functional MRI studies. This review was published in *Frontiers in Neurology* (See footnote for full reference).

1.5.1 Overview

In light of evidence implying the presence of centrally mediated mechanisms in the pathophysiology of SUDEP, an increase in efforts to characterise structural and functional brain changes among salient regulatory brain structures has emerged. Neuroimaging presents a unique and powerful opportunity to non-invasively explore changes in brain morphology and connectivity within and between structures mediating control of autonomic and respiratory processes. These techniques have enabled examination of structural (tissue) abnormalities or disrupted functional brain networks in people who (after being scanned) succumb to SUDEP, and those at varying degrees of risk (including healthy populations). Such assessments have the potential to shed light on underlying mechanisms, provide biomarkers to prospectively identify living patients at heightened risk, and guide preventive strategies. In the following sections, evidence from existing structural and functional MRI investigations into SUDEP will be discussed, together with pathways for future experiments.

¹ Allen, L. A., Harper, R. M., Lhatoo, S., Lemieux, L., & Diehl, B. (2019). Neuroimaging of Sudden Unexpected Death in Epilepsy (SUDEP): Insights From Structural and Resting-State Functional MRI Studies. *Frontiers in neurology*, 10.

1.5.2 Evidence from structural MRI

Structural MRI enables the identification and characterisation of brain tissue abnormalities, regional alterations in brain volume, cortical thickness and morphometry, and abnormal structural connections (fibre tracts). Such techniques have been widely applied to epilepsy (Salmenpera and Duncan, 2005; Koepp and Woermann, 2005; Winston et al, 2014), and have the potential to improve understanding of underlying brain physiology and highlight quantifiable disease biomarkers (Orru et al, 2012; Moffat et al, 2005). Although the precise pathological mechanisms of SUDEP are not known, some imaging studies have highlighted structural changes to cortical, sub-cortical and brainstem structures in those who subsequently succumbed to SUDEP and those at greatest risk, indicating morphological disturbances among sites involved in central autonomic and respiratory regulation. The remainder of this section will provide an overview of the main relevant imaging findings, and interpret them in relation to other, independent work.

1.5.2.1 Tissue loss in thalamic, brainstem and frontal sites

Voxel-based morphometry (VBM) has been used to investigate regional grey matter changes in subjects who later died from SUDEP (n=12) and comparable high-risk, low-risk and healthy controls (Wandschneider et al., 2015). Grey matter volume of the bilateral posterior thalamus (pulvinar nuclei) was found to be reduced in SUDEP cases and those at high-risk, compared with healthy and low-risk controls. Grey matter volume of the bilateral pulvinar also correlated negatively with disease duration in all subjects, suggesting an effect specific to epilepsy in general. Thalamic volume loss in patients who experience GTCS, and therefore who are at greatest risk of SUDEP, has

been widely demonstrated (Wang et al, 2012; Huang et al, 2011; Ciumas and Savic, 2006), including loss specifically within the pulvinar (Wang et al., 2012).

Posterior thalamic grey matter volume loss could be interpreted in the context of its known roles in respiratory regulation. A wealth of evidence, from lesion and stimulation studies in sheep (Koos et al., 1998, 2004), to fMRI studies of individuals with congenital central hypoventilation syndrome (Macey et al., 2005; Harper et al., 2005), demonstrate the role of the posterior thalamus in mediating breathing responses to manipulation of oxygen levels, and more particularly in the inhibition of breathing following hypoxemic exposure (Koos et al., 1998, 2004). Posterior thalamic injury may be common to people with epilepsy, and evidence suggests that disease duration may potentiate that injury. In other conditions involving impaired autonomic and respiratory function, such as obstructive sleep apnoea (Joo et al, 2010) and heart failure (Woo et al, 2003), posterior thalamic volume loss also appears. Such injury might pose a risk (in light of hypoxemia and other respiratory disturbances known to accompany ictal episodes) for thalamic structures to fail to adequately recover from low oxygen.

A recent investigation (Ogren et al, 2018) into neocortical morphometry in patients with GTCS (n=53) revealed widespread thinning, most prominently within the frontal lobe, including orbitofrontal sites, which are involved in cardiovascular regulation (Kimmerly et al., 2005), and in temporal and parietal cortices when compared with healthy controls (n=530). The results of volumetric studies are consistent with these findings, revealing tissue loss within the frontal cortex (Huang et al, 2011), including medial and lateral orbitofrontal regions (Wang et al., 2012) in patients with GTCS. Those cortical changes should be viewed in the context of volume changes in thalamic

sites, since sensory information classically synapses in the thalamus before projecting to cortical sites, with reticular thalamic sites providing an aspect of focus to afferent input. Many of these projections are reciprocal, providing a basis to induce structural alterations in subcortical areas following changes in cortical thickness.

In addition to changes among cortical and sub-cortical structures, more-caudal brain alterations have also been identified in cases of SUDEP. VBM revealed reduced volume of the periaqueductal grey (PAG; Mueller et al., 2014). Volume loss also appears in the medulla oblongata, which becomes progressively more extensive the closer to SUDEP from MRI (Mueller et al, 2018). Portions of the medulla form the final common pathway for cardiovascular and respiratory control. The PAG plays a significant role in cardiorespiratory patterning and recovery; deficient post-ictal PAG-driven compensatory mechanisms have been linked to SUDEP in a mouse model (Kommajosyula et al., 2018). That role stems from projections from forebrain areas, including the amygdala, and its own projections to parabrachial and ventrolateral regions for breathing control (Cameron et al, 1995); concerns of PAG contributions to breathing partially stem from susceptibility of its neurons to opiates (Pattinson, 2008), with their well-known depression of breathing. PAG neurons show time-locked relationships to both the respiratory (Ni et al, 1990a), and cardiac (Ni et al, 1990b) cycles, as revealed by animal studies, and these relationships are sleep-state dependent.

Overall, there is accumulating evidence of widespread structural loss, particularly within anatomic regions related to cardiorespiratory functions such as posterior

thalamic, frontal lobe (including medial and orbital divisions) as well as brainstem sites in people who suffered SUDEP and in those at greatest risk.

1.5.2.2 Tissue gain in limbic, insula and sensory sites

In addition to regional reductions, regional increased volume and cortical thickness in key autonomic, breathing and sensory sites have been observed in SUDEP cases and those at high risk. Compared with low-risk and healthy subjects, cases of SUDEP and those at high risk show increased grey matter volume of the amygdala and anterior hippocampus (Wandschneider et al, 2015). The breathing modulatory roles of the hippocampus and amygdala are well known, with stimulation of these areas eliciting central apnoea (Lacuey et al., 2017). Seizure spread to, as well as stimulation of, the amygdala results in central apnoea (Dlouhy et al, 2015). Bilateral increased mesial temporal structure volumes, including the amygdala, appear in a sub-type of mesial temporal lobe epilepsy (m-TLE) who also had poor post-surgical outcome (Bernhardt et al, 2015); patients in whom surgery has failed to reduce seizure frequency encompass the group at greatest risk of SUDEP, when compared with population-based incidence cohorts, prevalence cohorts, populations from epilepsy clinics, and even refractory epilepsy cohorts (Tomson, Nashef & Ryvlin, 2008). Increased volume may reflect gliosis or inflammation, potentially resulting from ongoing hypoxic damage (Aviles-Reyes et al, 2010) occurring following seizures (Farrell et al, 2017), although this must be confirmed in human epilepsy studies. Uncontrolled GTCS, often seen in subjects who die and those at high-risk, could accelerate such processes, although further work is required to confirm this process.

Patients who experience GTCS also show cortical thickening across a number of sites (Ogren et al, 2018): the post-central gyri, anterior insulae and the subgenual, anterior, posterior and isthmus cingulate exhibited cortical thickening in GTCS patients compared with healthy controls. While patients who experience GTCS are at highest risk of SUDEP, assessments of cortical thickness are additionally needed in patients who died from SUDEP, since studies including only at-risk populations are complicated by limited interpretability. Elevations in volume and cortical thickness are traditionally considered as being linked to improved function or compensatory mechanisms, such as the increased volume within visual cortex observed in deaf vs hearing individuals (Allen et al, 2013), and elevated peripheral V1 volume in those with macular degeneration (Burge et al, 2016). In the context of seizures, however, the explanation for increased volume and thickening is poorly developed, and further investigation is required. For SUDEP, elevated volumes in selected areas, e.g., the amygdala, raise concerns; if the increased volumes indeed reflect enhanced function, then the potential for those structures to induce apnoea (amygdala) or hypotension (subcallosal region) may be enhanced, thus putting these patients at greater risk.

1.5.2.3 Summary of structural imaging findings

Evidence from morphometry and cortical thickness studies in SUDEP and at-risk groups (i.e. patients with GTCS) demonstrates reduced volume and cortical thinning in thalamic (primarily within posterior portions), frontal (medial and orbital cortex) and midbrain/cerebellar/brainstem sites (Figure 1.4). Increased volume and regional cortical thickness appear in limbic regions, primarily anterior mesial temporal, especially the amygdala, and cingulate structures, the insula, and sensory areas

(Figure 1.4). Overall, the highlighted volumetric alterations indicate structural injury to key autonomic and respiratory control pathways, including cortical, sub-cortical and caudal structures; therefore, a possible interpretation is that these abnormalities reflect a mechanism that increases the risk for dysfunction, particularly in circumstances under which autonomic and respiratory processes are challenged, such as during and after GTCS (Ryvlin et al, 2013). However, a causal link between volume changes and autonomic and respiratory dysfunction is yet to be established in the SUDEP literature and further work is required to elucidate the relationship between volumetric changes and the extent of autonomic and respiratory dysfunction. Further studies which utilise segmentations of regional structures to validate differences in volume are required to overcome the constraints of the typically limited sample size of SUDEP studies.

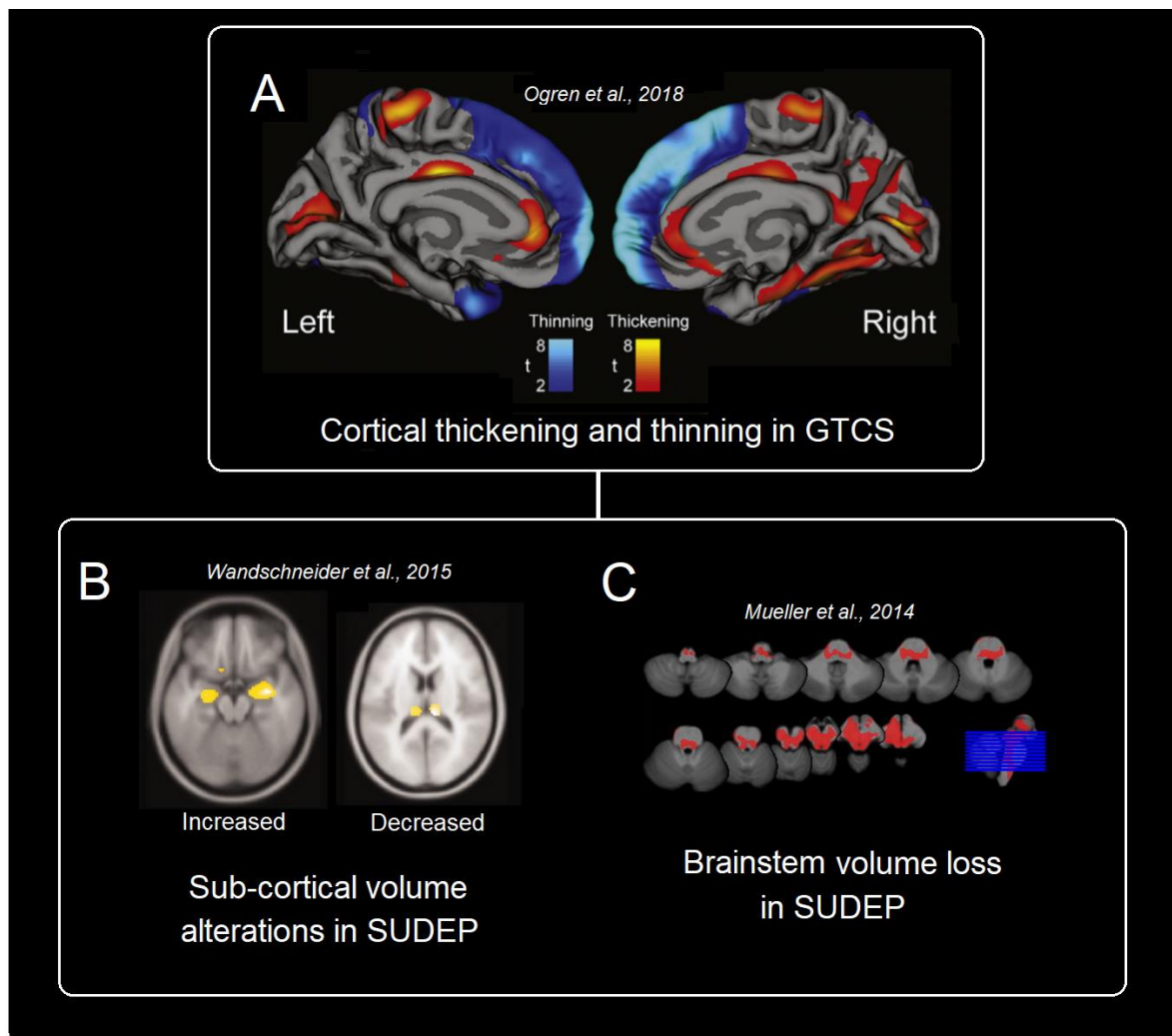


Figure 1.4. Summary of structural findings from imaging studies in SUDEP and populations at high-risk of SUDEP. Part A shows cortical thickness changes in patients with GTCS (Ogren et al., 2018). Part B show sub-cortical grey matter alterations in SUDEP (Wandschneider et al., 2015, and D depicts brainstem volume loss related to SUDEP (Mueller et al., 2014). Figure adapted from Allen et al., 2019¹.

1.5.3 Evidence from resting-state fMRI

1.5.3.1 Altered connectivity between central autonomic and respiratory sites

Resting state (RS)-fMRI is a brain imaging technique in which subjects undergo fMRI scanning whilst lying 'at rest', in the sense that they are not subjected to any experimental stimulus or task; they are usually asked to lie quietly and stay awake, with their eyes closed. Although it has been argued that the 'resting state' in question lacks specificity, this technique has the advantage of being applicable to a wide range of subjects, such as those incapable of performing a specific task (such as in comatose individuals, i.e. Achard et al., 2012) and thus has become an important tool in the study of the patterns of functional connectivity (FC; Cole, Smith and Beckman, 2010). FC describes the connectivity between spatially distant neurophysiological events which share functional properties (Aertsen et al., 1989; Friston et al., 1993). FC is based on the temporal correlations of spontaneous (i.e., resting state) BOLD (blood oxygen level dependent) fMRI signal fluctuations between regions (usually calculated as Pearson r correlation coefficients). From these measurements, resting brain functional connectivity can be explored in multiple ways (for a comprehensive review, see Van Den Heuvel & Pol, 2010).

To date, one study has used RS-fMRI to explore FC between brain regions of interest (ROIs) related to central mediation of autonomic and respiratory processes in patients with epilepsy (Figure 1.5). Tang et al, (2014) evaluated FC between 13 brain structures (medulla, midbrain, pons, and bilateral amygdala, hypothalamus, thalamus, insula and anterior cingulate) in patients at high-($n=13$) and low-risk ($n=12$) for SUDEP. High-risk patients were those who satisfied the key risk factors outlined earlier (Hesdorffer et al.,

201); > 3 GTCS per year, disease duration > 15 years, age at onset < 15 years and presence of nocturnal seizures. Low-risk patients were those who did not satisfy this criteria. FC between all ROIs was then compared between the two groups. High-risk patients showed reduced FC between the pons and right thalamus, midbrain and right thalamus, bilateral anterior cingulate and right thalamus, and between the left and right thalamus. These results demonstrate altered communication between key parts of the brainstem and the thalamus, as well as between the thalamus and other cortical sites involved in autonomic, somatosensory and affective regulation – the anterior cingulate (Bush et al., 2000; Critchley et al., 2003). Differences in connectivity among such brain areas between patients at high- and low-risk may represent potential neural network dysfunction linked to SUDEP, though the absence of a cohort of confirmed SUDEP cases in this study prohibits such a claim; to date, no resting-state fMRI studies have included cases of actual SUDEP.

Overall, RS-fMRI has provided insights into connectivity changes associated with elevated SUDEP risk which indicates altered communication among key brain regions contributing to autonomic and breathing regulatory processes. Larger studies, and investigations involving healthy controls and cases of SUDEP, are needed to confirm and further characterise disturbed connectivity which may offer further insights into the (proposed centrally mediated) pathogenesis of SUDEP, which remains undefined.

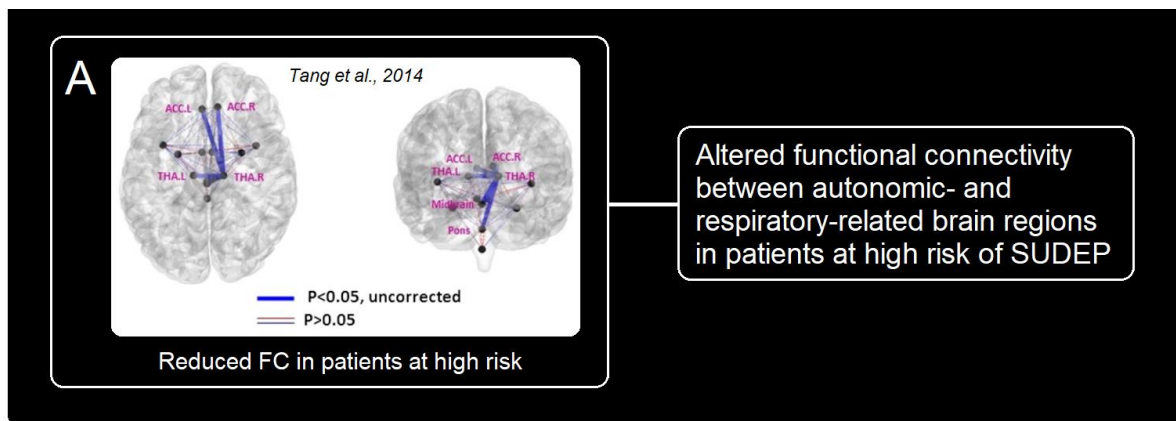


Figure 1.5. Summary of RS-FC findings in patients at risk of SUDEP. Altered connectivity between cortical and sub-cortical autonomic- and breathing-related sites. A shows reduced functional connectivity in patients at high risk (Adapted from Tang et al., 2014) between the brainstem, thalamus and anterior cingulate.

1.5.4 Discussion and considerations

1.5.4.1 Relationships between brain alterations and clinical epilepsy variables

The volume and FC of some brain structures is known to correlate with clinical epilepsy-related variables, particularly in the thalamus. Disease duration, for example, correlates negatively with thalamic volume, as has been demonstrated extensively (Wang et al., 2012; Bernhardt et al., 2009; Bernasconi et al, 2003; Natsume et al, 2003; Keller et al, 2002), including grey matter within the pulvinar nuclei (Wandschneider et al, 2015) – volume loss here is also associated with greater seizure frequency (Coan et al, 2009). Additionally, GTCS frequency correlates with cortical thickness of the cingulate and insula (Ogren et al, 2018). However, both disease duration and seizure frequency are also SUDEP risk factors (Hesdorffer et al, 2012); thus, a central objective

for the field lies within disentangling the effects of the former from what is believed to be related to SUDEP – representing a major challenge, since it is likely that they both contribute to the underlying mechanisms of SUDEP. This issue brings to light an overarching concern for all studies into SUDEP, namely the problem of defining imaging correlates of such underdefined pathology. Modelling and controlling for clinical factors (e.g. disease duration, medications and seizure frequency) in relation to regional brain volume and FC changes are important aspects of SUDEP research, and should be carried out when considering group differences, since the observed changes may be related to a particular seizure type or duration of epilepsy. Long-term prospective studies are needed to investigate all contributory factors of volume loss and connectivity alterations.

1.5.4.2 Imaging studies of other syndromes involving autonomic and respiratory dysfunction

Alterations in brain structure, function and connectivity are not unique to subjects with epilepsy at risk of SUDEP. Neuroimaging studies of other syndromes in which the risk of sudden death is high reveal both structural and functional brain alterations in autonomic brain areas among patient groups compared with controls, providing insights into the alterations observed in SUDEP. Heart failure (HF) patients, for example, show damage to cortical autonomic regions including the insula, anterior cingulate, subgenum and the ventro-medial pre-frontal cortex (VMPFC) (Woo et al., 2009). Obstructive sleep apnoea (OSA) subjects show significant amplitude and phase changes in functional MRI signals belonging to autonomic and respiratory regulatory structures in response to blood pressure and ventilator challenges (Harper et al., 2013;

Harper et al., 2014), as well as highly altered FC of the insular cortices (Park et al., 2016) and volumetric alterations of the putamen (Kumar et al., 2014). OSA is commonly observed among refractory epilepsy patients (Malow et al., 2000). Patients with congenital central hypoventilation syndrome (CCHS), a syndrome accompanied by severe disturbances in both autonomic and respiratory function (Ogren et al., 2010), show cortical thinning of the insular, cingulate, and VMPFC (Harper et al., 2015; Kumar et al., 2005; Macey et al., 2011), as well as injury to hippocampal, limbic and thalamic structures (Harper et al., 2015).

Imaging changes seen in these cohorts may provide important insights into the alterations related to SUDEP, as will be discussed in relation to later findings in the current body of work.

1.5.5 Conclusions & outlook

Given the relative rarity of SUDEP, multi-centre collaborations, including such consortia as the Center for SUDEP Research (CSR; a *Center Without Walls* initiative, funded by the US National Institute of Neurological Disorders and Stroke), which bring together investigators from multiple institutions and utilise open data sharing, are crucial. Additionally, the integration of multi-modal imaging data, acquired prospectively is essential for improving characterisation of structural and functional brain alterations; such an approach will enable investigations of how volume changes and structural and functional connectivity alterations among regulatory structures arise and change in relation to clinical (seizure frequency, disease duration) and autonomic/respiratory (i.e. hypoxemia) manifestations.

In summary, imaging studies have so far revealed changes in structure and functional connectivity among brain sites which are involved in the regulation of autonomic and respiratory action. Although, few studies are yet to include confirmed cases of SUDEP, and the underlying generators of volume and connectivity disturbances in both those who succumb and those who are at greatest risk are unknown. Key future aims (such are the goals of the work in the remainder of this thesis) are to corroborate findings in larger retrospective datasets and in confirmed SUDEP cases, as well as explore associations between volume/connectivity alterations and observed clinical, neurophysiological and autonomic/respiratory risk factors using prospectively acquired data. Such explorations may shed light on the genesis of injury to salient brain sites and enrich models of SUDEP pathophysiology.

Chapter 2: Common methods

The purpose of this chapter is to provide an overview of the methodologies employed throughout the thesis, describe the basic principles upon which they are based, justify the suitability of these approaches to address the goals of this work.

2.1: Ascertainment of SUDEP cases

A major challenge for investigations into SUDEP is the identification and definition of SUDEP cases, which can be difficult, or sometimes impossible if historical clinical data are inaccurate, missing or inaccessible. Deaths must first be identified from the cohort or data acquisition time period in question, which can include hundreds of patients and be time-consuming if performed manually.

In the following studies, a semi-automated approach was adopted to identify cases of SUDEP. For retrospective studies, hospital numbers of patients scanned within the case ascertainment period (selected such that scanner hardware was consistent), were entered into NHS spine – a service which automatically identifies deceased patients. For prospective studies, hospital numbers of all consented patients were queried. Once deaths were identified, the cause of death was determined to establish SUDEP and rule out other causes of death. Death certificates, if not already available in a patient's electronic or physical medical records, were obtained to verify this. With this information, SUDEP can then be classified (definite, probable or possible – as discussed in chapter [1.2.1](#)). Information stored in electronic medical records, or in physical patient notes, can also assist in these processes, but may not always contain information pertaining to the cause of death.

2.2: Magnetic Resonance Imaging and analysis procedures

2.1. MRI (overview)

MRI is a non-invasive medical imaging technique which can be used to generate 3D, and sometimes 4D, images revealing the anatomical structure and physiological processes of the body including, and most saliently here, the brain. As such, MRI is well suited to the aims of the current study, which are to characterise structural and functional brain architecture associated with SUDEP, and related risk factors.

MRI is based on the principle that hydrogen atoms (the most abundant particle in biological organisms, including the human body and brain), can absorb and emit radio frequency energy when placed in a magnetic field (such that is generated within and MRI scanner). Since hydrogen atoms are mostly contained in water and fat, structural MRI scanning fundamentally enables the localisation of those properties in space, revealing with it the underlying architecture of tissue types containing varying amounts of hydrogen. This is done by exciting the nuclear spin energy transition of hydrogen atoms with radiofrequency pulses. Magnetic field gradients are then used to localise the resultant signal which reflects the relaxation (recovery) of hydrogen atoms back to their equilibrium state (original spin direction) prior to excitation. The parameters of the pulse sequence can be changed to generate different contrasts between tissues based on the properties of the hydrogen atoms within them, and thus different types of image. Slice (a 2D cross-section) by slice an entire 3D image, containing voxels (similar to pixels in a photo or a television image), is reconstructed from the measured signals. Each voxel contains a numeric value reflecting the intensity at that particular

location in the image; the value of intensity depends on the tissue property at that location, and type of image sequence used.

The two basic types of image sequences are T1, and T2. In a T1-weighted image, tissues with high fat content and more myelinated axons (i.e. white matter) appear white, while tissues with fewer myelinated axons (i.e. grey matter) appear grey, and water-filled compartments (i.e. CSF) appears black (Figure 2.1 A). In a T2-weighted image, white matter appears dark grey, grey matter appears a lighter grey, and CSF appears bright (Figure 2.1 B). While both T1 and T2 weighted images are used in clinical and diagnostic settings, often in complement to one another, each are sensitive to different tissue types and are thus slightly better for different purposes. T1-weighted images give provide good contrast between the three primary brain tissue types (grey matter, white matter and CSF) and are thus slightly better for demonstrating anatomical structure. T2-weighted images provide a stronger signal for water-based tissues types, which appear brighter, making them slightly better for visually demonstrating pathology, since many brain lesions are water-based.

T1 and T2 images can be used to evaluate volume and morphology of structures throughout the brain, and be combined to approximate myelin content (Ganzetti, Wendearth and Mantini, 2014). Descriptions of such analysis procedures will be described in the following section (Image processing and analysis techniques).

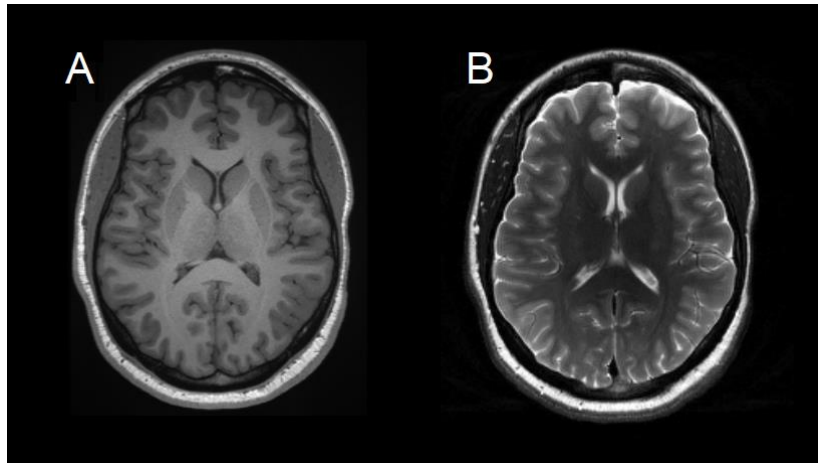


Figure 2.1. Example T1 and T2 MR images for a representative subject. A = T1-weighted image; B = T2-weighted image.

2.2 Functional MRI and resting-state fMRI (overview)

While the images outlined above describe static structural images, MRI can also be used to map neural activity within the brain. Functional MRI (fMRI) uses the blood-oxygen-level-dependent contrast (BOLD; Ogawa et al., 1990) to map changes in blood flow (hemodynamic response) related to neural energy consumption. BOLD fMRI rests on the physiological basis that neurons require glucose when they become active. Blood flow to active areas increases to bring in more glucose and oxygen, in the form of oxygenated haemoglobin. The magnetic properties of oxygenated haemoglobin are such that they interfere far less with the magnetic field than those of deoxygenated haemoglobin, and thus provide a better MR signal. This improved signal is then mapped to show activated regions at that specific time and across multiple volumes. When performed in conjunction with a cognitive task, fMRI can be used to map the related changes in brain activity across the whole brain or within a specific region. This then gives an indication of the involvement of a particular region, or regions, in specific tasks.

Since the brain is always active, even at rest and without carrying out a cognitive task, spontaneous activity of brain regions can be measured through the spontaneous fluctuations in BOLD signal which they exhibit. This can be assessed with resting-state fMRI (RS-fMRI), in which subjects lay idly in the scanner whilst volumes are continuously acquired. 3D images of the subject's brain are acquired at every volume, which are joined together to create a 4D image (with the 4th dimension being time). This approach allows the assessment of functional interactions between brain regions at rest, and characterisation of functional connectivity between regions and among networks based on temporal correlations between time-series of regions. Such approaches allow exploration of brain functional organisation and characterisation of resting brain networks (Damoiseaux et al., 2006).

fMRI is susceptible to many sources of noise, including scanner, physiological, sleep, drowsiness, vigilance and movement related artefacts, as well as individual strategies to cognitive tasks. These confounders are addressed with pre-processing steps carried out prior to statistical analyses or modelling of brain networks. The relatively low temporal resolution of fMRI makes it poorly suited to exploring fast changes in brain activity or connectivity (i.e. less than 1 second), which can be modelled more accurately with approaches such as electroencephalography (EEG) or magnetoencephalography (MEG). However, fMRI has superior spatial resolution, permitting localisation of activation to several millimetres (mm), and allowing connectivity to be assessed between brain areas as small as the amygdala.

RS-fMRI data are particularly vulnerable to movement related artifacts, including subtle sub-millimetre movements, which are known to increase RSFC correlations in a distant

dependent manner (Power et al., 2014). As such, pre-processing methods to detect and deal with movement, and tackle resultant spurious connectivity, have undergone extensive development over the years (Power, Schlagger and Peterson, 2015). Other pre-processing steps to clean data and improve resulting measurements are removal of nuisance covariates, such as the signals belonging to the white matter and CSF, which are known sources of physiological noise. Global signal regression (GSR; removal of the total mean signal of all voxels in the brain) can also be used to effectively deal with movement (Power et al., 2014). However, performing GSR comes at the cost of introducing unexplained anti-correlated networks and additional negative correlations (Murphy et al., 2009), which alter the natural underlying inter-regional correlation structure (Saad et al., 2012). Important information within the signals pertaining to the grey matter are intrinsically entwined with this global signal, hence it's removal comes at the cost of potentially losing valuable information relating to the structure of functional connectivity and resulting networks. GSR remains a controversial topic (Murphy and Fox, 2017), and while many studies conduct analyses with and without GSR, alternate methods to optimally deal with physiological and movement noise, such as wavelet filtering and motion scrubbing, are well-developed. Finally, most fMRI data undergo some sort of filtering to further clean the data and focus analyses on activations or connectivity pertaining to grey matter. The most common range between which RS-fMRI data are band-pass filtered is 0.01 – 0.08Hz, since fluctuations in this low-frequency (LF) range are reported to be of physiological importance (Biswal et al., 1995) and are believed to reflect spontaneous neuronal activity, primarily within the grey matter (Yu-Feng et al., 2007; Zuo et al., 2008, 2010). Wavelet filtering, an alternate approach to bandpass filtering, has become a popular

technique in RS-fMRI data pre-processing, enabling assessment of multiple frequency bands and offering improved denoising (Zaroubi and Goelman, 2000; Zhang, 2016).

2.3 Image processing and analysis techniques

2.3.1 Voxel-based morphometry

One aim of the present work was to determine the nature of brain structure in patients who suffered SUDEP and those at risk (as per [chapter 3.1](#) and [3.2](#)), in the hope that indications as to the proposed central mechanisms of SUDEP may be provided, along with imaging-based biomarkers with which to identify those at risk.

To characterise potential brain (grey and white matter) structural alterations, voxel-based morphometry (VBM; Ashburner and Friston, 2000) was employed. VBM is an established and flexible framework for evaluating focal, or global, changes in brain morphology, within the Statistical Parametric Mapping (SPM; <https://www.fil.ion.ucl.ac.uk/spm/>) framework.

VBM involves a sequence of pre-processing steps to analyse 3D structural images which enables characterisation of structural brain morphology within and between groups of individuals. Specifically, VBM allows regional grey and white matter (volume / amount, or intensity / concentration), to be quantified from (most commonly) an individual's T1-weighted MRI scan. Tissue probability maps (TPMs) can then be compared between groups, or assessed in relation to other scalar observations (i.e. continuous variables), under the statistical framework of the general linear model (GLM). VBM is a popular and widely used approach to investigate changes in structural brain morphology related to a specific neurological disease or any measurably variables, such as age. Prior to generating normalized tissue maps which can be

compared between groups, a number of steps are carried out to account for scan inhomogeneities and individual differences in brain size and structure.

2.3.1.1 Segmentation

Prior to segmentation, images may be resliced to ensure consistent voxel size across subjects (for example 1mm isotropic) and are normally bias corrected to account for intensity inhomogeneities and improve segmentation; the result of bias correction is visualised in Figure 2.2 A (before) and B (after). Segmentation involves separating the different tissue classes within the image using a prior tissue probability map to estimate the expected amount of a particular tissue (i.e. grey matter, white matter or CSF) at each location (voxel) in the image expressed as a probabilistic value between 0 and 1. Separate images for each tissue class are then generated; for the purposes of the following studies, only the grey (Figure 2.2 C) and white (Figure 2.2 D) matter TPMs were used for structural analysis (i.e. for evaluation of differences in grey and white matter).

2.3.1.2 Spatial normalisation and modulation

Spatial normalization involves registering each individual's image (T1, and TPMs) to the same common space; in this case, Montreal Neurological Institute (MNI) space. A common space is required for comparisons between groups of individuals to be made. Given the individual differences in neuroanatomical structure (brain size and shape), the point of normalization is to ensure that image locations, and thus brain regions, roughly correspond across subjects.

Since the brains of individuals take different shapes and sizes, the amount each TPM is expanded and contracted to fit the normalized template varies across subjects also.

To account for this, each TPM is scaled by the amount of contraction/expansion such that the total amount of modulated grey or white matter is the same as the original image (prior to normalization). Modulated images are of particular interest if one is interested in exploring 'volume' as opposed to 'concentration' or intensity, in which case unmodulated images are used. In the following studies, modulated images are used (Figure 2.2 E and F).

2.3.1.3 Spatial smoothing and masking

Segmented, normalized and modulated grey and white images are finally smoothed to improve the signal to noise ratio and further account for subtle anatomical variations across subjects and the approximate nature of spatial normalisation. Spatial smoothing is achieved by applying a Gaussian Kernel (full width at half maximum; FWHM), specified in millimetres (mm); most VBM studies apply between 8 and 12mm of smoothing (Mechelli, Price, Friston and Ashburner, 2005; Figure 2.2 G and H shows grey and white matter TPMs smoothed at 8mm). Another advantage of smoothing prior to statistical analysis is improved normality of the data. Smoothing does however come at the cost of slightly reducing the accuracy of localisation of regional effects.

Masking can be achieved in two ways and is performed to remove or omit values within an image. Threshold masking involves excluding values within an image below a specified threshold, primarily to avoid partial volume effects (values at the border between white and grey matter), and can be absolute (excluding values below a given voxel value) or proportional (removing n% of the lowest values). The threshold used often depends on the type of data and hypothesis, though an absolute threshold of 0.2 is the standard recommended, and default, option (Ashburner, 2015) and was used in

the VBM studies carried out in the following chapters. Image-masking involves using a separate image (usually binary) to exclude, or include, voxels within the image of interest.

2.3.1.4 Statistics

Once pre-processed, TPMs can be entered into voxel-wise statistical models to make group comparisons (i.e. T and F tests) or perform linear regression with relevant covariates, all of which are implemented under the GLM. The GLM is a flexible statistical framework which, within SPM, lets the hypothesis of interest (i.e. group 1 > group 2, or a regression with disease duration) be tested at every voxel. Since there are often hundreds of thousands of voxels for which a statistical test is performed, a multiple comparison problem emerges and thus with it a need to account for this. With so many comparisons, the probability of falsely rejecting the null hypothesis (making a type I error) for a proportion of those tests increases. The family wise error rate (FWER; Freedman and Lane, 1983) is a way of controlling for that probability and was employed in the following studies.

2.3.1.5 Limitations

The processes used in VBM, such as segmentation and normalisation, are sensitive to drastic neuroanatomical abnormalities and instances of severe pathology (such as large stroke lesions or sites of neurosurgical resection). VBM thus may not be best suited to studying neurological diseases involving severe brain abnormalities, and hence in the following studies patients with large lesions were excluded. Movement of individuals within the scanner, as well as the use of different scanners, can also

introduce systematic variance and affect the interpretability of results. Careful consideration over these factors must therefore be taken.

There is some debate over precisely what aspects of cell properties are captured by VBM, and what 'grey' and 'white' matter represents (Mechelli, Price, Friston and Ashburner, 2005). For example, neuronal size, axonal density or pathological cell alterations cannot be derived from VBM; one may only speculate about the nature of increases or decreases in volume. Additionally, different types of grey or white matter cannot be distinguished with VBM, and the interpretation is generally limited to 'average grey and white matter volume' (or concentration).

However, VBM is well suited to explorative investigations of neurological diseases, such as the experiments in this thesis, since it allows exploration of structural changes across the entire brain, without the need for a priori hypotheses regarding particular brain areas. A disadvantage of this, though, is that with such an explorative approach involving the whole brain, the correction for multiple comparisons is much more severe (greater number of voxels, and thus more comparisons, to correct for), therefore some important effects may be missed with stringent controlling for multiple comparisons.

2.3.2 Volumetry

Secondary volumetric analysis was performed in chapters 3.1 and 3.2 in order to complement and validate VBM findings. While the primary concept underlying VBM is segmentation of the entire grey and white matter, other methods enable segmentation and parcellation of individual brain structures such that volume, or other properties (such as shape), can be quantified for a specific region at the individual level. Geodesic information flows (GIF; Cardoso et al., 2012, 2015) is one such approach for doing so,

and involves propagating information regarding segmentation and parcellation from existing (already processed datasets), greatly improving the accuracy of these processes. Briefly, tissue classes are segmented and then, using the Brain Collaborative Open Labelling Online Resource (BrainCOLOR) whole-brain atlas (Klein and Tourville, 2012), anatomical labels are defined, which include 100 cerebral cortical areas, 16 subcortical grey matter areas, 16 cerebral white matter areas, and 5 cerebellar regions (an example T1-weighted image and resulting GIF parcellation can be seen in Figure 2.2 I and J). The volume of each region can then be calculated by multiplying the number of voxels in each ROI by the voxel volume. The main advantage of this approach is that the volume of entire, and individual defined, anatomical grey or white matter structures can be quantified, instead of relying on average grey or white matter TPMs as per VBM.

2.3.3 Resting-state fMRI data analysis

An abundance of approaches to RS-fMRI data analysis are now in existence. These include seed-based approaches (enabling connectivity of a specific region with the remaining voxels in the brain to be explored), independent components analysis (the data driven separation of functional imaging data into resting state networks [RSNs]), as well as graph theoretical and network-based approaches (Lee, Smyser and Shimony, 2013). With such a wealth of methods to choose from, or elaborate on, it becomes quickly apparent that there is no single optimal way to analyse RS-fMRI data, but it is rather more appropriate to select an approach based on the nature of hypotheses and questions to be asked. As such, and considering the goals of this

thesis are to explore regional interactions and network properties among specific structures involved in regulatory processes, a network-based approach was adopted.

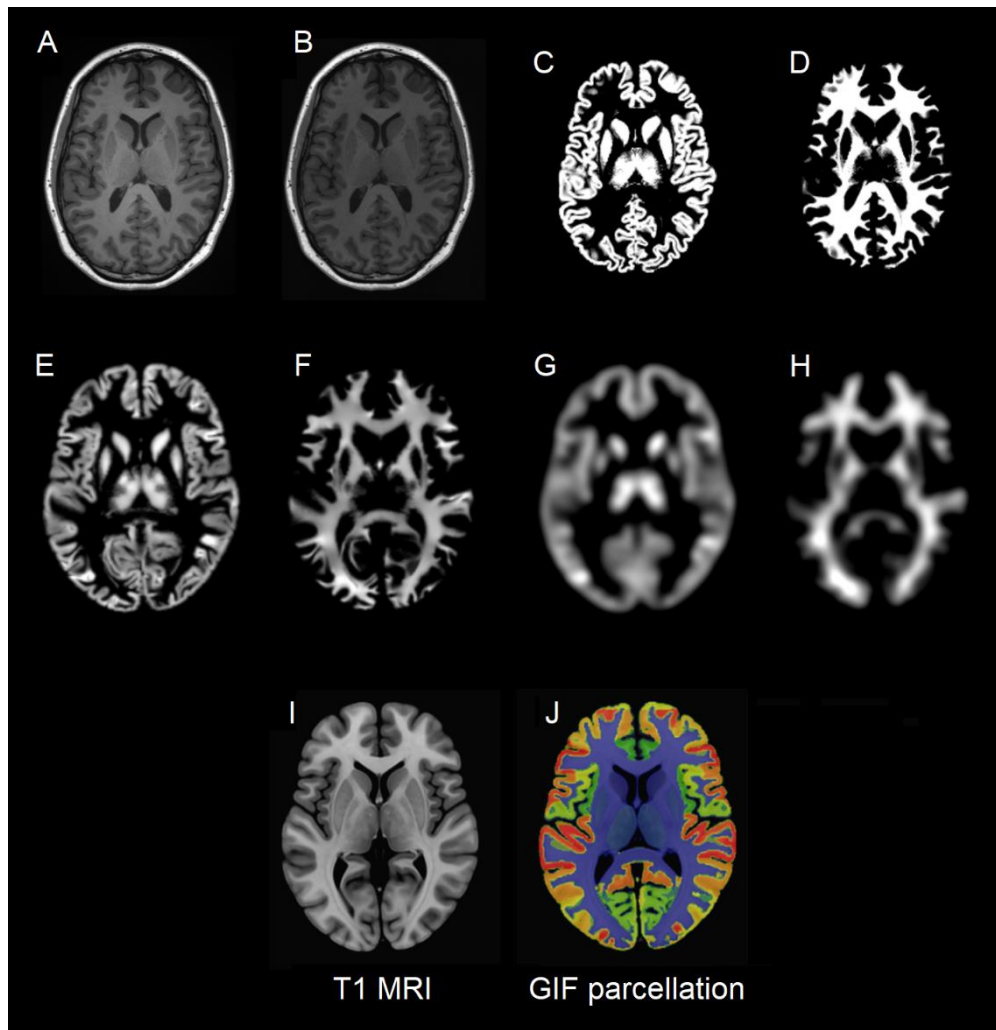


Figure 2.2. Example images from morphometric and volumetric processing steps. A = raw T1; B = bias corrected T1; C = grey matter TPM; D = white matter TPM; E and F are normalised, modulated grey and white matter TPMs respectively; G and H are smoothed and thresholded versions of E and F respectively; I is a template MRI scan and J is the GIF parcellation applied to that image.

2.3.3.1 Pre-processing

Prior to analysis network analysis, some pre-processing (as with VBM discussed above) is required to remove noise and prepare data for network and statistical modelling. Basic pre-processing steps include correcting for the fact that slices are acquired at slightly different times (slice-time correction), and realignment of volumes since subjects often move subtly over the course of the scan and sometimes abruptly during. If available, an anatomical image (i.e. T1-weighted MRI) can be registered to the space of the functional images, and segmented as described above. This allows an individualised extraction of the fMRI signals from the white matter and CSF which, along with the realignment parameter generated during image realignment, are traditionally removed as part of nuisance covariate regression to account for related noise (as mentioned above).

2.3.3.2 Network analysis and graph theory

Since the hypotheses of the present work are centred around functional connectivity between specific regions, and among networks of regions, a network / graph theory approach was adopted and employed in functional imaging studies of this work (chapter [4.1](#) and [4.2](#)). Graph theory is a flexible framework in which the mathematical study of networks is implemented, allowing characterisation of a range of network properties. Both structural and functional connectivity can be explored, involving directional or non-directional networks; the focus of the present work is on functional (based on RS-fMRI) and non-directional networks, since a direction cannot be inferred from such connections.

Once data are pre-processed, an anatomical (or functional) brain atlas can then be used to extract the mean signal of each ROI from the RS-fMRI volumes, yielding a time-series for each region. By performing correlations (usually a Pearson r) between every possible inter-regional pair of ROIs, a connectivity matrix, or network, can be generated, for the whole brain or a subnetwork of predefined ROIs (Figure 2.3). A network is also known as a 'graph', the primary features of which are nodes (in this case brain regions) and the edges (RS-fMRI derived connectivity) connecting them (Figure 2.4).

Graph theoretical measures (Rubinov and Sporns, 2010) are then computed on these graphs, which may be weighted or binary, to explore network properties. Since many of the smaller connections (lower weighted edges) may be spurious, or noisier, a common approach is to threshold weighted graphs to focus on the strongest connections in the network. Thresholding, as touched upon above in VBM processing, can be absolute (thresholding above a certain correlation value, i.e. 0.3) or proportional (keeping only 20% of the highest connections in the network). The latter is preferred since this preserves the same number of connections in every individual, whereas absolute thresholding can lead to greater variability in individual networks. However, proportional thresholding may lead to inclusion of more spurious connections if overall FC is not corrected for (van den Heuvel et al., 2017).

Weighted graphs are usually thresholded and binarized across a range of network sparsities, (Ridley et al., 2015; Basset et al., 2012; Alexander-Bloch et al, 2010; Achard et al., 2006), computing network measures at each iteration. Binarization involves converting thresholded weights into 1s and excluded weights to 0s.

Computing network measures on binary networks across a range of sparsities brings the advantage of capturing a wider spectrum of connectivity in individuals, and eliminates the bias of arbitrarily selecting a single threshold. It does, however, require the arbitrary selection of a threshold range, and increment, though network sparsities above 50% become increasingly more random (Humphries et al., 2006). Statistical analyses are usually then employed to compare groups, or conditions, at each network sparsity.

Some examples of network measures include degree (the number of connections a node has after thresholding; a high degree node is shown in red in Figure 2.4), modularity (the separation of nodes into separate modules, higher values of which reflect improve organisation) and participation (how much a node participates in modules outside its own; Figure 2.4 in orange), which are described in greater detail later. Elaborate definitions of these and many more graph theoretical measures are well described (Rubinov and Sporns, 2010).

2.3.3.3 Limitations

The major advantage of RS-fMRI coupled with graph theory is that it enables the characterisation of complex network properties which cannot be otherwise revealed. Since RS-fMRI is fast and straightforward to acquire, it is a sought-after approach to non-invasively explore alterations in connectivity associated with neurological or psychiatric diseases.

However, there are a number of limitations which should be considered. RS-fMRI is especially susceptible to movement-related artifacts, which should be dealt with during pre-processing depending on the extent of movement. The abundance of methods

and pipelines with which to pre-process RS-fMRI is a pitfall within itself, since the optimal approach is rarely known (Caballero-Gaudes and Reynolds, 2017), and different types of pre-processing, as well as the order in which they are performed, greatly affect resulting network measures (Gargouri et al., 2018).

Functional connectivity is based on temporal correlations between time-series, meaning their connectivity is based on regions being active at similar times. There is some debate over the precise underlying physiology of such connectivity, and the value it holds in explaining communication between distinct brain areas.

Graph theory-specific critiques include the often non-normal distributions of network measures, which prevents parametric statistical testing, and high levels of inter-subject variability. This can be overcome with some normalisation techniques, such as log-scaling, though may not always be valid since network measures at very low sparsities (i.e. 5-10%) in some subjects may include zero values. One approach to resolve this, along with dealing with the subjectivity of selecting threshold sparsities, is to integrate network measures in the sparsity range, yielding one value per measure, as opposed to one value per sparsity per measure. Doing so reduces the number of statistical comparisons to control for and increases power to detect significant effects (Wang et al., 2011).

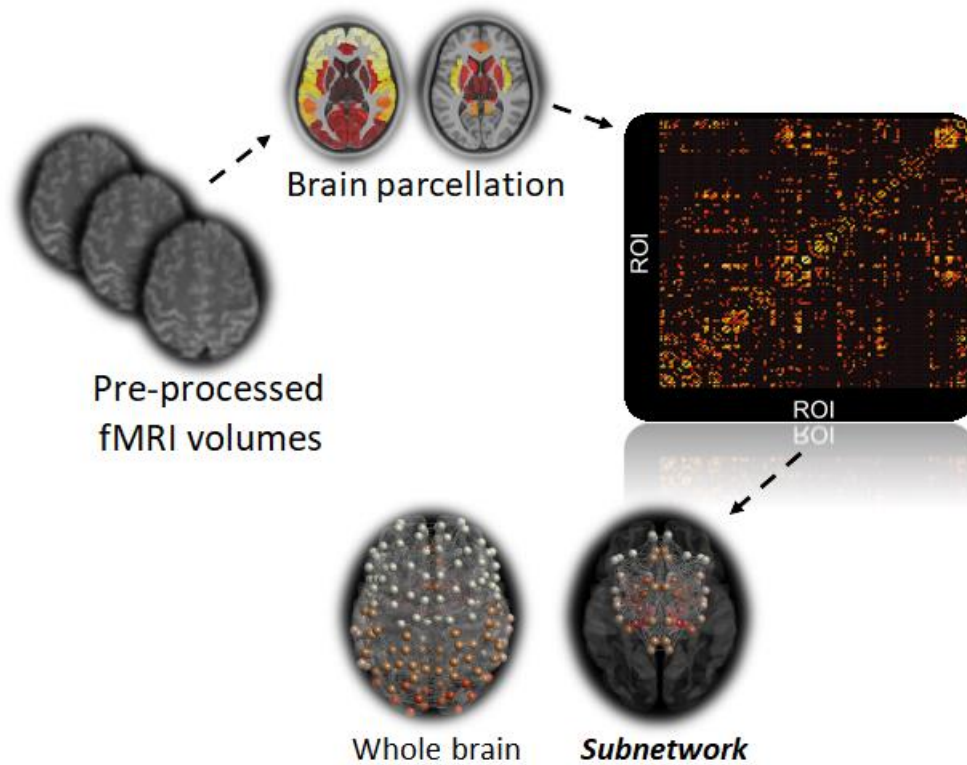


Figure 2.3. Simple schematic of ROI extraction and network (whole brain and subnetwork) construction. Brain atlas used to extract ROI signals from pre-processed fMRI volumes to generate connectivity matrices, or networks (clockwise).

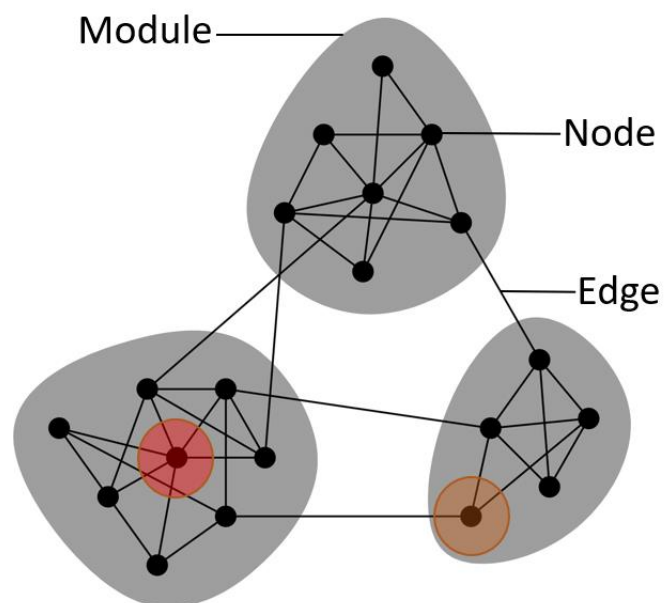


Figure 2.4. Example network consisting of three modules, nodes and edges. Red indicates a node with high degree (great number of connections), while orange indicates a node with greater participation (involvement in more than one module). Adapted from Newman (2006).

Chapter 3. Structural brain changes associated with SUDEP

In this chapter, two structural imaging studies are presented, the aims of which were to characterise morphometry and volumetry: 1) in individuals who later suffered SUDEP, and those at risk ([3.1](#)); and 2) related to a potential risk factor of SUDEP observed on the EMU; peri-ictal hypoxemia ([3.2](#)).

3.1: Cerebellar, midbrain and limbic volume alterations in SUDEP².

A retrospective study of 25 SUDEP cases, and matched high-risk, low-risk and healthy controls, published in *Epilepsia* (see footnote for full citation).

3.1.1. Background

As per chapter [1.5](#), recent structural MRI studies have revealed volumetric changes among brain structures involved in autonomic and breathing co-ordination associated with SUDEP and elevated risk. Such alterations may indicate injury to, or abnormal functioning of, sites important for recovery from cardiorespiratory dysfunction. Since the circumstances surrounding SUDEP suggest a centrally mediated cardiorespiratory collapse following a generalised tonic-clonic seizure (GTCS; Ryvlin et al., 2013), injury or dysfunction among central regulatory brain sites may shed light on proposed neural mechanisms. However, the majority of retrospective investigations have studied

² Allen, L. A., Vos, S. B., Kumar, R., Ogren, J. A., Harper, R. K., Winston, G. P., ... & Duncan, J. S. (2019). Cerebellar, limbic, and midbrain volume alterations in sudden unexpected death in epilepsy. *Epilepsia*, 60(4), 718-729.

populations at risk (i.e. those with GTCS or individuals stratified by clinical SUDEP risk factors), and the few studies which have included cases of SUDEP (i.e. Wandschneider et al., 2015; Mueller et al., 2014) have involved relatively small sample sizes. The goal of the present study was to explore volume changes related to SUDEP, confirming previously reported findings and revealing potential new changes, in a larger group of 25 SUDEP cases. Confirmed cases of SUDEP and living high-risk, low-risk and healthy controls were identified and VBM was used to compare brain-wide and regional volume between groups.

3.1.2 Methods

3.1.2.1 Subjects

As per chapter [2.1](#), twenty-five individuals who suffered definite (n=12) or probable (n=13) SUDEP (Nashef, So, Ryvlin, & Tomson, 2012), were retrospectively identified after updating an earlier initial search for cases of SUDEP at the epilepsy society, Chalfont St Peter, Buckinghamshire (Wandschneider et al., 2015). A database of subjects scanned between 2004 and 2017 were searched for deaths, and patient records were inspected to ascertain SUDEP and rule out other causes of death. Restricting the investigation to this time window ensured constancy in scanner hardware and software. All subjects underwent the same high-resolution 3D-T1-weighted scan, and Individuals with insufficient clinical data, large brain lesions, and/or previous neurosurgery were excluded.

Living high-(n=25) and low-risk (n=23) patients, and healthy controls (n=25), were identified from existing studies and were matched as closely as possible to SUDEP cases based on biological (age and sex) and clinical (epilepsy syndrome, seizure

localisation, disease duration and imaging findings) information (Table 3.1.1 shows group characteristics; Supplementary Table [S1](#) shows individual clinical characteristics of SUDEP, high-risk, low-risk and healthy individuals). Subjects were matched in this way to account for potential volume changes accompanying these factors.

Table 3.1.1. Group characteristics of SUDEP cases, high-risk, low-risk and healthy controls.

Characteristics	SUDEP (n=25)	High-risk (n=25)	Low-risk (n=23)	HC (n=25)
Age, years (mean±SD)	34.4±13.5	32±7.5	30±8.1	38±12.1
Sex (M:F)	18:07	18:07	16:07	18:07
Disease duration, years (mean±SD)	22.8±14.2	21.4±8.6	16.6±9.9	N.A.
GTCS/month, last 12 months (mean±SD)	2.7±2.5	2.5±1.5	N.A.	N.A.
Focal: generalised epilepsy	22:03	22:03	19:14	N.A.
No. AEDs ATOS (mean±SD)	2.2±0.8	2.7±1.1	2.1±0.9	N.A.
No. AEDs historic (mean±SD)	4.8±3.2	8.4±3.2	3.4±2.8	N.A.
Number exposed to Phenytoin	5	8	3	N.A.
Long term Phenytoin users (>10 years)	2	3	0	N.A.
Polytherapy (count)	10	15	8	N.A.
Duotherapy (count)	10	6	9	N.A.
Monotherapy (count)	5	4	6	N.A.
Seizure onset zone				
L temporal (HS)	1	2	1	N.A.
L temporal (no HS)	1	1	1	N.A.
R temporal (HS)	0	1	0	N.A.
R temporal (no HS)	2	1	2	N.A.
Frontal	6	5	6	N.A.
Temporal+	7	6	2	N.A.
Generalised	3	3	4	N.A.
Posterior head regions	2	1	2	N.A.
Focal, unknown	3	5	5	N.A.

SD=standard deviation, M=male, F=female, /per, HS = hippocampal sclerosis, AED=anti-epileptic drug, ATOS = at time of scan, HC=healthy control, N.A.=not applicable.

Patients at high-risk of SUDEP were those experiencing more than three GTCS per year, the most significant factor associated with SUDEP (DeGiorgio et al., 2017), and distinguished over 80% of SUDEP cases (21/25) in our data. Low-risk patients were those who did not experience GTCS. All clinical information used for risk stratification was obtained from multi-disciplinary team meeting reports and clinic letters closest to data collection, and confirmed with the most-recent follow-up. Survival of all non-SUDEP subjects was confirmed through examination of clinical records.

The study was approved by the UK National Research Ethics Committee under an ongoing database research project into autonomic and imaging biomarkers of SUDEP (04/Q0512/77 and 14/SW/0021), and a local audit into mortality in epilepsy.

3.1.2.2 Magnetic resonance imaging (MRI) acquisition

Scanning was performed at the Epilepsy Society (Chalfont St Peter, Buckinghamshire, UK) on a 3.0-Tesla Signa HDx, GE Medical Systems scanner, using standard imaging gradients (maximum strength of 40 mT/m, slew rate 150 T/m/s). All subjects underwent the same fast spoiled gradient-echo (FSPGR) 3D-T1 scan (repetition time = 8.3, echo time = 3.1, slices = 170, slice thickness = 1.1 mm, matrix size = 256 x 256, field-of-view = 240 x 240 mm).

3.1.2.3 Voxel-based morphometry

Voxel-based morphometry (VBM) was implemented using the computational anatomy toolbox (CAT12; Gaser & Dahnke, 2016), using SPM12 (Statistical Parametric Mapping; <http://www.fil.ion.ucl.ac.uk/spm>) and Matlab 2017b (MathWorks, USA), to explore grey matter volume differences across the whole-brain between groups. Images were de-noised using the spatial-adaptive non-local means filter and

normalised to MNI152 template space, before being segmented into grey matter (GM), white matter (WM), and cerebrospinal fluid (CSF) classes. Modulated images were then smoothed with an 8mm full-width-at-half-maximum Gaussian kernel and entered into a full-factorial model, with group as factor, and age and sex as covariates. An absolute threshold mask of probability 0.2 was applied to account for edge effects between different tissue types. Total intracranial volume (TIV; the sum of WM, GM and CSF), was used to proportionally scale the data to account for differences in whole-brain size across subjects, and results were FWER corrected at $p < 0.05$, unless otherwise stated.

3.1.2.4 Regional structure parcellation using Geodesic Information Flows (GIF)

3.1.2.4.1 Parcellation method

As outlined in chapter [2.3.2](#), for validation and determination of difference magnitudes, structures showing significantly increased or reduced volume using VBM were segmented in each subject using a whole-brain parcellation scheme based on geodesic information flows (GIF; Cardoso et al., 2015). Regional brain volumes were obtained by extracting areas of interest from the parcellation and multiplying the number of voxels in each area by the voxel volume. These values were scaled by TIV.

3.1.2.4.2 Statistical analysis

Permutation tests were employed to assess group differences; for each contrast, members from each group were randomly permuted (10,000 times) to obtain an empirical null distribution. P-values were corrected for multiple comparisons using FWER. Data were adjusted for age and sex using linear regression before being

compared across groups. All processes were carried out in Matlab2017b (Mathworks, USA).

3.1.2.5 Correlations: brain volume and clinical variables

Partial correlations (carried out in IBM SPSS25) were used to assess whether structural sizes from whole brain parcellation depended on disease duration or GTCS frequency, controlling for age, sex and TIV. Correlations with GTCS frequency were considered in two ways: we first examined correlations with SUDEP and high-risk subjects as one group. We then correlated volume with GTCS frequency in SUDEP and high-risk groups separately. Additional partial correlation analyses were performed to assess relationships between structural size and the time between MRI and SUDEP, controlling for seizure frequency, age, sex and TIV. P-values were FWER-corrected.

3.1.2.6 Contributions to tissue loss from medications

Several anti-epileptic drugs (AEDs) induce structural changes via toxic processes (Meldrum & Rogawski, 2007). Medications in all patients were documented and summarized by group in Table 3.1.1. We compared the number of AEDs used at scan time, and the total number of AEDs tried across groups with non-parametric tests (IBM SPSS 25). Additionally, we repeated all volumetry analyses having removed individuals with known phenytoin exposure (n=5 SUDEP, n=8 high-risk, n=3 low-risk) due to known cerebellar atrophy related to its use (De Marcos, Ghizoni, Kobayashi, Li, & Cendes, 2003).

3.1.3 Results

Table 3.1.2 provides a breakdown of group contrasts, main results and related figures per method. Results are otherwise reported and discussed by anatomical region.

3.1.3.1 Cerebellar volume loss

Compared with healthy controls (Figure 3.1.1 A) and low-risk subjects (Figure 3.1.2 A), SUDEP cases showed bilateral cerebellar volume loss, across medial, lateral and vermal portions (VBM). High-risk subjects showed reduced grey matter volume compared with healthy controls in the vermis (Figure 3.1.3 A). Sub-analyses, removing those with a history of phenytoin use, revealed similar, but less extensive patterns of cerebellar volume loss (particularly in lateral portions) in SUDEP and high-risk vs healthy controls (Figure 3.1.4 A-B); no other results changed significantly as a consequence of removing these subjects. Regional segmentation comparisons revealed reduced volumes of the bilateral exterior cerebellar grey matter in SUDEP vs healthy controls (Figure 3.1.5 B-C) and the high- and low-risk groups did not show significantly reduced volumes of segmented cerebellar structures.

3.1.3.2 Thalamic and limbic alterations

The left posterior and medial thalamus and posterior hippocampus exhibited reduced grey matter volume in SUDEP (Figure 3.1.1 B-C) and high-risk (Figure 3.1.3 A) vs healthy controls (VBM). Additionally, SUDEP, but not high-risk, subjects showed volume loss in these areas when compared with low-risk subjects (Figure 3.1.2 A). VBM also revealed PAG and bilateral posterior cingulate grey matter volume loss in SUDEP vs healthy controls (Figure 3.1.1 B-C). Regional segmentation analysis showed

that the thalamus as a whole was smaller in SUDEP vs healthy controls (Figure 3.1.1 C, 3.1.5 A).

The bilateral amygdala, entorhinal cortex, parahippocampal gyrus and subcallosal cortex showed increased grey matter volume in SUDEP vs healthy controls (regional segmentation and VBM; Figure 3.1.5 E-L and Figure 3.1.6, respectively). Regional segmentation analysis also revealed that all of these structures were larger in SUDEP vs low-risk patients (Figure 3.1.5 E-L). High-risk patients showed increased right amygdala grey matter volume vs healthy controls, using VBM (Figure 3.1.3 C), while regional segmentation analysis showed increased bilateral amygdala and parahippocampal gyrus volume (vs healthy controls and low-risk; Figure 3.1.5 E-H), and the entorhinal cortex (vs healthy controls only; Figure 3.1.5 I-J). In addition, we note a tendency for increased right amygdala grey matter in high-risk and SUDEP compared with low-risk patients, using VBM ($p < 0.001$ uncorrected; Figure 3.1.2 B-C).

Table 3.1.2. Analysis contrasts and results per method

Voxel-based Morphometry contrast	Results	Correction for multiple comparisons	Figure
SUDEP < Healthy control	Left posterior / medial thalamus, posterior hippocampus, vermis, bilateral lateral cerebellum, PAG	FWER	3.1.1a-c
SUDEP < low-risk		Uncorrected < 0.001	3.1.2a
High-risk < healthy control	Left posterior thalamus, vermis	FWER	3.1.3a
High-risk < low-risk	nil	N.A.	N.A.
SUDEP < high-risk	nil	N.A.	N.A.
Low-risk < healthy control	nil	N.A.	N.A.
SUDEP > healthy control	Bilateral amygdala, parahippocampus gyrus, entorhinal and subcallosal cortex	FWER	3.1.3b, 3.1.6
SUDEP > low-risk	Right amygdala, left entorhinal cortex	Uncorrected <0.001	3.1.2b
High-risk > healthy control	Right amygdala	FWER	3.1.3c
High-risk > low-risk	Right amygdala, temporal lobe		3.1.2c
SUDEP > high-risk	nil	N.A.	N.A.
Volumetry (using GIF) contrast			
SUDEP < Healthy control	Left thalamus, bilateral cerebellar gray matter	FWER	3.1.1; 3.1.5
SUDEP < low-risk	Bilateral cerebellar gray matter	FWER	3.1.5
High-risk < healthy control	nil	N.A.	N.A.
High-risk < low-risk	nil	N.A.	N.A.
SUDEP < high-risk	nil	N.A.	N.A.
Low-risk < healthy control	nil	N.A.	N.A.
SUDEP > healthy control	Bilateral amygdala, parahippocampal gyrus, entorhinal cortex and subcallosal cortex	FWER	3.1.5; 3.1.6
SUDEP > low-risk	As per SUDEP > HC	FWER	3.1.5
High-risk > healthy control	Bilateral amygdala, parahippocampal gyrus and entorhinal cortex	FWER	3.1.5
High-risk > low-risk	Bilateral amygdala and parahippocampal gyrus	FWER	3.1.5
SUDEP > high-risk	nil	N.A.	N.A.
Low-risk > healthy control	nil	N.A.	N.A.

N.A. = not applicable; nil = no result; HC = healthy control.

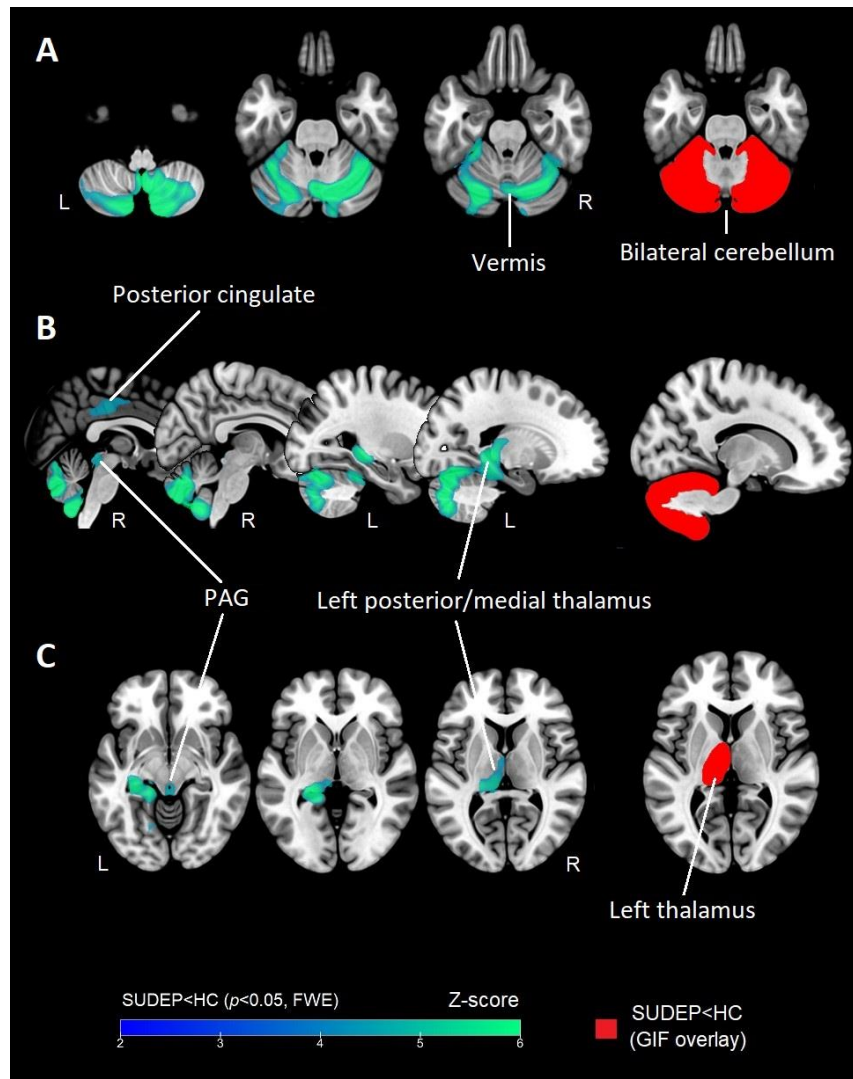


Figure 3.1.1. VBM-derived grey matter and ROI volume decreases in SUDEP compared with healthy controls. Bilateral cerebellum and vermis (A, B), PAG (B, C), the left medial and posterior thalamus (C), and the bilateral posterior cingulate (B). VBM contrast maps are overlaid onto a standard (MNI152) brain. Right column: ROI analysis results; The masks of segmented regions exhibiting reduced size in SUDEP < HC ($p < 0.05$, FWER) are overlaid in red.

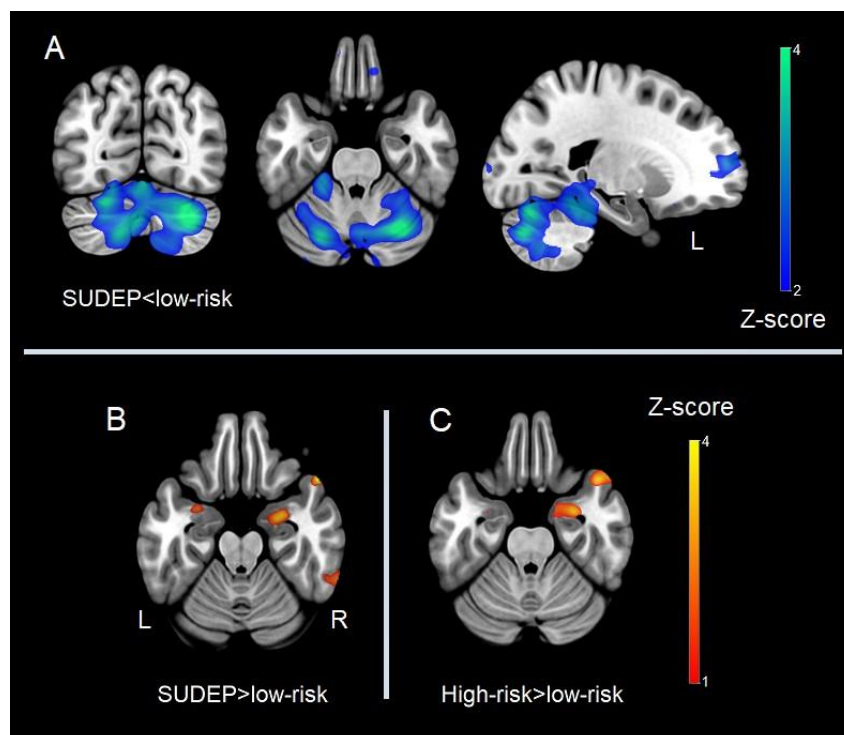


Figure 3.1.2. VBM grey matter volume alterations in SUDEP and high-risk subjects, compared with low-risk subjects. Volume loss in SUDEP compared with low-risk subjects within the cerebellum, vermis, left posterior hippocampus and thalamus, and right frontal lobe (A). Increased volume in SUDEP (B) and high-risk (C), compared with low-risk subjects in the right amygdala and aspects of the adjacent temporal lobe. $P < 0.001$.

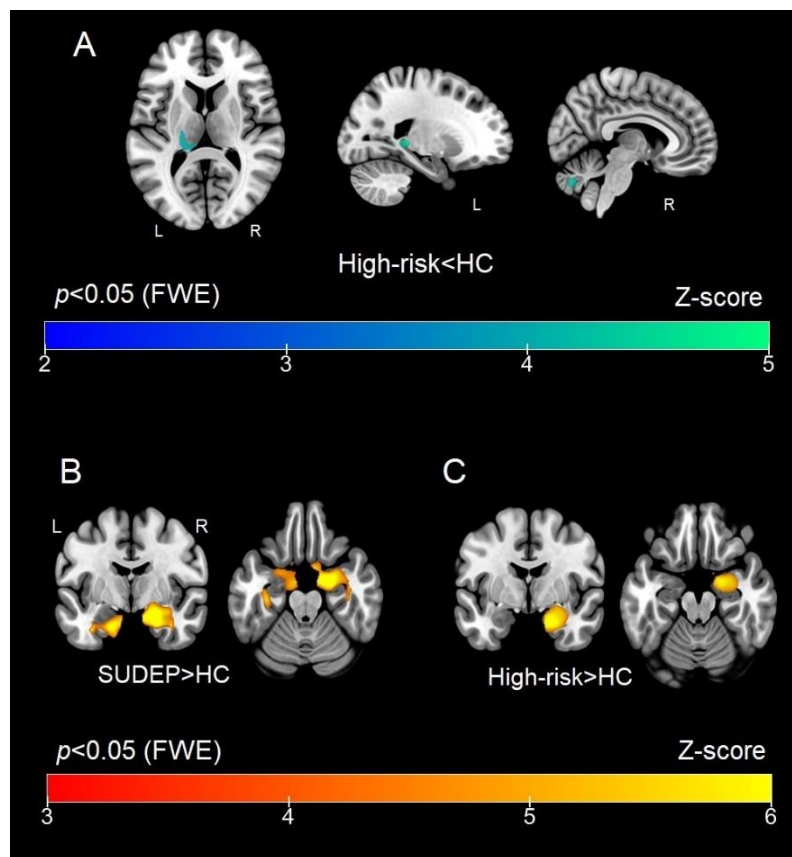


Figure 3.1.3. VBM grey matter volume alterations in SUDEP and high-risk subjects, compared with healthy controls. Reduced grey matter volume within the left posterior thalamus/hippocampus in high-risk subjects compared with healthy controls (A). Increased volume in the bilateral (B) and right (C) amygdala in SUDEP and high-risk, respectively.

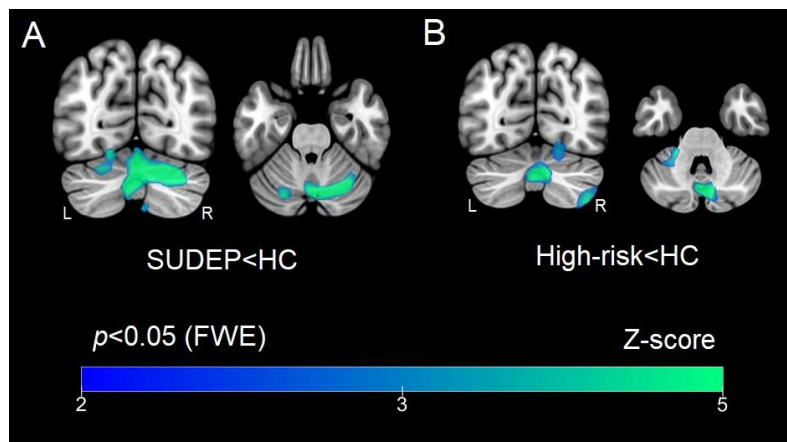


Figure 3.1.4. VBM grey matter reductions in non-phenytoin group. Grey matter loss was revealed in the cerebellum SUDEP (A) and high-risk (B) compared with healthy controls. Similar patterns of loss, particularly in the vermis are preserved. Results were FWER corrected ($p < 0.05$).

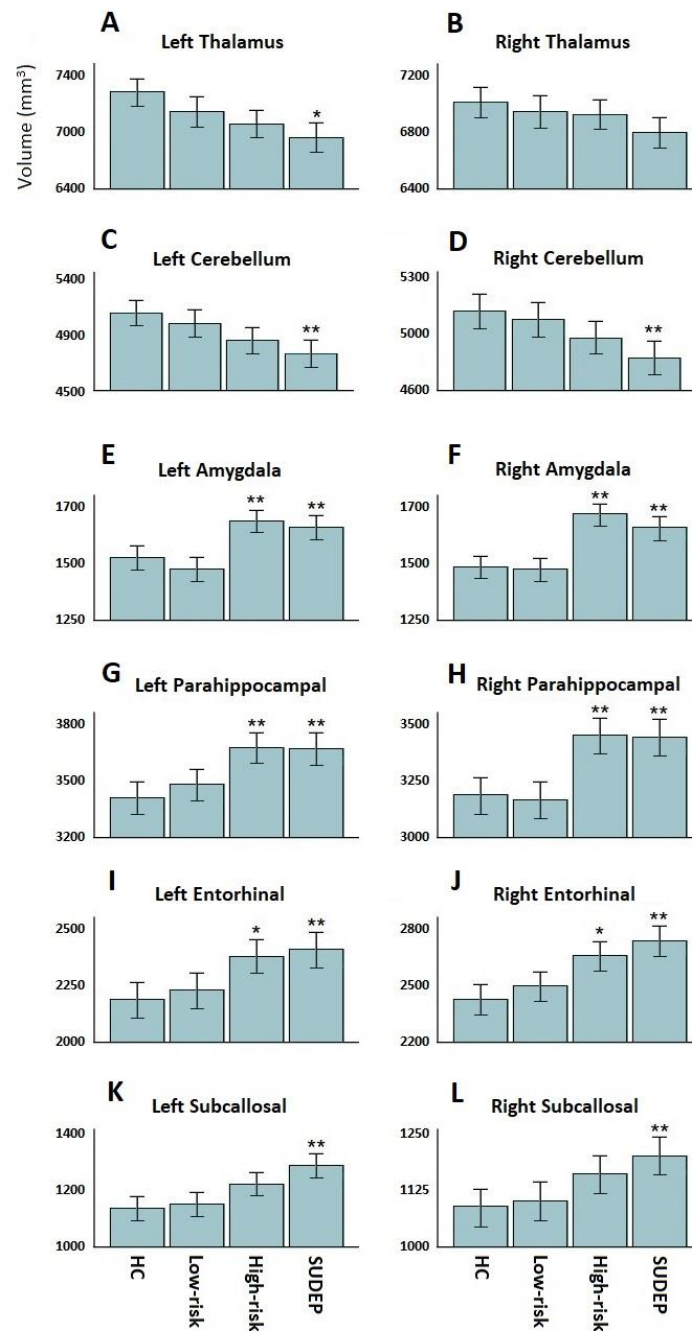


Figure 3.1.5. Results from ROI volume analysis displayed in bar graphs. Significant group volume differences were found in the thalamus (A, B), exterior cerebellar grey matter (C, D), amygdala (E, F), parahippocampal gyrus (G, H), entorhinal cortex (I, J) and subcallosal cortex (K, L). ** = significant at $p < 0.05$ (FWER) compared with low-risk and healthy controls. * = significant at $p < 0.05$ (FWER) compared with healthy controls only.

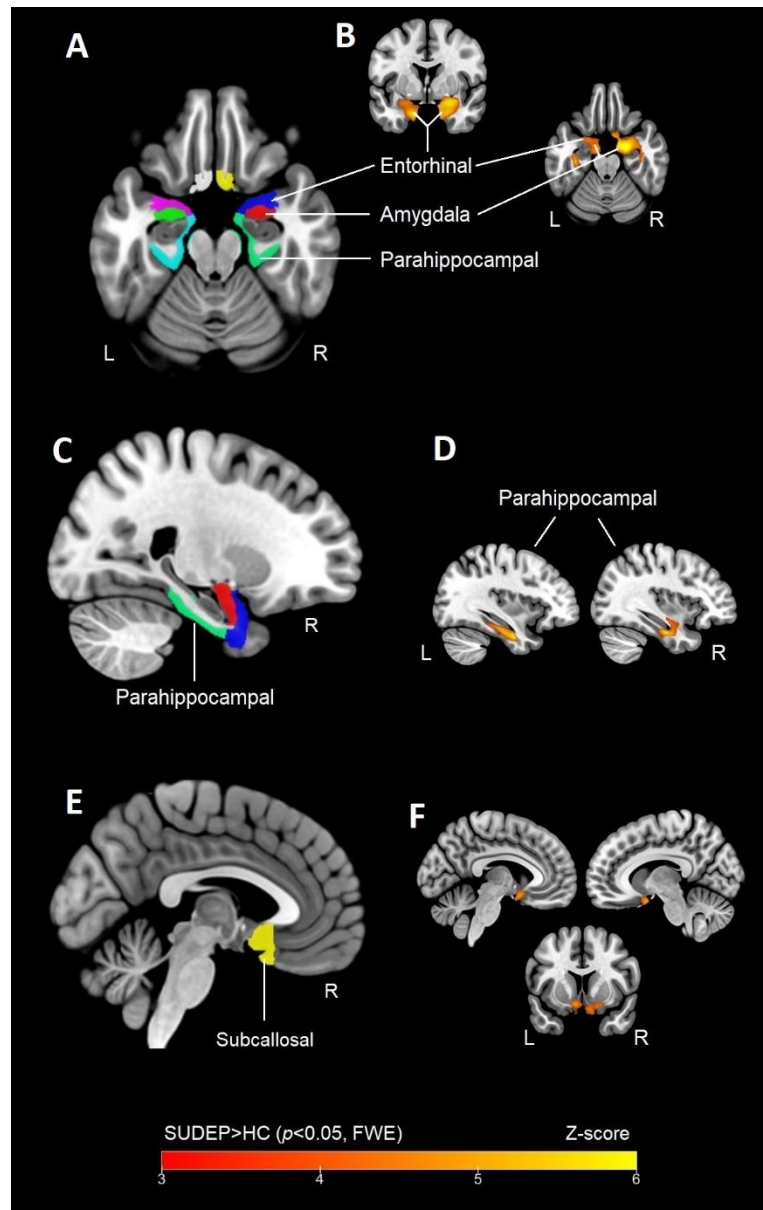


Figure 3.1.6. VBM grey matter and ROI volume increases in SUDEP. Regional volume increases in SUDEP compared with healthy controls, in the bilateral amygdala, entorhinal cortex, subcallosal cortex and parahippocampal gyrus (**B**, **D** and **F**). SPM contrast is overlaid in warm colours (red-yellow). Parcellation analyses (**A**, **C**, and **E**) show masks of segmented regions exhibiting increased size in SUDEP>HC ($p < 0.05$, FWER) overlaid in solid colours.

3.1.3.3 Correlational analyses

Significant partial correlations appeared between disease duration and left ($r = -0.325$, $p = 0.008$) and right ($r = -0.318$, $p = 0.009$) parahippocampal gyrus volume (Figure 3.1.7 A-B). Significant partial correlations also appeared between time-to-SUDEP from MRI in the left ($r = -0.4$, $p = 0.03$) and right ($r = -0.55$, $p = 0.006$) anterior insula (Figure 3.1.8 A-B), and the left ($r = -0.38$, $p = 0.04$) and right ($r = -0.47$, $p = 0.013$) midbrain (Figure 3.1.8 C-D).

GTCS frequency correlated positively with the right posterior cingulate ($r = 0.37$, $p = 0.005$) and bilateral anterior cingulate (left: $r = 0.28$, $p = 0.029$. right: $r = 0.26$, $p = 0.039$) volume, when SUDEP and high-risk were analysed in the same group ($n = 50$). When considered separately, high-risk ($n = 25$) showed positive correlations with the bilateral anterior cingulate (left: $r = 0.40$, $p = 0.036$. right: $r = 0.55$, $p = 0.005$), but insignificant correlations with the right posterior cingulate ($r = 0.35$, $p = 0.057$). When analysed alone, SUDEP cases ($n = 25$) showed positive correlations with the right hippocampus ($r = 0.54$, $p = 0.006$), but right posterior cingulate correlations were not significant ($r = 0.35$, $p = 0.063$). Negative correlations emerged with the left mid cingulate ($r = -0.39$, $p = 0.042$) and left anterior insula ($r = -0.45$, $p = 0.02$).

3.1.3.4 Anti-epileptic medication

The number of AEDs used at scan time did not significantly differ across patient groups. High-risk patients had been tried on a significantly greater number of AEDs throughout epilepsy duration vs SUDEP ($t = 3.97$, $p < 0.001$) and low-risk ($t = 6.1$, $p < 0.001$).

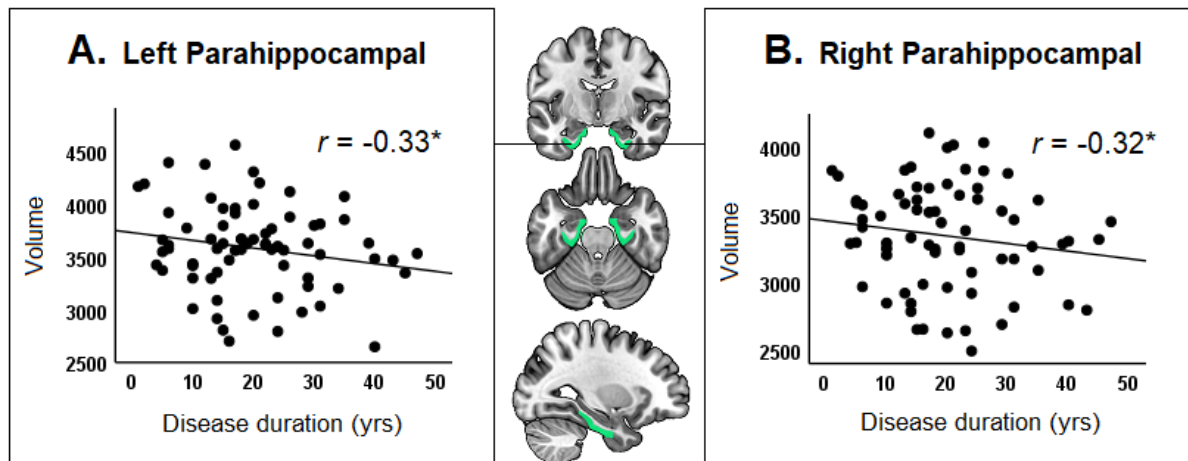
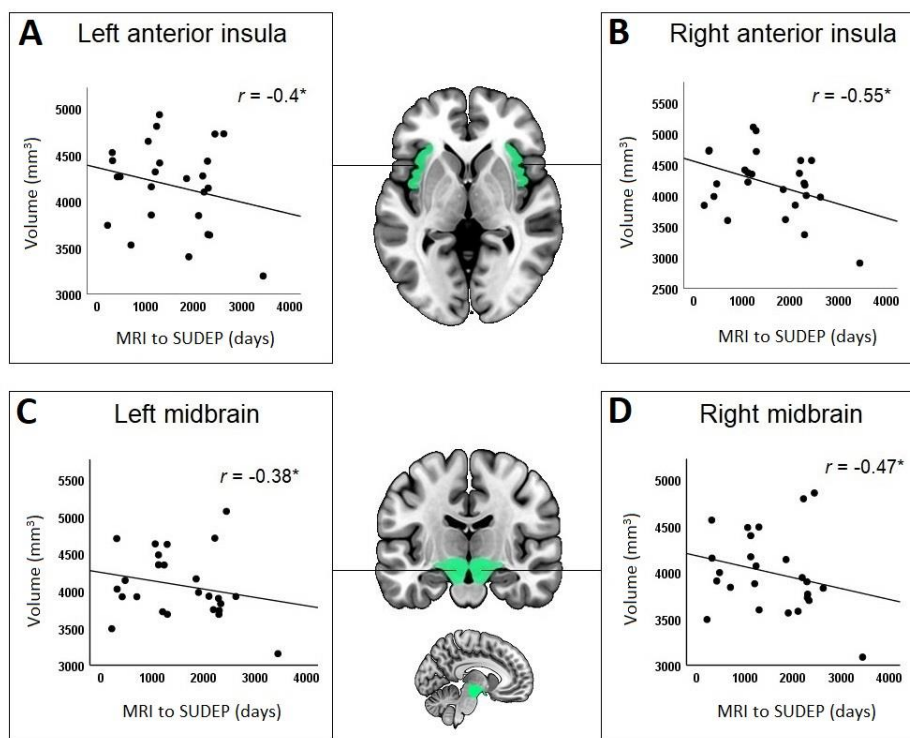


Figure 3.1.7. Partial correlations between parahippocampal volume and disease duration. Significant associations between Left (A) and Right (B) parahippocampal volume and disease duration across all epilepsy subjects. Covariates were seizure frequency, age, sex and total intracranial volume.



* $p < 0.05$ (FDR)

Figure 3.1.8. Partial correlations between regional volumes and time between MRI and SUDEP. Correlation plots showing associations between Left (A) and Right (B) anterior insula, and Left (C) and Right (D) midbrain, and time from MRI to SUDEP in SUDEP cases only. * = significant at $p < 0.05$ (FWER corrected). Covariates were seizure frequency, age, sex and total intracranial volume.

3.1.4 Discussion

3.1.4.1 Overview

SUDEP cases, and, to a lesser degree, those at high-risk, showed volume loss across a number of brain areas when compared with healthy controls and those at low-risk. Loss appeared in the thalamus, cerebellum and vermis, posterior cingulate and PAG. Increases in volume, of the amygdala, parahippocampal and entorhinal cortex, were also observed in high-risk and SUDEP cases. Changes were revealed using both conventional VBM, as well as through regional volumetry of brain structures.

Cerebellar and thalamic volume loss was most extensive in SUDEP, while PAG and posterior cingulate volume loss was exclusive to SUDEP, as was increased volume of the subcallosal cortex. Correlational analyses were performed between volumes and clinical variables, revealing associations with a number of brain areas though largely different from those showing loss in SUDEP and high-risk. Volume of the left mid/posterior cingulate showed a negative correlation with GTCS frequency, offering a potential explanation for the volume loss observed here in SUDEP. Otherwise, the direction of associations with clinical variables could not explain the volume alterations observed in SUDEP and high-risk.

3.1.4.2 Cerebellar volume loss

Extensive volume loss within the cerebellum was observed in SUDEP, and to a lesser extent in high-risk, compared with healthy controls and low-risk subjects; low-risk patients did not show significant loss compared to healthy controls. The cerebellum plays roles in movement coordination, recovering from blood pressure changes (Ramu & Bergmann, 1967), chemosensing, recovery from hypercarbia (Calton, Howard,

Harper, Goldowitz, & Mittleman, 2016) and compromised breathing circumstances (Xu & Frazier, 2002), and timing of upper airway and diaphragm action in obstructive and central apnea (Henderson et al., 2003); all potentially relevant issues in the circumstances surrounding SUDEP (Massey, et al., 2014). Cerebellar volume loss occurs commonly in epilepsy, and is associated with poor surgical outcome (Marcian et al., 2018), chronicity (Oyegbile et al., 2011), GTCS (Szabo et al., 2006) and AED use (De Marcos et al., 2003). These issues are of concern, since all, particularly poor surgical outcome (Tomson, Nashef, & Ryvlin, 2008) and GTCS (Harden et al., 2017) involve cohorts at greatest risk of SUDEP. However, the precise mechanisms and origins of cerebellar volume loss in epilepsy, and in the current study are not known.

One possible explanation is that cerebellar tissue loss may result from excitotoxic processes following excessive activation of pontine or long climbing fibres of olivary projections. The structural impingement of climbing fibres on Purkinje dendrites is such that excessive activation readily kills Purkinje neurons (Welsh et al., 2002), a process well-known in the neurotoxicity field, but potentially operating similarly during ictal events. Repeated or prolonged GTCS could establish a scenario for Purkinje cell death. If damaged Purkinje cells cannot effectively control the deep fastigial “autonomic” and “breathing” nuclei, recovery from hypotension or apnea, known to accompany ictal events in GTCS (Bozorgi et al., 2013; Lhatoo, Noebels, Whittemore, & Research, 2015) may be hampered; an inability to recover from such disturbances could contribute to SUDEP.

Overall, while the cerebellum plays important roles in the central control of autonomic and breathing action, further work is needed to ascertain the origins of tissue loss in epilepsy and those found to be associated with SUDEP.

3.1.4.3 Limbic and PAG volume loss

Volume loss appeared in the PAG and bilateral posterior cingulate in SUDEP, as well as the left posterior thalamus and hippocampus in both SUDEP and high-risk groups. Reduced posterior thalamic loss has been described earlier (Wandschneider et al., 2015). Damage here could potentially contribute to failure to sense low oxygen and hypercapnia (Harper et al., 2005); dysfunctional responses to hypercapnia (Harper et al., 2005) are pronounced in the left posterior thalamus in congenital central hypoventilation syndrome.

The PAG receives direct projections from the amygdala central nucleus (Hopkins & Holstege, 1978). Both the PAG and posterior cingulate assist respiratory and cardiovascular regulation, showing single neuron discharge related to both breathing and cardiac timing (Ni, Zhang, & Harper, 1990a, 1990b). PAG volume loss has been shown earlier in SUDEP (Mueller et al., 2014). The ventrolateral PAG can elicit substantial increases in sustained (i.e. “freezing”) muscle tone via the lateral vermis of the cerebellum, a source of concern when attempting to initiate cyclic breathing during an ictal event (Koutsikou et al., 2014). Deficient cardio-respiratory compensatory mechanisms mediate by the PAG have been shown to contribute to SUDEP in mice (Kommajosyula, Tupal, & Faingold, 2018). Volume loss may indicate dysfunction of the PAG, a concern given its roles in cardiorespiratory recovery (Kommajosyula, Tupal, & Faingold, 2018) and arousal processes (Edlow et al., 2012).

3.1.4.4 Anterior limbic volume increases

Increased amygdala volume is relevant because of its marked influences on breathing; stimulation elicits apnea in human epilepsy (Dlouhy et al., 2015), and triggering of respiratory phase changes in animal models (Harper, Frysinger, Trelease, & Marks, 1984). Similar amygdala volume increases have been described in SUDEP (Wandschneider et al., 2015), those at risk (Bernhardt, Hong, Bernasconi, & Bernasconi, 2015) and the common epilepsies (Whelan et al., 2018). While volume loss is known to be associated with atrophy and cell loss, implicating potential deficient processes, increases in volume are more difficult to interpret. As discussed in the previous chapter, increases in volume may reflect function gain, or compensatory processes, though they could also reflect responses to excessive neuronal injury, i.e. neuronal sprouting (Sobkowicz & Slapnick, 1992; Love et al., 2005). Either way, structural alterations in the amygdala are of concern given its role in breathing regulation. A potential explanation, and notable limitation of these findings, is that the elevated medial temporal volume may result from tissue sagging from brain atrophy in the posterior fossa, which can cause tissue accumulation in the medial fossa. Future studies evaluating epilepsy cohorts, particularly those involving subjects with chronic epilepsy, should take this possibility into account.

The subcallosal cortex was enlarged only in SUDEP, and represents a significant concern if enhanced volumes indicate increased influences; electrical stimulation of the subcallosal area results in profound hypotension (Lacuey et al., 2018b).

3.1.4.5 Antiepileptic drugs

Cerebellar atrophy in patients with epilepsy following use of particular AEDs, such as phenytoin, is well-described (De Marcos et al., 2003). We documented medication history of all patients, including exposure to phenytoin. The number of patients with phenytoin exposure in SUDEP, high-risk and low-risk groups was 5, 8 and 3, respectively, with only 2 SUDEP and 3 high-risk having use >10 years. Sub-analyses of SUDEP and high-risk groups, with removal of those with phenytoin exposure (and controlling for phenytoin use as a binary covariate), showed similar patterns of cerebellar volume loss to those groups before removal, although reduced in extent (particularly in lateral cerebellar areas; Figure 3.1.4), suggesting that tissue loss here, specifically in the vermis, cannot solely be attributed to phenytoin use. Notably, removing these subjects did not significantly alter other findings of increased or decreased volume. Across groups, the number of AEDs in the treatment regimen of patients at scan time did not significantly differ. However, high-risk patients had, on average, tried a greater number of AEDs throughout their epilepsy duration, which was significantly greater than SUDEP cases and low-risk patients. No significant differences between SUDEP and low-risk appeared with total number of AEDs historically trialled. While high-risk subjects and SUDEP cases had historically tried a greater number of AEDs compared with low-risk subjects, there is currently little evidence to suggest that any individual, or combination of AED(s) is responsible for SUDEP or a significant elevation in risk. Specifically, lamotrigine is not associated with increased SUDEP risk, as was previously thought, and the number of AEDs used is not an independent SUDEP risk factor (Hesdorffer et al., 2012). Rather, additional AEDs reduce the risk of SUDEP in drug refractory patients (Ryvlin, Cucherat, & Rheims, 2011). It should,

however, be noted that the precise role of AEDs in SUDEP risk is not entirely clear, and studies exploring this aspect are needed. In summary, the role of seizures or AED use in cerebellar atrophy in epilepsy remains unclear, despite evidence for both (De Marcos et al., 2003; Hagemann et al., 2002). However, either scenario is concerning, given the cerebellum's vital roles and the observed volume loss in SUDEP. Medication-induced injury remains an important consideration for epilepsy imaging studies.

3.1.4.6 Correlational analyses with clinical variables

Reduced parahippocampal volume correlated with disease duration across all epilepsy subjects. Progressive atrophy of mesial temporal structures occurs in temporal lobe epilepsy (Caciagli et al., 2017), and reduced volume of sub-cortical structures, including the parahippocampal gyri, is associated with greater disease duration in the common epilepsies (Whelan et al., 2018). Our data reinforce an association between reduced sub-cortical volume and disease duration. It should, however, be noted that, being a cross-sectional design, the current study did not assess progressive changes in structural volumes due to lack of follow-up scans in many subjects. Progressive changes could be assessed with longitudinal imaging studies, which may elucidate the evolution of volumetric alterations and their association with SUDEP risk, a future objective of imaging research into epilepsy and SUDEP.

Bilateral anterior insula and midbrain volumes correlated negatively ($p < 0.05$, FWER) with time-to-SUDEP from MRI, meaning volumes were increased the closer to SUDEP from scan time. This suggests that progressive enlargement of certain structures may accompany processes leading to SUDEP, although this would need to be assessed with longitudinal imaging studies.

3.1.4.7 Generalized tonic-clonic seizures

Since both people at high-risk and cases of SUDEP experience GTCS, a key aim of imaging studies is to outline their association with regional volume and consider any changes in relation to group comparisons with people not experiencing GTCS (healthy controls and people at low-risk). The association between GTCS and regional volumes was assessed by performing correlational analyses. If regional increases or decreases in volume resulted from GTCS, significant correlations between GTCS frequency and volume changes should occur. However, correlation analyses with GTCS frequency and the size of structures which showed group differences (i.e. the reduced cerebellar, vermal and thalamic volume, or the increased amygdala, entorhinal, parahippocampal or subcallosal volume) were small (non-significant) in the SUDEP and high-risk patients. One structure which showed a significant group difference (SUDEP < healthy control), the right posterior cingulate, showed a weak significant positive correlation with GTCS frequency (only when SUDEP and high-risk were considered in the same group). However, since this was a positive correlation, it may not offer insight into the volume loss of this structure observed in SUDEP. Significant positive correlations between GTCS frequency and volume were also observed for the bilateral anterior cingulate, when combining both SUDEP and high-risk subjects in one group. Cortical thickening of the cingulate has been recently demonstrated in GTCS patients (Ogren et al., 2018). Volume elevations associated with gliosis resulting from hyperexcitability due to repeated seizures may be operating (Binder & Steinhäuser, 2006), and may be indicative of limbic network dysfunction linked to GTCS (Bernhardt et al., 2009).

When high-risk and SUDEP groups were considered separately, correlations between the right posterior cingulate volume and GTCS frequency became non-significant in both groups, and the finding of increased anterior cingulate volume with GTCS frequency remained the same in high-risk, but became non-significant in SUDEP. In SUDEP cases only, additional significant correlations between volume and GTCS frequency emerged, including a positive correlation with the right hippocampus and negative correlations with the left mid cingulate and left anterior insula. These findings suggest that brain volumetric processes related to elevated GTCS frequency may be manifested differently in high-risk and SUDEP.

Finally, a critical difference between high-risk and SUDEP groups (who had very similar GTCS frequencies and disease durations) was volume loss in the PAG and posterior cingulate, and increased volume of the subcallosal cortex, which was evident only in SUDEP. We believe this to be important since if specific to GTCS, such volume alterations might be expected in high-risk subjects as well. This was not the case, however, suggesting that these alterations may be separate from GTCS processes. GTCS and disease duration, along with other clinically relevant factors, will remain critical considerations for all studies investigating SUDEP, especially imaging ones, and efforts to take this into account should be made in any future studies.

3.1.4.8 Stratification of living subjects into high- and low-risk

Living high- and low-risk patients were classified based on experience and frequency of GTCS. High-risk subjects were those experiencing more than three GTCS per year. Although risk-stratification is difficult (as discussed previously in chapter [2.1](#)), the current classification was based on the leading SUDEP risk-factor, which also

distinguished more than 80% of SUDEP cases here. The only variable to distinguish a greater number of SUDEP cases was presence of GTCS, which is a weaker SUDEP risk factor (Harden et al., 2017), and its use to define high-risk would only limit interpretation of results. While this may be seen as a limitation, it should also be noted that, in doing so, other factors known to influence volume changes, such as age, sex and disease duration, could be partially accounted for by attempting to match subjects with similar attributes; thus, we were able to shed light on imaging changes related not only to SUDEP but the greatest risk-factor associated with the fatal event.

3.1.4.9 Conclusion

We found SUDEP to be accompanied by tissue changes in brain structures involved in cardiovascular and breathing patterning, and in cerebellar and brainstem structures which involved in recovery from cardiorespiratory dysfunction. High-risk subjects showed alterations within similar regions, suggesting such features could be used to prospectively identify patients at risk. Non-invasive volumetric assessments within identified sites may shed light on potential neural predispositions and represent further biomarkers of SUDEP. However, the precise origins and mechanisms of volume alterations found in SUDEP and those at risk are unknown, and a clear link between such changes and SUDEP remains lacking.

3.2: Brain morphometric alterations accompanying GTCS with hypoxemia: a prospective structural imaging study

3.2.1 Rationale and motivation

Previous structural imaging studies, as discussed in chapter [1.5](#) and demonstrated in chapter [3.1](#), have shown regional brain structural changes in patients who later succumb to SUDEP, as well as those at elevated risk, as assessed with morphometry and volumetry procedures.

Increases and decreases in grey matter appear across a number of sites important for autonomic, breathing, sensory and other processes, but the mechanisms of these alterations remain poorly understood, as does their precise relationship with SUDEP.

Lacking are prospective studies investigating the link between SUDEP risk factors observed in epilepsy monitoring units (such as physiological, autonomic and respiratory alterations) and brain structural changes. Such findings may provide neurobiological markers for early detection of SUDEP risk, and shed light on SUDEP mechanisms.

The focus of this study is centred around the work of an ongoing prospective investigation into autonomic and imaging biomarkers of SUDEP being undertaken at the National Hospital for Neurology and Neurosurgery, the goal of which is to characterise the nature of injury to autonomic and breathing sites as previously found, in terms of their association with measurable SUDEP risk factors, and potential biomarkers of SUDEP, observed in the EMU; namely hypoxemia in this case.

3.2.2 Background

As outlined in chapter 1, the processes leading to SUDEP appear to involve a centrally mediated post-ictal pattern of breathing and cardiovascular dysfunction; namely transient periods of apnea and normal breathing leading to terminal apnea and asystole (Ryvlin et al., 2013). Hypoxemia – abnormally low concentrations of oxygen in the blood – is associated with post-convulsive central apnea (Vilella et al., 2019b), and hypoventilation (Bateman et al., 2008); both potentially involved in the processes leading to SUDEP. Hypoxic exposure is known to result in neuronal injury to central autonomic structures (such as the fastigial nuclei of the cerebellum; Pae, Chien & Harper, 2005), and is linked to dysfunctional responses in thalamic respiratory sites (Macey et al., 2005; Koos et al., 2016).

Hypoxemia could impair recovery from significant cardiovascular or respiratory distress if the central nervous system, including regulatory brain sites, are damaged and/or cannot appropriately respond due to inadequate oxygenation, representing a potential SUDEP mechanism. As such, the goal of the present study was to assess regional brain morphometric (grey and white matter volume) alterations relative to the degree of reductions in peripheral capillary oxygen (SpO₂) saturation (hypoxemia) as well as duration of hypoxemia in patients with GTCS. Such an assessment would enable characterisation of neuronal injury associated with hypoxemia and may enhance understandings of processes underlying brain structural alterations in SUDEP, and clarify the nature of strategies that might be incorporated to prevent neural injury during ictal events.

3.2.3 Methods

3.2.3.1 Subjects

Subjects were identified from a database of patients recruited as part of an ongoing prospective investigation into autonomic and imaging biomarkers of SUDEP (the center for SUDEP research; CSR) being conducted at University College London (UCL) and Case Western Reserve University (CWRU). All subjects gave written informed consent. Included subjects were those with a GTCS captured during their epilepsy monitoring unit (EMU) admission, with available pulse oximetry data and a T1-weighted MRI scan (carried out at either UCL or CWRU). Exclusion criteria were: incomplete physiological data (missing or incomplete pulse oximetry data), previous neurosurgery, large brain lesions, incomplete clinical data, incomplete (or artefact degraded) MRI scan and those undergoing intra-cranial investigations.

N=43 subjects were included for image analysis (23 UCL, 20 CWRU) and separated into two groups: '*GTCS-hypox*': subjects who had a GTCS with hypoxemia; and '*GTCS-hypox-no*': those in which hypoxemia did not feature in their GTCS. A group of age- and sex-comparable healthy controls, scanned at UCL, were included for comparisons with patient cohorts. Group characteristics were compared using non-parametric statistical tests in IBM SPSS v25 (Armonk, NY: IBM Corp). Clinical characteristics of groups can be found in table 3.2.1.

Two SUDEP cases were identified from this cohort of subjects. Though not included in statistical analysis, details regarding these cases, and the potential relevance to the results observed here, are outlined in the discussion, section [3.2.5.5](#).

3.2.3.2 Identification and definition of hypoxemia

Subjects underwent continuous SpO₂ monitoring during a prolonged video-EEG (electroencephalography) investigation. SpO₂ was measured using pulse oximetry (NONIN 8000J [Plymouth, MN, USA]). Subjects with hypoxemia were defined as those with oxygen desaturations reaching below 94% peri-GTCS. Measurements were obtained from the onset of the generalized phase until SpO₂ recovered to baseline. Those with SpO₂ measurements above 94% were allocated to the non-hypoxemia group (Lacuey et al., 2018a). Hypoxemia duration was calculated as the length of time during which sPO₂ was below 94%, in seconds (s). The *GTCS-hypox* group were further split into two groups for sub analyses: those in whom oxygen desaturations reached below 75% (*GTCS-hypox-severe*; n=10), indicating severe hypoxemia; and those in whom SpO₂ remained between 75%-94% (*GTCS-hypox-mild/moderate*; n=12), indicating mild-moderate hypoxemia. Group cut-off values were based on Lacuey et al., 2018a. Details of these sub-groups can be found in table 3.2.2.

Additionally, we calculated the difference in SpO₂ between baseline and the lowest recorded, giving an individual measure of peri-ictal oxygen desaturation (degree of SpO₂ loss). We then used this a covariate of interest in ROI analyses to explore associations between regional brain volumes and oxygen desaturation. For subjects with more than one GTCS recorded, the single lowest SpO₂ measurements were averaged across each seizure before subtracting from averaged baseline, and duration of hypoxemia (s) was averaged across seizures. Baseline SpO₂ readings were obtained during periods of resting inter-ictal wakefulness. Correlations were also

performed between duration of hypoxemia, degree of oxygen desaturation and GTCS frequency.

3.2.3.3 MRI acquisition

High-resolution 3D T1-weighted images were acquired on 3.0-Tesla MRI scanners at two centres; University College London (London, United Kingdom), and Case Western Reserve University Hospitals (Cleveland, Ohio, United States). Image acquisition parameters (UCL/UH) were as follows: FOV (mm) = 224×256×256 / 230×173×230; acquisition matrix = 224×256×256 / 256×192×256; voxel size (mm) = 1.0×1.0×1.0 / 0.7×0.9×0.7; TR (repetition time, ms) = 7.4 / 7.3; TE (echo time, ms) = 3.1 / 2.38; TI (inversion time, ms) = 400 / 900; flip angle (degrees) = 11 / 9.

3.2.3.4 Image analysis

3.2.3.4.1 Voxel-based morphometry (VBM)

To explore brain-wide differences in grey and white matter volume across groups, VBM was implemented using CAT12, as per methods in chapter [3.1.2.3](#).

Images were processed identically to the previous chapter in this study, apart from undergoing z-score normalization (-mean/standard deviation), following modulation, in order to correct for potential intensity differences related to using data from two separate scanners. Z-score maps were then smoothed with an 8mm full-width-at-half-maximum (FWHM) Gaussian kernel before statistical analysis in SPM. Total grey and white matter volume was combined per subject to generate a measure of total brain volume which was used as a covariate in subsequent statistical modelling, to account for differences in whole brain volume across subjects. Two-sample t-tests were used

for group comparisons in SPM, with age, sex and total brain volume as covariates. Reported p -values were FWER corrected (largest cluster at $p < 0.05$).

3.2.3.4.2 Region of interest analysis

In addition to VBM, volumetric measurements of regions of interest (ROIs) were calculated in order to compare volumes across sub-groups and quantify relationships between regional volumes and peri-ictal oxygen desaturation and hypoxemia duration. Each subject's (non-normalized and bias corrected) T1 image was segmented and parcellated into 146 brain regions using GIF (Cardoso et al., 2015) and volumes were derived as described in chapter [3.1.2.4.1](#). ROI volumes were Z-score normalized before comparison. For structures where an appropriate ROI parcel was not available using GIF (i.e. the PAG), mean grey or white matter values were extracted from each subject's (grey or white) tissue probability map by isolating the corresponding region-specific cluster from the group SPM map, and using this as a mask; these procedures were carried out in Matlab using Marsbar and SPM functions. ROI volumes were compared across all sub-groups using multi-variate analysis of covariance (MANCOVA) and post-hoc permutation two-sample t-tests (with covariates age, sex and total brain volume; 10000 permutations). Partial correlations between regional volumes and degree of oxygen desaturation / hypoxemia duration were performed, accounting for GTCS frequency, disease duration, and total brain volume. Covariates (i.e. GTCS frequency and disease duration) were also explored as variables of interest to highlight any associations with regional volumes. Since age and disease duration were correlated, these variables were entered in separate models to avoid problems

with collinearity. Statistical tests were carried out in SPSS and P-values were FWER corrected in Matlab.

Table 3.2.1. Group demographics and clinical characteristics.

CHARACTERISTICS	HC (N=43)	ALL GTCS (N=43)	GTCS-HYPOX (N=22)	GTCS-HYPOX- NO (N=21)
AGE, YEARS (MEAN±SD)	35.3 ± 12.9	34.1 ± 11.1	36.9 ± 13.1	31.2 ± 7.9
SEX (M:F)	26:17	26:17	9:13	17:4
DISEASE DURATION, YEARS (MEAN±SD)		15.8 ± 9.7	18.09 ± 11.1	13.3 ± 7.3
GTCS/YEAR (MEAN±SD)		16.7 ± 24.1	18.09 ± 24.9	15.12 ± 23.60
NUMBER AEDS (MEAN±SD)		2.9 ± 1.0	2.86 ± 0.9	2.86 ± 1.1
TBV, ML (MEAN±SD)	1180.1 ± 118.4	1158.5 ± 116.7	1121.8 ± 105	1196.9 ± 118.3
DEGREE OF SPO₂ LOSS			24	
Median (%)			7 - 64	
Range (%)				
HYPOXEMIA DURATION			95	
Median (s)			21 - 415	
Range (s)				
SEIZURE ONSET ZONE				
FOCAL (COUNT)		35	16	19
MULTI-FOCAL (COUNT)		3	2	1
GENERALIZED (COUNT)		5	4	1

HC = healthy control; GTCS = generalized tonic-clonic seizure; hypox = hypoxemia; SD = standard deviation;

AEDs = anti-epileptic drugs; TBV = total brain volume; ML = millilitres; SpO₂ = peripheral oxygen saturation.

Table 3.2.2. Demographics and clinical characteristics of the GTCS hypoxemia sub-groups

<u>CHARACTERISTICS</u>	<i>HYPOX MILD/MODERATE (N=12)</i>	<i>HYPOX SEVERE (N=10)</i>	P-VALUE
AGE, YEARS (MEAN±SD)	38.1 ± 12.1	35.4 ± 14.7	0.50
SEX (M:F)	5:7	4:6	0.47
DISEASE DURATION (YEARS, MEAN±SD)	19.9 ± 11.2	15.9 ± 10.6	0.25
GTCS/YEAR (MEAN±SD)	23.8 ± 28.6	11.4 ± 19.2	0.42
NUMBER AEDS (MEAN±SD)	2.75 ± 1.1	3.0 ± 0.8	0.67
TBV, ML³ (MEAN±SD)	1106 ± 109.6	1140.7 ± 101.6	0.28
HYPOX DURATION (S, MEAN±SD)	169.5 ± 117.2	81.9 ± 38.4	0.31
DEGREE HYPOX (% , MEAN±SD)	13.3 ± 6.1	41.9 ± 15	<0.001*
<u>SEIZURE ONSET ZONE (COUNT)</u>			
FOCAL	10	7	N.A.
MULTI-FOCAL	2	0	N.A.
GENERALIZED	2	3	N.A.

Hypox = hypoxemia, GTCS = generalized tonic-clonic seizure, AEDs = anti-epileptic drugs, TBV = total brain volume, ML = millilitres, S = seconds.

3.2.4 Results

3.2.4.1 Demographic and clinical characteristics

All groups were comparable for age. *GTCS-hypox-no* had significantly fewer females compared with the *GTCS-hypox* group ($\chi^2 = 7.2$, $p = 0.007$). Otherwise, groups were comparable for ratio of males to females.

Disease duration was greater in *GTCS-hypox*, though this did not reach statistical significance. Number of GTCS per year and number of AEDs being taken did not significantly differ between *GTCS-hypox* and *GTCS-hypox-no* groups. Total brain volume did not significantly differ between groups after accounting for age effects.

The degree of SpO₂ desaturation was significantly greater in the *GTCS-hypox-severe* group, compared with the *GTCS-hypox-mild/moderate* group ($Z = 3.9$, $p < 0.001$). Age, sex, disease duration, GTCS frequency, number of AEDs, total brain volume and hypoxemia duration did not significantly differ between *GTCS-hypox-severe* and *GTCS-hypox-mild/moderate* (table 3.2.2).

GTCS frequency correlated positively with hypoxemia duration ($r = 0.6$, $p = 0.001$), controlling for sex and disease duration.

3.2.4.2 VBM

3.2.4.2.1 Grey matter

Compared with healthy controls, *GTCS-hypox* showed reduced grey matter volume in the bilateral cerebellum, vermis, temporal pole, periaqueductal grey (PAG), hypothalamus, thalamus and right superior temporal gyrus (Figure 3.2.1 a-d), and increased grey matter volume in the bilateral amygdala and entorhinal cortex (Figure

3.2.1 e-h). *GTCS-hypox-no* showed grey matter loss in the bilateral cerebellum only (Figure 3.2.1 i), when compared with healthy controls.

3.2.4.2.2 White matter

GTCS-hypox showed reduced white matter volume in the medulla (including dorsal and ventral respiratory groups; Figure 3.2.2 a-b, d) and the dorsal pons (including the parabrachial complex; Figure 3.2.2 c-g).

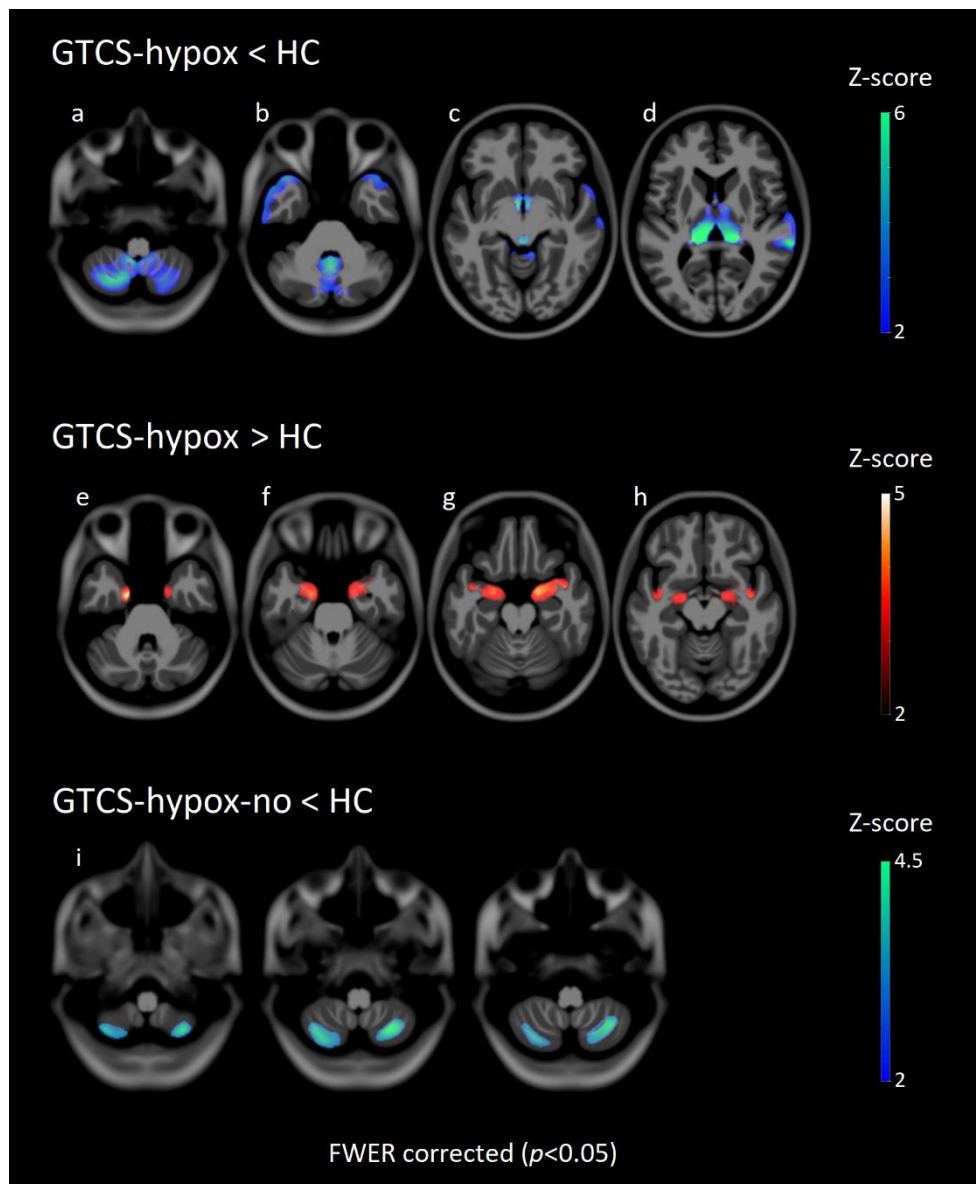


Figure 3.2.1. Grey matter VBM contrasts with healthy controls for GTCS-hypox and GTCS-hypox-no. Grey matter alterations in GTCS-hypox compared with HC: volume loss is seen in the cerebellum (a), vermis and temporal pole (b), hypothalamus and PAG (c) and bilateral thalamus (d). Volume increases are seen in the bilateral amygdala, entorhinal cortex (e-h) and ventral-anterior insula (h). Grey matter volume loss of bilateral lateral cerebellum in GTCS-hypox-no compared with HC (i).

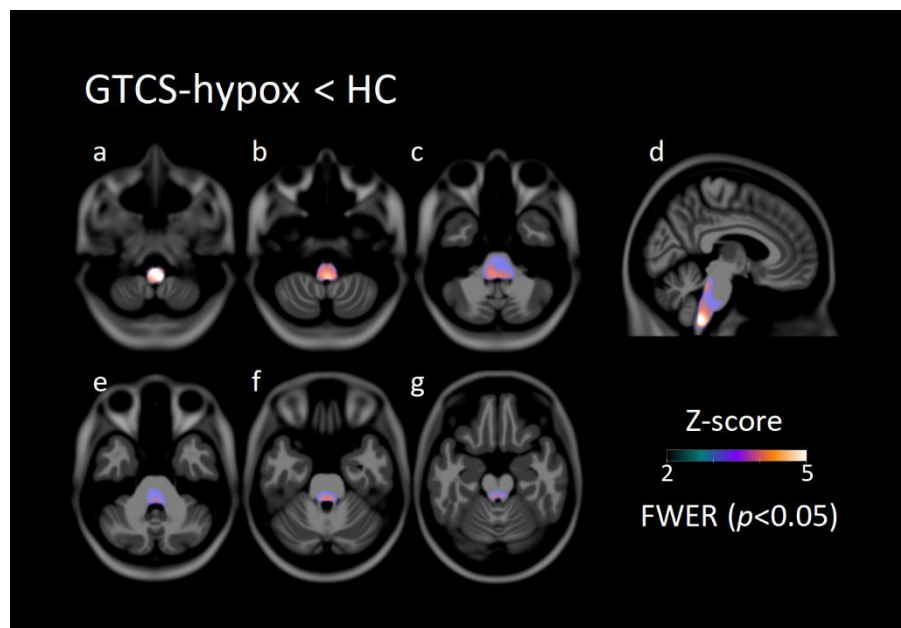


Figure 3.2.2. White matter VBM contrasts for GTCS-hypox compared with with healthy controls. Significantly reduced white matter in GTCS with hypoxemia compared with healthy controls. White matter loss was revealed in the medulla of the lower brainstem (a-b, d) and parabrachial area of the pons (c-g).

3.2.4.3 ROI analysis

3.2.4.3.1 Sub-group differences

ROI volumes of structures showing significant group-level VBM effects were compared across all sub-groups. Significant main effects were found for left ($F = 15.5$, $p = 5.12E-08$) and right ($F = 14.5$, $p = 1.34E-07$) thalamus, PAG ($F = 8.1$, $p = <0.0001$) and medulla ($F = 6.5$, $p = 0.002$). All ROI volume results are displayed in Figure 3.2.3.

Left and right thalamic volume was reduced in all sub-groups compared with healthy controls (*GTCS-hypox-no* [left: $t = 2.8$, $p = 0.007$ / right: $t = 2.5$, $p = 0.18$]; *GTCS-hypox-mild/mod* [left: $t = 3.6$, $p = 0.001$ / right: $t = 2.9$, $p = 0.005$]; *GTCS-hypox severe* [left: $t = 6.4$, $p = 4.43E-08$ / right: $t = 6.2$, $p = 9.66E-08$]).

Thalamic volumes in *GTCS-hypox-severe* were also significantly reduced when compared with *GTCS hypox-no* (left: $t = 3.2$, $p = 0.003$ / right: $t = 3.4$, $p = 0.002$) and *GTCS-hypox-mild/mod* (left: $t = 2.6$, $p = 0.016$ / right: $t = 3.4$, $p = 0.003$).

PAG volume was significantly reduced in *GTCS-hypox-severe* when compared with healthy controls ($t = 5.6$, $p = 7.58E-07$), *GTCS-hypox-no* ($t = 3.9$, $p = 0.001$) and *GTCS-hypox-mild/mod* ($t = 2.1$, $p = 0.48$). *GTCS-hypox-mod* had reduced PAG volume compared with healthy controls only ($t = 2.1$, $p = 0.042$).

Medulla volume was reduced in *GTCS-hypox-severe* compared with healthy controls ($t = 4.0$, $p = < 0.001$) and *GTCS-hypox-no*, ($t = 2.4$, $p = 0.024$) and in *GTCS-hypox-mild/mod* compared with healthy controls only ($t = 2.1$, $p = 0.041$).

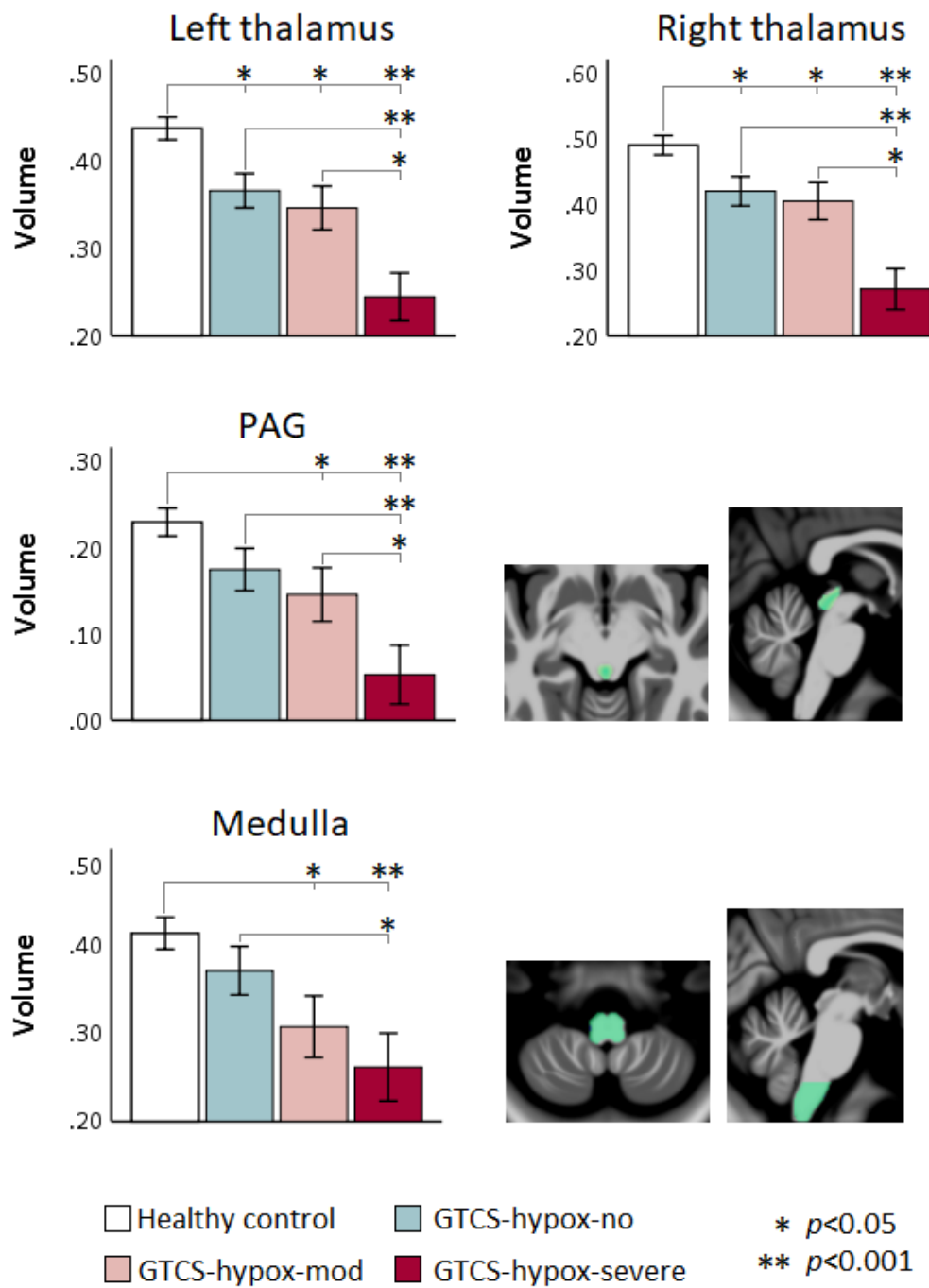


Figure 3.2.3. ROI volume analysis results displayed in bar graphs. Thalamic, PAG and medulla volume loss across groups. PAG = periaqueductal grey. Error bars represent standard error mean (SEM) +/-1.

3.2.4.3.2 Partial correlations

Significant negative partial correlations were found between degree of SpO₂ desaturation and left ($r = -0.429$, $p = 0.03$) and right ($r = -0.468$, $p = 0.02$) thalamus, and left ($r = -0.435$, $p = 0.03$) and right ($r = -0.66$, $p = 0.001$) hippocampus (Figure 3.2.4). Significant negative partial correlations were observed between duration of hypoxemia and the posterior vermis ($r = -0.58$, $p = 0.007$) and left ($r = -0.57$, $p = 0.006$) and right ($r = -0.58$, $p = 0.006$) accumbens (Figure 3.2.5). GTCS frequency correlated positively with left ($r = 0.67$, $p = 0.003$) and right ($r = 0.43$, $p = 0.04$) thalamic grey matter volume (Figure 3.2.6).

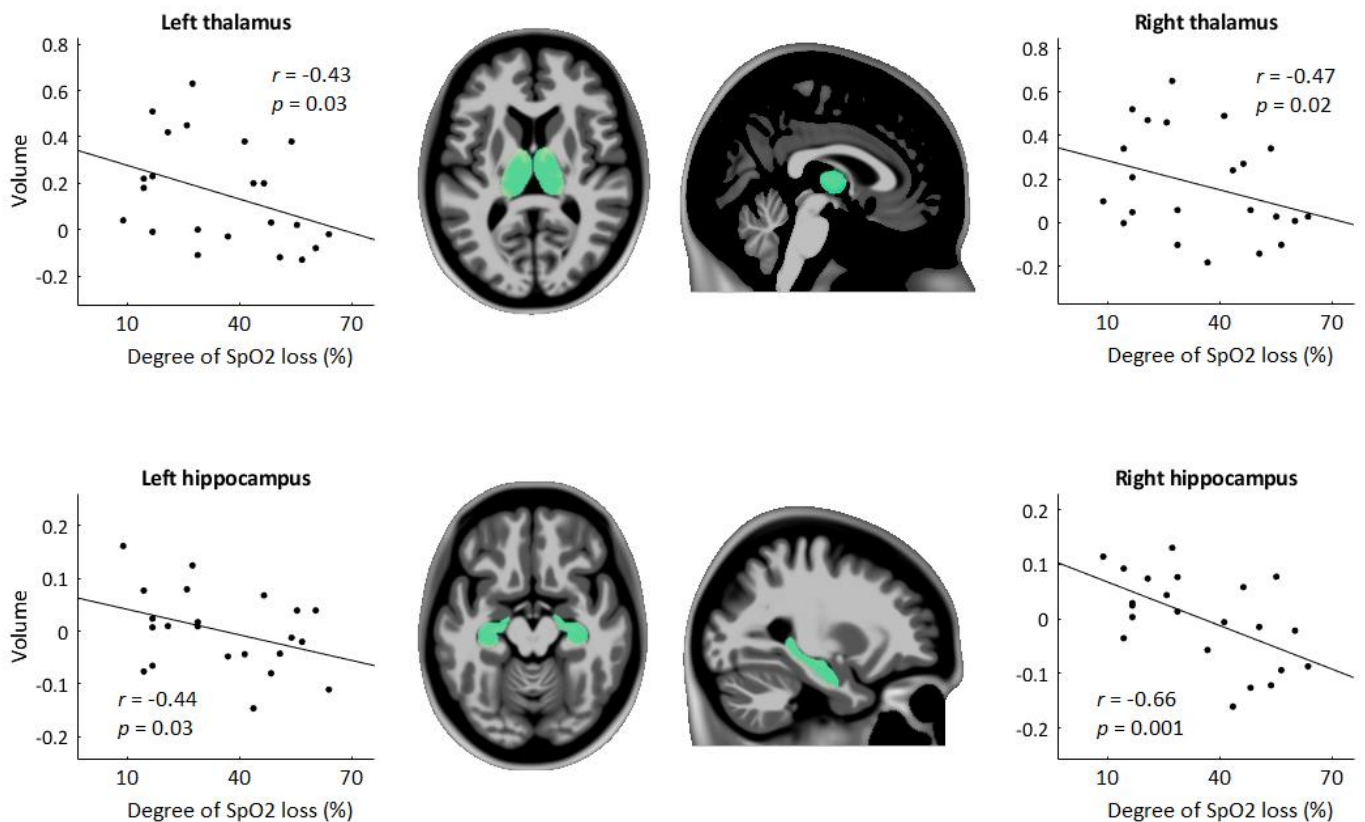


Figure 3.2.4. Partial correlations between thalamic and hippocampal volume and degree of SpO2 loss. Regions for which significant correlations with degree of SpO2 loss were found, overlaid in green on a template brain in MNI space. r = Pearson correlation coefficient. Covariates were, disease duration and total brain volume. P-values were FWER corrected.

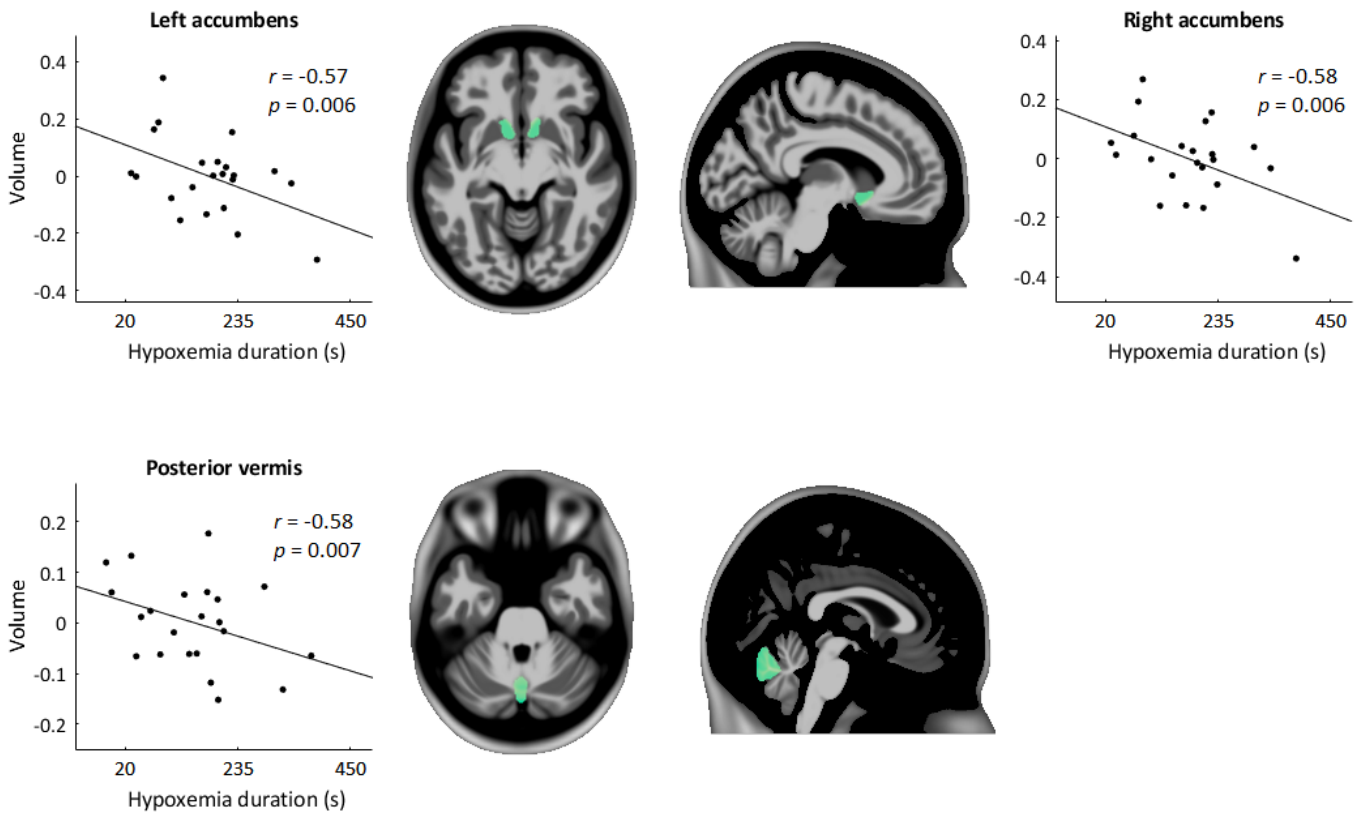


Figure 3.2.5. Partial correlations between accumbens and posterior vermis volume and duration of hypoxemia. Regions for which significant correlations with duration of hypoxemia were found, overlaid in green on a template MNI brain. r = Pearson correlation coefficient. Covariates were disease duration and total brain volume. P -values were FWER corrected.



Figure 3.2.6. Partial correlations between thalamic volume and GTCS frequency. Significant correlations between GTCS frequency and the bilateral thalamus in GTCS-hypox, overlaid in red on a template MNI brain. r = Pearson correlation coefficient. GTCS = generalized tonic-clonic seizure. Results reflect partial correlations, with GTCS frequency and thalamic volume as exploratory factors, and disease duration and total brain volume as covariates.

3.2.5 Discussion

3.2.5.1 Overview

In the current study, grey and white matter volume abnormalities associated with hypoxemia in patients with GTCS were assessed. Widespread volume loss was found in subjects whose seizures were accompanied by hypoxemia, including within grey matter sites previously shown to exhibit loss in patients who suffer SUDEP and those at highest risk (thalamus, cerebellum, vermis and PAG). Additionally, grey matter loss emerged in the hypothalamus and temporal pole, while white matter reductions known to be associated with SUDEP (Mueller et al., 2018) were seen in the medulla and pons of the brainstem. Increased grey matter was found in the bilateral amygdala and entorhinal cortex in GTCS with hypoxemia, which was absent in GTCS without hypoxemia.

Correlational analyses indicate an association between hypoxemia and volumes of specific sites known for their breathing roles, the posterior vermis (Xu & Frazier, 2002), thalamus (Koos et al., 1998; Koos et al., 2016; Macey et al., 2005) and hippocampus (Harper et al., 1998), which exhibit volume loss in previous imaging studies of SUDEP and at risk populations (Wandschneider et al., 2015; chapter [1.5](#)), as well as in other cohorts involving respiratory dysfunction (Macey et al., 2016). Data from two SUDEP cases indicates a potential role of hypoxemia degree and duration in SUDEP, though further work involving larger samples is needed.

3.2.5.2 Volume loss associated with hypoxemia

Volume loss of the thalamus, PAG and medulla followed a progressive pattern, in the direction of increasingly elevated peri-GTCS hypoxemia, across groups; subjects with severe hypoxemia showed the most extensive loss within these sites, while subjects with mild/moderate hypoxemia showed less, and those with no hypoxemia showing the least. As described in previous chapters, thalamic and brainstem volume loss is well described in SUDEP and those at risk, including GTCS patients (Allen et al., 2019a). Hypothalamic grey matter was also reduced in GTCS with hypoxemia, a finding not previously reported in those at risk for SUDEP.

The thalamus is a known oxygen-sensitive site (Dawes et al., 1983; Koos et al., 1998), which directs and receives respiratory information to and from the medulla (Neubauer & Sunderram, 2004) where the dorsal and ventral respiratory groups for controlling inspiration, exhalation and their timings (Tortora & Derrickson, 2008) are housed. The pons, which showed loss in GTCS-hypox compared with healthy controls, provides synaptic medullary input for shaping and adaptation of breathing patterns (Dutschmann & Dick, 2012) and is involved in hypoxic depression of breathing in foetal rabbits (Martin-Body & Johnston, 1988). The PAG, as detailed earlier, is involved in recovery from cardiorespiratory dysfunction, deficient responses of which can result in SUDEP (Kommajosyula, Tupal, & Faingold, 2018). Portions of the hypothalamus play roles in a variety of regulatory processes, including thermoregulation (Boulant, 2000), blood pressure regulation (Rodbard, 1948) and arousal (Harris & Aston-Jones, 2006). Since volumes of certain structures followed a progressive, seemingly linear, pattern of loss across groups, a logical next step was to determine whether the extent of site-

specific volume reductions could be explained by the degree or duration of hypoxemia, as assessed with correlation analyses. Consequently, the degree of hypoxemia correlated negatively with bilateral thalamic and hippocampal volumes, indicating that reduced volume of these structures is associated with greater degrees of hypoxemia. While a causal link cannot be established from these findings (since changes are associative and correlational), volume loss may reflect gliosis stemming from repeated hypoxic insult arising from frequent convulsions (Macey et al., 2009); hypoxemia certainly has the potential to damage these structures given the presence of oxygen-sensitive cells in these sites. Additionally, failure of oxygenation to cells undergoing high demands during ictal events, and presumably so during and after GTCS, establishes a scenario for excitotoxic injury (Johnston, 2001, et al., 2001; Dugan & Choi, 1999). However, regardless of injury mechanisms, volume loss to the thalamus, medulla and pons may represent impairment to sites and networks involved in central respiratory modulation and cardiorespiratory recovery in those with severe hypoxemia. Such impairment could predispose regulatory or recovery processes, and thus individuals.

Assessments of hypoxemia duration revealed negative correlations with volume of the accumbens (bilaterally) and posterior vermis, demonstrating that longer durations of hypoxemia are linked to greater volume loss in these areas. Intermittent hypoxemia is known to damage the posterior vermis, including the fastigial nuclei (Pae, Chien & Harper, 2005); similar processes of volume loss may be operating, whereby prolonged episodes of hypoxemia lead to cerebellar grey matter injury.

The nucleus accumbens forms part of the ventral striatum and plays well known roles in learning and reward circuitry, with strong dopaminergic and serotonergic inputs (Yoshimoto et al., 1992). A role in depression is also known; deep brain stimulation of the accumbens reduced anxiety and depression ratings in treatment resistant depression (Bewernick et al., 2010). We note that the accumbens is not known to directly participate in central autonomic or respiratory regulation, though reduced volume associated with extended durations of hypoxemia might indicate damage via sustained hypoxemia.

3.2.5.3 Grey matter increases in GTCS with hypoxemia

Compared with healthy controls, GTCS with hypoxemia showed increased grey matter volumes of bilateral amygdala, entorhinal cortex and ventral-anterior insula. As described in chapter 1 and 3, increased amygdala and entorhinal cortex volume associated with SUDEP and elevated risk has been highlighted before. The explanation for increased volume in these sites, as mentioned earlier in chapter [3.1.4.4](#), remains speculative, and explorations with clinical and hypoxemia measurements failed to outline associations other than the observed groups differences. Of note, disease duration or GTCS frequency did not correlate significantly with volume of these structures. Increased volume in these subjects could reflect inflammatory processes in breathing sites as a result of increased respiratory drives in response to hypoxemia (Eltzschig & Carmeliet, 2014). Though the role of the amygdala in breathing modulation is known, confirmation of such processes leading to grey matter volume alterations is required. Of note, and given the high prevalence of psychiatric co-morbidities in severe epilepsies, structures such as the amygdala play known roles in anxiety and

depression. One possibility is that elevated volume among such structures could reflect heightened physiological processes related to psychiatric disorder among these cohorts.

Insula cortex thickening has been demonstrated in patients with GTCS and is positively associated with GTCS frequency (Ogren et al., 2018). The bilateral anterior insula also shows elevations in volume closer to SUDEP from time of scanning (Allen et al., 2019b). The mechanism of elevations in insula volume and cortical thickness remain unknown, but could be a result of increased GTCS frequency which is also known to become progressively greater nearer to the time of SUDEP (Harden et al., 2017).

3.2.5.4 Clinical variables

GTCS frequency was positively associated with hypoxemia duration. If successive GTCS leads to more prolonged hypoxemic exposure, then repeated GTCS may be indirectly contributing to volume alterations in individuals with hypoxemia, provided that the mechanisms of injury can be confirmed as hypoxemic or excitotoxic in nature. Such a scenario could represent the bases of observed volume loss in the vermis – a region highly susceptible to excitotoxic cell loss (Slemmer, De Zeeuw & Webber, 2005) and showing reductions in volume in association with greater hypoxemia duration in this study.

Bilateral thalamic volumes correlated positively with GTCS frequency in GTCS patients with hypoxemia; when considered across all GTCS subjects and in GTCS without hypoxemia separately, correlations became weaker and non-significant (all GTCS: $r = 0.11$, $p = 0.6$ / GTCS-hypox-no: $r = 0.24$, $p = 0.3$). This provides evidence of two prospects: 1) that observed thalamic volume loss in GTCS patients, and associated

with hypoxemia, cannot be solely attributed to GTCS frequency; and 2) that seizure frequency and volume-related processes are likely operating under different conditions in GTCS with and without hypoxemia. Notably, no other clinical variables showed meaningful or significant correlations with regional structure volumes, including disease duration which has been previously associated with thalamic volume loss (Wandschneider et al., 2015).

3.2.5.5 Relevance to SUDEP research: hypoxemia data from two cases

Two confirmed SUDEP cases were identified in this cohort. Both exhibited peri-ictal hypoxemia. The first case had a 10% degree of hypoxemia (above 75%; mild/moderate), but with a longer duration (385s; the longest observed). This individual also had post-convulsive central apnea; one of 3 in the cohort. The second case had a shorter duration of hypoxemia (95s), but greater degree (55%; the 3rd greatest observed). While little inference can be derived from so few observations, highlighting the characteristics of these cases is worthwhile given the rarity of SUDEP and the objectives of this work. Of note, many of the observations of peri-ictal hypoxemia were based on one seizure alone – it could be the durations and extents of hypoxemia vary on a within subject basis, and are influenced by, or interact with, other factors (such as state at seizure onset, time of day or other peri-ictal autonomic / respiratory manifestations). Both duration and degree of hypoxemia may be relevant for SUDEP, and may involve separate mechanisms (i.e. apnea vs hypoventilation) but neither one could differentiate both SUDEP cases in this study and further work is required to characterise the role of, and pathways to, hypoxemia in SUDEP.

3.2.5.6 Limitations of this work

3.2.5.6.1 Interpretation of volume loss and link to SUDEP

The major pitfall of the present study is that the reported volume changes are associative only. Group differences of static volumetric measures, and correlational analyses, do not permit causal inference. As such, it cannot be claimed from the current study that hypoxemia causes the observed volume alterations outlined; it could equally be that smaller thalami, PAG and medulla (resulting from alternative, unknown, mechanisms) lead to a greater propensity for hypoxemia. Additionally, while hypoxemia may be a key risk factor and potential SUDEP mechanism, this is not confirmed and thus one can only indicate, with speculation, the possibility that volume alterations related to hypoxemia may be linked with processes involved in SUDEP. However, these findings do outline important relationships and provide insights into potential mechanisms of volume loss, and indicate target sites for future studies and potential interventions.

3.2.5.6.2 Measurements and mechanisms of hypoxemia

SpO₂ measurements were assessed via pulse oximetry to establish hypoxemia. While such measurements correlate strongly enough with the more desirable arterial oxygen saturation (SaO₂) monitoring, and are thus perfectly valid for clinical use, SpO₂ is considered inferior to SaO₂ in terms of susceptibility to inaccurate reading and artefacts. Future, more focussed studies addressing hypotheses regarding hypoxemia, SUDEP and neuroimaging correlates (which should be pursued in light of the current findings), should employ superior approaches to measuring oxygen saturation.

The current study did not assess the pathway to hypoxemia during GTCS, which could be a key investigation to ascertaining the pathophysiological processes leading to

SUDEP. Hypoxemia can arise in a number of ways, including from central (Vilella et al., 2019b) or obstructive apnea (Dewan et al., 2015; Friedman et al., 2001), or from hypoventilation (Bateman et al., 2008).

In this context, the current study can only interpret findings based on observations of reductions in oxygen saturation, and not how those desaturations arose. Future experiments should seek to determine the precise mechanisms of hypoxemia around the time of seizures, particularly during and after GTCS; a significant stride towards enhancing understandings of respiratory dysfunction in epilepsy and events resulting in SUDEP.

Another important consideration in light of the present results is that the seizures recorded, and subsequent occurrences and measurements of hypoxemia, may not reflect what typically happens during a seizure for a given patient. In controlled settings such as on the EMU, conditions are often very different from those in which a patient normally has a seizure. For example, patients are often sleep deprived and medication is usually tapered in order to provoke seizures. The interactions between provocative techniques such as these and other observations during seizures should be explored in the future, though it is likely that a more 'severe' form of seizure might be observed on the EMU compared with what might be typical for a patient. The relationship between seizure severity and the occurrence of hypoxemia should thus be examined in the future.

3.2.5.6.3 Cohort

Subjects in this study were selected based on the availability of recorded breathing parameters and imaging in recruited subjects, and thus were not confined to a specific

sub-group of epilepsy, such as TLE. As such, the cohort is represented by an inhomogeneous group of patients and reported results are thus confounded by variance related to differing disease aetiologies, epilepsy types, seizure onset zones and imaging findings. Ultimately, the findings do not provide insight into associations between hypoxemia and other aspects such epileptogenic zone, owed to a limited sample size.

Additionally, only patients with GTCS were included in the current study, and the lack of focal seizure sub-group, means interpretation is limited to these patients only. However, given the context that SUDEP is mostly associated with GTCS, relating findings to focal seizures remained a lesser priority here. Future studies should attempt to evaluate hypoxemia and associated brain changes in focal seizures as well.

3.2.5.6.4 ROI sub-divisions

The lack of regional sub-divisions of ROIs limits the neuroanatomical and neurobiological specificity of the findings. Future work should look to further parcellate structures such as the thalamus, to determine site-specific alterations with greater neuroanatomical accuracy, leading to more specific interpretations.

3.2.5.6.5 Data from two scanners

Since the current study forms part of larger a multi-center effort, data came from two sites, UCL and Case-Western Reserve University, and thus two separate scanners. A major advantage of multi-center studies is increased subjects numbers, and hence statistical power, particularly in the context of rare diseases and observations.

VBM measurements from longitudinal studies are known to differ across multiple scanners, and even scanner upgrades (Takao, Hayashi & Ohtomo, 2013). Importantly, in this study, as with others (Stonnington et al., 2008), scanner differences did not appear within sites showing significant effects of interest between disease groups. Additionally, group membership of subjects from either site was approximately even ensuring a balance of representatives across groups.

3.2.6 Conclusions

To our knowledge this study is the first to outline brain morphological and volumetric alterations associated with GTCS accompanied by hypoxemia. The changes we observed indicate injury to sites known to be involved in oxygen sensing, breathing regulation and cardiovascular recovery.

Though the reported volume changes are associative only, in that they are evidenced through observed group differences and correlational analyses, the results strongly indicate an association between hypoxemia and volume loss in salient brain structures.

The results give reasonable indications as to mechanisms of injury seen in SUDEP, though the underlying cause of volume loss in observed sites remain unknown, and determination of how, or if, volume alterations are truly linked to SUDEP will require further work.

Chapter 4. Functional brain network alterations related to SUDEP

The work of this thesis has focussed so far on the use of structural MRI techniques in the exploration of brain morphometric and volumetric alterations associated with SUDEP and related risk factors. Such approaches have primarily revealed damage to brain regions, many of which are involved in central autonomic and breathing regulatory processes. Even less, however, is known about functional alterations among those regions, and whether SUDEP is associated with changes in communication between them. The aims of the following two studies are to characterise functional connectivity changes linked to SUDEP, and consider whether such changes might shed light on SUDEP pathophysiology and be used to prospectively identify those at risk. The first of these studies examines functional connectivity alterations in temporal lobe epilepsy patients at high- and low-risk of SUDEP and was published in *Frontiers in Neurology* ([4.1](#)), while the second explores a group of confirmed SUDEP cases, relative to high-risk, low-risk and healthy controls, and is currently under review ([4.2](#)).

4.1: Dysfunctional Brain Networking among Autonomic Regulatory Structures in Temporal Lobe Epilepsy Patients at High Risk of Sudden Unexpected Death in Epilepsy³.

4.1.1 Background

Little is known regarding whether, or to what extent, communication among brain regions involved in autonomic and respiratory regulation is altered in TLE patients as a consequence of increased SUDEP risk (which includes a higher frequency of GTCS). The main objective of the current study was to investigate potential differences in functional connectivity (FC) among a subnetwork of key structures related to autonomic and respiratory regulation. We investigated this subnetwork using RS-fMRI, and applying the network-based statistic (NBS; Zalesky et al., 2010) to compare connections among the subnetwork between high- and low-risk of SUDEP patients. The NBS is a graph theory-based approach to FC analysis which exploits the clustering structure of between-group differences in network topology. That is, connections within a network which significantly differ across groups often form a connected subnetwork or 'component'. Similar to conventional neuroimaging analysis (Nichols & Holmes, 2001), whereby clusters are identified among voxels in physical space, the NBS identifies clusters in topological space and possesses greater power to detect strength-based differences as opposed to methods which ignore such a topological

³ Allen, L. A., Harper, R. M., Kumar, R., Guye, M., Ogren, J. A., Lhatoo, S. D., ... & Diehl, B. (2017). Dysfunctional brain networking among autonomic regulatory structures in temporal lobe epilepsy patients at high risk of sudden unexpected death in epilepsy. *Frontiers in neurology*, 8, 544.

structure. Altered communication among regulatory regions of interest (ROIs) in patients at high-risk may shed light on central regulatory disturbances related to TLE and elevated risk of SUDEP.

4.1.2 Methods

4.1.2.1 Subjects and risk stratification

Sixty-two patients with TLE underwent RS-fMRI scanning (34 left TLE; 26 right TLE). Twenty-eight of these subjects were excluded from further analyses due to the presence of large lesions (9), inter-ictal epileptic discharges (IEDs) recorded during the RS-fMRI scan acquisition (8), excessive head movement (9; see fMRI pre-processing in section [4.1.2.3](#)), and two cases who suffered SUDEP. We excluded patients who suffered from SUDEP, so as not to mix potential pathological differences which may be present in these cases.

Of 32 patients remaining for further analysis, 17 had left TLE (9 females) and 15 right TLE (7 females). Subjects were classified as being at high- or low-risk of SUDEP based on clinical factors (Wandschneider et al., 2015, Tang et al., 2014; Hesdorffer et al., 2011) as follows: An odds ratio (OR) score was generated for each patient using duration of epilepsy > 15 years (OR = 1.95), epilepsy onset < 16 years (OR = 1.72), > 3 generalised tonic clonic seizures (GTCS) per year (OR = 15.46), and nocturnal seizures present (OR = 3.9). Patients with > 3 GTCS per year (OR = 15.46) or nocturnal seizures (OR = 3.9) were classified as high-risk. The OR cut off value of 3.9 for the high-risk label was selected based on a previous SUDEP neuroimaging study (Wandschneider et al., 2015), in which 90% of SUDEP cases were correctly identified as high-risk if their summed OR score was at least 3.9 (presence of nocturnal seizures).

Therefore, any patients above 3.9 were classed as ‘high-risk’ and any below were classed as ‘low-risk’. In our cohort, this classification resulted in 14 high-risk (8 L TLE, 7 females) and 18 low-risk (9 L TLE, 9 females) subjects. Patient characteristics are shown in Table 4.1.1.

Table 4.1.1. Summary of patients at low and high-risk of SUDEP.

CHARACTERISTICS	LOW-RISK (N = 18)	HIGH-RISK (N = 14)	P
MEAN AGE AT SCAN (YEARS) ± SD	30.0 ± 7.1	33.5 ± 9.1	0.332
SEX (M:F)	9:9	7:7	1
EPILEPSY LATERALISATION (L:R)	9:9	8:6	0.693
MEAN AGE ONSET (YEARS) ± SD	12.9 ± 9.5	12.4 ± 8.5	0.203
MEAN DURATION (YEARS) ± SD	17.6 ± 10.3	21.2 ± 12.3	0.068
> 3 GTCS PER YEAR	0	14	< 0.001
MEAN NUMBER OF GTCS PER YEAR	0.3 ± 0.6	62 ± 58	< 0.001
NOCTURNAL SEIZURES	0	6	0.002
HIPPOCAMPAL SCLEROSIS	7	9	0.161
POLYTHERAPY	13	12	0.367
MONOTHERAPY	5	2	0.367
MEAN AED DOSE (MG) ± SD	1219 ± 811	1412 ± 845	0.517
TOTAL AED INTAKE PER DAY (MG) ± SD	2349 ± 1692	2790 ± 1664	0.468
MEAN SUDEP RISK (OR) SCORE ± SD	1.6 ± 1.7	19.2 ± 2.2	< 0.001

SUDEP = Sudden death in epilepsy, L = left, R = right, GTCS, generalized tonic-clonic seizures, SD = standard deviation, OR = odds ratio, AED = antiepileptic drug, mg = milligram.

4.1.2.2 Functional MRI

All subjects underwent a 20-minute resting-state electroencephalogram-functional magnetic resonance imaging (EEG-fMRI) scan (3.0 tesla scanner, Signa Excite HDX, GE Medical Systems), during which they were instructed to lay idly with eyes closed. The echo planar imaging (EPI)-based blood oxygen level dependent (BOLD) functional

MRI scans were acquired with the following parameters: repetition time = 3000 ms, echo time = 30 ms; flip angle = 90°, matrix size = 64 × 64, field of view = 24 × 24 cm², slice thickness = 3 mm, number of slices = 43, 44 or 47. Simultaneous EEGs with 32 channels recorded with MRI compatible electrodes were acquired (Brain Products, Munich, Germany). The EEG recordings were used to exclude patients with epileptiform activity during the scan. The study was approved by the National Research Ethics Committee (04/Q0512/77 and 14/SW/0021).

4.1.2.3 Data pre-processing

The RS-fMRI time-series data were pre-processed in MATLAB 2016a (MathWorks inc) with DPARSFA (data processing assistant for resting state fMRI; Yan et al., 2016) software, which calls functions from the software packages REST (Song et al., 2011) and SPM12 (statistical parametric mapping; <http://www.fil.ion.ucl.ac.uk/spm>). The following steps were carried out: slice time correction, realignment, co-registration of structural and functional MRI images, segmentation via DARTEL (diffeomorphic anatomical registration through exponential lie algebra; Ashburner, 2007), and spatial normalisation to Montreal Neurological Institute (MNI) space.

To reduce the effects of physiological noise, and to improve the specificity of signals pertaining to grey matter (GM), the white matter (WM), and cerebrospinal fluid (CSF), signals were regressed out using the (principal components analysis) component-based noise correction method CompCor (Behzadi et al., 2007), in which 5 principal components derived from noise regions-of-interest based on each subject's segmented WM and CSF mask (mask threshold = 0.99) were removed (Muschelli et al., 2014). The 6 motion realignment parameters calculated by SPM12 were also regressed out. Head motion “scrubbing” was implemented, using DPARSFA's built-in

functions, to account for excessive head movements which are known to affect inter-regional correlations (Power et al., 2012; Satterthwaite et al., 2012; Van Dijk et al., 2012; Power et al., 2014; Lemieux et al., 2007). For every scan in a given time series, the frame-wise displacement (FD), an index of head-movement from one volume to the next, was calculated as the sum of the absolute values of the realignment estimates relative to the preceding scan (Power et al., 2012). Scans to be scrubbed were defined as those which FD exceeded 0.25 mm; for each of those, the preceding 1 and subsequent 2 scans were replaced via linear interpolation. In 9 of the original 60 patients, this procedure resulted in 75%, or more, of the scans being scrubbed, and these scans were excluded from further analysis. In the remaining datasets, the proportion of scrubbed scans was below 50%. Finally, the linear trend was removed, and a bandpass filter of 0.01 – 0.08 Hz was applied, which is consistent with the frequency range most relevant to BOLD signal fluctuations. Spatial smoothing was not applied to not extend the BOLD signal between nearby regions of interest.

4.1.2.4 Region of interest (ROI) selection

The Harvard-Oxford (HO) cortical & subcortical atlas (http://www.cma.mgh.harvard.edu/fsl_atlas.html) was used to extract ROI-averaged time-series from the processed fMRI time series. We selected 11 bilateral brain regions (22 total) from the HO atlas based on their known involvement in the central control of autonomic regulation (see Figure 4.1.1). These regions included structures belonging to the limbic system: hippocampus, amygdala, anterior cingulate cortex (ACC), and subcallosal cortex (SC); the insulae, thalamus, orbitofrontal cortex (OFC), frontal medial cortex (FMC), brainstem, and two regions of the basal ganglia: caudate and putamen.

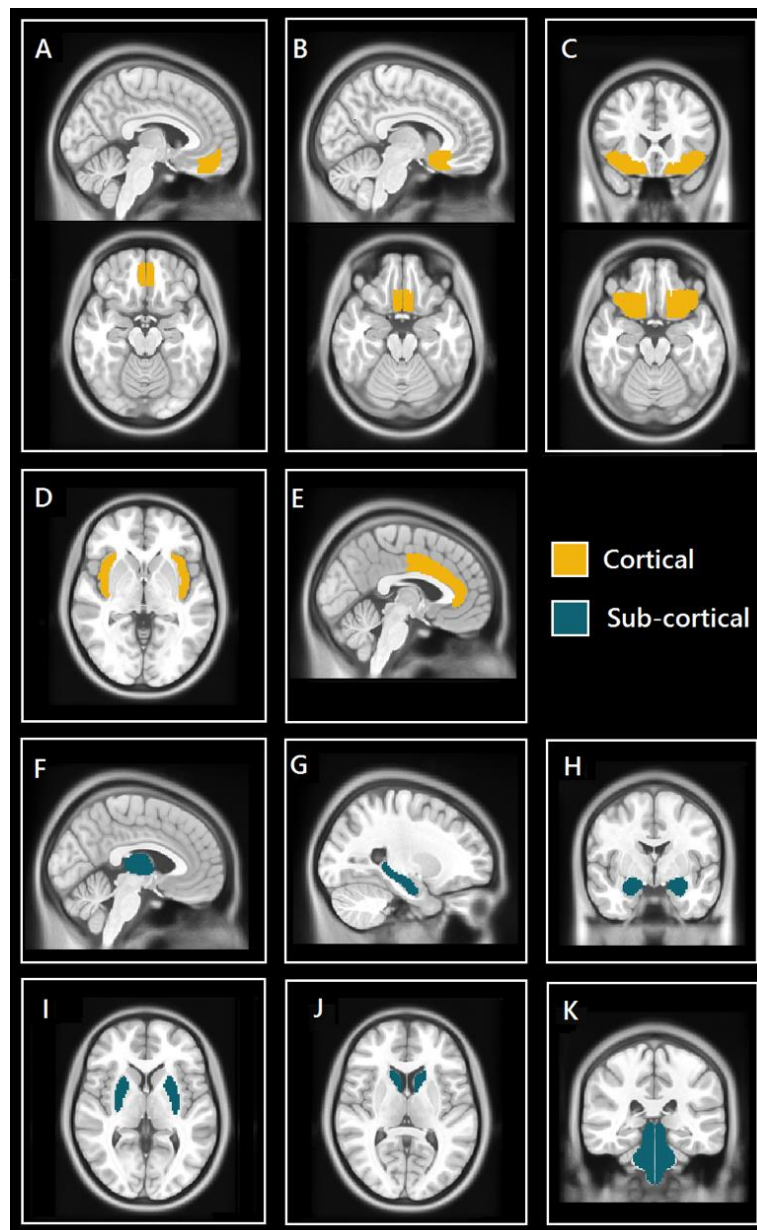


Figure 4.1.1. Selected cortical and sub-cortical regions of interest (ROIs) masks from HO atlas. A, sagittal (top) and axial (bottom) views of the frontal medial cortex (FMC); B, sagittal (top) and axial (bottom) views of the subcallosal cortex (SC); C, coronal (top) and axial (bottom) views of orbitofrontal cortex (OFC); D, axial view of insulae (Ins); E, sagittal view of anterior cingulate cortex (ACC); F, sagittal view of thalamus; G sagittal view of hippocampus; H, coronal view of amygdalae; I, axial view of putamen; J, axial view of caudate; K, coronal view of brainstem (includes midbrain, pons, and medulla).

4.1.2.5 Resting-state FC analysis and Network Based Statistic (NBS)

After extracting the time-series belonging to each ROI (network node), the absolute value of the Pearson r correlation coefficient was calculated for every possible ROI pair (each ROI pair defining a network edge or 'path' between two structures) and a Fisher Z-transform normalisation applied, yielding a 22×22 FC matrix for every subject. We then used the Network Based Statistic (NBS; Zalesky et al., 2010) to compare the FC strength of every edge in the matrices between high-risk and low-risk of SUDEP patients. We sought to identify increased and decreased FC (contrasts: high-risk < low-risk; high-risk > low-risk) using analysis of covariance, with the following covariates: age, sex, lateralisation of epilepsy, and presence of hippocampal sclerosis (HS). In addition to using presence of HS as a covariate, we also performed analysis whereby hippocampal grey matter volume of the epileptogenic hemisphere was regressed out (see supplementary methods [S1](#)).

In summary, the NBS consists of the following steps: independently test the null hypothesis at every connection in the network using a two-sample t test (ANCOVA), endowing each edge with a t -statistic. A t -statistic threshold is required and must be specified prior to testing. Any edges for which the t -statistic threshold is exceeded are defined as supra-thresholded connectivity. Clusters, or any set of nodes between which a path can be found, are then identified among the supra-thresholded connectivity. The main assumption of the NBS is that any supra-thresholded edges which form a cluster are not isolated from each other and therefore comprise a connected component, or subnetwork, differentiating the two groups (Zalesky et al., 2010; Figure 4.1.2). Finally, a family-wise error rate (FWER)-corrected p value is

calculated using permutation testing (Freedman & Lane 1983). For each permutation, members of the two samples are randomly permuted, and the size of the extended cluster is calculated (10000 permutations). These calculations yield an empirical null distribution of the maximal supra-threshold cluster size.

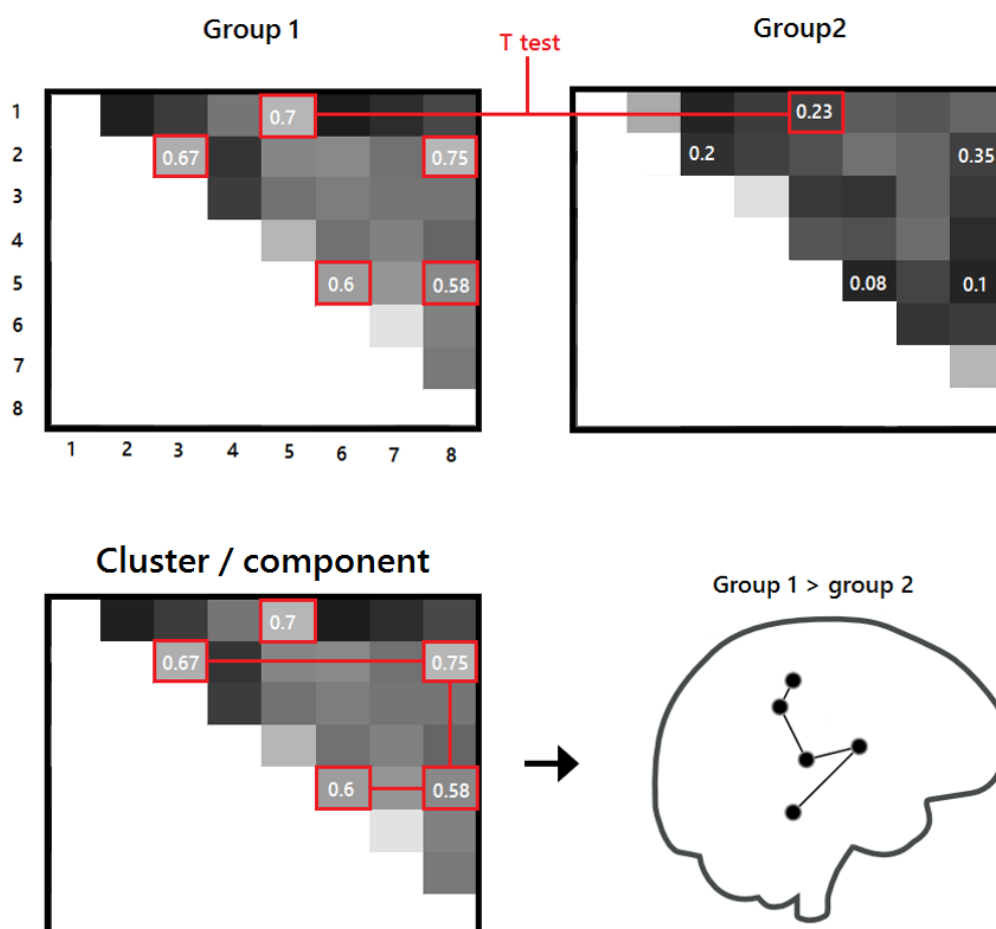


Figure 4.1.2. Visual schematic of the NBS method. *T*-tests are calculated for every possible edge in the network, between the two groups (top panel), after specifying a *T*-statistic threshold. Connections which exceed the *T*-threshold, and form a connected subnetwork (bottom panel), represent the suprathreshold cluster, for which a *p*-value is calculated after permuting the same test with random group membership 10000 times.

4.1.3 Results

The comparison between high- and low-risk SUDEP patients revealed a subnetwork of significantly reduced FC ($t = 2.5$, $p = .029$) and one subnetwork of significantly enhanced FC ($t = 2.1$, $p = .033$). The reduced FC subnetwork consisted of 9 edges between the following 9 nodes: bilateral ACC, bilateral thalamus, bilateral brainstem, left amygdala, and bilateral putamen (Figure 4.1.3; Table 4.1.2). The subnetwork of enhanced FC consisted of 16 nodes (bilateral FMC, bilateral SC, bilateral OFC, bilateral insula, bilateral hippocampus, bilateral amygdala, right caudate, right putamen, right brainstem and left thalamus) and 24 edges (Figure 4.1.4; Table 4.1.3). Comparable significant subnetworks emerged following regression of hippocampal GM volume (instead of “presence of HS”). The high-risk < low-risk contrast revealed a significantly reduced subnetwork of 11 nodes (bilateral brain stem, bilateral thalamus, left amygdala, right insula, bilateral ACC, bilateral putamen and right SC) and 14 edges ($t = 2.5$, $p = 0.035$). The high-risk > low-risk contrast showed a significantly enhanced subnetwork comprising 15 nodes (bilateral hippocampus, amygdala, putamen, insula, SC, orbitofrontal cortex, medial frontal cortex, and right caudate) and 27 edges ($t = 2.5$, $p = 0.028$) (Results and Figures [S1](#) and [S2](#) in Supplementary Material).

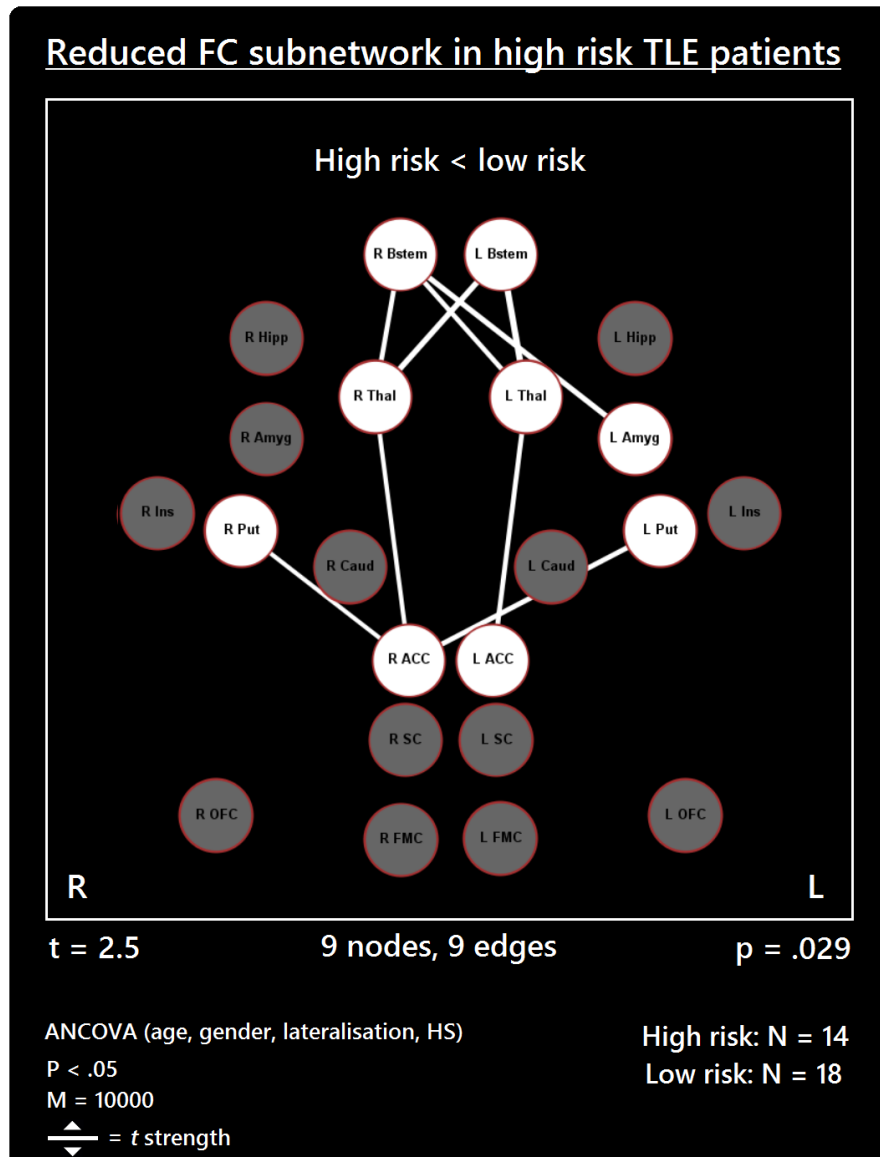


Figure 4.1.3. Reduced FC subnetwork in high-risk over lower risk of SUDEP patients.

Subnetwork of reduced FC involving the bilateral brainstem (Bstem), bilateral thalamus (Thal), bilateral putamen (Put), bilateral ACC, and left amygdala (Amyg). L = Left, R = Right; HS: hippocampal sclerosis; ANCOVA: analysis of covariance; t = t -statistic threshold; M = number of permutations; P value was set at < 0.05, FWER corrected. Nodes in white are those which were involved in the significant subnetwork. Red node outline represents search for reduced connectivity (high<low). Visualisation using Gephi (<https://gephi.org/>).

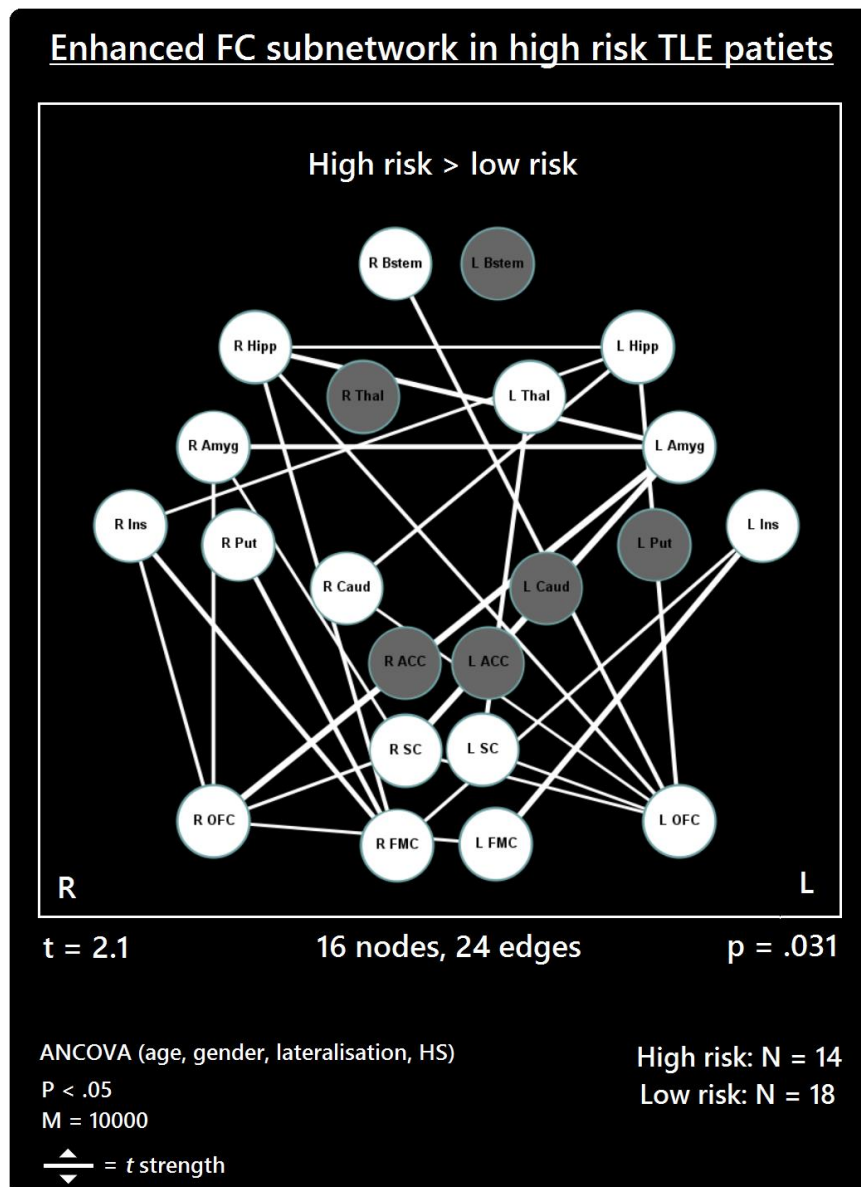


Figure 4.1.4. Subnetwork of enhanced FC in high-risk TLE patients when compared with low-risk TLE patients. Regions include: bilateral amygdala (L Amyg, R Amyg), right brainstem (R Bstem), right caudate (R Caud), bilateral frontal medial cortex (L FMC, R FMC), bilateral hippocampus (L Hipp, R Hipp), bilateral insula (L Ins, R Ins), bilateral orbitofrontal cortex (L OFC, R OFC), right putamen (R Put), bilateral subcallosal cortex (L SC, R SC), and the left thalamus (L Thal). L = left, R = Right. White nodes represent ROIs involving significant connections. Blue node outline represents search for increased connectivity (high>low).

Table 4.1.2. List of decreased connections belonging to the subnetwork of reduced connectivity found (high-risk < low-risk), with a threshold of $t = 2.5$. $t = t$ -test statistic.

Connection	t
<i>L ACC – L Thalamus</i>	2.91
<i>L Brainstem – L Thalamus</i>	3.76
<i>L Brainstem – R Thalamus</i>	3.38
<i>R_ACC – R Thalamus</i>	2.66
<i>R ACC – L Putamen</i>	3.04
<i>R ACC – R Putamen</i>	2.59
<i>R Brainstem – L Amygdala</i>	3.23
<i>R Brainstem – L Thalamus</i>	2.87
<i>R Brainstem – R Thalamus</i>	2.89

Table 4.1.3. List of enhanced connections belonging to the subnetwork of increased connectivity found in high-risk > low-risk, with a threshold of $t = 2.1$. $t = t$ -test statistic.

Connection	t
<i>L Amygdala – R Amygdala</i>	2.68
<i>L FMC – R OFC</i>	2.21
<i>L OFC - L Hipp</i>	2.51
<i>L OFC – R Brainstem</i>	2.58
<i>L OFC – R Caudate</i>	2.10
<i>L OFC – R Hipp</i>	2.42
<i>L Hipp– R Hipp</i>	2.16
<i>L Ins – L FMC</i>	2.99
<i>L ins – R FMC</i>	2.29
<i>L SC – L OFC</i>	2.14
<i>L SC – L Thalamus</i>	2.62

<i>R Caudate – L Hipp</i>	2.46
<i>R FMC – R Hipp</i>	2.49
<i>R FMC – R Putamen</i>	2.69
<i>R OFC – L Amygdala</i>	3.19
<i>R OFC – R Amygdala</i>	2.39
<i>R Hipp – L Amygdala</i>	2.78
<i>R Ins – L Hipp</i>	2.24
<i>R Ins – R FMC</i>	2.66
<i>R Ins – R OFC</i>	2.35
<i>R SC – L Amygdala</i>	3.17
<i>R SC – L OFC</i>	2.15
<i>R SC – R Amygdala</i>	2.18
<i>R SC – R OFC</i>	2.35

4.1.4 Discussion

4.1.4.1 Overview

This investigation examined whether, and to what extent, the FC between a group of structures associated with autonomic and respiratory regulation differs between TLE patients at high- and low-risk of SUDEP. High-risk TLE patients exhibited altered FC among a number of regions when compared with patients at low risk. A subnetwork of reduced FC was found, the regions of which involved several areas previously linked to increased SUDEP risk (Tang et al., 2014), including the thalamus, brainstem, and anterior cingulate. However, here involvement of additional brain regions which have not been previously linked to FC investigations into SUDEP, including the bilateral putamen and left amygdala, was revealed. Additionally, a subnetwork of enhanced FC in TLE patients at high-risk of SUDEP was found, the connections of which extended

to many of the regions in the subnetwork. A large proportion of enhanced connections involved medial/orbital frontal cortices, the insulae, limbic areas (amygdalae and hippocampus) and the subcallosal cortex. The cingulate was not involved in enhanced FC in high risk TLE patients. These findings prompt the need for further investigations into these structures, given their known involvement in cortical/sub-cortical autonomic control functions.

4.1.4.2 Reduced FC subnetwork

The current findings lend further support to the importance of altered ACC-thalamus and thalamus-brainstem connectivity in epilepsy patients at high-risk of SUDEP (Tang et al., 2014). Given the known, and earlier discussed, roles of the thalamus in oxygen sensing (Harper et al., 2015; Koos et al., 1998) and in relaying afferent activity essential for breathing, disruptions of the thalamic-brainstem link, as shown here in high-risk SUDEP patients, is particularly concerning given the apparent involvement of respiratory failure in SUDEP (Ryvlin et al., 2013). Reduced thalamic connectivity parallels the direction of structural changes seen in earlier described studies in which reductions in grey matter are observed among high-risk subjects and SUDEP victims (Wandschneider et al., 2015). The link between volumetric/morphometric and functional connectivity findings is unclear, and was not assessed in the current study. However, reduced connectivity of the thalamus may be related to injury and may predispose thalamic processes to recover from hypoxia accompanying ictal episodes. The ACC involvement in autonomic regulation is well documented. Early stimulation studies demonstrated an ACC role in blood-pressure regulation (Pool & Ransohoff, 1949). Neuroimaging studies corroborated these findings (Macefield & Henderson,

2015) and showed consistent fMRI activation and deactivation patterns of the ACC in association with heart rate changes (Shoemaker et al., 2012; Critchley et al., 2003), and cold pressor and hand-grip responses (Macey et al., 2016). In human epilepsy, thalamic-cingulate circuitry alterations were previously described (Bonilha et al., 2005; Tang et al., 2014). Upon stimulation of the cingulate, asystole – a potential SUDEP mechanism - has been observed (Leung et al., 2007). The reduced thalamic-ACC connectivity among patients at high-risk for SUDEP reflects a disruption of key pathways involved in central modulation of cardiorespiratory and blood-pressure mechanisms, which may be implicated in SUDEP (Bozorgi et al., 2013).

The current findings reveal a role of the putamen in the reduced connectivity subnetwork found in high-risk SUDEP patients. The putamen serves significant autonomic regulatory behaviours, and has major projections to insular and limbic sites (Saper, 1982; Pazo & Belforte, 2002). The putamen also serves to integrate sensory information for preparation of movements (Alexander & Crutcher, 1990; Marchand et al., 2008). Reduced connectivity between the putamen and ACC could alter communication between autonomic and motor regulatory pathways in patients at high-risk of SUDEP. Furthermore, we show reduced FC of the bilateral putamen with the right ACC only. The right ACC is preferentially involved in baroreflex-mediated autonomic cardiovascular function in humans (Kimmerly et al., 2005). Patients with congenital central hypoventilation syndrome (CCHS), who are also at high risk of sudden death, show BOLD signal reductions within the putamen when compared with controls (Macey et al., 2005).

Reduced FC between the right brainstem and left amygdala also occurred in high-risk patients. The final common path nuclei for cardiac, respiratory, and blood pressure control lie within the brainstem. The involvement of the amygdala in cardiovascular and respiratory activities has been described (Harper et al., 1998; Lacuey et al., 2017), as have the afferent and efferent pathways through which the amygdala projects to the midbrain, pons, and brainstem (Hopkins and Holstege, 1978; Saper & Loewy, 1980; Usnoff et al., 2006; Price & Drevets, 2010). Single-pulse stimulation of the amygdala central nucleus will trigger state-dependent inspiration (Harper et al., 1984). Animal models reveal a vital role of the amygdala in the propagation of seizures from the brainstem to the forebrain (Hirsch et al., 1997). Upon stimulation of the amygdala in patients with epilepsy, apnoea and oxygen desaturation are observed (Lacuey et al., 2017; Dlouhy et al., 2015), demonstrating the significant influences of this structure on brainstem respiratory nuclei in humans. The reduced FC we found between the amygdala and brainstem in high-risk patients is of considerable concern, especially given the occurrence of terminal apnoea in the majority of SUDEP cases (Ryvlin et al., 2013). It could be speculated that the FC reduction may contribute to a failure of amygdala influences to trigger inspiratory efforts and recover from possible hypoventilation or apnoea during seizures, or possibly result in sustained apnoea. Reduced FC may provide a marker for the respiratory alterations in epilepsy and mechanisms underpinning SUDEP.

4.1.4.3 Enhanced FC subnetwork

As well as reduced connectivity, an enhanced FC subnetwork emerged in high-risk SUDEP patients which involved 24 increased functional links in 16 of the 22 regions

investigated (Figure 4). The majority of enhanced connectivity patterns found in high-risk patients was represented by connections from the frontal medial or orbital frontal cortex to the insula and limbic cortices (hippocampus and amygdala).

The enhanced FC of orbital frontal and frontal medial cortices found here is of particular interest given their involvement in blood-pressure modulation (Harper et al., 1998; Harper et al., 2000). Portions of the medial prefrontal cortex also influence key areas involved in modulating cardiac sympathetic and parasympathetic responses and baroreflex activity (Resstel & Corrêa, 2006; Guyenet, 2006; Ziegler et al., 2009). Hand grip tasks, which induce heart rate changes, are associated with reduced activity within the hippocampus, orbitofrontal and medial prefrontal cortex in human subjects (Kimmerly et al., 2005; Wong et al., 2007; Shoemaker et al., 2012), demonstrating the largely inhibitory role of the medial and orbital frontal cortices in autonomic regulation (Owens & Verberne, 2000; Kimmerly et al., 2005; Shoemaker et al., 2015). Enhanced connectivity between medial prefrontal cortices and limbic structures in high-risk SUDEP patients could reflect an imbalance in the medial prefrontal-hippocampal circuitry involved in blood pressure regulation (Harper et al., 2015; Shoemaker & Goswami, 2015). A recent RS-fMRI study showed that increased vagal modulation, as measured by post-exercise heart rate variability, is accompanied by increased FC between the right anterior hippocampus and the ventral medial prefrontal cortex (Bär et al., 2016). Of interest, enhanced FC between the right hippocampus and the right FMC emerged in our study, and not in the left in high-risk patients at rest. One possibility, therefore, is that this increased connectivity is linked to resting elevated sympathetic tone, which is exhibited among poorly-controlled epilepsy patients (Mukherjee et al., 2009).

Connections with the insulae were also observed. A role of the insula in autonomic regulation has long been known (Oppenheimer, 1992), with neuroimaging studies confirming earlier stimulation studies (Henderson et al., 2002). The inhibitory role of the medial prefrontal cortex is well known for both autonomic processes and somatic reflexes (Chase & Clemente, 1968). Projections from the insular cortex to the medial frontal cortex, if exaggerated by seizure discharge, could lead to enhanced suppression of blood pressure levels, with the potential for hypotension. Such an imbalance at rest provides evidence of dysfunctional networking among these structures which may alter their ability to recover following a significant disturbance, such as a seizure.

The current data also demonstrate increased FC between the left and right hippocampus and left and right amygdalae in high-risk patients. Human electrophysiological studies demonstrate homotopic connectivity of bilateral mesial temporal structures in drug-resistant focal epilepsy patients (Wilson et al., 1991). Stimulation of the fornix results in contralateral hippocampal responses without involvement from the neocortex, establishing a link between bilateral mesial temporal structures (Lacuey et al., 2015). These findings also demonstrate that temporal lobe seizures likely propagate between the hemispheres via the limbic system. Elevated functional interconnectivity among high-risk patients between the bilateral amygdalae and bilateral hippocampi poses a risk of exaggerated descending influences on both breathing and blood pressure. The role of the amygdala in both sustaining inspiration (Harper et al., 1984) with the potential for apneusis or generating apnea has been described earlier (Dlouhy et al, 215). If both amygdalae combine to exert influences to the phase-switching brainstem areas, the risk for apneusis or apnea is raised. The

hippocampus plays an essential role in the diencephalic blood pressure regulatory circuitry (Shoemaker et al., 2015; Harper et al., 1998, 2000). Safe constraints of the system may exist with unilateral influences, but bilateral extreme activation, as may happen by recruitment in ictal discharge, may pose overwhelming drives to lower blood pressure final common path structures. Resting inter-ictal imbalances as shown here could result in erroneous and disturbed autoregulation during extreme circumstances, such as during ictal or post-ictal periods. Given the much higher frequency of seizures experienced by the high-risk cohort, it is plausible to suggest that these enhanced connections may be evidence of long-term seizure-induced hyper-connectivity of these structures. However, further work is required to establish whether and how seizure frequency influences the homotopic connectivity of these structures in TLE and other epilepsies.

4.1.4.4 Results after Regression of Hippocampal GM Volume, Not Presence of HS

As well as using presence/non-presence of HS as a covariate, we conducted further analyses using a more quantitative approach to control for connectivity changes related to morphological differences of the mesial temporal structures (hippocampus) between high- and low-risk patients. Similar reduced and enhanced subnetworks were revealed following this approach and, importantly, the core effects observed using presence of HS as a covariate were mirrored in this analysis. In summary, these were: reduced connectivity of the brain stem, thalamus, amygdala and putamen; and enhanced connectivity involving medial and orbital frontal cortices, the insulae, hippocampi and amygdalae, putamen, and caudate (see Results and Figures [S1](#) and [S2](#) in Supplementary Material). Additional edges were revealed in the reduced

subnetwork and comprised connections from the brain stem to the insula, putamen, and SC, and from the subcallosal to the ACC. In the high-risk > low-risk contrast, a greater number of connections involving the left medial frontal cortex emerged, and enhanced bilateral homotopic connectivity of the frontal medial and SC is shown. These connections highlight further altered connectivity in relation to increased SUDEP risk which must be explored in future studies. These data also demonstrate the importance of taking into account volumetric alterations in connectivity analyses, which should be considered in future studies.

4.1.4.5 Inter-ictal autonomic disturbances in epilepsy and relation to current findings

TLE patients show highly altered inter-ictal heart rate variability (HRV) (Ansakorpi et al., 2002) which reflect imbalances in sympathetic and parasympathetic control over cardiorespiratory actions, and is particularly disturbed in refractory epilepsy patients and those who experience GTCS (Evrengül et al., 2005; Mukherjee et al., 2009). Increased SUDEP risk has been associated with such alterations in HRV (DeGiorgio et al, 2010), particularly reductions in RMSSD (root-mean square differences of successive R-R intervals; Stein, 1994) - a measure of HRV which reflects vagus nerve-mediated autonomic control of the heart (DeGiorgio et al, 2010). The findings outlined in the current study may shed light on the underlying neural correlates of such autonomic imbalances in TLE patients at high risk of SUDEP.

4.1.4.6 Limitations

4.1.4.6.1 ROIs

A potential drawback of the current study is the incomplete parcellation of the template used to define ROIs. Many of the structures investigated here contain subdivisions

which may be important for interpreting the relevance of our findings with respect to their specific autonomic function. For example, the insular cortices are large structures, the subdivisions of which have differential roles in autonomic function (Macey et al., 2012). The lack of insular subdivisions in the current study hampers interpretation of enhanced connections found involving this structure. Similarly, subdivisions of the hippocampus also serve different functions (Strange et al., 2014), and future brainstem studies should include, at least, separation of the midbrain, pons, and medulla. The thalamus also contains multiple subdivisions, each with specialized functions and which project to different sites (Behrens et al., 2003).

The current study did not consider the cerebellum among the selected ROIs due to inadequate scan coverage. The cerebellum has been extensively linked to autonomic and respiratory functions, and especially with its role in dampening extremes of blood pressure changes (Harper et al., 2015), and is another structure which exhibits damage in HF patients, who are at considerable risk of sudden death (Ogren et al., 2012). Exploring functional interactions between the cerebellum and other brain structures in epilepsy, and with particular respect to SUDEP, is of significant interest. Future studies investigating structural and functional changes in this setting should include both cerebellar cortex and deep “autonomic” nuclei in the evaluation.

4.1.4.6.2 NBS limitations and choice of statistical significance threshold

The NBS enables detection of cluster-based differences (components) among a set of connections (in a network), enabling differentiation of two group-based significant subnetworks. Thus, the NBS has reduced power to detect stand-alone connections as belonging to the significant detected component. Furthermore, identification of a

cluster relies first, on detection of edges which surpass a given threshold (t), which must be specified a priori. One drawback of this approach is that it is rarely known which t should be used in practise, resulting in an unavoidable level of arbitrariness. To limit this bias here, we chose the minimum threshold at which a significant subnetwork for each contrast was revealed. The threshold required to reveal the reduced subnetwork (high-risk < low-risk) was $t = 2.5$, while $t = 2.1$ was required to reveal the enhanced subnetwork. The relatively higher threshold used in the high-risk < low-risk contrast reflects the discovery of a smaller, but more intense subnetwork of reduced FC, while the slightly lower threshold used for the high-risk > low-risk contrast explains the more extended yet less intense subnetwork of increased FC found (Zalesky et al., 2010).

4.1.4.6.3 Cohort

Future neuroimaging studies investigating SUDEP would benefit from applying network-based FC approaches to larger samples involving more epilepsy sub-types and patients who are subsequent victims of SUDEP. Furthermore, comparisons involving a group of healthy subjects is also necessary to evaluate findings in patients with reference to the healthy brain. Further sampling issues relate to inclusion of left and right TLE patients in the same group which, although controlled in statistical analysis, does not offer the opportunity to independently explore high-risk vs low-risk differences in each sub-group separately. Such an investigation would be of interest, given the lateralisation of autonomic brain circuitry (Macey et al., 2016) and the known whole-brain network differences between left and right TLE patients (Riddley et al., 2015).

Neuroimaging studies have demonstrated altered FC of mesial temporal structures, including the hippocampus and amygdala (Cullen et al., 2014), and medial prefrontal regions, including the subcallosal cortex (Sawaya et al., 2015), among patients with depression. Given the overlap involving epilepsy and psychiatric complications such as depression and anxiety (Thapar et al., 2009), future efforts should include methods to partition variance due to the incidence and severity of psychiatric diagnoses.

4.1.4.6.4 Use of connectivity strength

Comparisons of connection strength, while able to provide insights into communication between two distinct regions, is a relatively simplistic connectivity measure. Other, more elaborate, techniques under the graph theory framework, allow more sophisticated characterisation of connectivity and brain network architecture using rs-MRI. Future studies, and as will be demonstrated in the second study of this chapter, should employ approaches to characterise multiple aspects of connectivity, and thus allowing a more comprehensive assessment of network alterations related to SUDEP and elevated risk.

4.1.5 Conclusions

Alterations in FC observed indicate altered, potentially dysfunctional, communication among cortical and sub-cortical brain regions involved in autonomic and respiratory regulation. Resting-state FC imbalances among these regulatory structures may predispose such a network of regions to fail to recover from extremities caused by seizures, particularly GTCS. However, further work is required, particularly exploration of altered connectivity among individuals who go on to suffer SUDEP, as will be assessed in the next study ([4.2](#)). The present results build on existing findings and

shed further light on interactions between affected structures related to increased SUDEP risk and underline the need to consider integration from multiple brain sites in evaluating autonomic or breathing outcomes in SUDEP mechanisms.

4.2: Altered modularity and local connectivity amongst cortical and sub-cortical regulatory structures in confirmed cases of SUDEP.

4.2.1 Background

Non-invasive determination of risk for sudden unexpected death in epilepsy (SUDEP) and unearthing of processes leading to that outcome are major goals in the epilepsy field. Although the precise mechanisms of SUDEP remain elusive, circumstances surrounding the fatal event suggest a sudden cardiovascular collapse or cessation of respiratory efforts (Ryvlin et al. 2013; Massey et al. 2014), implying a failure of central regulatory control.

Earlier resting-state functional magnetic resonance imaging (RS-fMRI) studies, including the results of the previous chapter ([4.1](#)), show that patients at high risk of SUDEP show altered functional connectivity between key cortical and sub-cortical autonomic and respiratory control regions (Allen et al. 2017; Tang et al. 2014). Disrupted functional interactions among these regions along the cortico-diencephalic-brainstem pathway for cardiovascular and breathing control are suspected of contributing to SUDEP by interfering with normal control of autonomic or breathing processes. The RS-fMRI methodology allows non-invasive assessment of alterations to underlying functional neural pathways.

Previous studies assessing functional interactions between areas mediating autonomic and respiratory functions focused on specific epilepsy subgroups, e.g., temporal lobe

epilepsy, in risk-stratified living patients (Allen et al. 2017; Tang et al. 2014) and no confirmed or suspected SUDEP cases have been studied to date.

The current study sought to characterize noninvasively the functional architecture of a network of brain sites known to mediate cardiovascular and breathing control in confirmed SUDEP cases. Network analysis procedures in patient groups that included SUDEP cases, patients at high and low SUDEP risk, and matched healthy controls, was undertaken. The goal was to provide insights into potential mechanisms of failure and suggest possible non-invasive means to evaluate risk for SUDEP.

4.2.2 Methods

4.2.2.1 Subjects

Cases of SUDEP, high- and low-risk patients, and healthy controls were selected from an ongoing investigation into the fMRI correlates of interictal epileptiform discharges (Coan et al. 2016), with a case ascertainment period between 2005 and 2014. During this time, scanner hardware and software remained unchanged. The inclusion criteria were the availability of: 1) a resting-state EEG-fMRI scan, and 2) a high-resolution T1-weighted scan. The exclusion criteria were: 1) large brain lesions or previous neurosurgery (we considered large to be anything greater than a small area of FCD or sclerosis – i.e. tumours, cavernomas etc.); 2) incomplete clinical or imaging data (e.g., abandoned scans); and 3) excessive head movement during the EEG-fMRI scan (inter-scan displacement exceeding 3mm in any direction).

We searched the database for deaths, by querying each subject's medical record profile on a local clinical records database, and confirming these with death certificates. Of 12 deaths, nine were identified as SUDEP, one of which was excluded

due to the presence of a large brain lesion (previous neurosurgery). The resulting eight SUDEP cases (4 males, mean age 26.6 ± 6.1 ; see Table 4.2.1 for patient characteristics) were then classified as either probable or definite SUDEP based on established criteria (Nashef et al. 2012). We matched each SUDEP case as closely as possible with 2 high-risk and 2 low-risk patients, based on epilepsy syndrome and localization, disease duration, age, sex and lesion pathology.

Table 4.2.1. Clinical characteristics of the SUDEP cases

CASE	SUDEP CLASS	AGE AT SCAN/ DEATH (YEARS)	EPILEPSY SYNDROME	DISEASE DURATION (YEARS)	GTCS PER MONTH	MRI FINDINGS
01 (M)	Def	25 / 28	Focal, L frontal	18	0.75	Normal
02 (M)	Def	23 / 29	JME	2	10	Normal
03 (F)	Prob	28 / 30	JME	6	1.5	Normal
04 (M)	Def	34 / 40	Focal, L hemisphere	29	1	L parietal ischaemia
05 (F)	Def	36 / 42	Focal, L frontal	30	2	L frontal FCD
06 (F)	Prob	17 / 25	Focal, R parietal	10	1	R parietal FCD
07 (M)	Prob	24 / 26	Focal, L temporal	20	2	L anterior temporal FCD
08 (F)	Prob	26 / 32	Focal, L hemisphere	18	5	Normal

*M=*male, *F=*female, *def=*definite, *prob=*probable, *JME=*juvenile myoclonic epilepsy, *L=*left, *R=*right, *FCD=*focal cortical dysplasia.

All clinical information used for risk stratification and subject-matching was obtained from multidisciplinary team meeting reports and clinic letters at the time closest to the RS-fMRI scan. We chose to classify the matched patients according to a single criterion based on close examination of the SUDEP cases in our cohort: experiencing more than 3 GTCS per year, which has been found to be the most predictive SUDEP risk factor (DeGiorgio et al. 2017; Harden et al. 2017; Hesdorffer et al. 2012), and was the only common clinical factor in the SUDEP cases in our cohort. Thus, high-risk patients were defined as those experiencing more than 3 GTCS per year. Since SUDEP is dominantly a GTCS-related event, 2 low-risk patients were those not experiencing any GTCS. Survivorship of the living patient controls was confirmed by referring to the patient status in the clinical records database, which is regularly updated, prior to analysis.

In addition to living patient controls, each SUDEP case was matched to two healthy controls, of comparable age and same sex (individual patient and healthy control characteristics are shown in Supplementary Table [S2](#)). This selection resulted in 4 sub-groups; SUDEP (n=8), high-risk (n=16), low-risk (n=16) and healthy (n=16) for further analysis of RS-fMRI data and inter-group comparisons (group demographics and clinical details are shown in supplementary Table [S3](#)). The study was approved by the National Research Ethics Committee (United Kingdom; 04/Q0512/77 and 14/SW/0021) and all patients gave written informed consent.

4.2.2.2 Magnetic Resonance Imaging Acquisition

4.2.2.2.1 Resting-state fMRI

Scanning was performed at the Epilepsy Society (Chalfont St Peter, Buckinghamshire, UK) on a 3.0 Tesla GE (Signa Excite HDX) scanner. A 20-minute (400 volume) resting-

state EEG-fMRI scan was collected for each subject with the following characteristics: repetition time (TR) = 3000ms, echo time (TE) = 30 ms; flip angle = 90°, matrix size = 64×64, field of view (FOV) = 24×24cm, slice thickness = 3 mm, 44 slices. Subjects were instructed to keep their eyes closed, avoid falling asleep, and not think about anything in particular. A 64-channel EEG was recorded during the fMRI scanning using an MRI-compatible amplifier and cap (Brain Products GmbH, Gilching, Germany). In this study, the EEG recordings were used solely to record occurrence of interictal epileptiform discharges.

4.2.2.2.2 Structural MRI

A single high-resolution T1-weighted image was also acquired immediately before RS-fMRI collection using a FSPGR (fast spoiled gradient recalled echo) sequence, with the following parameters: TR/TE = 8.10/3.2, 24cm FOV, 100 slices, slice thickness = 1.5mm, with a matrix size of 256×160 for a voxel size of 1×1×1.5mm.

4.2.2.3 Data Processing

4.2.2.3.1 RS-fMRI pre-processing

'Data Processing Assistant for Resting-State fMRI' (DPARSFA; Yan & Zang, 2010), running in Matlab 2017b (MathWorks, USA), was used to pre-process the fMRI data. DPARSFA utilises functions from the software packages REST (Resting-State fMRI Data Analysis Toolkit; Song et al., 2011) and SPM12 (Statistical Parametric Mapping; www.fil.ion.ucl.ac.uk/spm). For each subject, the high-resolution T1 image was segmented using a fast-diffeomorphic image registration algorithm (DARTEL; Ashburner, 2007). The functional MRI volumes were slice timing-corrected and realigned. The 6-motion realignment parameters (generated during functional image

realignment), together with the mean white matter and CSF (generated during segmentation), were removed during nuisance covariate regression. Further motion correction (or 'scrubbing') was implemented to account for subtle (sub-millimetre) head movements which confound RS-fMRI data despite routine motion correction (Power et al., 2012). This correction was achieved by calculating the frame-wise displacement (FD – the sum of the absolute values of the realignment estimates relative to the preceding scan; Power et al., 2012), and replacing the volumes for which FD exceeded 0.5mm with linearly interpolated values. A threshold of 0.5mm was selected as a trade-off between appropriate control over movement and a reasonable amount of un-corrected data remaining per subject (in our data, no more than 30% of the volumes were corrected for a given subject). Lastly, the Brainnetome (BNA) atlas (Fan et al, 2016) was warped into individual scan space, using the parameters generated by DARTEL, for RS-fMRI time series extraction.

4.2.2.3.2. Wavelet filtering

Wavelet filtering was carried out due to superior denoising capabilities (Bullmore et al, 2004; Fadili & Bullmore, 2004). Prior to filtering, all time-series were shortened to 200 volumes (approximately 10 mins), due to 5 subjects having undergone a shortened scan. The average fMRI time series was calculated over all voxels in each of the 246 regions of the Brainnetome atlas and decomposed using the maximal overlap discrete wavelet transform (MODWT; Percival & Walden, 2000). Analysis was restricted to scale 2 of the wavelet decomposition which, in our data, corresponded to the frequency range 0.03~0.06Hz, since grey matter-derived network properties are most are most

salient within this frequency range (Achard et al., 2006; Bullmore et al., 2004). Wavelet filtering was carried out using the Matlab Wavelet Toolbox.

Time-courses from 246 brain regions were then extracted for each subject using the BNA. The BNA is composed of 7 'lobes' (frontal, temporal, parietal, insular, cingulate, occipital and sub-cortical nuclei), with a total of 24 'sub-lobes' (or gyri) , sub-divided into a total of 246 regions, and was selected because of its high level of regional subdivision and its anatomical, structural and functional relevance.

4.2.2.3.3 Regulatory subnetwork: ROI selection

The regulatory subnetwork was constructed from regions which play a significant role in cardiovascular and respiratory control, on the assumption that the fatal SUDEP event develops from a blood pressure collapse, significant arrhythmia, or failed respiratory efforts resulting in hypoxia (Massey et al. 2014). Regions of interest (ROIs) were selected from the BNA in a systematic fashion by including all regions within the structures belonging to lobes known to be associated with autonomic and respiratory functions, namely the cortico-diencephalic-brainstem pathways for autonomic and respiratory control (Macey et al. 2015; Shoemaker and Goswami 2015; Loewy 1991). This resulted in seventy-four ROIs: medial/orbito-frontal cortex (12 regions), insular cortex (12) and cingulate cortex (14), and 8 medial temporal structures (4 amygdala, 4 hippocampus), 12 basal ganglia and 16 thalamic regions (see Figure 4.2.1 for visualization of network and Table [S4](#) for details).

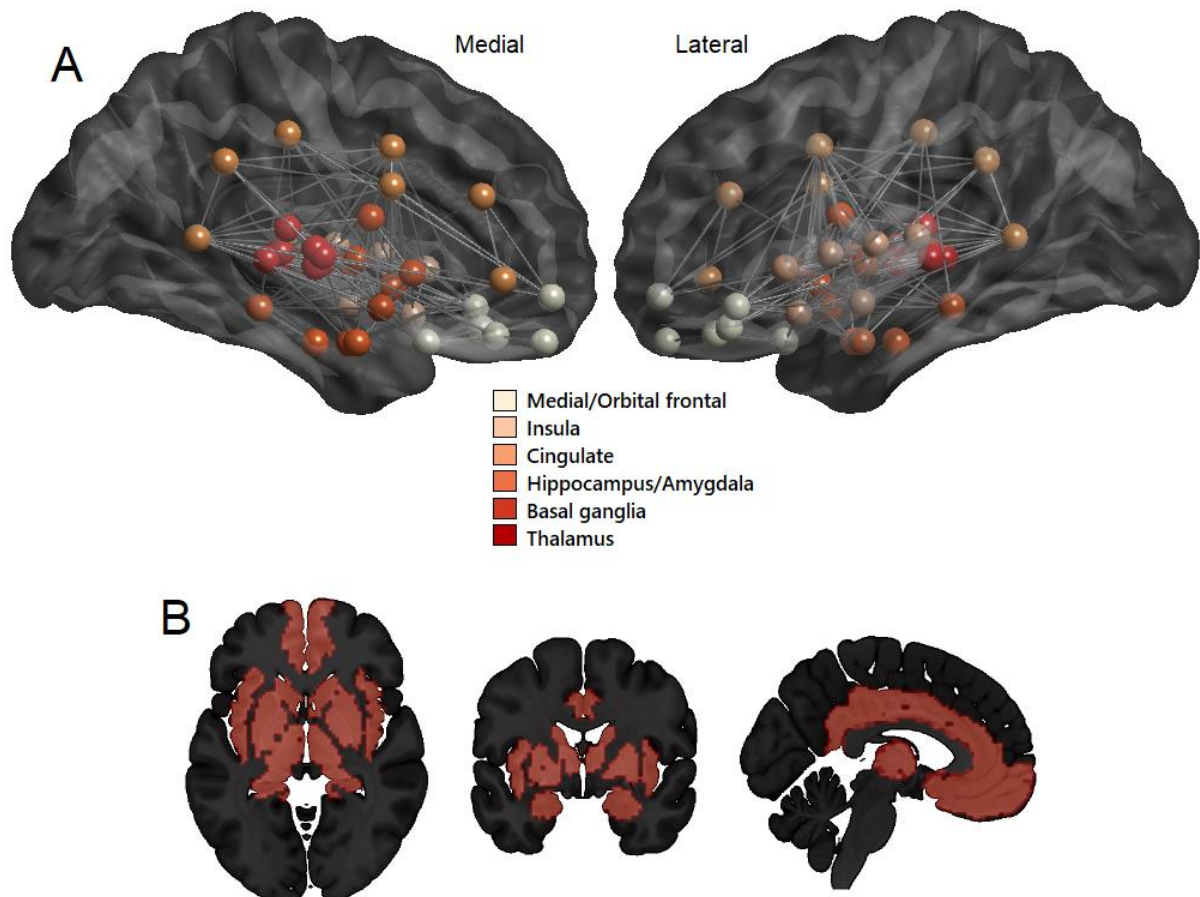


Figure 4.2.1. Visualisation of the selected subnetwork and ROI coverage displayed in standard space. A show medial (left) and lateral (right) views of the minimally connected subnetwork (MST), for visualisation of node locations, overlaid in render (MNI space). B shows ROIs displayed in 2D and overlaid in red, on axial (left), coronal (middle) and sagittal (right) planes.

4.2.2.3.4 Network Construction and Analysis

The wavelet coefficients obtained from the steps described above were used to perform inter-regional correlations between every brain region (or “node”), generating for each subject a 74×74 weighted network (or “graph”) for the regulatory subnetwork, and a 246×246 weighted network for the whole brain. Network construction and computation of the network measures were carried out using the Brain Connectivity Toolbox (BCT; Rubinov & Sporns, 2010) in Matlab. Weighted networks were thresholded using a minimal spanning tree (MST) approach, whereby the lowest weighted “edges” (connections between nodes) are used to minimally connect the network (Kruskal, 1956; Prim, 1957). Connections were then added back to the MST in descending order of the wavelet coefficients at network densities (proportion of connections) ranging from 50% to 5% in decrements of 1% (Alexander-Bloch et al, 2010). This procedure yielded a series of 46 binary undirected (involving non-directional connections) networks per subject, on which the four following measures were computed.

1. Network Modularity

Under our hypothesis that SUDEP may be linked to altered organization, and therefore communication, among brain regions involved in regulatory processes as well as the whole brain, we investigated modularity. Modularity is a network-wide assessment of how well a network can be sub-divided into clearly delineated groups (or modules) – a measure of how well-organised networks are.

Modularity was computed using the Louvain method for community detection (Blondel et al., 2008), which utilises a multi-iterative algorithm to determine the best possible

moduli of nodes into groups and thus an optimised (or ‘maximised’) modularity. In summary, modularity was estimated and optimised through a two-phase iterative process (Blondel et al., 2008), and was initially defined as:

$$Q = \frac{1}{2m} \sum_{ij} \left[A_{ij} - \frac{k_i k_j}{2m} \right] \delta (c_i, c_j)$$

Where A_{ij} represents the edge weight between nodes i and j ; for binary networks, as in the current instance, this value would be 0 or 1; k_i and k_j are the sum of the number of edges attached to nodes i and j respectively; $2m$ is the sum of all edges in the graph; c_i and c_j are the communities of the nodes; and δ is a delta function.

In order for this value to be efficiently optimised, two phases are repeated iteratively. First, each node in the network is assigned to its own community. Then for each node i , the change in modularity is calculated for removing i from its own community and moving it into the community of each neighbour j of i . This value is calculated by: (1) removing i from its original community, and (2) inserting i to the community of j . The equation for step 2 is as follows:

$$\Delta Q = \left[\frac{\Sigma_{in} + 2k_{i,in}}{2m} - \left(\frac{\Sigma_{tot} + k_i}{2m} \right)^2 \right] - \left[\frac{\Sigma_{in}}{2m} - \left(\frac{\Sigma_{tot}}{2m} \right)^2 - \left(\frac{k_i}{2m} \right)^2 \right]$$

Where Σ_{in} is sum of all links inside the community i is moving into, Σ_{tot} is the sum of all links to nodes in the community i is moving into, k_i is the degree of i , $k_{i,in}$ is the sum of the links between i and other nodes in the community that i is moving into, and m is the sum of all links in the network. Once this value is calculated for all communities to which i is connected, i is placed into the community that resulted in the greatest

increase in modularity. If no increase is possible, i remains in its original community. This process is carried out repeatedly and sequentially to all nodes until no modularity increase can occur.

The first phase is over once the local maximum of modularity is found. In the second phase, the nodes in the same community are grouped and a new network is built where nodes are the communities from the previous phase. Any links between nodes of the same community are now represented by self-loops on the new community node, and links from multiple nodes in the same community to a node in a different community are represented by links between communities. Once the new network is created, the second phase is over, and phase 1 can be re-applied to the new network.

2. Nodal Participation

Secondly, we computed participation (Guimera & Amaral, 2005), to understand if any particular brain regions exhibiting altered inter-modular communication are linked to SUDEP and/or elevated risk. The participation coefficient is a nodal measure associated with modularity, and assesses the extent to which a given region is connected to the other modules in the network. A node with high participation will have an equivalent number of connections to all the modules in the network. For a node with low participation, however, a larger proportion of its connections will lie within its own module. Participation is a measure of the diversity of a node, i.e., how much it ‘participates’ in other modules, and is defined as:

$$y_i = 1 - \sum_{m \in M} \left(\frac{k_i}{2m} \right)^2$$

Where M is the set of modules and $k_i(m)$ is the number of link between i and all nodes in module M .

3. Nodal Degree Centrality (DC)

We explored degree centrality (DC) to investigate whether differences in connectivity of specific regions, with the rest of the sub-network and whole brain, may be related to SUDEP. DC is a nodal network measure, which can be used to explore ‘hubness’ – the tendency of real-world complex systems, such as human brain networks, to be organised around highly-connected hubs (Achard et al. 2006). DC is simply defined as the number of connections incident upon a node (after thresholding connection strength). The greater the number of connections belonging to a node, the greater its connectivity.

4. Hub Distribution Index (HDI)

To examine whether SUDEP may be related to changes in how ‘hubs’ (highly connected brain regions) are organised across the whole brain and the regulatory network, we explored the hub distribution index (HDI). The HDI (Achard et al. 2012) characterizes the distribution of hubs within a network. Specifically, the HDI is a relative measure of regional topology that quantifies the reorganization of hubs between two given networks. Here, hub distribution was calculated for every patient network relative to the mean healthy control network.

To estimate the hub distribution index in a single subject, the healthy group mean degree (across subjects and network sparsities) for each region is simply subtracted from the mean (across sparsities) degree of the same region in an individual subject. The regional differences thus obtained are then plotted against the means of the

healthy control group and a least square regression line is fitted to the data. Typically, when calculated for an individual healthy control, the data points on the plot scatter to form a positive horizontal slope, indicating that the degree of a given region in a given healthy control is close to the average degree of the same region for the remainder of the healthy group (Achard et al., 2012). A negative slope for an individual subject, however, indicates that high-degree regions (hubs) in the healthy group have become low-degree regions (non-hubs) in the test subject, demonstrating a reorganization of hubs (Achard et al., 2012; Figure 4.2.2). The gradient of the slope was measured for each epilepsy subject, relative to the healthy control group, and compared across patient groups using non-parametric permutation t-tests, as described in statistical analysis.

Due to inadequate whole-brain parcellation (incomplete T1 scan) in one subject, the whole-brain network analysis was carried out in 55 subjects (8 SUDEP, 15 high-risk, 16 low-risk and 16 healthy).

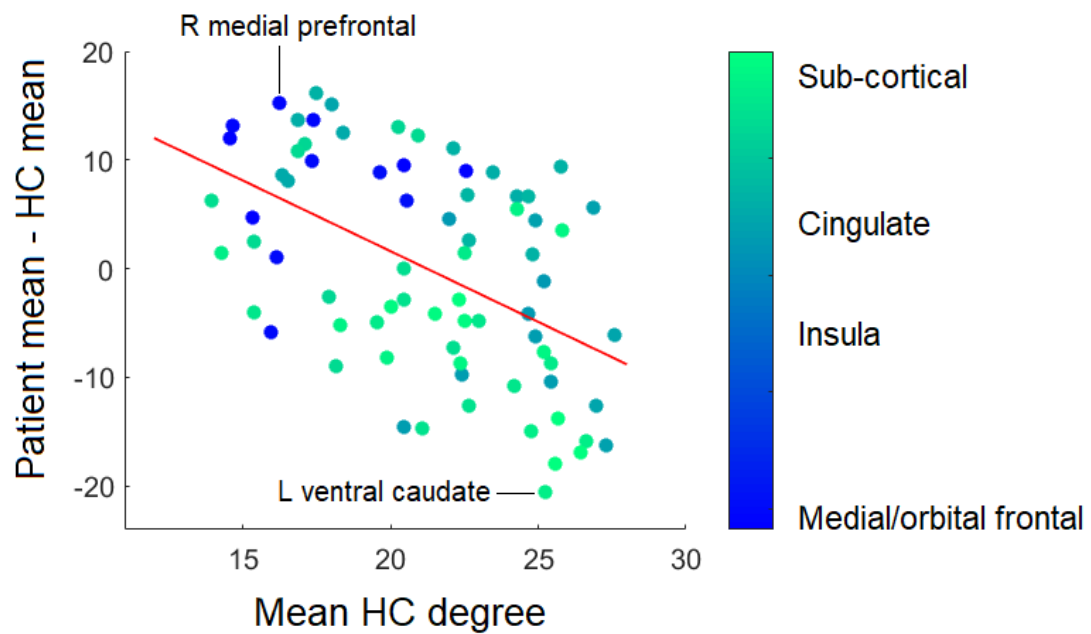


Figure 4.2.2. Hub distribution index computed for one subject. Scatter showing individual patient mean minus the HC mean on the y axis, and mean degree of healthy controls on the x axis. Red line is the least squares regression line fitted to the data, showing a slope of -0.78 in this example.

4.2.2.4 *Statistical analysis of network measures*

The following statistical analyses were carried out identically for the regulatory sub-network and whole-brain network.

4.2.2.4.1 Area under the curve (AUC) and permutation tests

The following calculations were carried out in Matlab: to establish between-group differences between each of the patient subgroups and the healthy controls for each network measure, we compared the area under the curve (AUC; Figure 4.2.3) using permutation tests. The AUC was obtained by integrating the network measure values across all 46 sparsities, yielding one value/network measure, and per node for DC and participation, as opposed to one per sparsity, greatly reducing the number of statistical tests required for group comparisons and increasing power to detect differences across multiple sparsities (Zhang et al. 2017; Xu et al. 2016).

Prior to statistical assessments, age, sex, and mean frame-wise displacement were regressed from the AUC using linear regression, and the residuals from these values were used for comparison. The AUC for each network measure was compared using permutation tests, whereby members from each sample were randomly permuted upon each of 10,000 iterations. This step generates an empirical null distribution, from which p-values were obtained. The nodal measures (degree centrality and participation) were corrected for multiple comparisons using the family wise error rate (FWER; Freedman and Lane, 1983) a correction which was unnecessary for the network-wide measures (network modularity and HDI), since only one value per subject is calculated.

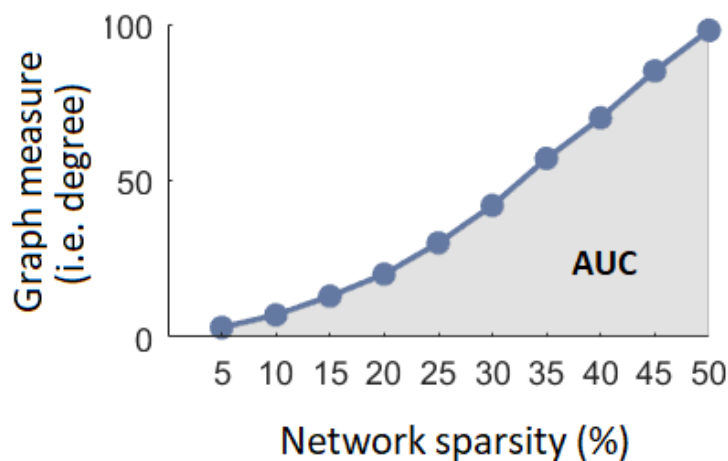


Figure 4.2.3. Area under the curve (AUC) of an example graph measure (degree centrality) in one subject. The AUC is represented by the grey shading below the data points which signify the observed graph measure at each network sparsity.

4.2.2.4.2 Correlation analysis

Partial correlations were carried out in IBM SPSS 25 to assess whether GTCS frequency correlated with the AUC of any of the graph measures computed on the subnetwork (modularity, participation, DC), as well as with hub distribution. SUDEP cases and high-risk subjects (n=24) were considered as one group for this correlation analysis. P-values were FWER corrected as per group comparisons.

4.2.2.4.3 Accounting for epileptiform discharges during RS-fMRI

For each epilepsy subject (SUDEP, high-risk and low-risk groups), data were checked for interictal epileptiform discharges (IED; or 'epileptic spikes'), by an experienced neurophysiologist. IEDs were visually counted and average (mean) IED counts (for each scan, per subject) were calculated and compared across patient groups using

non-parametric statistical tests. Spearman's rank correlation coefficients were also carried out between IED counts and each of the network measures computed.

4.2.3 Results

4.2.3.1 Demographics and clinical data

Age and sex distributions for all groups at scan time were similar, and epilepsy groups (SUDEP, high- and low-risk) were comparable for clinical variables, including localization and duration of epilepsy (Table S4.) All epilepsy groups had similar proportions of patients with a lesion identified on MRI (SUDEP: 50%, high-risk: 37.5%, low-risk: 50%).

4.2.3.2 Resting-state fMRI

The mean number of IEDs did not differ significantly between any of the patient groups, nor did it correlate significantly with the AUC of any of the network measures or hub distribution indices.

Modularity of the regulatory subnetwork was significantly reduced in cases of SUDEP ($t = 3.2$, $p = 0.004$) and high-risk subjects ($t = 2.4$, $p = 0.02$), compared with healthy controls (Figure 4.2.4 A). Subnetwork modularity was reduced in SUDEP when compared with low-risk subjects ($t = 2.1$, $p = 0.03$). Similarly, whole-brain modularity was reduced in SUDEP cases ($t = 2.2$, $p = 0.03$) and patients at high-risk ($t = 2.1$, $p = 0.04$), compared with healthy controls (Figure 4.2.4 B).

Nodal participation (the extent to which a region participated in modules outside its own) was significantly higher for 16 regions in high-risk patients and 23 in SUDEP

cases (Figure 4.2.5). Details of the affected nodes, their anatomical labels, and FWER-corrected p-values can be found in Table [S5](#).

Both elevated and reduced DC (degree centrality, a measure of hubness) across nodes were observed in every patient group relative to healthy controls. SUDEP and high-risk cases displayed similar patterns of change in DC, with reductions in the insula and cingulate, and increases in frontal and hippocampal structures (Figure 4.2.6 A-B). Low-risk subjects also showed increased and decreased DC vs controls, although these changes spanned a greater part of the network compared to high-risk and SUDEP cases (Figure 4.2.6 C; see Supplementary Table [S6](#) and [S7](#) for detailed affected nodes and FWER corrected p-values).

All patient groups exhibited hub reorganization (as measured with HDI) within the regulatory subnetwork; furthermore, this effect was entirely consistent within each subgroup (with negative slopes in all subjects). Compared with high-risk patients ($t = 2.6$, $p = 0.014$) and SUDEP cases ($t = 2.7$, $p = 0.012$), low-risk subjects showed significantly greater reorganization (Figure 4.2.7).

Lastly, GTCS frequency correlated positively with DC of the right posterior hippocampus ($r = 0.452$, $p = 0.045$), and negatively with DC of the right pregenual cingulate ($r = -0.52$, $p = 0.02$; Supplementary Figure [S3](#) A and B). Significant negative correlations were observed with nodal participation of the left rostroventral cingulate ($r = -0.64$, $p = 0.002$) and the right ventral caudate ($r = -0.58$, $p = 0.008$; Supplementary Figure [S3](#) C and D).

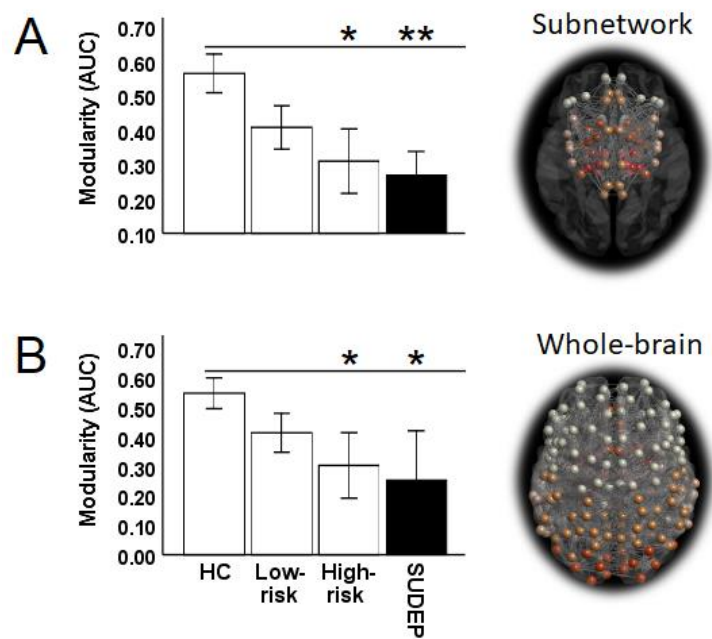


Figure 4.2.4. Reduced modularity in SUDEP and high-risk. A: Significantly reduced subnetwork modularity in high-risk patients and cases of SUDEP; *reduced compared to HC, **reduced compared to HC and low-risk. Error bars = standard error (SE) +/- 2. B: Significantly reduced whole brain modularity in high-risk subjects and SUDEP cases compared with healthy controls (HC) only.

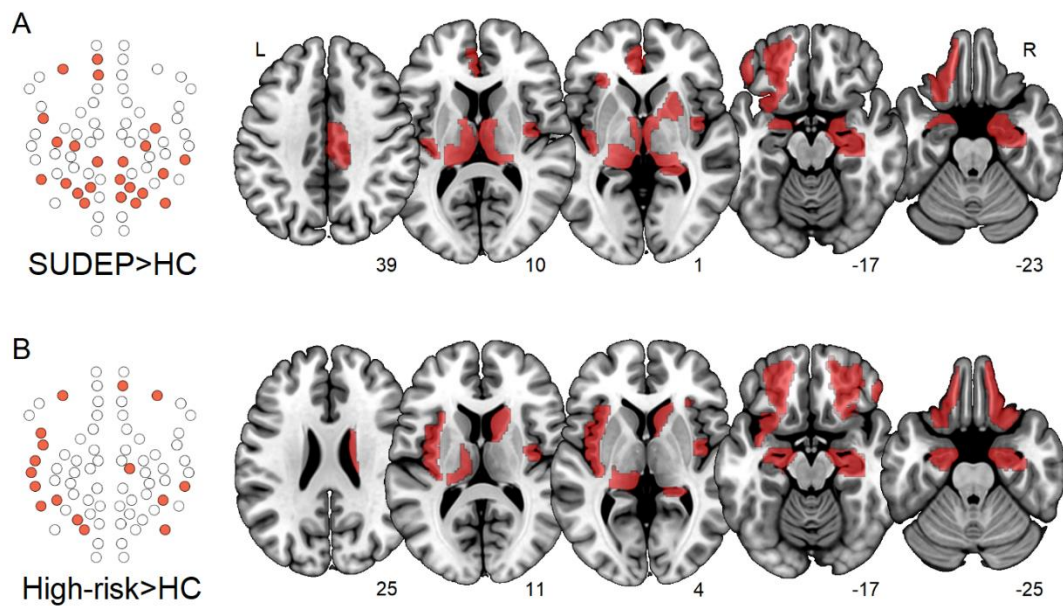


Figure 4.2.5. Elevated participation in SUDEP and high-risk subjects. Nodes with increased participation in SUDEP (A) and high-risk (B) compared with healthy controls. Left: Network schematics of affected regions among the subnetwork in SUDEP and high-risk. Right: affected regions overlaid in red on a standard brain, with slice numbers below. ($p < 0.05$, FWER).

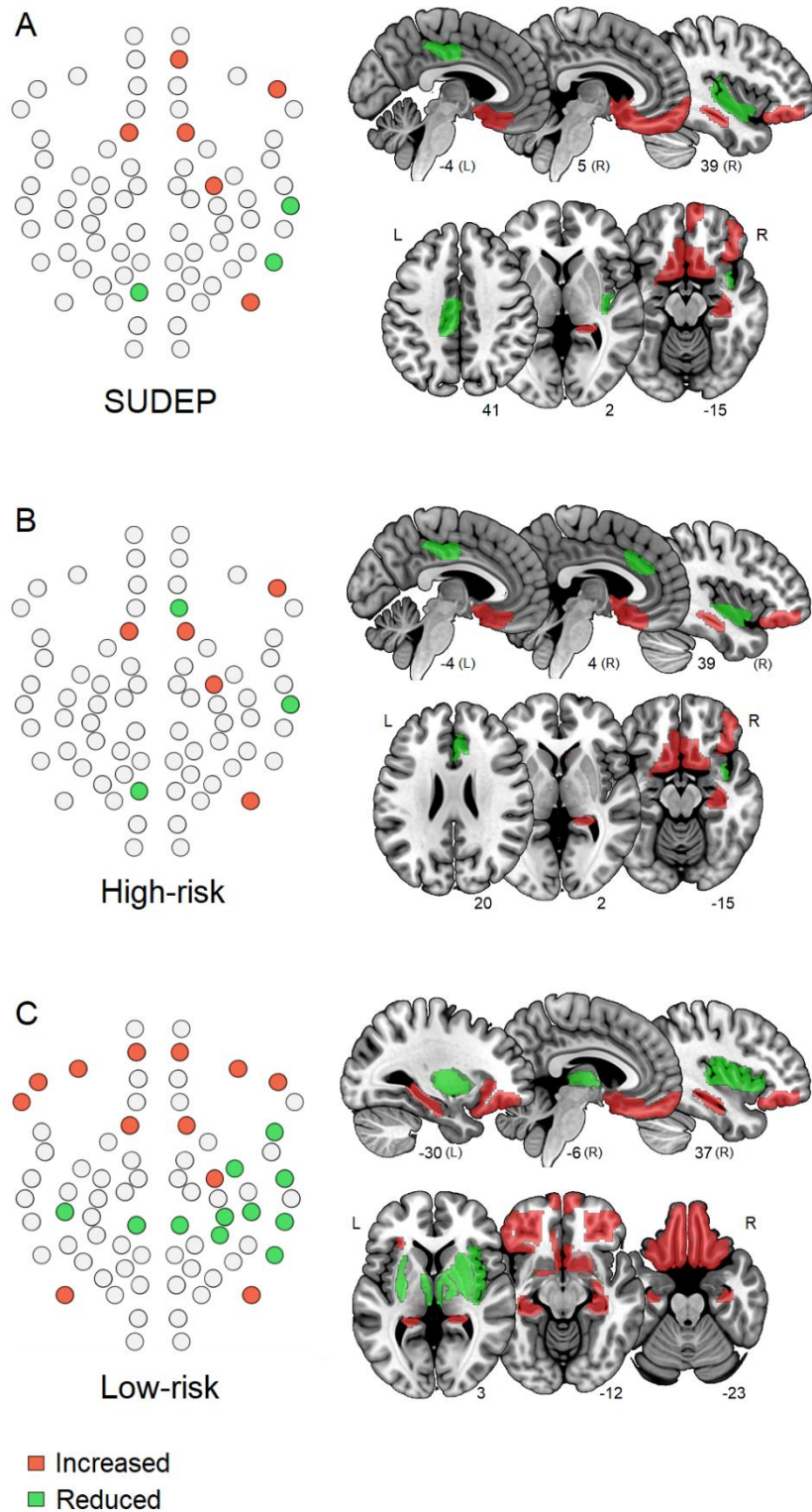


Figure 4.2.6. Altered degree centrality across groups compared with healthy controls. Increased (red) and reduced (green) degree centrality in SUDEP (A) high-risk (B) and low-risk (C) compared with healthy controls ($p < 0.05$, FWER). **Left:** regulatory subnetwork schematic, **right:** ROIs overlaid on standard brain.

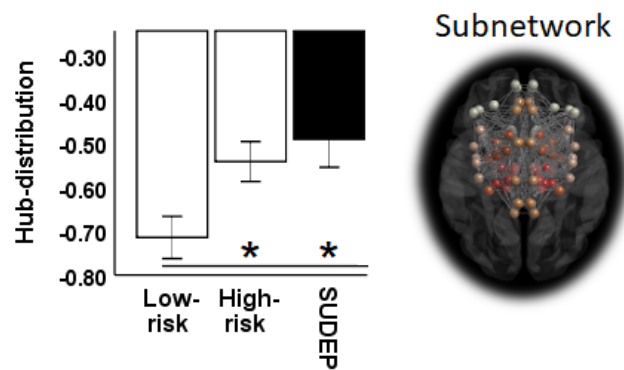


Figure 4.2.7. Subnetwork Hub distribution index across groups. Greater reorganisation (more negative hub-distribution index) amongst the regulatory subnetwork in low-risk compared with high-risk subjects and SUDEP cases. * ($p < 0.05$). Error bars = $SE \pm 1$.

4.2.4 Discussion

4.2.4.1 Overview of results

Significantly altered patterns of network connectivity emerged in high-risk individuals and SUDEP cases, who showed decreased network modularity and increased nodal participation relative to healthy controls amongst a subnetwork of critical brain regions involved in cardiovascular and breathing control. The findings suggest that the functional architecture among regulatory structures in SUDEP and those at greatest risk is more diffuse and less organised.

Differences in the number of connections belonging to a region (degree centrality) appeared across all patient subgroups relative to healthy controls, with SUDEP and high-risk patients eliciting similar patterns of alteration, and low-risk patients showing more drastic changes encompassing a greater number of regions. Patterns of centrality alterations and reorganization of hubs among regulatory structures differentiated low-risk patients from high-risk and SUDEP cases, suggesting different pathways to functional reorganization that are related to SUDEP risk.

4.2.4.2 Disrupted organization among regulatory structures in SUDEP and high-risk patients

A clear division of a network into modules (assessed with modularity) is a prominent feature of many biological networks, including the mammalian cortical architecture (Yamaguti and Tsuda 2015). Decreased modularity of resting-state functional brain networks occurs in several pathological states, e.g., childhood-onset schizophrenia, and with poorer responses to cognitive training in aging adults following traumatic brain injury (Gallen et al. 2016). Lower modularity implies a less organised network,

accompanied by a reduced ability to adapt to diverse and fluctuating situations (Kashtan and Alon 2005). We propose that aberrant organization among regulatory structures, as found here, may lead to a reduced ability of neural circuitry to adapt or respond to stimuli accompanying extreme challenges, e.g., baroreceptor, hypoxia or hypercarbia stimuli, such as might be experienced during recovery from the severe autonomic and respiratory imbalances known to accompany GTCS (Ryvlin et al. 2013; Lacuey, et al. 2018a; Schuele et al. 2011).

In this study nodal participation, a measure of the degree to which a brain region communicates with other modules in the regulatory subnetwork, was elevated across multiple regions in SUDEP and high-risk subjects, with the SUDEP group showing the greatest alterations, and further indicating lowered modular organization. SUDEP cases also showed increased participation vs low-risk subjects among 6 regions, (see details in Supplementary Material Table [S8](#) and Figure [S4](#)). A possible interpretation is that higher between-module connectivity, resulting from a greater number of connector nodes (regions with higher participation), may facilitate synchrony and could enhance “channelling” of cross-network action. Such “channelling” may exaggerate neural actions, potentially overloading the system under exacerbated neuronal activity, e.g., during a GTCS. These augmented interactions could involve brainstem regions via multiple descending influences from the diencephalon, including the thalamus. Such enhanced influences on critical nuclei in the brainstem may result in spreading depolarization (Aiba and Noebels 2015) or disruption to brainstem networks (Mueller et al., 2014; Mueller et al., 2018).

The nature of affected areas varied across the groups. Anterior mesial temporal structures were affected, including the bilateral medial amygdala in SUDEP and bilateral anterior hippocampus in high-risk groups. These regions exert critical influences on breathing, with stimulation eliciting apnea in human epilepsy patients (Lacuey et al. 2017; Nobis et al. 2018; Dlouhy et al. 2015). Ictal central apnea is common (Lacuey, et al. 2018a), prolonged instances of which may contribute to SUDEP. Increased amygdala grey matter volume has been linked with SUDEP and those at high-risk (Wandschneider et al. 2015). The current findings build on evidence of amygdala involvement in SUDEP and elevated risk, showing altered functional networking of these structures in high-risk and SUDEP cases. The thalamus was most affected in the SUDEP group, with 10 of 16 thalamic subregions showing increased participation, implying greater inter-modular connectivity of the thalamus with other structures in the subnetwork. Grey matter volume of the posterior thalamus is reduced in SUDEP and those at high-risk as shown earlier. Here, we demonstrate dysfunctional connectivity among many portions of the thalamus, including posterior, medial and lateral portions in high-risk and SUDEP cases.

The cingulate serves critical regulatory control for blood pressure (Burns and Wyss 1985), and interactions with other limbic structures for blood pressure control are substantial (Öngür, An, and Price 1998). Network alterations to portions of the cingulate cortex appeared only in those who succumbed to SUDEP.

At the whole-brain level, nodal participation did not significantly differ between patient groups and controls for any region considered here. However, when exploring connectivity among the regulatory network, participation was aberrant in the patient

groups. While communication between regions in the subnetwork was disrupted, these alterations went undetected when assessed in relation to the whole-brain, highlighting a well-known limitation of more-exploratory analyses, and vindicating our overarching hypothesis that connectivity amongst this subset of structures (largely forming the limbic system) is of particular relevance for SUDEP, and epilepsy.

4.2.4.3 Connectivity patterns also differentiate patients at low-risk

Degree centrality, the number of connections a node possesses to others in the regulatory subnetwork, showed increases and decreases in each patient group compared with healthy controls, with SUDEP and high-risk cases showing similar patterns. In these two groups, increases appeared in the ventromedial prefrontal cortex and right posterior hippocampus, while reductions occurred in the cingulate and insula. Low-risk patients, however, showed more widespread changes in DC, spanning a greater number of regions compared with the SUDEP and high-risk groups. Increases were principally observed in the frontal cortex (9 nodes) and decreases involved the bilateral medial thalamus, basal ganglia (5) and insula (4). Across all groups, increases appeared in the right posterior hippocampus (bilaterally in low-risk patients) and right accumbens, which may represent markers of altered connectivity specific to epilepsy in this cohort.

The hub distribution index, the extent to which hubs (highly connected nodes) are topologically organised in patients with respect to the control group, was negative in all patients, reflecting reorganization of functional brain network hubs within the subnetwork; the same is apparent in comatose individuals (Achard et al. 2012). Moreover, the HDI was significantly altered (more negative) in low-risk patients vs

SUDEP and high-risk patients. This change indicates a shift in hub organization within the regulatory network in low-risk patients, which appears to link to the more dramatic alterations in DC. The same reorganization in low-risk patients did not appear when computed for the whole-brain.

Taken together, the alterations in DC and greater hub reorganization revealed by HDI differentiated patients at low-risk, and may provide evidence of network reorganization among regulatory structures in subjects with better-controlled epilepsy. Imaging features related to reduced SUDEP risk may provide further insight into mechanisms and prevention approaches; thus, these findings warrant further investigation, as they may one day have implications for clinical management.

4.2.4.4 GTCS frequency and graph measures

When considered over the subnetwork of interest only, GTCS frequency correlated negatively with participation in the left rostroventral anterior cingulate, a region which increased participation in SUDEP cases. None of the subnetwork regions showing increased participation in high-risk and SUDEP cases demonstrated significant positive correlations with GTCS frequency. The only significant negative correlation between GTCS frequency and DC was in the right pregenual cingulate, suggesting that repeated GTCS are related to reduced connectivity of this region, a concern, since stimulation near here leads to central apnea (Lacuey., et al. 2018b). Conversely, the only positive correlation between DC and GTCS frequency appeared in the right posterior hippocampus, suggesting more frequent GTCS are related to greater connectivity of this structure. GTCS frequency did not significantly correlate with modularity or hub distribution across the subnetwork. Overall, GTCS frequency is an

important SUDEP risk factor and correlates with connectivity measures of several regions. However, GTCS seizure frequency alone could not explain the drastic alterations in modularity and participation observed in cases of SUDEP or high-risk patients.

4.2.4.5 Autonomic dysregulation in epilepsy and functional imaging biomarkers of SUDEP

A meta-analysis of heart rate variability in epilepsy (Lotufo et al. 2012), revealed sympathovagal imbalance, with lower vagal and higher sympathetic tone in patients. High sympathetic tone poses a risk, leading to constriction of the arterial supply to vital organs, and to arrhythmia, especially if the outflow is asymmetric (Schwartz, Priori, and Napolitano 2000). Conversely, while routine vagal activity levels are often cardioprotective, excessive activity leads to bradycardia and impaired perfusion (Thayer, Yamamoto, and Brosschot 2010). The disrupted connectivity in key cardiovascular and breathing sites, including the amygdala and hippocampus (Frysinger and Harper 1989), in SUDEP and high-risk groups may provide insights into mechanisms of central autonomic dysfunction related to SUDEP.

The functional connectivity of mesial temporal (hippocampus and amygdala) and thalamic structures was extensively affected in SUDEP and in high-risk patients. This and other work has previously shown volumetric and functional connectivity changes occur in the hippocampus, amygdala, cingulate and thalamus in SUDEP and those at high-risk (Wandschneider et al. 2015; Ogren et al. 2018; Tang et al. 2014; Allen et al. 2017; Allen et al., 2019b), findings which reinforce the importance of these structures

to SUDEP and elevated risk. Altered connectivity among these structures has the potential to provide prospective and non-invasive biomarkers of SUDEP.

4.2.4.6 Limitations and future work

4.2.4.6.1 Cohort

The difficulty of identifying SUDEP cases makes imaging studies challenging, usually resulting in small sample sizes; a limitation of the current study. If future studies (particularly those employing novel imaging sequences such as RS-fMRI) are to expand their sample sizes, large multi-center collaborations should be sought and methodological issues surrounding multiple MRI scanners will require careful consideration.

4.2.4.6.2 ROIs

Methodological constraints precluded inclusion of the brainstem and cerebellum here, despite their central roles in autonomic and respiratory regulation. Typically, resting-state fMRI scans employing graph theory do not cover the brainstem region due to noise introduced from non-grey matter signals (Brooks et al. 2013). Future studies should also explore brainstem connectivity using diffusion MRI, which would allow assessment of white matter tracts in the region that are difficult to investigate with fMRI. Insufficient imaging coverage of the cerebellum in many subjects precluded its inclusion in this analysis.

Although the selection of regulatory sub-network nodes may be seen as somewhat arbitrary, extensive previous work demonstrated the regional roles in autonomic and respiratory control, (Macey et al. 2015; Shoemaker and Goswami 2015; Loewy 1991)

and earlier studies constructed similar (but less detailed) subnetworks (Allen et al. (2017). Future studies, however, should record autonomic and respiratory output (i.e. blood pressure, breathing rate, apnea) during fMRI for inclusion in connectivity analyses.

4.2.4.6.3 Differences and similarities between high-risk and SUDEP

Matching high-risk subjects to SUDEP cases based on clinical variables, such as epilepsy duration and seizure frequency, enabled us to account for epilepsy severity (a confound and popular critique of SUDEP studies). Doing so ensures that the main difference between these two groups is that the former were alive at the time of inclusion and the latter were not due to SUDEP. Interestingly, SUDEP and high-risk showed similar connectivity alterations compared with healthy controls. However, the differences between them are of note. For example, although modularity was reduced in both SUDEP and high-risk, the magnitude of difference was greater in SUDEP. Also, nodal participation was elevated in both SUDEP and high-risk, although the number and nature of affected nodes differed (SUDEP showed increases among 23 regions, involving mainly thalamic nodes, while high-risk exhibited increases among 16 nodes, with mainly insula nodes affected). Thus, while the differences for any of the network metrics did not reach statistical significance, the trends indicate progressive network disruption in the direction of SUDEP. Further investigation into these patterns is therefore key to understanding the processes leading to SUDEP.

4.2.4.6.4 Resting-state fMRI in exploration of brain connectivity

RS-fMRI provides a unique opportunity to characterise functional connectivity of the brain, and model network interactions in health and disease. The functional

interactions upon which fMRI is based, rests upon the assumption that correlated fluctuations of regionally averaged BOLD signals reflect connectivity and thus communication between brain areas. It is important to note that the physiological underpinnings, and thus the interpretation, of such connectivity remain under debate. In addition, this approach does not take into account the structural pathways which connect such sites, and they instead rely only on correlations between discrete, but functionally related, brain regions, which may not have a direct structural link with one another. A key goal for future work is thus to characterise functional connectivity and network alterations alongside structural connectivity and morphology, in order to enhance insight into, and amalgamate, observed structural and functional alterations linked to SUDEP.

4.2.5 Conclusions

The functional organization among a preselected network of regions involved in respiratory and cardiovascular regulation was less modular in patients who subsequently succumbed to SUDEP and in those at greatest risk. Disrupted organization could mean impaired communication and vulnerability under extreme circumstances. Greater inter-module connectivity may reflect an increased propensity to facilitate seizure spread and promote excessive neuronal interactions among vital structures. Alterations in degree centrality and reorganization of hubs among these regions was most prominent in low-risk patients. The characterization of altered network properties among essential autonomic and breathing regulatory brain areas may shed light on the processes underlying SUDEP and facilitate non-invasive evaluation of SUDEP risk stratification. Further work is required to establish the

processes leading to, and evolution of, brain network alterations related to SUDEP.

Clear mechanisms linking changes in brain connectivity to SUDEP remain to be seen.

Chapter 5: Conclusions, limitations and future work

The current body of work employed MRI techniques to explore and characterise structural and functional brain alterations associated with SUDEP and related risk factors. The purpose of this chapter is to summarise key findings, highlight limitations and consider future directions of the work carried out as part of this thesis. Structural and functional connectivity findings will first be summarised, and overarching limitations of neuroimaging as a technique to investigate SUDEP will be detailed. The future of neuroimaging studies of SUDEP will be briefly discussed, followed by final concluding remarks.

5.1: Key findings

5.1.1 Structural brain alterations

As part of the current collection of work, three structural MRI experiments were carried out, revealing several key outcomes:

1. As revealed in chapter [3.1](#), individuals who went on to suffer SUDEP, and those at high risk, exhibited grey matter volume loss in the thalamus (particularly posterior portions, as reported previously, i.e. Wandschneider et al, 2015), and vermis; sites known to participate in autonomic and respiratory action. Both SUDEP and high-risk additionally demonstrated increased amygdala, parahippocampal and entorhinal cortex grey matter volume. Together, such changes, if confirmed in much larger datasets, may provide potential predictive markers. Volume alterations exclusive to SUDEP were grey matter volume loss of the PAG and increased

subcallosal grey matter volume, which may more closely reflect patho-mechanistic changes related to SUDEP.

2. Individuals with GTCS accompanied by hypoxemia exhibited regional brain volume reductions across a number of sites, some of which showed loss in confirmed cases of SUDEP (the thalamus, PAG and vermis), as shown in chapter [3.2](#). Additional areas, including the pons, medulla and hypothalamus, also showed loss. The direction of thalamic, PAG and medulla volume loss across groups indicates injury related to increasing levels of peri-GTCS hypoxemic exposure. Thalamic and hippocampal volume loss was linked to elevated degrees of hypoxemia, and vermal and accumbens volume loss was linked with greater durations of hypoxemia.
3. The latter of the described studies attempted to characterise associations between structural alterations among important brain sites and a respiratory manifestation which may be involved in SUDEP (hypoxemia). However, while indications of potential injury mechanisms may be speculated, the exact processes leading to SUDEP, and the links between brain structural changes and the final events involved, remain unknown.

5.1.2 Resting-state functional connectivity and brain network alterations

The two resting-state fMRI experiments described in this thesis set out to characterise the presence and extent of altered functional connectivity associated with SUDEP and elevated risk.

1. Assessments of functional connectivity strength in risk-stratified living patients with temporal lobe epilepsy, as per chapter [4.1](#), demonstrated increased and decreased subnetworks in patients at high-risk, compared with subjects classified as low-risk. Reductions in connectivity were consistent with previous work, and demonstrated reduced connectivity between the thalamus, brainstem, anterior cingulate, amygdala and putamen. Increases in connectivity were largely observed between medial/orbital prefrontal cortex and mesial temporal structures (hippocampus and amygdala).
2. Confirmed cases of SUDEP and those at high-risk exhibited altered functional organisation of the whole-brain and a regulatory subnetwork, evidenced by reduced modularity and increased regional participation (which was most prominent among thalamic regions in those who subsequently suffered SUDEP) in chapter [4.2](#). A shift in the topological organisation of network hubs in the regulatory subnetwork was apparent in patients relative to healthy controls, as were alterations in degree centrality, both of which were most dramatic in those at low-risk.

5.2 Overarching limitations, considerations and future work

5.2.1 Overview

The findings reported across the current body of work demonstrate structural alterations and aberrant resting-state functional connectivity associated with SUDEP and increased risk. It is, however, important to highlight a number of considerations and limitations of the methods employed and what can be derived from them. While technique-specific limitations have been outlined within the discussion sections of each respective study, there are several limitations which apply to the general use of neuroimaging to investigate SUDEP.

5.2.2 Limitations of findings and interpretation

The current imaging findings demonstrate structural and functional connectivity changes among central autonomic and breathing regulatory brain regions. The primary interpretation of altered structure and functional connectivity rests on the assumptions that: 1) such sequelae equates to damage and dysfunction among autonomic regulatory structures and networks; and 2) that this may predispose or compromise central regulatory sites and processes to recover from post-ictal cerebral inhibition or cardiorespiratory dysfunction, ultimately contributing to SUDEP. The suggestion that such alterations could indeed lead to death, and be involved in SUDEP, while possible, is entirely speculative and will remain so until the exact cause (or *causes*) of SUDEP is confirmed. As such, and speaking to a wider issue of using neuroimaging to investigate disease processes and mechanisms, associative changes (i.e. those accompanying a particular patient cohort) such as those revealed in the present studies, do not permit causal inference of a process or mechanism.

Much of the findings reported across the current thesis were discussed and interpreted in relation to previous studies demonstrating the roles of certain brain regions in autonomic and breathing regulation, many of which were conducted on animals. Functional imaging studies involving triggered autonomic and breathing challenges and diseases accompanied by autonomic and respiratory dysfunction have confirmed much of what is known in animals (Macey et al., 2016). However, the precise processes and networks which govern the components of autonomic and respiratory regulation, and how compromised aspects may lead to SUDEP in humans, remains to be fully known.

Future studies, particularly ones exploring changes in, or interactions between, specific groups of ROIs would benefit from combined autonomic, respiratory and imaging investigations. This would not only guide ROI selection, but it would also enable assessment of changes involving brain areas and networks functionally related to breathing and autonomic action, and not in those selected on an a priori basis. Triggered fMRI experiments, for example, whereby functional brain responses to autonomic and breathing challenges can be measured, could be performed to characterise regional responses and networks related to those functions and reveal potential disturbances. This would enable assessment of functionally relevant disruptions among central autonomic and breathing regulatory areas, and may help to establish a functional basis for impaired central autonomic and breathing control related to SUDEP and elevated risk. Additionally, given that SUDEP often occurs at night (Lamberts, 2012), and that PGES occurs more commonly following sleep-bound compared with daytime GTCS (Peng, Danison & Seyal, 2017), changes in functional connectivity across states of wakefulness and sleep should be explored in relation to

SUDEP risk and simultaneously acquired autonomic (i.e. ECG) or breathing measurements. Such investigations would allow dynamic assessments of interactions between connectivity of individual or networks of regions and sleep, and how they may be modulated by, or interact with, cardiac and respiratory processes. This is particularly important for certain regions which play known roles in sleep/wake modulation of autonomic and breathing control, such as the PAG (Scammell, Arrigoni & Lipton, 2017).

5.2.3 Relationship with epilepsy severity

Since SUDEP is associated with greater severity of epilepsy, it is important to consider imaging findings associated with SUDEP in relation to clinical factors such as disease duration and GTCS frequency. Correlational analyses in the present studies were largely unsuccessful in revealing associations with such factors for sites exhibiting significant volumetric or functional connectivity differences related to SUDEP. This may lead one to believe that these factors are not driving, or associated with the observed alterations, though it is possible that they arise from more complex processes which cannot be captured by simplistic measurements of disease duration or seizure frequency (which are often inaccurate and non-normally distributed). However, earlier work has shown volume loss in posterior thalamus, found in SUDEP and high-risk, to be significantly negatively associated with disease duration (Wandschneider et al., 2015). Precisely how disease duration is related to SUDEP is unknown, though one may speculate that a longer duration of epilepsy is associated with a greater likelihood of having had experienced more seizures (and potentially developing more functional connectivity and structural changes), especially since

elevated GTCS frequency is the leading SUDEP risk factor. This suggests the possibility that SUDEP may result from progressive damage to, or degradation of, central autonomic/regulatory systems, and thus brain sites, due to repeated ictal episodes (namely GTCS). However, such progressive alterations require investigation through longitudinal studies.

5.2.4 The need for longitudinal experiments to assess progressive brain changes

So far, imaging studies investigating SUDEP have exclusively employed cross-sectional designs, examining data from one fixed point in time, and thus only one observation (scan) per subject. Such experiments prevent characterisation of progressive structural or functional changes related to disease evolution, which would be crucial to determine whether alterations observed in SUDEP are progressive or linked to other factors such as disease duration or changes in seizure frequency. Future studies investigating imaging correlates of SUDEP and related risk factors must go beyond the established static measures of neural structure and function, and extend to longitudinal assessments of brain structural and functional change.

5.2.5 Relationship between structural and RS-FC alterations

Some of the observed brain volume changes in SUDEP, and those at high risk for SUDEP, align with changes highlighted in the functional connectivity studies. For example, reduced volume within the thalamus observed in SUDEP and high-risk patients (Wandschneider et al., 2015), as well as those with GTCS (Wang et al., 2012; Huang et al., 2011; Ciumas and Savic, 2006), appears to relate to the reduced connectivity of the thalamus (Tang et al., 2014; Allen et al., 2017). Additionally, elevated volume and cortical thickening found in limbic structures such as the amygdala

(Wandschneider et al., 2015), bear resemblance to the increased FC of the bilateral mesial temporal structures in TLE patients at high risk (Allen et al., 2017).

Despite some homologous findings across structural and FC studies, further work is required for example to elucidate the link between volumetric changes and connectivity disruptions. In this respect, future studies should focus on combined volumetric and connectivity-based experiments (i.e. Wang et al., 2012) on the same cohorts of individuals and in larger datasets.

5.2.6 Relevance of findings to identification of preventative interventions

The observed network disruptions and structural alterations among brain regions which have the potential to elicit a cardiovascular or breathing crisis leading to SUDEP raise the issue of how one day we might be able to intervene in those dysfunctional pathways to avoid or overcome such crises. Potential targets for intervention are the neurotransmitters in the affected pathways or the enhancement of pathways for protective recovery circuitry. In addition, advances in neuromodulation procedures offer a means to intervene directly in disrupted functional pathways, which is of particular use here, since 31% of epilepsy patients are drug resistant (Tang, Hartz and Bauer, 2017). Neuromodulatory techniques, such as invasive stimulation of the vagus, has been effective for the decrease of seizure incidence (for a review, see Cukiert, 2015); Furthermore non-invasive vagal stimulation can both reduce seizure incidence, and modify breathing and cardiovascular patterns (Feulner et al., 2017; White et al., 2016; Rong et al., 2014; Bauer et al., 2016; He et al., 2013; Stefan et al., 2012). Therefore, the combination of identifying disrupted cardiovascular/respiratory functional pathways, and implementation of inputs from cranial nerves that will

influence those pathways through non-invasive or invasive neuromodulatory techniques have the potential to impact disrupted vital functions that lead to the fatal scenario in SUDEP.

5.2.7 Future for neuroimaging of SUDEP and towards biomarkers

The nature and rarity of SUDEP makes the various aspects of any investigation, not least imaging experiments, extremely challenging. This is perhaps most prominent for data collection, including identifying and categorising cases of SUDEP, and also for study design. While retrospective investigations yield greater numbers of SUDEP cases, scans of some patients may have been carried out years before death and others months, weeks or days before, representing a major confound and thus limitation of retrospective studies. Prospective and longitudinal studies would permit assessments of progressive change, though may require many years (10 – 20) to accumulate appropriate numbers of cases to sufficiently power statistical analyses. Large scale multi-center collaborations, such as the CSR and ENIGMA (i.e. Whelan et al, 2018) consortiums, involving many centers worldwide, enable pooling of large datasets and thus acquisition of larger numbers of cases. Such studies and collaborations should be sought in order to advance the use of neuroimaging to investigate SUDEP, the future goals of which should be based around moving closer toward establishing concrete imaging biomarkers. Once numbers of included cases are large enough, approaches including meta-analyses of p-values (Whelan et al., 2018) to determine concrete findings, and predictive modelling to forecast SUDEP risk, may be considered.

Whether functional or structural in nature, such markers could additionally be used to prospectively identify those at risk, contribute to calculation of individualised SUDEP risk, and assist in understanding mechanisms (by, for example, guiding neurophysiological / stimulation studies to affected sites). Large datasets would enable enhanced inference of alterations in brain structure or functional associated with SUDEP and would allow improved characterisation of brain changes related to many other disease (i.e. disease duration and seizure frequency), and non-disease, related factors (including sex differences, which remains an important issue for SUDEP). Additionally, the combination of imaging and genetic data would permit major leaps forward towards understanding neurophenotypic components of SUDEP.

While imaging alone may not be capable of proving underlying mechanisms, it can, as demonstrated across the current work, provide evidence of alterations in brain structure and functional connectivity associated with SUDEP and related risk factors. Such changes, as well as further indicating the possibility of disturbed central regulatory processes – as a result of damaged sites or aberrant connectivity – may also serve as biomarkers to identify those at risk. If such markers can be confirmed in much larger cohorts, and if extent of injury is able to accurately predict the extent of risk, then an individual's brain structural or functional architecture may be used to calculate individual risk level.

Much work is required before imaging outcomes such as those revealed here can be extrapolated at the individual level to evaluate risk, though preparation for such an eventuality is worth considering, especially in terms of clinical and ethical contexts. Even if clinical or imaging information could be used to quantify a given individual's

risk of SUDEP, there are still ethical issues surrounding the disclosure of such information to patients, and questions around the current translation of value to individuals. While the exact cause of SUDEP is not known, and since preventive strategies are not established and integrated into clinical frameworks, informing patients of their risk level may be seen as futile. Consider, for example, telling an individual that they are at risk of a particular disease or are at elevated risk of mortality, but that we do not know precisely how and why this will happen, or how to prevent it yet. For risk-indicating biomarkers to be meaningful to an individual, and to aid prevention, the clinical and preventative strategies to which biomarkers could guide must be equally developed. Simple, yet powerful, strategies have been outlined and include information-based strategies to encourage AED compliance and ensure patient engagement with medical management to reduce seizure frequency (Harden et al., 2017).

Since many cases are unwitnessed, lack of supervision or intervention is likely to play a major role in the occurrence of SUDEP (Ryvlin et al, 2013, Peng, Danison & Seyal, 2017). Associations between SUDEP risk and the prone position following a seizure are known (Liebenthal et al., 2015; Harden, 2015); airway obstruction, particularly if the patient is unconscious, may become more likely. Enhanced monitoring and night-time supervision of at-risk individuals may reduce the incidence of SUDEP in at risk cohorts, provided individuals can be identified and that support can be efficiently guided.

One might consider initial value in such risk-indicating imaging biomarkers for guiding such enhanced monitoring to those at greatest risk. However, one must also appreciate that such a healthcare feat would involve resources far beyond what can

be currently provided. Thus, experimental imaging techniques, clinical and care streams, as well as the bodies which govern them, must align before such involved pathways to prevent SUDEP can be considered.

5.3 Concluding remarks

The current work demonstrates associations between SUDEP, and elevated risk, and changes in brain structure and functional networking among brain areas mediating cardiovascular and breathing processes. The data may indicate a structural and functional basis for impaired functioning or communication between areas necessary for recovery from compromised vital circumstances.

Although limited in sample sizes, findings are sufficiently apparent that indications of structural and functional changes may signal risk for SUDEP. However, further work is needed to elucidate the underlying mechanisms and evolution of neural changes to provide a direct link between such findings and sudden death.

A more immediate application of such findings may be their utilisation in biomarker development, once findings are refined and confirmed in larger cohorts. As well as shedding further light on potential mechanisms, such markers may one day be incorporated into unified approaches to risk identification and stratification among individuals.

Additionally, both the structural and functional outcomes suggest means for potential interventions with specialized pharmacologic or neuromodulatory procedures. The proper characterisation of the respective roles of the known risk factors, such as GTCS and disease duration (through longitudinal assessments), in relation to imaging findings can contribute to understanding SUDEP mechanisms, and warrant further investigation to disentangle clinical factors from what may be related to SUDEP.

Supplementary material

Supplementary Methods

S1. Pre-processing (regression of hippocampal gray matter volume)

As well as using presence of hippocampal sclerosis as a covariate, we also performed analysis with hippocampal volume of epileptogenic hemisphere regressed out. To do this, hippocampal volumes were calculated for each patient using the Harvard-Oxford sub-cortical atlas hippocampal (left and right where applicable) masks. For each patient, the respective ROI mask (depending on lateralisation of epilepsy) was used to extract the amount gray matter volume within the mask using the normalised gray matter segmentations created in pre-processing via DARTEL. This yielded a value representing the total amount of gray matter volume within the mask. This was then used as a covariate in statistical analysis within the NBS formalism, replacing the binary 'presence or non-presence of hippocampal sclerosis' covariate.

Supplementary tables

Table S1. Individual characteristics of those at high- and low-risk as well as healthy controls.

Control case	Group	Sex	Age at scan (yrs)	Epilepsy syndrome	Disease duration	GTCS per month, last 12 months	Findings on MRI
01	High-risk	M	38	Multi-focal	2.5	5	Tuberous sclerosis, R frontal, L frontal, R temporo-parietal-occipital.
02	High-risk	M	27	Focal, R temporal+	10	4	Cerebellar atrophy
03	High-risk	F	47	Focal, L temporal (no HS)	30	3	Normal
04	High-risk	F	34	Focal, L frontal	11	2	Normal
05	High-risk	M	33	Focal, L temporal (HS)	2	5	L HS
06	High-risk	F	25	Focal, L parietal	11	3	FCD - L inferior parietal
07	High-risk	M	39	Focal, R temporal (no HS)	14	2	Normal
08	High-risk	F	33	Focal, bi-fronto-temporal	23	4	Normal
09	High-risk	M	37	Focal, L frontal	8	4	Normal
10	High-risk	M	25	Focal, R frontal	6	1	Normal
11	High-risk	M	49	Focal, L frontal	4	3	Normal
12	High-risk	M	39	Focal, unown	14	1.5	Mature damage left>right gyrus rectus
13	High-risk	F	26	Generalised	11	2	Normal
14	High-risk	M	22	Focal, L temporal (HS)	4	2.5	L HS
15	High-risk	M	38	Focal, L fronto-temporal	15	2.5	Normal
16	High-risk	M	35	Focal, temporal+	6	1.5	Normal
17	High-risk	M	17	Focal, R temporal (HS)	11	0.33	R HS
18	High-risk	M	27	Focal, L temporo-occipital	13	4	FCD - L temporal
19	High-risk	M	35	Focal, unown	13	5	Normal
20	High-risk	F	30	Generalised	6	1.5	Normal
21	High-risk	M	27	Focal, R fronto-temporal	21	0.5	Normal
22	High-risk	F	27	Focal, temporal+	5	2	Normal
23	High-risk	M	24	Focal, L frontal	7	2	Normal
24	High-risk	M	33	Focal, L hemisphere	11	0.33	FCD - L supuerior temporal gyrus
25	High-risk	M	33	Generalised	16	0.33	Normal
26	Low-risk	M	44	Focal, L frontal	5	N.A	DNET - Superior frontal gyrus
27	Low-risk	M	22	Focal, unown	16	N.A	Normal
28	Low-risk	M	27	Focal, L frontal	14	N.A	Normal
29	Low-risk	M	30	Focal, L frontal	18	N.A	Normal
30	Low-risk	F	31	Focal, L fronto-temporal	15	N.A	Normal
31	Low-risk	M	39	Focal, L fronto-temporal	4	N.A	Hypothalamic hamartoma
32	Low-risk	M	24	Focal, L frontal	4	N.A	FCD, anterior bank of left post-central sulcus
33	Low-risk	F	19	Generalised	9	N.A	cystic area, right putamen. Small suprasellar cyst optic chiasm.
34	Low-risk	F	38	Generalised	7	N.A	Normal
35	Low-risk	M	27	Focal, L parietal	7	N.A	FCD, lying inferior and posterior to motor cortex
36	Low-risk	F	42	Focal, L central	18	N.A	Normal
37	Low-risk	M	28	Focal, L temporal (no HS)	5	N.A	FC D - L superior temporal gyrus
38	Low-risk	M	31	Focal, R temporal (no HS)	16	N.A	FCD - R temporal occipital
39	Low-risk	M	48	Generalised	20	N.A	Normal
40	Low-risk	F	22	Focal, unown	17	N.A	Normal
41	Low-risk	M	37	Generalised	16	N.A	Normal
42	Low-risk	F	19	Focal, unown	13	N.A	Normal
43	Low-risk	F	28	Focal, unown	13	N.A	Normal
44	Low-risk	M	30	Focal, L occipital	16	N.A	FCD - L superior posterior calcarine sulcus
45	Low-risk	M	28	Focal, R temporal (no HS)	27	N.A	Cavernoma - right anterior temporal/amygdala
46	Low-risk	M	30	Focal, frontal	12	N.A	Normal
47	Low-risk	M	29	Focal, unown	16	N.A	exophytic cavernoma or lipoma left inferior colliculus
48	Low-risk	M	18	Focal, L temporal (HS)	13	N.A	L HS

49	Healthy	F	37	N.A	N.A	N.A	Normal
50	Healthy	M	46	N.A	N.A	N.A	Normal
51	Healthy	M	40	N.A	N.A	N.A	Normal
52	Healthy	M	25	N.A	N.A	N.A	Normal
53	Healthy	F	21	N.A	N.A	N.A	Normal
54	Healthy	M	37	N.A	N.A	N.A	Normal
55	Healthy	M	37	N.A	N.A	N.A	Normal
56	Healthy	F	53	N.A	N.A	N.A	Normal
57	Healthy	M	49	N.A	N.A	N.A	Normal
58	Healthy	M	41	N.A	N.A	N.A	Normal
59	Healthy	F	19	N.A	N.A	N.A	Normal
60	Healthy	M	26	N.A	N.A	N.A	Normal
61	Healthy	M	42	N.A	N.A	N.A	Normal
62	Healthy	M	58	N.A	N.A	N.A	Normal
63	Healthy	F	22	N.A	N.A	N.A	Normal
64	Healthy	M	49	N.A	N.A	N.A	Normal
65	Healthy	F	64	N.A	N.A	N.A	Normal
66	Healthy	F	26	N.A	N.A	N.A	Normal
67	Healthy	M	44	N.A	N.A	N.A	Normal
68	Healthy	M	54	N.A	N.A	N.A	Normal
69	Healthy	M	39	N.A	N.A	N.A	Normal
70	Healthy	M	40	N.A	N.A	N.A	Normal
71	Healthy	M	25	N.A	N.A	N.A	Normal
72	Healthy	M	35	N.A	N.A	N.A	Normal
73	Healthy	M	34	N.A	N.A	N.A	Normal

M = male, F = female, R = right, L = left, temporal+ = temporal plus, HS = hippocampal sclerosis, GTCS = generalised tonic-clonic seizure, FCD = focal cortical dysplasia, DNET = Dysembryoplastic neuroepithelial tumour, N.A. = not applicable.

Table S2. Clinical characteristics of low- and high-risk patient- and healthy-control subjects.

Case # [sex]	Risk group	Age at time of scan (years)	Epilepsy syndrome	Disease duration (years)	Number of GTCS (per month)	MRI findings at time of scan
1 [M]	High-risk	20	Focal, L frontal	9	2	Normal
2 [M]	High-risk	25	Focal, L frontal	15	3	L MFG FCD
3 [M]	High-risk	33	Generalised (JME)	20	1	Normal
4 [M]	High-risk	35	Generalised	29	2	Normal
5 [F]	High-risk	18	Generalised (JME)	15	2.5	Normal
6 [F]	High-risk	26	Generalised (JME)	24	1.5	Normal
7 [M]	High-risk	49	Focal, L frontal	45	3	Normal
8 [M]	High-risk	23	Focal, L fronto-temporal	11	1	Normal
9 [F]	High-risk	37	Focal, L frontal	21	1.5	Normal
10 [F]	High-risk	46	Focal, L frontal	41	10	L IFG FCD
11 [F]	High-risk	19	Focal, R parietal	17	2	L parietal FCD
12 [F]	High-risk	25	Focal, R parietal	24	5	L parietal FCD
13 [M]	High-risk	22	Focal, L temporal	18	8	L HS
14 [M]	High-risk	33	Focal, L temporal	31	6.5	L HS
15 [F]	High-risk	31	Focal, L fronto-temporal	25	8	Normal
16 [F]	High-risk	26	Focal, L fronto-temporal	17	10	Normal
17 [M]	Low-risk	24	Focal, L frontal	17	0	Normal
18 [M]	Low-risk	24	Focal, L frontal	20	0	L frontal FCD
19 [M]	Low-risk	39	Generalised	35	0	Normal
20 [M]	Low-risk	33	Generalised	17	0	Normal
21 [F]	Low-risk	30	Generalised (JME)	17	0	Normal
22 [F]	Low-risk	38	Generalised	31	0	Normal

Case # [sex]	Risk group	Age at time of scan (years)	Epilepsy syndrome	Disease duration (years)	Number of GTCS (per month)	MRI findings at time of scan
23 [M]	Low-risk	27	Focal, L Parietal	20	0	L parietal FCD
24 [M]	Low-risk	33	Focal, L hem	18	0	Normal
25 [F]	Low-risk	24	Focal, L frontal	21	0	Normal
26 [F]	Low-risk	42	Focal, L frontal	24	0	L frontal FCD
27 [F]	Low-risk	28	Focal, R parieto-occipital	21	0	R parieto-occipital FCD
28 [F]	Low-risk	32	Focal, R parietal	30	0	R superior parietal FCD
29 [M]	Low-risk	26	Focal, L temporal	19	0	L HS
30 [M]	Low-risk	28	Focal, L temporal	23	0	L STG FCD
31 [F]	Low-risk	19	Focal, L frontal	13	0	L inferior frontal infarct
32 [F]	Low-risk	24	Focal, L frontal	20	0	Normal
33 [F]	HC	30	N.A.	N.A.	N.A.	N.A.
34 [M]	HC	30	N.A.	N.A.	N.A.	N.A.
35 [F]	HC	49	N.A.	N.A.	N.A.	N.A.
36 [M]	HC	22	N.A.	N.A.	N.A.	N.A.
37 [M]	HC	28	N.A.	N.A.	N.A.	N.A.
38 [M]	HC	28	N.A.	N.A.	N.A.	N.A.
39 [F]	HC	29	N.A.	N.A.	N.A.	N.A.
40 [F]	HC	25	N.A.	N.A.	N.A.	N.A.
41 [M]	HC	35	N.A.	N.A.	N.A.	N.A.
42 [F]	HC	27	N.A.	N.A.	N.A.	N.A.
43 [M]	HC	34	N.A.	N.A.	N.A.	N.A.
44 [M]	HC	30	N.A.	N.A.	N.A.	N.A.
45 [F]	HC	33	N.A.	N.A.	N.A.	N.A.
46 [F]	HC	28	N.A.	N.A.	N.A.	N.A.
47 [M]	HC	28	N.A.	N.A.	N.A.	N.A.
48 [M]	HC	33	N.A.	N.A.	N.A.	N.A.

*M=*male, *F=*female, *L=*left, *R=*right, *JME=*juvenile myoclonic epilepsy, *FCD=*focal cortical dysplasia, *MFG=*middle frontal gyrus, *IFG=*inferior frontal gyrus, *STG=*superior temporal gyrus, *hem=*hemisphere, *HS=*hippocampal sclerosis, *HC=*healthy control, *N.A.=*not applicable.

Table S3. Group summaries of SUDEP cases, high-risk, low-risk and healthy controls.

Variable	SUDEP (n=8)	High-risk (n=16)	Low-risk (n=16)	HC (n=16)
Age (mean±SD)	26 ± 6.1	29.3 ± 9.2	29.4 ± 6.3	30.6 ± 6
Sex (M:F)	4:4	8:8	8:8	9:7
Disease duration (years)	16.6 ± 10.1	22.6 ± 10.0	21.6 ± 5.8	N.A.
GTCS/month (mean±SD)	3.0 ± 3.1	5.4 ± 7.1	N.A.	N.A.
Number of AEDs (mean±SD)	2.6 ± 0.5	2.6 ± 0.9	2.8 ± 0.9	N.A.
Number polytherapy	5	8	9	N.A.
Number duotherapy	3	7	7	N.A.
Number monotherapy	N.A.	1	N.A.	N.A.

SD=standard deviation, M=male, F=female, /=per, AED=anti-epileptic drug, HC=healthy control, N.A.=not applicable.

Table S4. Brainnetome atlas regions, labels, abbreviations and MNI co-ordinates.

Structure	Sub-region label	Abbrev	MNI Left (X, Y, Z)	MNI Right (X, Y, Z)
Medial/orbital-frontal cortex	Medial prefrontal (anterior 1)	aMpf1	-7, 54, -7	6, 47, -7
	Orbital (ventrolateral 1)	vOrb1	-36, 33, -16	40, 39, -14
	Orbital (ventrolateral 2)	vOrb2	-23, 38, -18	23, 36, -18
	Medial prefrontal (anterior 2)	aMpf2	-6, 52, -19	6, 57, -16
	Ventromedial prefrontal	vMpf	-10, 18, -19	9, 20, -19
	Orbital (dorsolateral)	dOrb	-41, 32, -9	42, 31, -9
Insula	hypergranular ins	Hg_ins	-36, -20, 10	37, -18, 8
	ventral agranular ins	vAng_ins	-32, 14, -13	33, 14, -13
	dorsal agranular ins	dAng_ins	-34, 18, 1	36, 18, 1
	ventral dysgranular+granular ins	vD&G_ins	-38, -4, -9	39, -2, -9
	dorsal granular ins	dGran_ins	-38, -8, 8	39, -7, 8
	dorsal dysgranular ins	dDysg_ins	-38, 5, 5	38, 5, 5
Cingulate	dorsal area	dCing	-4, -39, 31	4, -37, 32
	rostroventral area	rvCing	-3, 8, 25	5, 22, 12
	pregenual area	Pregen	-6, 34, 21	5, 28, 27
	ventral area	vCing	-8, -47, 10	9, -44, 11
	caudodorsal area	cd_Cing	-5, 7, 37	4, 6, 38
	caudal area	cCing	-7, -23, 41	6, -20, 40
	subgenual area	Subgen	-4, 39, -2	5, 41, 6
Amygdala	medial amygdala	mAmyg	-19, -2, -20	19, -2, -19
	lateral amygdala	lAmyg	-27, -4, -20	28, -3, -20
Hippocampus	rostral hippocampus	aHipp	-22, -14, -19	22, -12, -20
	caudal hippocampus	pHipp	-28, -30, -10	29, -27, -10
Basal Ganglia	ventral caudate	vCaud	-12, 14, 0	15, 14, -2
	globus pallidus	GP	-22, -2, 4	22, -2, 3
	NAC, nucleus accumbens	NAC	-17, 3, -9	15, 8, -9
	ventromedial putamen	vmPut	-23, 7, -4	22, 8, -1
	dorsal caudate	dCaud	-14, 2, 16	14, 5, 14
	dorsolateral putamen	dIPut	-28, -5, 2	29, -3, 1
Thalamus	medial pre-frontal thalamus	mPFtha	-7, -12, 5	7, -11, 6
	pre-motor thalamus	mPMtha	-18, -13, 3	12, -14, 1
	sensory thalamus	Stha	-18, -23, 4	18, -22, 3
	rostral temporal thalamus	rTtha	-7, -14, 7	3, -13, 5
	posterior parietal thalamus	Pptha	-16, -24, 6	15, -25, 6
	occipital thalamus	Octha	-15, -28, 4	13, -27, 8
	caudal temporal thalamus	cTtha	-12, -22, 13	10, -14, 14
	lateral pre-frontal thalamus	IPFtha	-11, -14, 2	13, -16, 7

Abbrev = abbreviation.

Table S5. Increased regional participation in SUDEP and high-risk groups compared with healthy controls.

Structure	Sub-region	SUDEP (p-value)	High-risk (p-value)
Medial/orbital-frontal cortex	aMpf1_L	0.198	0.144
	aMpf1_R	0.288	0.095
	vIOrb1_L	0.085	0.114
	vIOrb1_R	0.288	0.144
	vIOrb2_L	0.038	0.044
	vIOrb2_R	0.150	0.039
	aMpf2_L	0.110	0.079
	aMpf2_R	0.358	0.091
	vMpf_L	0.103	0.140
	vMpf_R	0.060	0.119
	dIOrb_L	0.035	0.126
	dIOrb_R	0.361	0.044
Insula	Hg_ins_L	0.038	0.044
	Hg_ins_R	0.362	0.218
	vAng_ins_L	0.028	0.024
	vAng_ins_R	0.288	0.126
	dAng_ins_L	0.193	0.044
	dAng_ins_R	0.097	0.061
	vD&G_ins_L	0.129	0.039
	vD&G_ins_R	0.064	0.052
	dGran_ins_L	0.080	0.024
	dGran_ins_R	0.038	0.039
	dDysg_ins_L	0.288	0.024
dDysg_ins_R	0.129	0.052	
Cingulate	dCing_L	0.164	0.119
	dCing_R	0.187	0.111
	rvCing_L	0.063	0.065
	rvCing_R	0.131	0.059
	Pregen_L	0.077	0.052
	Pregen_R	0.097	0.358
	vCing_L	0.251	0.230
	vCing_R	0.085	0.252
	cd_Cing_L	0.080	0.144
	cd_Cing_R	0.086	0.080
	cCing_L	0.288	0.144
	cCing_R	0.035	0.132
Subgen_L	0.043	0.091	

Structure	Sub-region	SUDEP (p-value)	High-risk (p-value)
	Subgen_R	0.077	0.137
Amygdala	mAmyg_L	0.005	0.052
	mAmyg_R	0.033	0.093
	lAmyg_L	0.028	0.144
	lAmyg_R	0.358	0.618
Hippocampus	aHipp_L	0.080	0.039
	aHipp_R	0.039	0.039
	pHipp_L	0.077	0.182
	pHipp_R	0.015	0.040
Basal Ganglia	vCaud_L	0.322	0.097
	vCaud_R	0.164	0.343
	GP_L	0.288	0.272
	GP_R	0.074	0.097
	NAC_L	0.138	0.091
	NAC_R	0.080	0.052
	vmPut_L	0.080	0.080
	vmPut_R	0.030	0.119
	dCaud_L	0.430	0.243
	dCaud_R	0.223	0.024
	dIPut_L	0.361	0.097
	dIPut_R	0.288	0.144
Thalamus	mPFtha_L	0.007	0.146
	mPFtha_R	0.006	0.144
	mPMtha_L	0.059	0.052
	mPMtha_R	0.147	0.097
	Stha_L	0.035	0.097
	Stha_R	0.063	0.272
	rTtha_L	0.308	0.067
	rTtha_R	0.033	0.093
	Pptha_L	0.038	0.039
	Pptha_R	0.007	0.209
	Octha_L	0.021	0.040
	Octha_R	0.021	0.091
	cTtha_L	0.033	0.108
	cTtha_R	0.036	0.141
	IPFtha_L	0.201	0.126
	IPFtha_R	0.069	0.163

Table S6. Increased degree centrality (DC) in SUDEP, high-risk and low-risk compared with healthy controls.

Structure	Sub-region	SUDEP (p-value)	High-risk (p-value)	Low-risk (p-value)
Medial/orbital- frontal cortex	aMpf1_L	0.164	0.751	0.574
	aMpf1_R	0.508	0.877	0.341
	vIOrb1_L	0.135	0.064	0.003
	vIOrb1_R	0.038	0.002	0.007
	vIOrb2_L	0.187	0.247	0.005
	vIOrb2_R	0.096	0.096	0.023
	aMpf2_L	0.083	0.234	0.030
	aMpf2_R	0.008	0.261	0.028
	vMpf_L	0.028	0.010	0.002
	vMpf_R	0.009	0.013	0.026
	dIOrb_L	0.335	0.476	0.034
	dIOrb_R	0.464	0.520	0.508
Insula	Hg_ins_L	0.864	0.878	0.471
	Hg_ins_R	0.985	0.885	0.983
	vAng_ins_L	0.127	0.184	0.143
	vAng_ins_R	0.321	0.537	0.464
	dAng_ins_L	0.939	0.719	0.482
	dAng_ins_R	0.675	0.798	0.993
	vD&G_ins_L	0.765	0.682	0.451
	vD&G_ins_R	0.959	0.988	0.854
	dGran_ins_L	0.671	0.847	0.649
	dGran_ins_R	0.833	0.755	0.994
	dDysg_ins_L	0.828	0.541	0.450
dDysg_ins_R	0.884	0.385	0.959	
Cingulate	dCing_L	0.148	0.687	0.140
	dCing_R	0.174	0.577	0.526
	rvCing_L	0.061	0.030	0.109
	rvCing_R	0.491	0.250	0.139
	Pregen_L	0.784	0.751	0.826
	Pregen_R	0.290	0.977	0.945
	vCing_L	0.185	0.170	0.073
	vCing_R	0.277	0.166	0.064
	cd_Cing_L	0.818	0.766	0.762
	cd_Cing_R	0.334	0.623	0.507
	cCing_L	0.998	0.998	0.687
cCing_R	0.893	0.990	0.655	

Structure	Sub-region	SUDEP (p-value)	High-risk (p-value)	Low-risk (p-value)
	Subgen_L	0.404	0.865	0.660
	Subgen_R	0.435	0.891	0.826
Amygdala	mAmyg_L	0.080	0.284	0.108
	mAmyg_R	0.098	0.331	0.544
	lAmyg_L	0.467	0.459	0.351
	lAmyg_R	0.817	0.465	0.726
Hippocampus	aHipp_L	0.510	0.187	0.134
	aHipp_R	0.176	0.085	0.156
	pHipp_L	0.302	0.061	0.036
	pHipp_R	0.003	0.018	0.036
Basal Ganglia	vCaud_L	0.401	0.694	0.603
	vCaud_R	0.554	0.750	0.895
	GP_L	0.895	0.828	0.950
	GP_R	0.525	0.687	0.965
	NAC_L	0.723	0.639	0.902
	NAC_R	0.025	0.010	0.036
	vmPut_L	0.870	0.945	0.937
	vmPut_R	0.765	0.794	0.960
	dCaud_L	0.595	0.750	0.686
	dCaud_R	0.396	0.189	0.167
	dIPut_L	0.948	0.701	0.955
	dIPut_R	0.920	0.941	0.971
Thalamus	mPFtha_L	0.561	0.588	0.984
	mPFtha_R	0.197	0.780	0.982
	mPMtha_L	0.177	0.094	0.592
	mPMtha_R	0.967	0.796	0.975
	Stha_L	0.695	0.402	0.941
	Stha_R	0.824	0.238	0.916
	rTtha_L	0.835	0.247	0.697
	rTtha_R	0.885	0.291	0.862
	Pptha_L	0.962	0.258	0.852
	Pptha_R	0.735	0.767	0.569
	Octha_L	0.187	0.445	0.396
	Octha_R	0.322	0.351	0.307
	cTtha_L	0.745	0.558	0.604
	cTtha_R	0.564	0.552	0.089
IPFtha_L	0.978	0.803	0.872	
IPFtha_R	0.925	0.972	0.944	

FDR corrected p-values are displayed and those below 0.05 are highlighted in red.

Table S7. Degree centrality in SUDEP, high-risk and low-risk compared with healthy controls.

Structure	Sub-region	SUDEP (<i>p</i> -value)	High-risk (<i>p</i> -value)	Low-risk (<i>p</i> -value)
Medial/orbital- frontal cortex	aMpf1_L	0.836	0.249	0.426
	aMpf1_R	0.492	0.123	0.659
	vIOrb1_L	0.865	0.936	0.997
	vIOrb1_R	0.962	0.998	0.993
	vIOrb2_L	0.813	0.753	0.995
	vIOrb2_R	0.904	0.904	0.977
	aMpf2_L	0.917	0.766	0.970
	aMpf2_R	0.992	0.739	0.972
	vMpf_L	0.972	0.990	0.998
	vMpf_R	0.991	0.987	0.974
	dIOrb_L	0.665	0.524	0.966
	dIOrb_R	0.536	0.480	0.492
Insula	Hg_ins_L	0.136	0.122	0.529
	Hg_ins_R	0.015	0.115	0.017
	vAng_ins_L	0.873	0.816	0.857
	vAng_ins_R	0.679	0.463	0.536
	dAng_ins_L	0.061	0.281	0.518
	dAng_ins_R	0.325	0.202	0.007
	vD&G_ins_L	0.235	0.318	0.549
	vD&G_ins_R	0.041	0.012	0.146
	dGran_ins_L	0.329	0.153	0.351
	dGran_ins_R	0.167	0.245	0.006
	dDysg_ins_L	0.172	0.459	0.550
dDysg_ins_R	0.116	0.615	0.041	
Cingulate	dCing_L	0.852	0.313	0.860
	dCing_R	0.826	0.423	0.474
	rvCing_L	0.939	0.970	0.979
	rvCing_R	0.509	0.750	0.861
	Pregen_L	0.216	0.249	0.174
	Pregen_R	0.710	0.023	0.055
	vCing_L	0.815	0.830	0.927
	vCing_R	0.723	0.834	0.936
	cd_Cing_L	0.182	0.234	0.238
	cd_Cing_R	0.666	0.377	0.493
	cCing_L	0.002	0.002	0.313
	cCing_R	0.107	0.198	0.345

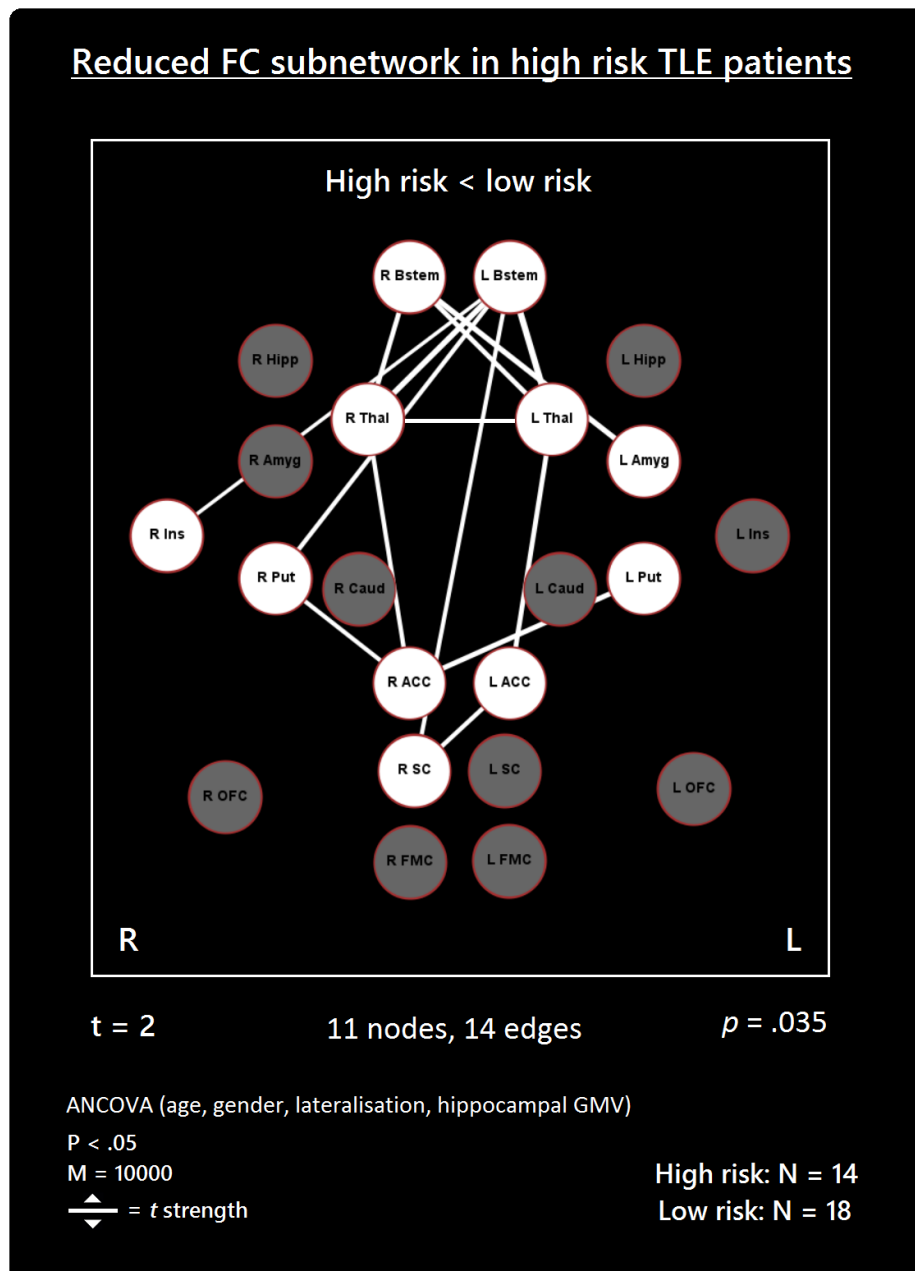
Structure	Sub-region	SUDEP (p-value)	High-risk (p-value)	Low-risk (p-value)
	Subgen_L	0.596	0.135	0.340
	Subgen_R	0.565	0.109	0.174
Amygdala	mAmyg_L	0.920	0.716	0.892
	mAmyg_R	0.902	0.669	0.456
	lAmyg_L	0.533	0.541	0.649
	lAmyg_R	0.183	0.535	0.274
Hippocampus	aHipp_L	0.490	0.813	0.866
	aHipp_R	0.824	0.915	0.844
	pHipp_L	0.698	0.939	0.964
	pHipp_R	0.997	0.998	0.964
Basal Ganglia	vCaud_L	0.599	0.306	0.397
	vCaud_R	0.446	0.250	0.105
	GP_L	0.105	0.172	0.050
	GP_R	0.475	0.313	0.035
	NAC_L	0.277	0.361	0.098
	NAC_R	0.975	0.999	0.964
	vmPut_L	0.130	0.055	0.063
	vmPut_R	0.235	0.206	0.040
	dCaud_L	0.405	0.250	0.314
	dCaud_R	0.604	0.811	0.833
	dIPut_L	0.052	0.299	0.045
	dIPut_R	0.080	0.059	0.029
Thalamus	mPFtha_L	0.439	0.412	0.016
	mPFtha_R	0.803	0.220	0.018
	mPMtha_L	0.823	0.906	0.408
	mPMtha_R	0.033	0.204	0.025
	Stha_L	0.305	0.598	0.059
	Stha_R	0.176	0.762	0.084
	rTtha_L	0.165	0.753	0.303
	rTtha_R	0.115	0.709	0.138
	Pptha_L	0.038	0.742	0.148
	Pptha_R	0.265	0.233	0.431
	Octha_L	0.813	0.555	0.604
	Octha_R	0.678	0.649	0.693
	cTtha_L	0.255	0.442	0.396
	cTtha_R	0.436	0.448	0.911
IPFtha_L	0.236	0.197	0.128	
IPFtha_R	0.075	0.276	0.056	

FDR corrected p-values are displayed and those below 0.05 are highlighted in green.

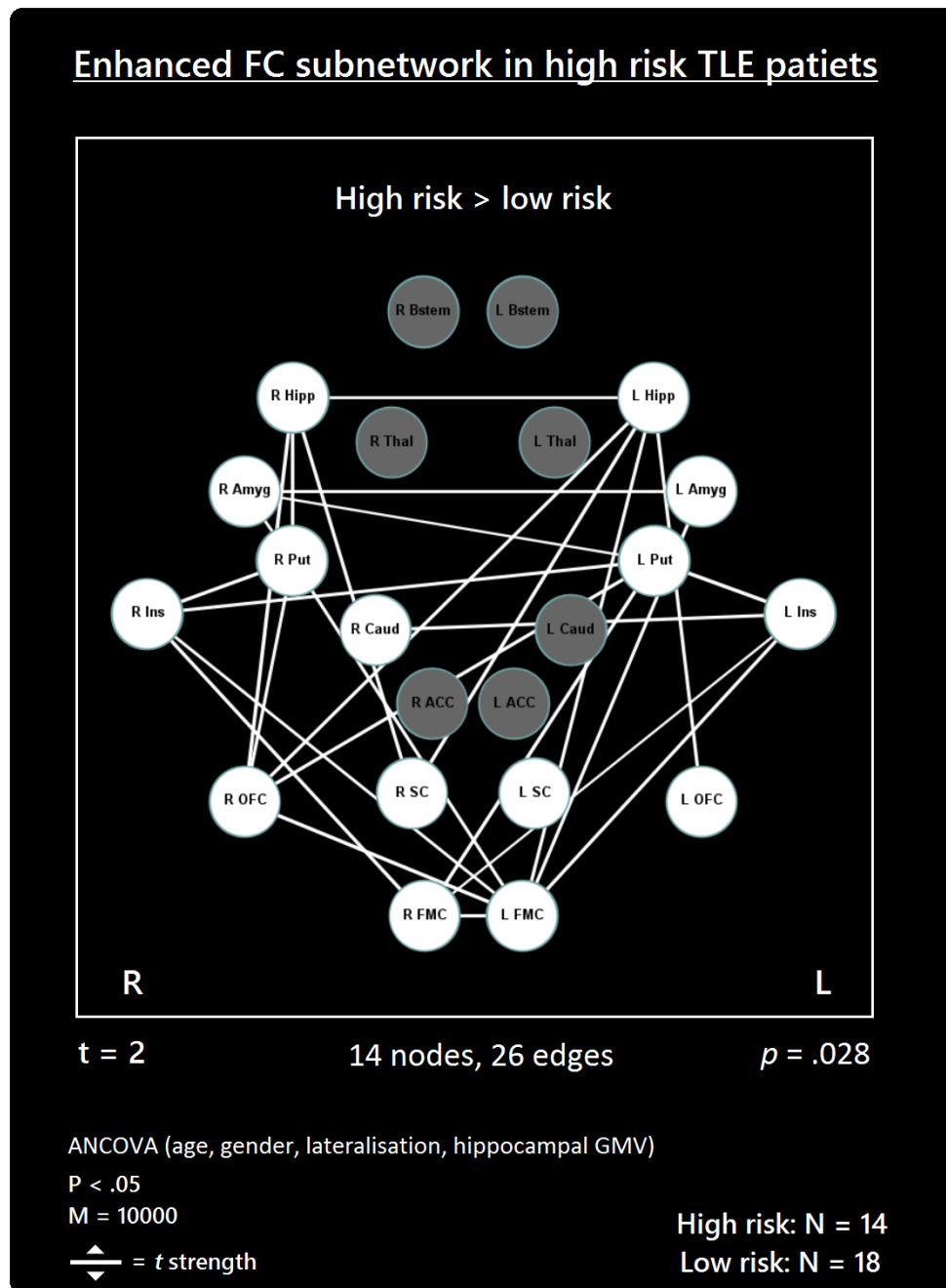
Table S8. Increased participation in SUDEP compared with low-risk patients at the uncorrected significance level ($p < 0.05$).

Sub-region	SUDEP (p-value)
Subgen_L	0.021
mAmyg_L	0.045
pHipp_R	0.044
vCaud_R	0.040
mPFtha_L	0.016
mPFtha_R	0.003

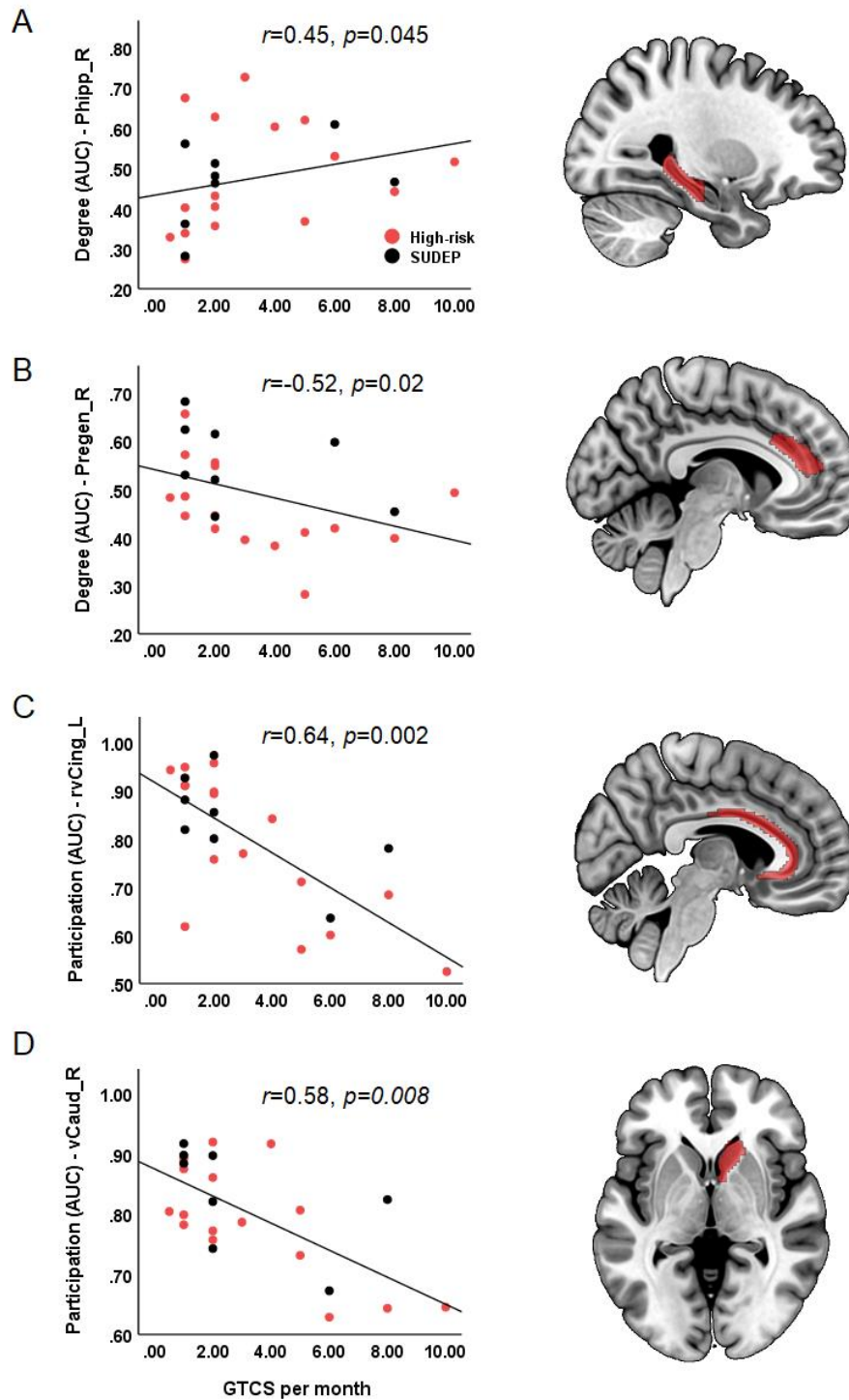
Supplementary figures

**Figure S1**

Reduced FC subnetwork with hippocampal grey matter volume of epileptogenic hemisphere, not presence of HS, regressed out. Subnetwork involves bilateral brainstem (Bstem), bilateral thalamus (Thal), bilateral putamen (Put), bilateral ACC, left amygdala (Amyg), right subcallosal cortex (SC) and right Insula (Ins). L = Left, R = Right; ANCOVA: analysis of covariance; t = t -statistic threshold; M = number of permutations; P value was set at < 0.05 , FWER corrected. Visualisation using Gephi (<https://gephi.org>).

**Figure S2**

Subnetwork of enhanced FC in high-risk TLE patients compared with low-risk TLE patients, with hippocampal grey matter volume of epileptogenic hemisphere regressed out. Regions include: bilateral amygdala (L Amyg, R Amyg), right caudate (R Caud), frontal medial cortex (L FMC, R FMC), hippocampus (L Hipp, R Hipp), insula (L Ins, R Ins), orbitofrontal cortex (L OFC, R OFC), putamen (L Put, R Put), and subcallosal cortex (L SC, R SC). L = left, R = Right.

**Figure S3**

Significant correlations between GTCS frequency and network measures degree (A and B) and participation (C and D). Right: Related sites; right posterior hippocampus (A), right pregenual cingulate (B), rostroventral cingulate (C), and right ventral caudate (D).

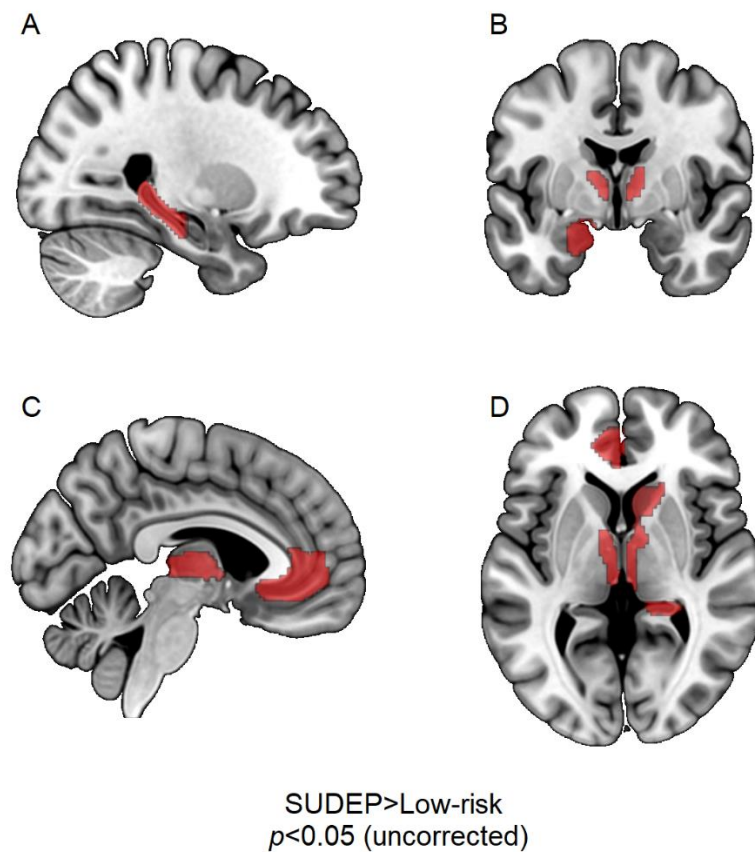


Figure S4

Regions of significantly greater participation in SUDEP cases compared with low-risk patients (uncorrected). BNA ROIs are overlaid onto a standard brain in red. A: sagittal section showing the right posterior hippocampus, B: coronal section showing left medial amygdala and bilateral medial prefrontal thalamus, C: sagittal section showing left pregenual cingulate and left medial prefrontal thalamus, D: axial section showing right ventral caudate, left pregenual cingulate, bilateral medial prefrontal thalamus and right posterior hippocampus.

References

- Achard, S., Delon-Martin, C., Vértes, P. E., Renard, F., Schenck, M., Schneider, F., ... & Bullmore, E. T. (2012). Hubs of brain functional networks are radically reorganized in comatose patients. *Proceedings of the National Academy of Sciences*, 109(50), 20608-20613.
- Achard, S., Salvador, R., Whitcher, B., Suckling, J., & Bullmore, E. D. (2006). A resilient, low-frequency, small-world human brain functional network with highly connected association cortical hubs. *Journal of Neuroscience*, 26(1), 63-72.
- Aertsen, A. M., Gerstein, G. L., Habib, M. K., & Palm, G. (1989). Dynamics of neuronal firing correlation: modulation of "effective connectivity". *Journal of neurophysiology*, 61(5), 900-917.
- Aiba, I., & Noebels, J. L. (2015). Spreading depolarization in the brainstem mediates sudden cardiorespiratory arrest in mouse SUDEP models. *Science translational medicine*, 7(282), 282ra46-282ra46.
- Alexander, G. E., & Crutcher, M. D. (1990). Functional architecture of basal ganglia circuits: neural substrates of parallel processing. *Trends in neurosciences*, 13(7), 266-271.
- Alexander-Bloch, A. F., Gogtay, N., Meunier, D., Birn, R., Clasen, L., Lalonde, F., ... & Bullmore, E. T. (2010). Disrupted modularity and local connectivity of brain functional networks in childhood-onset schizophrenia. *Frontiers in systems neuroscience*, 4, 147.
- Allen, J. S., Emmorey, K., Bruss, J., & Damasio, H. (2013). Neuroanatomical differences in visual, motor, and language cortices between congenitally deaf signers, hearing signers, and hearing non-signers. *Frontiers in neuroanatomy*, 7, 26.
- Allen, L. A., Harper, R. M., Kumar, R., Guye, M., Ogren, J. A., Lhatoo, S. D., ... & Diehl, B. (2017). Dysfunctional brain networking among autonomic regulatory structures in temporal lobe epilepsy patients at high risk of sudden unexpected death in epilepsy. *Frontiers in neurology*, 8, 544.
- Allen, L. A., Harper, R. M., Lhatoo, S., Lemieux, L., & Diehl, B. (2019a). Neuroimaging of Sudden Unexpected Death in Epilepsy (SUDEP): Insights From Structural and Resting-State Functional MRI Studies. *Frontiers in neurology*, 10.
- Allen, L. A., Vos, S. B., Kumar, R., Ogren, J. A., Harper, R. K., Winston, G. P., ... & Duncan, J. S. (2019b). Cerebellar, limbic, and midbrain volume alterations in sudden unexpected death in epilepsy. *Epilepsia*, 60(4), 718-729.
- Andreuzik, J. A., Dormer, K. J., Foreman, R. D., & Person, R. J. (1984). Fastigial nucleus projections to the brain stem in beagles: pathways for autonomic regulation. *Neuroscience*, 11(2), 497-507.

- Ansakorpi, H., Korpelainen, J. T., Huikuri, H. V., Tolonen, U., Myllylä, V. V., & Isojärvi, J. I. T. (2002). Heart rate dynamics in refractory and well controlled temporal lobe epilepsy. *Journal of Neurology, Neurosurgery & Psychiatry*, *72*(1), 26-30.
- Ashburner, J. (2007). A fast diffeomorphic image registration algorithm. *Neuroimage*, *38*(1), 95-113.
- Ashburner, J. (2015). VBM tutorial. *Tech. rep Wellcome Trust Centre for Neuroimaging, London, UK*.
- Ashburner, J., & Friston, K. J. (2000). Voxel-based morphometry—the methods. *Neuroimage*, *11*(6), 805-821.
- Bär, K. J., Herbsleb, M., Schumann, A., de la Cruz, F., Gabriel, H. W., & Wagner, G. (2016). Hippocampal-brainstem connectivity associated with vagal modulation after an intense exercise intervention in healthy men. *Frontiers in neuroscience*, *10*, 145.
- Bassett, D. S., Nelson, B. G., Mueller, B. A., Camchong, J., & Lim, K. O. (2012). Altered resting state complexity in schizophrenia. *Neuroimage*, *59*(3), 2196-2207.
- Bateman, L. M., Li, C. S., & Seyal, M. (2008). Ictal hypoxemia in localization-related epilepsy: analysis of incidence, severity and risk factors. *Brain*, *131*(12), 3239-3245.
- Bauer, S., Baier, H., Baumgartner, C., Bohlmann, K., Fauser, S., Graf, W., ... & Mayer, T. (2016). Transcutaneous vagus nerve stimulation (tVNS) for treatment of drug-resistant epilepsy: a randomized, double-blind clinical trial (cMPsE02). *Brain stimulation*, *9*(3), 356-363.
- Beheshti, I., Sone, D., Farokhian, F., Maikusa, N., & Matsuda, H. (2018). gray Matter and White Matter abnormalities in Temporal lobe epilepsy Patients with and without hippocampal sclerosis. *Frontiers in neurology*, *9*, 107.
- Behrens, T. E., Johansen-Berg, H., Woolrich, M. W., Smith, S. M., Wheeler-Kingshott, C. A. M., Boulby, P. A., ... & Thompson, A. J. (2003). Non-invasive mapping of connections between human thalamus and cortex using diffusion imaging. *Nature neuroscience*, *6*(7), 750.
- Behzadi, Y., Restom, K., Liau, J., & Liu, T. T. (2007). A component based noise correction method (CompCor) for BOLD and perfusion based fMRI. *Neuroimage*, *37*(1), 90-101.
- BENARROCH, E. E. (1993, October). The central autonomic network: functional organization, dysfunction, and perspective. In *Mayo Clinic Proceedings* (Vol. 68, No. 10, pp. 988-1001). Elsevier.
- Benarroch, E. E. (Ed.). (2014). *Autonomic neurology* (Vol. 86). Oxford University Press.
- Berg, A. T., Berkovic, S. F., Brodie, M. J., Buchhalter, J., Cross, J. H., van Emde Boas, W., ... & Moshé, S. L. (2010). Revised terminology and concepts for organization of seizures and epilepsies: report of the ILAE Commission on Classification and Terminology, 2005–2009. *Epilepsia*, *51*(4), 676-685.

- Bernasconi, A., Bernasconi, N., Natsume, J., Antel, S. B., Andermann, F., & Arnold, D. L. (2003). Magnetic resonance spectroscopy and imaging of the thalamus in idiopathic generalized epilepsy. *Brain*, *126*(11), 2447-2454.
- Bernhardt, B. C., Hong, S. J., Bernasconi, A., & Bernasconi, N. (2015). Magnetic resonance imaging pattern learning in temporal lobe epilepsy: classification and prognostics. *Annals of neurology*, *77*(3), 436-446.
- Bernhardt, B. C., Rozen, D. A., Worsley, K. J., Evans, A. C., Bernasconi, N., & Bernasconi, A. (2009). Thalamo-cortical network pathology in idiopathic generalized epilepsy: insights from MRI-based morphometric correlation analysis. *Neuroimage*, *46*(2), 373-381.
- Bernhardt, B. C., Worsley, K. J., Kim, H., Evans, A. C., Bernasconi, A., & Bernasconi, N. (2009). Longitudinal and cross-sectional analysis of atrophy in pharmaco-resistant temporal lobe epilepsy. *Neurology*, *72*(20), 1747-1754.
- Bewernick, B. H., Hurlemann, R., Matusch, A., Kayser, S., Grubert, C., Hadrysiewicz, B., ... & Brockmann, H. (2010). Nucleus accumbens deep brain stimulation decreases ratings of depression and anxiety in treatment-resistant depression. *Biological psychiatry*, *67*(2), 110-116.
- Binder, D. K., & Steinhäuser, C. (2006). Functional changes in astroglial cells in epilepsy. *Glia*, *54*(5), 358-368.
- Biswal, B., Zerrin Yetkin, F., Haughton, V. M., & Hyde, J. S. (1995). Functional connectivity in the motor cortex of resting human brain using echo-planar MRI. *Magnetic resonance in medicine*, *34*(4), 537-541.
- Blondel, V. D., Guillaume, J. L., Lambiotte, R., & Lefebvre, E. (2008). Fast unfolding of communities in large networks. *Journal of statistical mechanics: theory and experiment*, *2008*(10), P10008.
- Blume, W. T., Lüders, H. O., Mizrahi, E., Tassinari, C., van Emde Boas, W., & Engel Jr, E. (2001). Glossary of descriptive terminology for ictal semiology: report of the ILAE task force on classification and terminology. *Epilepsia*, *42*(9), 1212-1218.
- Blumhardt, L. D., Smith, P. E. M., & Owen, L. (1986). Electrocardiographic accompaniments of temporal lobe epileptic seizures. *The Lancet*, *327*(8489), 1051-1056.
- Bonilha, L., Rorden, C., Castellano, G., Cendes, F., & Li, L. M. (2005). Voxel-based morphometry of the thalamus in patients with refractory medial temporal lobe epilepsy. *Neuroimage*, *25*(3), 1016-1021.
- Boulant, J. A. (2000). Role of the preoptic-anterior hypothalamus in thermoregulation and fever. *Clinical infectious diseases*, *31*(Supplement_5), S157-S161.
- Boylan, L. S., Flint, L. A., Labovitz, D. L., Jackson, S. C., Starner, K., & Devinsky, O. (2004). Depression but not seizure frequency predicts quality of life in treatment-resistant epilepsy. *Neurology*, *62*(2), 258-261.

- Bozorgi, A., Chung, S., Kaffashi, F., Loparo, K. A., Sahoo, S., Zhang, G. Q., ... & Lhatoo, S. D. (2013). Significant postictal hypotension: expanding the spectrum of seizure-induced autonomic dysregulation. *Epilepsia*, *54*(9), e127-e130.
- Britton, J. W., Ghearing, G. R., Benarroch, E. E., & Cascino, G. D. (2006). The ictal bradycardia syndrome: localization and lateralization. *Epilepsia*, *47*(4), 737-744.
- Brodie, M. J. (2013). Road to refractory epilepsy: The Glasgow story. *Epilepsia*, *54*, 5-8.
- Brooks, J. C. W., Faull, O. K., Pattinson, K. T., & Jenkinson, M. (2013). Physiological noise in brainstem fMRI. *Frontiers in human neuroscience*, *7*, 623.
- Bullmore, E., Fadili, J., Maxim, V., Şendur, L., Whitcher, B., Suckling, J., ... & Breakspear, M. (2004). Wavelets and functional magnetic resonance imaging of the human brain. *Neuroimage*, *23*, S234-S249.
- Burge, W. K., Griffis, J. C., Nenert, R., Elkhatali, A., DeCarlo, D. K., Lawrence, W., ... & Visscher, K. M. (2016). Cortical thickness in human V1 associated with central vision loss. *Scientific reports*, *6*, 23268.
- Burns, S. M., & Wyss, J. M. (1985). The involvement of the anterior cingulate cortex in blood pressure control. *Brain research*, *340*(1), 71-77.
- Bush, G., Luu, P., & Posner, M. I. (2000). Cognitive and emotional influences in anterior cingulate cortex. *Trends in cognitive sciences*, *4*(6), 215-222.
- Caballero-Gaudes, C., & Reynolds, R. C. (2017). Methods for cleaning the BOLD fMRI signal. *Neuroimage*, *154*, 128-149.
- Caciagli, L., Bernasconi, A., Wiebe, S., Koepp, M. J., Bernasconi, N., & Bernhardt, B. C. (2017). A meta-analysis on progressive atrophy in intractable temporal lobe epilepsy: time is brain?. *Neurology*, *89*(5), 506-516.
- Calton, M. A., Howard, J. R., Harper, R. M., Goldowitz, D., & Mittleman, G. (2016). The cerebellum and SIDS: disordered breathing in a mouse model of developmental cerebellar Purkinje cell loss during recovery from hypercarbia. *Frontiers in neurology*, *7*, 78.
- Camacho, D. L., & Castillo, M. (2007, December). MR imaging of temporal lobe epilepsy. In *Seminars in Ultrasound, CT and MRI* (Vol. 28, No. 6, pp. 424-436). WB Saunders.
- Cameron, A. A., Khan, I. A., Westlund, K. N., & Willis, W. D. (1995). The efferent projections of the periaqueductal gray in the rat: a Phaseolus vulgaris-leucoagglutinin study. II. Descending projections. *Journal of Comparative Neurology*, *351*(4), 585-601.
- Cardoso, M. J., Modat, M., Wolz, R., Melbourne, A., Cash, D., Rueckert, D., & Ourselin, S. (2015). Geodesic information flows: spatially-variant graphs and their application to segmentation and fusion. *IEEE transactions on medical imaging*, *34*(9), 1976-1988.

- Cardoso, M. J., Wolz, R., Modat, M., Fox, N. C., Rueckert, D., & Ourselin, S. (2012, October). Geodesic information flows. In *International Conference on Medical Image Computing and Computer-Assisted Intervention* (pp. 262-270). Springer, Berlin, Heidelberg.
- Cauda, F., D'Agata, F., Sacco, K., Duca, S., Geminiani, G., & Vercelli, A. (2011). Functional connectivity of the insula in the resting brain. *Neuroimage*, *55*(1), 8-23.
- Chase, M.H., & Clemente, C. D. (1968). Central neural components of the autonomic nervous system. *Journal of the American Society of Anesthesiology*. *29*(4),625–33.
- Ciomas, C., & Savic, I. (2006). Structural changes in patients with primary generalized tonic and clonic seizures. *Neurology*, *67*(4), 683-686.
- Coan, A. C., Appenzeller, S., Bonilha, L., Li, L. M., & Cendes, F. (2009). Seizure frequency and lateralization affect progression of atrophy in temporal lobe epilepsy. *Neurology*, *73*(11), 834-842.
- Cole, D. M., Smith, S. M., & Beckmann, C. F. (2010). Advances and pitfalls in the analysis and interpretation of resting-state FMRI data. *Frontiers in systems neuroscience*, *4*, 8.
- Cook, M. J., Fish, D. R., Shorvon, S. D., Straughan, K., & Stevens, J. M. (1992). Hippocampal volumetric and morphometric studies in frontal and temporal lobe epilepsy. *Brain*, *115*(4), 1001-1015.
- Craig, A. D. (2003). Interoception: the sense of the physiological condition of the body. *Current opinion in neurobiology*, *13*(4), 500-505.
- Critchley, H. D., Mathias, C. J., Josephs, O., O'Doherty, J., Zanini, S., Dewar, B. K., ... & Dolan, R. J. (2003). Human cingulate cortex and autonomic control: converging neuroimaging and clinical evidence. *Brain*, *126*(10), 2139-2152.
- Cukiert, A. (2016). Vagus nerve stimulation for epilepsy: an evidence-based approach. In *Stimulation of the Peripheral Nervous System* (Vol. 29, pp. 39-52). Karger Publishers.
- Cullen, K. R., Westlund, M. K., Klimes-Dougan, B., Mueller, B. A., Houry, A., Eberly, L. E., & Lim, K. O. (2014). Abnormal amygdala resting-state functional connectivity in adolescent depression. *JAMA psychiatry*, *71*(10), 1138-1147.
- Dahnke, R., & Gaser, C. (2016). Computational Anatomy Toolbox-CAT12. University of Jena: Structural Brain Mapping Group.
- Damoiseaux, J. S., Rombouts, S. A. R. B., Barkhof, F., Scheltens, P., Stam, C. J., Smith, S. M., & Beckmann, C. F. (2006). Consistent resting-state networks across healthy subjects. *Proceedings of the national academy of sciences*, *103*(37), 13848-13853.
- Dawes, G. S., Gardner, W. N., Johnston, B. M., & Walker, D. W. (1983). Breathing in fetal lambs: the effect of brain stem section. *The Journal of physiology*, *335*(1), 535-553.

- De Marco, F. A., Ghizoni, E., Kobayashi, E., Li, L. M., & Cendes, F. (2003). Cerebellar volume and long-term use of phenytoin. *Seizure, 12*(5), 312-315.
- De Tisi, J., Bell, G. S., Peacock, J. L., McEvoy, A. W., Harkness, W. F., Sander, J. W., & Duncan, J. S. (2011). The long-term outcome of adult epilepsy surgery, patterns of seizure remission, and relapse: a cohort study. *The Lancet, 378*(9800), 1388-1395.
- DeGiorgio, C. M., Markovic, D., Mazumder, R., & Moseley, B. D. (2017). Ranking the leading risk factors for sudden unexpected death in epilepsy. *Frontiers in neurology, 8*, 473.
- DeGiorgio, C. M., Miller, P., Meymandi, S., Chin, A., Epps, J., Gordon, S., ... & Harper, R. M. (2010). RMSSD, a measure of vagus-mediated heart rate variability, is associated with risk factors for SUDEP: the SUDEP-7 Inventory. *Epilepsy & Behavior, 19*(1), 78-81.
- Devinsky, O. (2004). Effects of seizures on autonomic and cardiovascular function. *Epilepsy currents, 4*(2), 43-46.
- Devinsky, O., Perrine, K., & Theodore, W. H. (1994). Interictal autonomic nervous system function in patients with epilepsy. *Epilepsia, 35*(1), 199-204.
- Dewan, N. A., Nieto, F. J., & Somers, V. K. (2015). Intermittent hypoxemia and OSA: implications for comorbidities. *Chest, 147*(1), 266-274.
- Di Gennaro, G., Quarato, P. P., Sebastiano, F., Esposito, V., Onorati, P., Grammaldo, L. G., ... & Eusebi, F. (2004). Ictal heart rate increase precedes EEG discharge in drug-resistant mesial temporal lobe seizures. *Clinical neurophysiology, 115*(5), 1169-1177.
- Dlouhy, B. J., Gehlbach, B. K., & Richerson, G. B. (2016). Sudden unexpected death in epilepsy: basic mechanisms and clinical implications for prevention. *J Neurol Neurosurg Psychiatry, 87*(4), 402-413.
- Dlouhy, B. J., Gehlbach, B. K., Kreple, C. J., Kawasaki, H., Oya, H., Buzza, C., ... & Richerson, G. B. (2015). Breathing inhibited when seizures spread to the amygdala and upon amygdala stimulation. *Journal of Neuroscience, 35*(28), 10281-10289.
- Dow, R. S., & Moruzzi, G. (1958). *The physiology and pathology of the cerebellum*. U of Minnesota Press.
- Dugan, L. L., & Choi, D. W. (1999). Hypoxia-ischemia and brain infarction. *Basic neurochemistry: molecular, cellular and medical aspects, 6th edn*. Lippincott-Raven, Philadelphia. Available from: <http://www.ncbi.nlm.nih.gov/books/NBK28046>.
- Dutschmann, M., & Dick, T. E. (2012). Pontine mechanisms of respiratory control. *Comprehensive Physiology, 2*(4), 2443-2469.
- Edlow, B. L., Takahashi, E., Wu, O., Benner, T., Dai, G., Bu, L., ... & Folkerth, R. D. (2012). Neuroanatomic connectivity of the human ascending arousal system critical to

- consciousness and its disorders. *Journal of Neuropathology & Experimental Neurology*, 71(6), 531-546.
- Engel Jr, J. (2006). ILAE classification of epilepsy syndromes. *Epilepsy research*, 70, 5-10.
- Evrengül, H., Tanriverdi, H., Dursunoglu, D., Kaftan, A., Kuru, O., Unlu, U., & Kilic, M. (2005). Time and frequency domain analyses of heart rate variability in patients with epilepsy. *Epilepsy research*, 63(2-3), 131-139.
- Fadili, M. J., & Bullmore, E. T. (2004). A comparative evaluation of wavelet-based methods for hypothesis testing of brain activation maps. *NeuroImage*, 23(3), 1112-1128.
- Fan, L., Li, H., Zhuo, J., Zhang, Y., Wang, J., Chen, L., ... & Fox, P. T. (2016). The human brainnetome atlas: a new brain atlas based on connectional architecture. *Cerebral cortex*, 26(8), 3508-3526.
- Farrell, J. S., Colangeli, R., Wolff, M. D., Wall, A. K., Phillips, T. J., George, A., ... & Teskey, G. C. (2017). Postictal hypoperfusion/hypoxia provides the foundation for a unified theory of seizure-induced brain abnormalities and behavioral dysfunction. *Epilepsia*, 58(9), 1493-1501.
- Feulner, L. C., Yan-Go, F., Snodgrass, D., Jen, J., Harper, R., Sauerland, E., & Harper, R. M. (2017). A79 TAKING CONTROL OF BREATHING: RESPIRATORY MUSCLES, INNERVATION, AND GAS EXCHANGE: Neuromodulation Of Cranial Nerves In Migraine Subjects Reduces Respiratory Rate And Variability. *American Journal of Respiratory and Critical Care Medicine*, 195.
- Ficker, D. M., So, E. L., Shen, W. K., Annegers, J. F., O'brien, P. C., Cascino, G. D., & Belau, P. G. (1998). Population-based study of the incidence of sudden unexplained death in epilepsy. *Neurology*, 51(5), 1270-1274.
- Fisher, R. S., Acevedo, C., Arzimanoglou, A., Bogacz, A., Cross, J. H., Elger, C. E., ... & Hesdorffer, D. C. (2014). ILAE official report: a practical clinical definition of epilepsy. *Epilepsia*, 55(4), 475-482.
- Fisher, R. S., Boas, W. V. E., Blume, W., Elger, C., Genton, P., Lee, P., & Engel Jr, J. (2005). Epileptic seizures and epilepsy: definitions proposed by the International League Against Epilepsy (ILAE) and the International Bureau for Epilepsy (IBE). *Epilepsia*, 46(4), 470-472.
- Fisher, R. S., Cross, J. H., French, J. A., Higurashi, N., Hirsch, E., Jansen, F. E., ... & Scheffer, I. E. (2017). Operational classification of seizure types by the International League Against Epilepsy: Position Paper of the ILAE Commission for Classification and Terminology. *Epilepsia*, 58(4), 522-530.
- Freedman, D., & Lane, D. (1983). A nonstochastic interpretation of reported significance levels. *Journal of Business & Economic Statistics*, 1(4), 292-298.
- Friedman, M., Landsberg, R., & Ascher-Landsberg, J. (2001). Treatment of hypoxemia in obstructive sleep apnea. *American journal of rhinology*, 15(5), 311-313.

- Friston, K. J., Frith, C. D., Liddle, P. F., & Frackowiak, R. S. J. (1993). Functional connectivity: the principal-component analysis of large (PET) data sets. *Journal of Cerebral Blood Flow & Metabolism*, *13*(1), 5-14.
- Frysinger, R. C., Engel, J., & Harper, R. M. (1993). Interictal heart rate patterns in partial seizure disorders. *Neurology*, *43*(10), 2136-2136.
- Gallen, C. L., Baniqued, P. L., Chapman, S. B., Aslan, S., Keebler, M., Didehbani, N., & D'Esposito, M. (2016). Modular brain network organization predicts response to cognitive training in older adults. *PloS one*, *11*(12), e0169015.
- Ganzetti, M., Wenderoth, N., & Mantini, D. (2014). Whole brain myelin mapping using T1- and T2-weighted MR imaging data. *Frontiers in human neuroscience*, *8*, 671.
- Gargouri, F., Kallel, F., Delphine, S., Ben Hamida, A., Lehericy, S., & Valabregue, R. (2018). The influence of preprocessing steps on graph theory measures derived from resting state fMRI. *Frontiers in computational neuroscience*, *12*, 8.
- Glasscock, E. (2014). Genomic biomarkers of SUDEP in brain and heart. *Epilepsy & Behavior*, *38*, 172-179.
- Guimera, R., & Amaral, L. A. N. (2005). Functional cartography of complex metabolic networks. *nature*, *433*(7028), 895.
- Guyenet, P. G. (2006). The sympathetic control of blood pressure. *Nature Reviews Neuroscience*, *7*(5), 335.
- Guyenet, P. G. (2006). The sympathetic control of blood pressure. *Nature Reviews Neuroscience*, *7*(5), 335.
- Hagemann, G., Lemieux, L., Free, S. L., Krakow, K., Everitt, A. D., Kendall, B. E., ... & Shorvon, S. D. (2002). Cerebellar volumes in newly diagnosed and chronic epilepsy. *Journal of neurology*, *249*(12), 1651-1658.
- Hanna, N. J., Black, M., Sander, J. W., Smithson, W. H., Appleton, R., Brown, S., & Fish, D. R. (2002). National Sentinel clinical audit of epilepsy-related death: report 2002. Epilepsy-death in the shadows.
- Harden, C., Tomson, T., Gloss, D., Buchhalter, J., Cross, J. H., Donner, E., ... & Spitz, M. C. (2017). Practice guideline summary: sudden unexpected death in epilepsy incidence rates and risk factors: report of the Guideline Development, Dissemination, and Implementation Subcommittee of the American Academy of Neurology and the American Epilepsy Society. *Epilepsy currents*, *17*(3), 180-187.
- Harper, R. M., Bandler, R., Spriggs, D., & Alger, J. R. (2000). Lateralized and widespread brain activation during transient blood pressure elevation revealed by magnetic resonance imaging. *Journal of Comparative Neurology*, *417*(2), 195-204.

- Harper, R. M., Frysinger, R. C., Trelease, R. B., & Marks, J. D. (1984). State-dependent alteration of respiratory cycle timing by stimulation of the central nucleus of the amygdala. *Brain research*, 306(1-2), 1-8.
- Harper, R. M., Kumar, R., Macey, P. M., Harper, R. K., & Ogren, J. A. (2015). Impaired neural structure and function contributing to autonomic symptoms in congenital central hypoventilation syndrome. *Frontiers in neuroscience*, 9, 415.
- Harper, R. M., Kumar, R., Macey, P. M., Woo, M. A., & Ogren, J. A. (2014). Affective brain areas and sleep-disordered breathing. In *Progress in brain research* (Vol. 209, pp. 275-293). Elsevier.
- Harper, R. M., Kumar, R., Ogren, J. A., & Macey, P. M. (2013). Sleep-disordered breathing: effects on brain structure and function. *Respiratory physiology & neurobiology*, 188(3), 383-391.
- Harper, R. M., Macey, P. M., Woo, M. A., Macey, K. E., Keens, T. G., Gozal, D., & Alger, J. R. (2005). Hypercapnic exposure in congenital central hypoventilation syndrome reveals CNS respiratory control mechanisms. *Journal of neurophysiology*, 93(3), 1647-1658.
- Harper, R. M., Poe, G. R., Rector, D. M., & Kristensen, M. P. (1998). Relationships between hippocampal activity and breathing patterns. *Neuroscience & Biobehavioral Reviews*, 22(2), 233-236.
- Harris, G. C., & Aston-Jones, G. (2006). Arousal and reward: a dichotomy in orexin function. *Trends in neurosciences*, 29(10), 571-577.
- He, W., Jing, X., Wang, X., Rong, P., Li, L., Shi, H., ... & Zhu, B. (2013). Transcutaneous auricular vagus nerve stimulation as a complementary therapy for pediatric epilepsy: a pilot trial. *Epilepsy & Behavior*, 28(3), 343-346.
- He, X., Doucet, G. E., Pustina, D., Sperling, M. R., Sharan, A. D., & Tracy, J. I. (2017). Presurgical thalamic “hubness” predicts surgical outcome in temporal lobe epilepsy. *Neurology*, 88(24), 2285-2293.
- Henderson, L. A., Gandevia, S. C., & Macefield, V. G. (2007). Somatotopic organization of the processing of muscle and cutaneous pain in the left and right insula cortex: a single-trial fMRI study. *Pain*, 128(1-2), 20-30.
- Henderson, L. A., Macey, P. M., Macey, K. E., Frysinger, R. C., Woo, M. A., Harper, R. K., ... & Harper, R. M. (2002). Brain responses associated with the Valsalva maneuver revealed by functional magnetic resonance imaging. *Journal of neurophysiology*, 88(6), 3477-3486.
- Henderson, L. A., Woo, M. A., Macey, P. M., Macey, K. E., Frysinger, R. C., Alger, J. R., ... & Harper, R. M. (2003). Neural responses during Valsalva maneuvers in obstructive sleep apnea syndrome. *Journal of Applied Physiology*, 94(3), 1063-1074.

- Hesdorffer, D. C., Tomson, T., Benn, E., Sander, J. W., Nilsson, L., Langan, Y., ... & ILAE Commission on Epidemiology; Subcommittee on Mortality. (2011). Combined analysis of risk factors for SUDEP. *Epilepsia*, *52*(6), 1150-1159.
- Hesdorffer, D. C., Tomson, T., Benn, E., Sander, J. W., Nilsson, L., Langan, Y., ... & ILAE Commission on Epidemiology; Subcommittee on Mortality. (2012). Do antiepileptic drugs or generalized tonic-clonic seizure frequency increase SUDEP risk? A combined analysis. *Epilepsia*, *53*(2), 249-252.
- Hirsch, E., Danober, L., Simler, S., De Vasconcelos, A. P., Maton, B., Nehlig, A., ... & Vergnes, M. (1997). The amygdala is critical for seizure propagation from brainstem to forebrain. *Neuroscience*, *77*(4), 975-984.
- Hitiris, N., Suratman, S., Kelly, K., Stephen, L. J., Sills, G. J., & Brodie, M. J. (2007). Sudden unexpected death in epilepsy: a search for risk factors. *Epilepsy & behavior*, *10*(1), 138-141.
- Holst, A. G., Winkel, B. G., Risgaard, B., Nielsen, J. B., Rasmussen, P. V., Haunsø, S., ... & Tfelt-Hansen, J. (2013). Epilepsy and risk of death and sudden unexpected death in the young: a nationwide study. *Epilepsia*, *54*(9), 1613-1620.
- Holstege, G., Meiners, L., & Tan, K. (1985). Projections of the bed nucleus of the stria terminalis to the mesencephalon, pons, and medulla oblongata in the cat. *Experimental brain research*, *58*(2), 379-391.
- Hopkins, D. A., & Holstege, G. (1978). Amygdaloid projections to the mesencephalon, pons and medulla oblongata in the cat. *Experimental Brain Research*, *32*(4), 529-547.
- Huang, W., Lu, G., Zhang, Z., Zhong, Y., Wang, Z., Yuan, C., ... & Zhang, Z. (2011). Gray-matter volume reduction in the thalamus and frontal lobe in epileptic patients with generalized tonic-clonic seizures. *Journal of Neuroradiology*, *38*(5), 298-303.
- Humphries, M. D., Gurney, K., & Prescott, T. J. (2005). The brainstem reticular formation is a small-world, not scale-free, network. *Proceedings of the Royal Society B: Biological Sciences*, *273*(1585), 503-511.
- Isojärvi, J. I., Ansakorpi, H., Suominen, K., Tolonen, U., Repo, M., & Myllylä, V. V. (1998). Interictal cardiovascular autonomic responses in patients with epilepsy. *Epilepsia*, *39*(4), 420-426.
- Johnston, M. V. (2001). Excitotoxicity in neonatal hypoxia. *Mental retardation and developmental disabilities research reviews*, *7*(4), 229-234.
- Johnston, M. V., Trescher, W. H., Ishida, A., & Nakajima, W. (2001). Neurobiology of hypoxic-ischemic injury in the developing brain. *Pediatric research*, *49*(6), 735-741.
- Joo, E. Y., Tae, W. S., Lee, M. J., Kang, J. W., Park, H. S., Lee, J. Y., ... & Hong, S. B. (2010). Reduced brain gray matter concentration in patients with obstructive sleep apnea syndrome. *Sleep*, *33*(2), 235-241.

- Kang, J. Y., Rabiei, A. H., Myint, L., & Nei, M. (2017). Equivocal significance of post-ictal generalized EEG suppression as a marker of SUDEP risk. *Seizure*, *48*, 28-32.
- Kanner, A. M. (2003). Depression in epilepsy: prevalence, clinical semiology, pathogenic mechanisms, and treatment. *Biological psychiatry*, *54*(3), 388-398.
- Kashtan, N., & Alon, U. (2005). Spontaneous evolution of modularity and network motifs. *Proceedings of the National Academy of Sciences*, *102*(39), 13773-13778.
- Keller, S. S., & Roberts, N. (2008). Voxel-based morphometry of temporal lobe epilepsy: an introduction and review of the literature. *Epilepsia*, *49*(5), 741-757.
- Keller, S. S., Ahrens, T., Mohammadi, S., Gerdes, J. S., Möddel, G., Kellinghaus, C., ... & Deppe, M. (2013). Voxel-based statistical analysis of fractional anisotropy and mean diffusivity in patients with unilateral temporal lobe epilepsy of unknown cause. *Journal of Neuroimaging*, *23*(3), 352-359.
- Keller, S. S., Wiesmann, U. C., Mackay, C. E., Denby, C. E., Webb, J., & Roberts, N. (2002). Voxel based morphometry of grey matter abnormalities in patients with medically intractable temporal lobe epilepsy: effects of side of seizure onset and epilepsy duration. *Journal of Neurology, Neurosurgery & Psychiatry*, *73*(6), 648-655.
- Kimmerly, D. S., O'Leary, D. D., Menon, R. S., Gati, J. S., & Shoemaker, J. K. (2005). Cortical regions associated with autonomic cardiovascular regulation during lower body negative pressure in humans. *The Journal of physiology*, *569*(1), 331-345.
- Klein, A., & Tourville, J. (2012). 101 labeled brain images and a consistent human cortical labeling protocol. *Frontiers in neuroscience*, *6*, 171.
- Koepp, M. J., & Woermann, F. G. (2005). Imaging structure and function in refractory focal epilepsy. *The Lancet Neurology*, *4*(1), 42-53.
- Kommajosyula, S. P., Tupal, S., & Faingold, C. L. (2018). Deficient post-ictal cardiorespiratory compensatory mechanisms mediated by the periaqueductal gray may lead to death in a mouse model of SUDEP. *Epilepsy research*, *147*, 1-8.
- Koos, B. J., Chau, A., Matsuura, M., Punla, O., & Kruger, L. (1998). Thalamic locus mediates hypoxic inhibition of breathing in fetal sheep. *Journal of Neurophysiology*, *79*(5), 2383-2393.
- Koos, B. J., Chau, A., Matsuura, M., Punla, O., & Kruger, L. (2000). Thalamic lesions dissociate breathing inhibition by hypoxia and adenosine in fetal sheep. *American Journal of Physiology-Regulatory, Integrative and Comparative Physiology*, *278*(4), R831-R837.
- Koos, B. J., Kawasaki, Y., Hari, A., Bohorquez, F., Jan, C., Roostaeian, J., ... & Kruger, L. (2004). Electrical stimulation of the posteromedial thalamus modulates breathing in unanesthetized fetal sheep. *Journal of Applied Physiology*, *96*(1), 115-123.

- Koos, B. J., Rajaei, A., Ibe, B., Guerra, C., & Kruger, L. (2016). Thalamic mediation of hypoxic respiratory depression in lambs. *American Journal of Physiology-Regulatory, Integrative and Comparative Physiology*, *310*(7), R586-R595.
- Koutsikou, S., Crook, J. J., Earl, E. V., Leith, J. L., Watson, T. C., Lumb, B. M., & Apps, R. (2014). Neural substrates underlying fear-evoked freezing: the periaqueductal grey–cerebellar link. *The Journal of physiology*, *592*(10), 2197-2213.
- Kruskal, J. B. (1956). On the shortest spanning subtree of a graph and the traveling salesman problem. *Proceedings of the American Mathematical Society*, *7*(1), 48-50.
- Kumar, R., Ahdout, R., Macey, P. M., Woo, M. A., Avedissian, C., Thompson, P. M., & Harper, R. M. (2009). Reduced caudate nuclei volumes in patients with congenital central hypoventilation syndrome. *Neuroscience*, *163*(4), 1373-1379.
- Kumar, R., Farahvar, S., Ogren, J. A., Macey, P. M., Thompson, P. M., Woo, M. A., ... & Harper, R. M. (2014). Brain putamen volume changes in newly-diagnosed patients with obstructive sleep apnea. *NeuroImage: Clinical*, *4*, 383-391.
- Kumar, R., Macey, P. M., Woo, M. A., Alger, J. R., Keens, T. G., & Harper, R. M. (2005). Neuroanatomic deficits in congenital central hypoventilation syndrome. *Journal of Comparative Neurology*, *487*(4), 361-371.
- Kuo, J., Zhao, W., Li, C. S., Kennedy, J. D., & Seyal, M. (2016). Postictal immobility and generalized EEG suppression are associated with the severity of respiratory dysfunction. *Epilepsia*, *57*(3), 412-417.
- Lacuey, N., Hampson, J. P., Theeranaew, W., Zonjy, B., Vithala, A., Hupp, N. J., ... & Lhatoo, S. D. (2018b). Cortical structures associated with human blood pressure control. *JAMA neurology*, *75*(2), 194-202.
- Lacuey, N., Zonjy, B., Hampson, J. P., Rani, M. S., Zaremba, A., Sainju, R. K., ... & Nei, M. (2018a). The incidence and significance of periictal apnea in epileptic seizures. *Epilepsia*, *59*(3), 573-582.
- Lacuey, N., Zonjy, B., Londono, L., & Lhatoo, S. D. (2017). Amygdala and hippocampus are symptomatogenic zones for central apneic seizures. *Neurology*, *88*(7), 701-705.
- Lamberts, R. J., Thijs, R. D., Laffan, A., Langan, Y., & Sander, J. W. (2012). Sudden unexpected death in epilepsy: people with nocturnal seizures may be at highest risk. *Epilepsia*, *53*(2), 253-257.
- Langan, Y., Nashef, L., & Sander, J. W. (2005). Case-control study of SUDEP. *Neurology*, *64*(7), 1131-1133.
- Laxer, K. D., Trinkaus, E., Hirsch, L. J., Cendes, F., Langfitt, J., Delanty, N., ... & Benbadis, S. R. (2014). The consequences of refractory epilepsy and its treatment. *Epilepsy & behavior*, *37*, 59-70.

- Lee, M. H., Smyser, C. D., & Shimony, J. S. (2013). Resting-state fMRI: a review of methods and clinical applications. *American Journal of neuroradiology*, *34*(10), 1866-1872.
- Lemieux, L., Salek-Haddadi, A., Lund, T. E., Laufs, H., & Carmichael, D. (2007). Modelling large motion events in fMRI studies of patients with epilepsy. *Magnetic resonance imaging*, *25*(6), 894-901.
- Leung, H., Schindler, K., Kwan, P., & Elger, C. (2007). Asystole induced by electrical stimulation of the left cingulate gyrus. *Epileptic disorders*, *9*(1), 77-81.
- Leutmezer, F., Scherthaner, C., Lurger, S., Pötzelberger, K., & Baumgartner, C. (2003). Electrocardiographic changes at the onset of epileptic seizures. *Epilepsia*, *44*(3), 348-354.
- Lhatoo, S., Noebels, J., Whittemore, V., & NINDS Center for SUDEP Research. (2015). Sudden unexpected death in epilepsy: Identifying risk and preventing mortality. *Epilepsia*, *56*(11), 1700-1706.
- Liebenthal, J. A., Wu, S., Rose, S., Ebersole, J. S., & Tao, J. X. (2015). Association of prone position with sudden unexpected death in epilepsy. *Neurology*, *84*(7), 703-709.
- Loewy, A. D. (1982). Descending pathways to the sympathetic preganglionic neurons. In *Progress in brain research* (Vol. 57, pp. 267-277). Elsevier.
- Loewy, A. D. (1991). Forebrain nuclei involved in autonomic control. In *Progress in brain research* (Vol. 87, pp. 253-268). Elsevier.
- Lotufo, P. A., Valiengo, L., Benseñor, I. M., & Brunoni, A. R. (2012). A systematic review and meta-analysis of heart rate variability in epilepsy and antiepileptic drugs. *Epilepsia*, *53*(2), 272-282.
- Lotufo, P. A., Valiengo, L., Benseñor, I. M., & Brunoni, A. R. (2012). A systematic review and meta-analysis of heart rate variability in epilepsy and antiepileptic drugs. *Epilepsia*, *53*(2), 272-282.
- Love, S., Plaha, P., Patel, N. K., Hotton, G. R., Brooks, D. J., & Gill, S. S. (2005). Glial cell line-derived neurotrophic factor induces neuronal sprouting in human brain. *Nature medicine*, *11*(7), 703.
- Macefield, V. G., & Henderson, L. A. (2015). Autonomic responses to exercise: cortical and subcortical responses during post-exercise ischaemia and muscle pain. *Autonomic Neuroscience*, *188*, 10-18.
- Macey, P. M., Moiyadi, A. S., Kumar, R., Woo, M. A., & Harper, R. M. (2011). Decreased cortical thickness in central hypoventilation syndrome. *Cerebral Cortex*, *22*(8), 1728-1737.
- Macey, P. M., Ogren, J. A., Kumar, R., & Harper, R. M. (2016). Functional imaging of autonomic regulation: methods and key findings. *Frontiers in neuroscience*, *9*, 513.

- Macey, P. M., Richard, C. A., Kumar, R., Woo, M. A., Ogren, J. A., Avedissian, C., ... & Harper, R. M. (2009). Hippocampal volume reduction in congenital central hypoventilation syndrome. *PLoS One*, *4*(7), e6436.
- Macey, P. M., Woo, M. A., Macey, K. E., Keens, T. G., Saeed, M. M., Alger, J. R., & Harper, R. M. (2005). Hypoxia reveals posterior thalamic, cerebellar, midbrain, and limbic deficits in congenital central hypoventilation syndrome. *Journal of Applied Physiology*, *98*(3), 958-969.
- Macey, P. M., Wu, P., Kumar, R., Ogren, J. A., Richardson, H. L., Woo, M. A., & Harper, R. M. (2012). Differential responses of the insular cortex gyri to autonomic challenges. *Autonomic Neuroscience*, *168*(1-2), 72-81.
- Maglajlija, V., Walker, M. C., & Kovac, S. (2012). Severe ictal hypoxemia following focal, subclinical temporal electrographic scalp seizure activity. *Epilepsy & Behavior*, *24*(1), 143-145.
- Malow, B. A., Levy, K., Maturen, K., & Bowes, R. (2000). Obstructive sleep apnea is common in medically refractory epilepsy patients. *Neurology*, *55*(7), 1002-1007.
- Marchand, W. R., Lee, J. N., Thatcher, J. W., Hsu, E. W., Rashkin, E., Suchy, Y., ... & Barbera, S. S. (2008). Putamen coactivation during motor task execution. *Neuroreport*, *19*(9), 957-960.
- Marcián, V., Mareček, R., Korit'áková, E., Pail, M., Bareš, M., & Brázdil, M. (2018). Morphological changes of cerebellar substructures in temporal lobe epilepsy: A complex phenomenon, not mere atrophy. *Seizure*, *54*, 51-57.
- Martin-Body, R. L., & Johnston, B. M. (1988). Central origin of the hypoxic depression of breathing in the newborn. *Respiration physiology*, *71*(1), 25-32.
- Massetani, R., Strata, G., Galli, R., Gori, S., Gneri, C., Limbruno, U., ... & Murri, L. (1997). Alteration of cardiac function in patients with temporal lobe epilepsy: different roles of EEG-ECG monitoring and spectral analysis of RR variability. *Epilepsia*, *38*(3), 363-369.
- Massey, C. A., Sowers, L. P., Dlouhy, B. J., & Richerson, G. B. (2014). Mechanisms of sudden unexpected death in epilepsy: the pathway to prevention. *Nature Reviews Neurology*, *10*(5), 271.
- Mechelli, A., Price, C. J., Friston, K. J., & Ashburner, J. (2005). Voxel-based morphometry of the human brain: methods and applications. *Current medical imaging reviews*, *1*(2), 105-113.
- Meldrum, B. S., & Rogawski, M. A. (2007). Molecular targets for antiepileptic drug development. *Neurotherapeutics*, *4*(1), 18-61.
- Messenheimer, J. A., Quint, S. R., Tennison, M. B., & Keaney, P. (1990). Monitoring heart period variability changes during seizures. I. Methods. *Journal of Epilepsy*, *3*(1), 47-54.

- Miura, M., & Reis, D. J. (1969). Cerebellum: a pressor response elicited from the fastigial nucleus and its efferent pathway in brainstem. *Brain Research*, *13*(3), 595-599.
- Moffat, B. A., Chenevert, T. L., Lawrence, T. S., Meyer, C. R., Johnson, T. D., Dong, Q., ... & Robertson, P. L. (2005). Functional diffusion map: a noninvasive MRI biomarker for early stratification of clinical brain tumor response. *Proceedings of the national academy of sciences*, *102*(15), 5524-5529.
- Moseley, B. D., Britton, J. W., Nelson, C., Lee, R. W., & So, E. (2012). Periictal cerebral tissue hypoxemia: a potential marker of SUDEP risk. *Epilepsia*, *53*(12), e208-e211.
- Mueller, S. G., Bateman, L. M., & Laxer, K. D. (2014). Evidence for brainstem network disruption in temporal lobe epilepsy and sudden unexplained death in epilepsy. *NeuroImage: Clinical*, *5*, 208-216.
- Mueller, S. G., Nei, M., Bateman, L. M., Knowlton, R., Laxer, K. D., Friedman, D., ... & Goldman, A. M. (2018). Brainstem network disruption: A pathway to sudden unexplained death in epilepsy?. *Human brain mapping*, *39*(12), 4820-4830.
- Mufson, E. J., & Mesulam, M. M. (1984). Thalamic connections of the insula in the rhesus monkey and comments on the paralimbic connectivity of the medial pulvinar nucleus. *Journal of Comparative Neurology*, *227*(1), 109-120.
- Mukherjee, S., Tripathi, M., Chandra, P. S., Yadav, R., Choudhary, N., Sagar, R., ... & Deepak, K. K. (2009). Cardiovascular autonomic functions in well-controlled and intractable partial epilepsies. *Epilepsy research*, *85*(2-3), 261-269.
- Murphy, K., & Fox, M. D. (2017). Towards a consensus regarding global signal regression for resting state functional connectivity MRI. *Neuroimage*, *154*, 169-173.
- Murphy, K., Birn, R. M., Handwerker, D. A., Jones, T. B., & Bandettini, P. A. (2009). The impact of global signal regression on resting state correlations: are anti-correlated networks introduced?. *Neuroimage*, *44*(3), 893-905.
- Muschelli, J., Nebel, M. B., Caffo, B. S., Barber, A. D., Pekar, J. J., & Mostofsky, S. H. (2014). Reduction of motion-related artifacts in resting state fMRI using aCompCor. *Neuroimage*, *96*, 22-35.
- Myers, K. A., Bello-Espinosa, L. E., Symonds, J. D., Zuberi, S. M., Clegg, R., Sadleir, L. G., ... & Scheffer, I. E. (2018). Heart rate variability in epilepsy: a potential biomarker of sudden unexpected death in epilepsy risk. *Epilepsia*, *59*(7), 1372-1380.
- Nashef, L., Hindocha, N., & Makoff, A. (2007). Risk factors in sudden death in epilepsy (SUDEP): the quest for mechanisms. *Epilepsia*, *48*(5), 859-871.
- Nashef, L., So, E. L., Ryvlin, P., & Tomson, T. (2012). Unifying the definitions of sudden unexpected death in epilepsy. *Epilepsia*, *53*(2), 227-233.

- Nashef, L., Walker, F., Allen, P., Sander, J. W., Shorvon, S. D., & Fish, D. R. (1996). Apnoea and bradycardia during epileptic seizures: relation to sudden death in epilepsy. *Journal of Neurology, Neurosurgery & Psychiatry*, *60*(3), 297-300.
- Natsume, J., Bernasconi, N., Andermann, F., & Bernasconi, A. (2003). MRI volumetry of the thalamus in temporal, extratemporal, and idiopathic generalized epilepsy. *Neurology*, *60*(8), 1296-1300.
- Nei, M., Ho, R. T., & Sperling, M. R. (2000). EKG abnormalities during partial seizures in refractory epilepsy. *Epilepsia*, *41*(5), 542-548.
- Neubauer, J. A., & Sunderram, J. (2004). Oxygen-sensing neurons in the central nervous system. *Journal of Applied Physiology*, *96*(1), 367-374.
- Ni, H., Zhang, J., & Harper, R. M. (1990a). Cardiovascular-related discharge of periaqueductal gray neurons during sleep-waking states. *Brain research*, *532*(1-2), 242-248.
- Ni, H., Zhang, J., & Harper, R. M. (1990b). Cardiovascular-related discharge of periaqueductal gray neurons during sleep-waking states. *Brain research*, *532*(1-2), 242-248.
- Nichols, T. E., & Holmes, A. P. (2002). Nonparametric permutation tests for functional neuroimaging: a primer with examples. *Human brain mapping*, *15*(1), 1-25.
- Nobis, W. P., Schuele, S., Templer, J. W., Zhou, G., Lane, G., Rosenow, J. M., & Zelano, C. (2018). Amygdala-stimulation-induced apnea is attention and nasal-breathing dependent. *Annals of neurology*, *83*(3), 460-471.
- Ogawa, S., Lee, T. M., Kay, A. R., & Tank, D. W. (1990). Brain magnetic resonance imaging with contrast dependent on blood oxygenation. *proceedings of the National Academy of Sciences*, *87*(24), 9868-9872.
- Ogren, J. A., Macey, P. M., Kumar, R., Fonarow, G. C., Hamilton, M. A., Harper, R. M., & Woo, M. A. (2012). Impaired cerebellar and limbic responses to the valsalva maneuver in heart failure. *The Cerebellum*, *11*(4), 931-938.
- Ogren, J. A., Macey, P. M., Kumar, R., Woo, M. A., & Harper, R. M. (2010). Central autonomic regulation in congenital central hypoventilation syndrome. *Neuroscience*, *167*(4), 1249-1256.
- Ogren, J. A., Tripathi, R., Macey, P. M., Kumar, R., Stern, J. M., Eliashiv, D. S., ... & Lhatoo, S. D. (2018). Regional cortical thickness changes accompanying generalized tonic-clonic seizures. *NeuroImage: Clinical*, *20*, 205-215.
- Öngür, D., & Price, J. L. (2000). The organization of networks within the orbital and medial prefrontal cortex of rats, monkeys and humans. *Cerebral cortex*, *10*(3), 206-219.
- Öngür, D., An, X., & Price, J. L. (1998). Prefrontal cortical projections to the hypothalamus in macaque monkeys. *Journal of Comparative Neurology*, *401*(4), 480-505.

- Opherk, C., Coromilas, J., & Hirsch, L. J. (2002). Heart rate and EKG changes in 102 seizures: analysis of influencing factors. *Epilepsy research*, 52(2), 117-127.
- Oppenheimer, S. M., Gelb, A., Girvin, J. P., & Hachinski, V. C. (1992). Cardiovascular effects of human insular cortex stimulation. *Neurology*, 42(9), 1727-1727.
- Oppenheimer, S. M., Kedem, G., & Martin, W. M. (1996). Left-insular cortex lesions perturb cardiac autonomic tone in humans. *Clinical Autonomic Research*, 6(3), 131-140.
- Orru, G., Pettersson-Yeo, W., Marquand, A. F., Sartori, G., & Mechelli, A. (2012). Using support vector machine to identify imaging biomarkers of neurological and psychiatric disease: a critical review. *Neuroscience & Biobehavioral Reviews*, 36(4), 1140-1152.
- Owens, N. C., & Verberne, A. J. (2000). Medial prefrontal depressor response: involvement of the rostral and caudal ventrolateral medulla in the rat. *Journal of the autonomic nervous system*, 78(2-3), 86-93.
- Oyegbile, T. O., Bayless, K., Dabbs, K., Jones, J., Rutecki, P., Pierson, R., ... & Hermann, B. (2011). The nature and extent of cerebellar atrophy in chronic temporal lobe epilepsy. *Epilepsia*, 52(4), 698-706.
- Pae, E. K., Chien, P., & Harper, R. M. (2005). Intermittent hypoxia damages cerebellar cortex and deep nuclei. *Neuroscience letters*, 375(2), 123-128.
- Park, B., Palomares, J. A., Woo, M. A., Kang, D. W., Macey, P. M., Yan-Go, F. L., ... & Kumar, R. (2016). Aberrant insular functional network integrity in patients with obstructive sleep apnea. *Sleep*, 39(5), 989-1000.
- Pattinson, K. T. (2008). Opioids and the control of respiration. *British journal of anaesthesia*, 100(6), 747-758.
- Pazo, J. H., & Belforte, J. E. (2002). Basal ganglia and functions of the autonomic nervous system. *Cellular and molecular neurobiology*, 22(5-6), 645-654.
- Peng, W., Danison, J. L., & Seyal, M. (2017). Postictal generalized EEG suppression and respiratory dysfunction following generalized tonic-clonic seizures in sleep and wakefulness. *Epilepsia*, 58(8), 1409-1414.
- Percival, D. B., & Walden, A. T. (2000). *Wavelet methods for time series analysis* (Vol. 4). Cambridge university press.
- Pool, J. L., & Ransohoff, J. (1949). Autonomic effects on stimulating rostral portion of cingulate gyri in man. *Journal of neurophysiology*, 12(6), 385-392.
- Power, J. D., Barnes, K. A., Snyder, A. Z., Schlaggar, B. L., & Petersen, S. E. (2012). Spurious but systematic correlations in functional connectivity MRI networks arise from subject motion. *Neuroimage*, 59(3), 2142-2154.

- Power, J. D., Mitra, A., Laumann, T. O., Snyder, A. Z., Schlaggar, B. L., & Petersen, S. E. (2014). Methods to detect, characterize, and remove motion artifact in resting state fMRI. *Neuroimage*, *84*, 320-341.
- Power, J. D., Schlaggar, B. L., & Petersen, S. E. (2015). Recent progress and outstanding issues in motion correction in resting state fMRI. *Neuroimage*, *105*, 536-551.
- Price, J. L., & Drevets, W. C. (2010). Neurocircuitry of mood disorders. *Neuropsychopharmacology*, *35*(1), 192.
- Prim, R. C. (1957). Shortest connection networks and some generalizations. *The Bell System Technical Journal*, *36*(6), 1389-1401.
- Ramu, A., & Bergmann, F. (1967). The role of the cerebellum in blood pressure regulation. *Experientia*, *23*(5), 383-384.
- Resstel, L. B. M., & Correa, F. M. A. (2006). Involvement of the medial prefrontal cortex in central cardiovascular modulation in the rat. *Autonomic Neuroscience*, *126*, 130-138.
- Ridley, B. G. Y., Rousseau, C., Wirsich, J., Le Troter, A., Soulier, E., Confort-Gouny, S., ... & Guye, M. (2015). Nodal approach reveals differential impact of lateralized focal epilepsies on hub reorganization. *Neuroimage*, *118*, 39-48.
- Rocamora, R., Kurthen, M., Lickfett, L., Von Oertzen, J., & Elger, C. E. (2003). Cardiac asystole in epilepsy: clinical and neurophysiologic features. *Epilepsia*, *44*(2), 179-185.
- Rodbard, S. (1948). Body temperature, blood pressure, and hypothalamus. *Science*, *108*(2807), 413-415.
- Rong, P., Liu, A., Zhang, J., Wang, Y., He, W., Yang, A., ... & Wu, P. (2014). Transcutaneous vagus nerve stimulation for refractory epilepsy: a randomized controlled trial. *Clinical Science*, CS20130518.
- Ronkainen, E., Ansakorpi, H., Huikuri, H. V., Myllylä, V. V., Isojärvi, J. I. T., & Korpelainen, J. T. (2005). Suppressed circadian heart rate dynamics in temporal lobe epilepsy. *Journal of Neurology, Neurosurgery & Psychiatry*, *76*(10), 1382-1386.
- Rubinov, M., & Sporns, O. (2010). Complex network measures of brain connectivity: uses and interpretations. *Neuroimage*, *52*(3), 1059-1069.
- Rugg-Gunn, F. J., Simister, R. J., Squirrell, M., Holdright, D. R., & Duncan, J. S. (2004). Cardiac arrhythmias in focal epilepsy: a prospective long-term study. *The Lancet*, *364*(9452), 2212-2219.
- Ryvlin, P., Cucherat, M., & Rheims, S. (2011). Risk of sudden unexpected death in epilepsy in patients given adjunctive antiepileptic treatment for refractory seizures: a meta-analysis of placebo-controlled randomised trials. *The Lancet Neurology*, *10*(11), 961-968.

- Ryvlin, P., Nashef, L., Lhatoo, S. D., Bateman, L. M., Bird, J., Bleasel, A., ... & Lerche, H. (2013). Incidence and mechanisms of cardiorespiratory arrests in epilepsy monitoring units (MORTEMUS): a retrospective study. *The Lancet Neurology*, *12*(10), 966-977.
- Saad, Z. S., Gotts, S. J., Murphy, K., Chen, G., Jo, H. J., Martin, A., & Cox, R. W. (2012). Trouble at rest: how correlation patterns and group differences become distorted after global signal regression. *Brain connectivity*, *2*(1), 25-32.
- Salmenpera, T. M., & Duncan, J. S. (2005). Imaging in epilepsy. *Journal of Neurology, Neurosurgery & Psychiatry*, *76*(suppl 3), iii2-iii10.
- Sander, J. W. (2003). The epidemiology of epilepsy revisited. *Current opinion in neurology*, *16*(2), 165-170.
- Sander, J. W. (2004). The use of antiepileptic drugs—principles and practice. *Epilepsia*, *45*, 28-34.
- Sander, J. W., & Sillanpää, M. (1997). Natural history and prognosis. In: Engel Jr J, Pedly TA, eds. *Epilepsy: a comprehensive textbook*. Philadelphia: *Lippincott Raven Publishers*, 69–85.
- Saper, C. B. (2002). The central autonomic nervous system: conscious visceral perception and autonomic pattern generation. *Annual review of neuroscience*, *25*(1), 433-469.
- Saper, C. B., & Loewy, A. D. (1980). Efferent connections of the parabrachial nucleus in the rat. *Brain research*, *197*(2), 291-317.
- Satterthwaite, T. D., Wolf, D. H., Loughhead, J., Ruparel, K., Elliott, M. A., Hakonarson, H., ... & Gur, R. E. (2012). Impact of in-scanner head motion on multiple measures of functional connectivity: relevance for studies of neurodevelopment in youth. *Neuroimage*, *60*(1), 623-632.
- Sawaya, H., Johnson, K., Schmidt, M., Arana, A., Chahine, G., Atoui, M., ... & Nahas, Z. (2015). Resting-state functional connectivity of antero-medial prefrontal cortex sub-regions in major depression and relationship to emotional intelligence. *International Journal of Neuropsychopharmacology*, *18*(6), pyu112.
- Scammell, T. E., Arrigoni, E., & Lipton, J. O. (2017). Neural circuitry of wakefulness and sleep. *Neuron*, *93*(4), 747-765.
- Scheffer, I. E., Berkovic, S., Capovilla, G., Connolly, M. B., French, J., Guilhoto, L., ... & Nordli, D. R. (2017). ILAE classification of the epilepsies: position paper of the ILAE Commission for Classification and Terminology. *Epilepsia*, *58*(4), 512-521.
- Schuele, S. U., Afshari, M., Afshari, Z. S., Macken, M. P., Asconape, J., Wolfe, L., & Gerard, E. E. (2011). Ictal central apnea as a predictor for sudden unexpected death in epilepsy. *Epilepsy & Behavior*, *22*(2), 401-403.

- Schwartz, P. J., S. G. Priori, and C. Napolitano. (2000). 'The long QT syndrome.' in D. P. Zipes and J. Jalife (eds.), *Cardiac electrophysiology: from cell to bedside* (W. B. Saunders: Philadelphia).
- Seyal, M., Pascual, F., Lee, C. Y. M., Li, C. S., & Bateman, L. M. (2011). Seizure-related cardiac repolarization abnormalities are associated with ictal hypoxemia. *Epilepsia*, 52(11), 2105-2111.
- Shankar, R., Donner, E. J., McLean, B., Nashef, L., & Tomson, T. (2017). Sudden unexpected death in epilepsy (SUDEP): what every neurologist should know. *Epileptic Disorders*, 19(1), 1-9.
- Shoemaker, J. K., & Goswami, R. (2015). Forebrain neurocircuitry associated with human reflex cardiovascular control. *Frontiers in physiology*, 6, 240.
- Shoemaker, J. K., Wong, S. W., & Cechetto, D. F. (2012). Cortical circuitry associated with reflex cardiovascular control in humans: does the cortical autonomic network “speak” or “listen” during cardiovascular arousal. *The Anatomical Record: Advances in Integrative Anatomy and Evolutionary Biology*, 295(9), 1375-1384.
- Shoemaker, J. Kevin, Katelyn N. Norton, J. Baker, and T. Luchyshyn. "Forebrain organization for autonomic cardiovascular control." *Autonomic Neuroscience* 188 (2015): 5-9.
- Shorvon, S., & Tomson, T. (2011). Sudden unexpected death in epilepsy. *The Lancet*, 378(9808), 2028-2038.
- Slemmer, J. E., De Zeeuw, C. I., & Weber, J. T. (2005). Don't get too excited: mechanisms of glutamate-mediated Purkinje cell death. *Progress in brain research*, 148, 367-390.
- Sobkowicz, H. M., & Slapnick, S. M. (1992). Neuronal sprouting and synapse formation in response to injury in the mouse organ of Corti in culture. *International journal of developmental neuroscience*, 10(6), 545-566.
- Song, X. W., Dong, Z. Y., Long, X. Y., Li, S. F., Zuo, X. N., Zhu, C. Z., ... & Zang, Y. F. (2011). REST: a toolkit for resting-state functional magnetic resonance imaging data processing. *PloS one*, 6(9), e25031.
- Stefan, H., Kreiselmeyer, G., Kerling, F., Kurzbuch, K., Rauch, C., Heers, M., ... & Ellrich, J. (2012). Transcutaneous vagus nerve stimulation (t-VNS) in pharmacoresistant epilepsies: A proof of concept trial. *Epilepsia*, 53(7), e115-e118.
- Stein, P. K., Bosner, M. S., Kleiger, R. E., & Conger, B. M. (1994). Heart rate variability: a measure of cardiac autonomic tone. *American heart journal*, 127(5), 1376-1381.
- Stonnington, C. M., Tan, G., Klöppel, S., Chu, C., Draganski, B., Jack Jr, C. R., ... & Frackowiak, R. S. (2008). Interpreting scan data acquired from multiple scanners: a study with Alzheimer's disease. *Neuroimage*, 39(3), 1180-1185.

- Strange, B. A., Witter, M. P., Lein, E. S., & Moser, E. I. (2014). Functional organization of the hippocampal longitudinal axis. *Nature Reviews Neuroscience*, *15*(10), 655.
- Surges, R., Henneberger, C., Adjei, P., Scott, C. A., Sander, J. W., & Walker, M. C. (2009). Do alterations in inter-ictal heart rate variability predict sudden unexpected death in epilepsy?. *Epilepsy research*, *87*(2-3), 277-280.
- Surges, R., Scott, C. A., & Walker, M. C. (2010). Enhanced QT shortening and persistent tachycardia after generalized seizures. *Neurology*, *74*(5), 421-426.
- Szabo, C. A., Lancaster, J. L., Lee, S., Xiong, J. H., Cook, C., Mayes, B. N., & Fox, P. T. (2006). MR imaging volumetry of subcortical structures and cerebellar hemispheres in temporal lobe epilepsy. *American Journal of Neuroradiology*, *27*(10), 2155-2160.
- Takao, H., Hayashi, N., & Ohtomo, K. (2014). Effects of study design in multi-scanner voxel-based morphometry studies. *Neuroimage*, *84*, 133-140.
- Tang, F., Hartz, A., & Bauer, B. (2017). Drug-resistant epilepsy: multiple hypotheses, few answers. *Frontiers in neurology*, *8*, 301.
- Tang, Y., Chen, Q., Yu, X., Xia, W., Luo, C., Huang, X., ... & Zhou, D. (2014). A resting-state functional connectivity study in patients at high risk for sudden unexpected death in epilepsy. *Epilepsy & Behavior*, *41*, 33-38.
- Télliez-Zenteno, J. F., Dhar, R., & Wiebe, S. (2005). Long-term seizure outcomes following epilepsy surgery: a systematic review and meta-analysis. *Brain*, *128*(5), 1188-1198.
- Thapar, A., Kerr, M., & Harold, G. (2009). Stress, anxiety, depression, and epilepsy: investigating the relationship between psychological factors and seizures. *Epilepsy & Behavior*, *14*(1), 134-140.
- Thayer, J. F., Yamamoto, S. S., & Brosschot, J. F. (2010). The relationship of autonomic imbalance, heart rate variability and cardiovascular disease risk factors. *International journal of cardiology*, *141*(2), 122-131.
- Thompson, P. J., & Duncan, J. S. (2005). Cognitive decline in severe intractable epilepsy. *Epilepsia*, *46*(11), 1780-1787.
- Tomson, T., Ericson, M., Ihrman, C., & Lindblad, L. E. (1998). Heart rate variability in patients with epilepsy. *Epilepsy research*, *30*(1), 77-83.
- Tomson, T., Nashef, L., & Ryvlin, P. (2008). Sudden unexpected death in epilepsy: current knowledge and future directions. *The Lancet Neurology*, *7*(11), 1021-1031.
- Tortora, G. J., & Derrickson, B. H. (2008). *Principles of anatomy and physiology*. John Wiley & Sons.
- Usunoff, K. G., Itzev, D. E., Rolfs, A., Schmitt, O., & Wree, A. (2006). Brain stem afferent connections of the amygdala in the rat with special references to a projection from the

- parabigeminal nucleus: a fluorescent retrograde tracing study. *Anatomy and embryology*, 211(5), 475-496.
- Van Buren, J. M. (1958). Some autonomic concomitants of ictal automatism: a study of temporal lobe attacks. *Brain*, 81(4), 505-528.
- Van Den Heuvel, M. P., & Pol, H. E. H. (2010). Exploring the brain network: a review on resting-state fMRI functional connectivity. *European neuropsychopharmacology*, 20(8), 519-534.
- van den Heuvel, M. P., de Lange, S. C., Zalesky, A., Seguin, C., Yeo, B. T., & Schmidt, R. (2017). Proportional thresholding in resting-state fMRI functional connectivity networks and consequences for patient-control connectome studies: Issues and recommendations. *Neuroimage*, 152, 437-449.
- van der Lende, M., Surges, R., Sander, J. W., & Thijs, R. D. (2016). Cardiac arrhythmias during or after epileptic seizures. *J Neurol Neurosurg Psychiatry*, 87(1), 69-74.
- Van Dijk, K. R., Sabuncu, M. R., & Buckner, R. L. (2012). The influence of head motion on intrinsic functional connectivity MRI. *Neuroimage*, 59(1), 431-438.
- Verberne, A. J., & OWENS, N. C. (1998). Cortical modulation of the cardiovascular system. *Progress in neurobiology*, 54(2), 149-168.
- Vilella, L., Lacuey, N., Hampson, J. P., Rani, M. S., Loparo, K., Sainju, R. K., ... & Scott, C. (2019a). Incidence, Recurrence, and Risk Factors for Peri-ictal Central Apnea and Sudden Unexpected Death in Epilepsy. *Frontiers in neurology*, 10.
- Vilella, L., Lacuey, N., Hampson, J. P., Rani, M. S., Sainju, R. K., Friedman, D., ... & Zonjy, B. (2019b). Postconvulsive central apnea as a biomarker for sudden unexpected death in epilepsy (SUDEP). *Neurology*, 92(3), e171-e182.
- Wandschneider, B., Koeppe, M., Scott, C., Micallef, C., Balestrini, S., Sisodiya, S. M., ... & Duncan, J. S. (2015). Structural imaging biomarkers of sudden unexpected death in epilepsy. *Brain*, 138(10), 2907-2919.
- Wang, J. H., Zuo, X. N., Gohel, S., Milham, M. P., Biswal, B. B., & He, Y. (2011). Graph theoretical analysis of functional brain networks: test-retest evaluation on short-and long-term resting-state functional MRI data. *PloS one*, 6(7), e21976.
- Wang, Z., Zhang, Z., Jiao, Q., Liao, W., Chen, G., Sun, K., ... & Lu, G. (2012). Impairments of thalamic nuclei in idiopathic generalized epilepsy revealed by a study combining morphological and functional connectivity MRI. *PloS one*, 7(7), e39701.
- Weaver, K. E., Chaovalitwongse, W. A., Novotny, E. J., Poliakov, A., Grabowski Jr, T. J., & Ojemann, J. G. (2013). Local functional connectivity as a pre-surgical tool for seizure focus identification in non-lesion, focal epilepsy. *Frontiers in neurology*, 4, 43.
- Welsh, J. P., Yuen, G. S., Placantonakis, D. G., Vu, T. Q., Haiss, F., O Hearn, E., ... & Aicher, S. A. (2002). Why do Purkinje cells die so easily after global brain ischemia?

- Aldolase C, EAAT4 and the cerebellar contribution to posthypoxic myoclonus. *ADVANCES IN NEUROLOGY-NEW YORK-RAVEN PRESS*-, 89, 331-360.
- Wenker, I. C., Abe, C., Viar, K. E., Stornetta, D. S., Stornetta, R. L., & Guyenet, P. G. (2017). Blood pressure regulation by the rostral ventrolateral medulla in conscious rats: effects of hypoxia, hypercapnia, baroreceptor denervation, and anesthesia. *Journal of Neuroscience*, 37(17), 4565-4583.
- Whelan, C. D., Altmann, A., Botía, J. A., Jahanshad, N., Hibar, D. P., Absil, J., ... & Bergo, F. P. (2018). Structural brain abnormalities in the common epilepsies assessed in a worldwide ENIGMA study. *Brain*, 141(2), 391-408.
- White, C. R., Snodgrass, D., Yazdizadeh, M., Yan-Go, F., Jen, J., Harper, R. K., ... & Harper, R. M. (2016). Neuromodulation of cranial nerves for migraine and trigeminal neuropathy pain: cardiac effects. *The FASEB Journal*, 30(1_supplement), 731-4.
- Wilson, C. L., Isokawa, M., Babb, T. L., Crandall, P. H., Levesque, M. F., & Engel, J. (1991). Functional connections in the human temporal lobe. *Experimental Brain Research*, 85(1), 174-187.
- Winston, G. P., Micallef, C., Symms, M. R., Alexander, D. C., Duncan, J. S., & Zhang, H. (2014). Advanced diffusion imaging sequences could aid assessing patients with focal cortical dysplasia and epilepsy. *Epilepsy research*, 108(2), 336-339.
- Wong, S. W., Massé, N., Kimmerly, D. S., Menon, R. S., & Shoemaker, J. K. (2007). Ventral medial prefrontal cortex and cardiovagal control in conscious humans. *Neuroimage*, 35(2), 698-708.
- Woo, M. A., Kumar, R., Macey, P. M., Fonarow, G. C., & Harper, R. M. (2009). Brain injury in autonomic, emotional, and cognitive regulatory areas in patients with heart failure. *Journal of cardiac failure*, 15(3), 214-223.
- Woo, M. A., Macey, P. M., Fonarow, G. C., Hamilton, M. A., & Harper, R. M. (2003). Regional brain gray matter loss in heart failure. *Journal of applied physiology*, 95(2), 677-684.
- Xu, F., & Frazier, D. T. (2002). Role of the cerebellar deep nuclei in respiratory modulation. *The Cerebellum*, 1(1), 35.
- Xu, T., Cullen, K. R., Mueller, B., Schreiner, M. W., Lim, K. O., Schulz, S. C., & Parhi, K. K. (2016). Network analysis of functional brain connectivity in borderline personality disorder using resting-state fMRI. *NeuroImage: Clinical*, 11, 302-315.
- Yamaguti, Y., & Tsuda, I. (2015). Mathematical modeling for evolution of heterogeneous modules in the brain. *Neural Networks*, 62, 3-10.
- Yan, C., & Zang, Y. (2010). DPARSF: a MATLAB toolbox for " pipeline" data analysis of resting-state fMRI. *Frontiers in systems neuroscience*, 4, 13.

- Yıldız, G. U., Dogan, E. A., Dogan, U., Tokgoz, O. S., Ozdemir, K., Genc, B. O., & İlhan, N. (2011). Analysis of 24-hour heart rate variations in patients with epilepsy receiving antiepileptic drugs. *Epilepsy & behavior*, *20*(2), 349-354.
- Yoshimoto, K., McBride, W. J., Lumeng, L., & Li, T. K. (1992). Alcohol stimulates the release of dopamine and serotonin in the nucleus accumbens. *Alcohol*, *9*(1), 17-22.
- Yu-Feng, Z., Yong, H., Chao-Zhe, Z., Qing-Jiu, C., Man-Qiu, S., Meng, L., ... & Yu-Feng, W. (2007). Altered baseline brain activity in children with ADHD revealed by resting-state functional MRI. *Brain and Development*, *29*(2), 83-91.
- Zalesky, A., Fornito, A., & Bullmore, E. T. (2010). Network-based statistic: identifying differences in brain networks. *Neuroimage*, *53*(4), 1197-1207.
- Zanchetti, A., & Zoccolini, A. (1954). Autonomic hypothalamic outbursts elicited by cerebellar stimulation. *Journal of Neurophysiology*, *17*(5), 475-483.
- Zaroubi, S., & Goelman, G. (2000). Complex denoising of MR data via wavelet analysis: application for functional MRI. *Magnetic resonance imaging*, *18*(1), 59-68.
- Zhang, J., Su, J., Wang, M., Zhao, Y., Zhang, Q. T., Yao, Q., ... & Liu, Y. S. (2017). The posterior insula shows disrupted brain functional connectivity in female Migraineurs without Aura based on Brainnetome atlas. *Scientific reports*, *7*(1), 16868.
- Zhang, Z., Telesford, Q. K., Giusti, C., Lim, K. O., & Bassett, D. S. (2016). Choosing wavelet methods, filters, and lengths for functional brain network construction. *PloS one*, *11*(6), e0157243.
- Ziegler, G., Dahnke, R., Yeragani, V. K., & Bär, K. J. (2009). The relation of ventromedial prefrontal cortex activity and heart rate fluctuations at rest. *European Journal of Neuroscience*, *30*(11), 2205-2210.
- Zijlmans, M., Flanagan, D., & Gotman, J. (2002). Heart rate changes and ECG abnormalities during epileptic seizures: prevalence and definition of an objective clinical sign. *Epilepsia*, *43*(8), 847-854.
- Zou, Q. H., Zhu, C. Z., Yang, Y., Zuo, X. N., Long, X. Y., Cao, Q. J., ... & Zang, Y. F. (2008). An improved approach to detection of amplitude of low-frequency fluctuation (ALFF) for resting-state fMRI: fractional ALFF. *Journal of neuroscience methods*, *172*(1), 137-141.
- Zuo, X. N., Di Martino, A., Kelly, C., Shehzad, Z. E., Gee, D. G., Klein, D. F., ... & Milham, M. P. (2010). The oscillating brain: complex and reliable. *Neuroimage*, *49*(2), 1432-1445.